Novologue Therapy Improves Mitochondrial Bioenergetics and Modulates Transcriptome Changes in Diabetic Sensory Neurons

By

Jiacheng Ma

Submitted to the graduate degree program in Department of Pharmacology and Toxicology and the Graduate Faculty of the University of Kansas in partial fulfillment of the requirements for the degree of Doctor of Philosophy

_____

Chairperson, Dr. Rick Dobrowsky

_____

Dr. Alexander Moise

_____

Dr. Honglian Shi

_____

Dr. Shidu Yan

_____

Dr. Douglas Wright

Date Defended: May 19, 2015

The Dissertation Committee for Jiacheng Ma

certifies that this is the approved version of the following dissertation:

Novologue Therapy Improves Mitochondrial Bioenergetics and Modulates Transcriptome Changes in Diabetic Sensory Neurons

_____

Chairperson, Dr. Rick Dobrowsky

Date approved: May 19, 2015

Abstract

Diabetic peripheral neuropathy (DPN) is a prevalent diabetic complication with scarce treatment options. Impaired neuronal mitochondrial bioenergetics contributes to the pathophysiologic progression of DPN and may be a focal point for disease management. We have demonstrated that modulating Hsp90 and Hsp70 with the small-molecule drug KU-32 ameliorates psychosensory, electrophysiologic, morphologic, and bioenergetic deficits of DPN in animal models of type 1 diabetes. The current study used mouse models of type 1 and type 2 diabetes to determine the relationship of changes in sensory neuron mitochondrial bioenergetics to the onset of and recovery from DPN. The onset of DPN showed a tight temporal correlation with a decrease in mitochondrial bioenergetics in a genetic model of type 2 diabetes. In contrast, sensory hypoalgesia developed 10 weeks before the occurrence of significant declines in sensory neuron mitochondrial bioenergetics in the type 1 model. KU-32 therapy improved mitochondrial bioenergetics in both the type 1 and type 2 models, and this tightly correlated with a decrease in DPN. Mechanistically, improved mitochondrial function following KU-32 therapy required Hsp70, since the drug was ineffective in diabetic Hsp70 knockout mice. Our data indicate that changes in mitochondrial bioenergetics may rapidly contribute to nerve dysfunction in type 2 diabetes, but not type 1 diabetes, and that modulating Hsp70 offers an effective approach toward correcting sensory neuron bioenergetic deficits and DPN in both type 1 and type 2 diabetes.

We also sought to determine whether KU-596, an analogue of KU-32, offers similar therapeutic potential for treating DPN. Similar to KU-32, KU-596 improved psychosensory and bioenergetic deficits of DPN in a dose-dependent manner. However,

the drug could not improve DPN in Hsp70 KO mice. Transcriptomic analysis using RNA sequencing (RNA-Seq) of DRG from diabetic wild type (WT) and Hsp70 KO mice revealed that KU-596 modulated transcription of genes involved in inflammatory pathways independently of Hsp70. In contrast, the effects of KU-596 on genes involved in the production of reactive oxygen species (ROS) are Hsp70-dependent. Our data indicate that modulation of molecular chaperones offers an effective approach towards correcting nerve dysfunction, and that normalization of inflammatory pathways alone by novologue therapy seems to be insufficient to reverse the deficits associated with insensate DPN in our model of type 1 diabetes.

Acknowledgement

First and foremost I would like to express my deepest gratitude to my mentor, Dr. Rick Dobrowsky. It has been my great honor to be his student. I appreciate all his contributions of time, ideas, and funding to make my Ph.D. experience productive and stimulating. The joy and enthusiasm he has for his research was contagious and motivational for me, even during tough times in the Ph.D. pursuit. Without his guidance and persistent help this dissertation would not have been possible. I would like to thank my committee members, Dr. Alexander Moise, Dr. Honglian Shi, Dr. Shidu Yan and Dr. Douglas Wright, for their support and precious suggestions during my graduate study. Dr. Brain Blagg had generously provided the compounds, KU-32 and KU-596, without which none of my dissertation work could have been done. I would also like to thank Jennifer Hackett in the Genome Sequencing Core for her help in the RNA sequencing study.

My time at KU was made enjoyable in large part due to the many friends and groups that became a part of my life. The members of the Dobrowsky group have contributed immensely to my personal and professional time at KU. The group has been a source of friendships as well as good advice and collaboration. I would like to thank Dr. Kevin Farmer, Dr. Liang Zhang, Dr. Chengyuan Li, Dr. Pan Pan and Michael Urban for teaching me the lab skills and providing precious suggestions for my research. I would like to thank Xinyue Zhang and Zhenyuan You, who shared my problems and listened to my complaints during the past year. Special thanks to Dr. Pan Pan, who spent the longest time with me in the lab and always cheered me up with her wild thoughts when I felt upset. Dr. Mengxi Sun and Zhen Mi have been great friends and roommates, their

encouragement and company has helped me to survive the hard times of graduate school. I would also like to thank everyone in the PTX department for making the past five years a great memory for me.

Lastly, I would like to thank my family for all their love and encouragement. For my parents who raised me with a love of science and supported me in all my pursuits. For my grandpa who taught me to always be optimistic and never give up. I would not have reached this far without their love and support.

Finally, I gratefully acknowledge the funding sources that made my Ph.D. work possible. This work was supported by grants from the Juvenile Diabetes Research Foundation (to R.T.D.); the National Institutes of Health National Institute of Neurological Disorders and Stroke [Grant NS054847] (to R.T.D.); National Institutes of Health National Institute of Diabetes and Digestive and Kidney Diseases [Grant DK095911] (to R.T.D.); National Institutes of Health National Cancer Institute [Grants CA120458 and CA109265] (to B.S.J.B.); the National Institute of Neurological Disorders and Stroke [Grant NS075311] (to B.S.J.B. and R.T.D.); COBRE funding; and a pilot grant from the National Institute of Diabetes and Digestive and Kidney Diseases Diabetes Complications Consortium (DiaComp).

Contents

List of Tables

List of Figures

List of Abbreviations

12/15-LO	12/15-lipoxygenase
17-AAG	17-allylamino-17-demethoxygeldanamycin
ACE	angiotensin-converting enzyme
ADA	American Diabetes Association
AGE	advanced glycation endproducts
AMPK	AMP-activated protein kinase
AR	aldose reductase
AT2	angiotensin II
AVONA	analysis of variance
bp	base pairs
Ca^{2+}	calcium
CAP	Cbl associated protein
CDC	Centers for Disease Control and Prevention
CGRP	calcitonin gene related peptide
CHIP	C terminus of Hsc70-Interacting Protein
CIDP	chronic inflammatory demyelinating polyneuropathy
CIPN	chemotherapeutics-induced peripheral neuropathy
CREB	cAMP responsive element binding protein
CRP	C-reactive peptides
CVD	cardiovascular diseases
DAG	diacylglycerol
DAN	Diabetic autonomic neuropathy
DBD	DNA binding domain
DCCT	Diabetes Control and Complications Trail
DKA	diabetic ketoacidosis
DPN	Distal symmetrical sensorimotor polyneuropathy, diabetic peripheral neuropathy

DRG	dorsal root ganglion
Drp1	dynamin-related protein 1
EDIC	Epidemiology of Diabetes Interventions and Complications
eEFs	eukaryotic elongation factors
eIFs	eukaryotic initiation factors
ER	endoplasmic reticulum
ERK	extracellular regulated kinase
ESRD	end-stage renal disease
FCCP	carbonylcyanide-4-(trifluoromethoxy)-phenylhydrazone
FDR	false discovery rate
FFA	free fatty acids
FKBP52	FK506-binding protein
FPG	fasting plasma glucose
FPKM	fragments per kb per millions of aligned reads
G6P	glucose-6-phosphate
GAD65	glutamic acid decarboxylase
GAPDH	glyceraldehyde 3-phosphate dehydrogenase
GDA	geldanamycin
GLP-1	glucagon-like peptide-1
GLUT	glucose transporter
GLUT-2	type 2 glucose transporter
GLUT-4	type 4 glucose transporter
GSH	glutathione
GSK	glycogen synthase kinase
HbA1c	glycated hemoglobin
HETE	hydroxyeicosatetraenoic acid
HFD	high fat diet
HLA	human leukocyte antigen

HNF	hepatocyte nuclear transcription factor
HOP	Hsp70-Hsp90 Organizing Protein
HR	hydrophobic repeat
HSE	heat shock element
HSF	heat shock factor
HSP	heat shock protein
HSR	heat shock response
IDDM	insulin-dependent diabetes mellitus
IDF	International Diabetes Federation
IENF	intraepidermal nerve fiber
IFG	impaired fasting glucose
IGF	insulin-like growth factor
IGRP	islet-specific glucose-6-phosphatase catalytic subunit-related protein
IGT	impaired glucose tolerance
IKK	inhibitor κB kinase
IL	interleukin
IP	intraperitoneal
IRS	insulin receptor substrates
IV	intravenous
JNK	c-jun N-terminal kinase
K^+/ATP	ATP-gated potassium channels
KO	knockout
LADA	latent autoimmune diabetes in adults
Lepr	leptin receptor
LPS	lipopolysaccharide
MAPK	mitogen-activated protein kinase
MI	myocardial infarction
MNCV	motor nerve conduction velocity

MODY	maturity-onset diabetes of the young
MRC	maximum respiratory capacity
mtBE	mitochondrial bioenergetics
mtDNA	mitochondrial DNA
mTOR	mammalian target of rapamycin
NC	nerve conduction
NCV	nerve conduction velocity
NEF	nuclear exchange factor
NF-κB	nuclear factor kappa B
NGF	nerve growth factor
NIDDM	noninsulin-dependent diabetes mellitus
NKHS	nonketotic hyperosmolar syndrome
NO	nitric oxide
NOD	non-obese diabetic
novologue	novobiocin analogue
NPDR	non-proliferative diabetic retinopathy
NRG1	neuregulin-1
NT-3	neurotrophin 3
OCR	oxygen consumption rate
OGTT	oral glucose tolerance test
PAI-1	plasminogen activator inhibitor-1
PARP	poly(ADP-ribose) polymerase
PCR	polymerase chain reaction
PDGF	platelet-derived growth factor
PDPN	painful diabetic peripheral neuropathy
PDR	proliferative diabetic retinopathy
PGE2	prostaglandin E2
PH	pleckstrin homology

PI3-K	phosphatidylinositol 3-kinase
PIP_2	3,4 bis-phosphate
PIP_3	phosphatidylinositol 3,4,5-triphosphate
PKC	protein kinase C
PP1	protein phosphatase 1
$PPAR\gamma$	peroxisome proliferator-activated receptor γ
PTB	phosphotyrosine binding
PTPase	protein tyrosine phosphatases
qRT-PCR	quantitative real-time PCR
RAGE	receptor for AGEs
RAS	renin-angiotensin system
RCR	respiratory control ratio
RNA-Seq	RNA sequencing
ROS	reactive oxygen species
rRNA	ribosomal RNA
SAR	structure-activity relationships
SDH	sorbitol dehydrogenase
SH2	Src-homology-2
SNCV	sensory nerve conduction velocity
SOD	superoxide dismutase
SoHo	sorbin homology
SOS	son-of-sevenless
SP	substance P
SRC	spare respiratory capacity
SREBP	steroid regulatory element-binding protein
STZ	streptozotocin
SUMO	small ubiquitin-like modifier
TCA	tricarboxylic acid

TGF-β	transforming growth factor-β
TNF-α	tumor necrosis factor-α
TPR	tetratricopeptide repeat
Trx	thioredoxin
Txnip	thioredoxin interacting/inhibiting protein
VEGF	vascular endothelial growth factor
WHO	World Health Organization
WT	wild type
ZDF	Zucker Diabetic Fatty
ZF	Zucker fatty

Chapter 1: Introduction

1.1. Diabetes Mellitus

1.1.1. Overview of Diabetes Mellitus

Diabetes mellitus is a metabolic disorder that characterized by chronic hyperglycemia and impaired carbohydrate, lipid and protein metabolism resulting from defects in insulin secretion, insulin action, or both. It is associated with reduced life expectancy, significant morbidity due to specific diabetes related microvascular complications (retinopathy, nephropathy and neuropathy), increased risk of macrovascular complications (ischemic heart disease, stroke and peripheral vascular disease), and diminished quality of life (WHO, 2006; WHO, 2013a).

First recognized around 1500 B.C.E. by the ancient Egyptians, diabetes mellitus was considered a rare condition in which a person urinated excessively and lost weight. The term diabetes mellitus reflects the fact that the urine of those affected had a sweet taste. When the disease was first recognized, no effective treatment was available, and diabetes was uniformly fatal within weeks to months after its diagnosis owing to insulin deficiency. With recent advances in our understanding towards the underlying causes of diabetes and the approaches to its prevention and treatment, many effective therapies are available for the controlling of hyperglycemia and its associated complications. Although diabetes is still associated with a reduced life expectancy, the outlook for patients with this disease has improved dramatically. However, although scientific advances have led to effective strategies for preventing and controlling diabetes, the pathway to cure has remained elusive. From the public health and overall societal standpoint, little progress

has been made toward conquering the disease during the past 200 years, with tremendous increase in the prevalence of diabetes worldwide (Polonsky, 2012).

Diabetes mellitus has become a worldwide epidemic that is among one of the most common and serious medical conditions humankind has had to face. Recent estimates indicate that there are an estimate of 382 million people in the world with diabetes and this is projected to increase to 592 million by 2035 (Guariguata, 2012; Guariguata, 2013; Whiting et al., 2011). According to a recent report released by the Centers for Disease Control and Prevention (CDC), 29.1 million people or 9.3% of the population in the United States have diabetes, with 8.1 million people being undiagnosed (CDC, 2014). As the number of people with diabetes grows worldwide, the disease takes an ever-increasing proportion of national health care budgets, having caused at least $548 billion in health expenditure in 2013 (Guariguata, 2013). In the US alone, the total cost of diagnosed diabetes in 2012 was $245 billion, including $176 billion in direct costs, and $69 billion for reduced productivity (American Diabetes, 2014).

1.1.2. Clinical Features and Diagnostic Criteria of Diabetes Mellitus

Diabetes mellitus normally presents with symptoms of polyuria, polydipsia and weight loss, and is sometimes accompanied by polyphagia and blurred vision. Impaired growth and susceptibility to certain infections may also present as clinical features of chronic hyperglycemia. Uncontrolled diabetes may lead to acute, life-threatening consequences such as diabetic ketoacidosis (DKA) or the nonketotic hyperosmolar syndrome (NKHS) (American Diabetes, 2013).

With progression of the disease, chronic hyperglycemia often leads to long-term complications including retinopathy with potential loss of vision; nephropathy leading to

renal failure; peripheral neuropathy with risk of foot ulceration, amputations, and Charcot joints; and autonomic neuropathy causing gastrointestinal, genitourinary, and cardiovascular symptoms and sexual dysfunction. Hypertension and abnormalities of lipoprotein metabolism often coexist with diabetes, especially in patients with type 2 diabetes. In addition, patients with diabetes have an increased incidence of atherosclerotic cardiovascular, peripheral arterial, and cerebrovascular disease (American Diabetes, 2013).

Diabetes mellitus is diagnosed on the basis of American Diabetes Association (ADA) recommendations, incorporating fasting plasma glucose (FPG), 2h values in the oral glucose tolerance test (OGTT) and HbA1c (Glycated hemoglobin) criteria (Table 1.1-1). FPG measures the plasma glucose level in a person who has been fasting for at least 8 hours and is the preferred method due to its convenience and low cost, however, it is not as powerful as the OGTT with respect to accuracy (NIDDK, 2011). Also performed after an at least 8-hour fast, the OGTT involves oral ingestion of a standard dose of glucose (75g) and measurement of plasma glucose levels two hours later, which indicates the efficiency of insulin to promote glucose uptake. HbA1c is a form of hemoglobin that is formed in a non-enzymatic glycation pathway by hemoglobin's exposure to plasma glucose. Whereas normal levels of glucose produce a normal amount of glycated hemoglobin, the fraction of glycated hemoglobin increases in a predictable way as the plasma glucose level increases. Since the HbA1c level could reflect average blood glucose levels over a 2- to 3-month period, it is a good tool for determining long-term glycemic condition. As a widely used biomarker of chronic glycemia, the HbA1c test correlates well with the onset of both microvascular and, to a lesser extent, macrovascular

complications, thus it plays a critical role in the disease management of diabetic patients (American Diabetes, 2013).

In 1997 and 2003, the Expert Committee on Diagnosis and Classification of Diabetes Mellitus recognized an intermediate group of individuals whose glucose levels do not meet criteria for diabetes, yet are higher than those considered normal (1997; 2003). These people are defined as having impaired fasting glucose (IFG) or impaired glucose tolerance (IGT) (Table 1.1-1), which are referred to as prediabetic states. Though IFG and IGT should not be viewed as clinical entities on their own, they are considered as risk factors for diabetes as well as cardiovascular diseases. The presence of IFG and IGT are closely associated with obesity, dyslipidemia with high triglycerides and/or low HDL cholesterol, and hypertension, which are also risk factors for diabetes. HbA1c also serves as a measure for the tendency to develop diabetes: an HbA1c range of 5.7-6.4% has been used to identify individuals with high risk for future diabetes, to whom the term prediabetes is applicable (American Diabetes, 2013).

Table 1.1-1: Diagnostic criteria of diabetes mellitus and other categories of hyperglycemia.

Diabetes mellitus	HbA1c ≥ 6.5%. **OR** FPG ≥ 126mg/dL (7.0 mmol/L). **OR** 2h post-glucose load ≥ 200 mg/dL (11.1 mmol/L). **OR** in patients with classic symptoms of hyperglycemia or hyperglycemic crisis, a random plasma glucose ≥ 200 mg/dL (11.1 mmol/L).
Impaired glucose tolerance (IGT)	2h post-glucose load ≥ 140 mg/dL (7.8 mmol/L) and < 199 mg/dL (11.0 mmol/L).
Impaired fasting glucose (IFG)	FPG ≥ 100 mg/dL (5.6 mmol/L) and ≤ 125 mg/dL (6.9 mmol/L)
*Glucose load = 75 g glucose orally	

1.1.3. Classification of Diabetes Mellitus

Depending on the origin of hyperglycemia, diabetes mellitus can be divided into different types, which mainly involves type 1 diabetes, type 2 diabetes and the gestational diabetes. Hyperglycemia resulting from an absolute lack of insulin is characterized as type 1 diabetes, which is also known as insulin-dependent diabetes mellitus (IDDM) or juvenile-onset diabetes. In contrast, type 2 diabetes, also known as noninsulin-dependent diabetes mellitus (NIDDM) or adult-onset diabetes, is resulted from a relative insufficiency of insulin production in the face of insulin resistance.

Type 1 Diabetes Mellitus

Type 1 diabetes mellitus, once known as the insulin-dependent diabetes mellitus (IDDM) or juvenile-onset diabetes, is a chronic condition in which the pancreas produces little or no insulin. Accounting for about 5-10% of cases in the US, type 1 diabetes is considered the result of a chronic, mainly T-cell mediated, autoimmune disease, which eventually leads to the virtually complete loss of pancreatic β-cells (Pugliese, 2013). Globally, the number of people with type 1 diabetes is unknown, although it is estimated that about 80,000 children develop the disease each year (WHO, 2013b). In the US, the number of type 1 diabetes patients is estimated to be around 3 million (JDRF). Although it has long been called “juvenile diabetes” due to the more frequent and relatively straightforward diagnosis in children, the majority of individuals living with the disease are adults. The increasing number of adult patients with type 1 diabetes is mainly due to two reasons: first, with increasing understanding of the disease and healthcare innovations, individuals with childhood-onset type 1 diabetes tend to live longer; second,

the rising number of new-onset cases of type 1 diabetes in adults, including those diagnosed with latent autoimmune diabetes in adults (LADA) (Andre et al., 1996).

Patients of type 1 diabetes experience progressive β-cell destruction. In the absence of β-cells, there is neither production nor secretion of insulin, and circulating insulin concentrations are near zero. In the absence of insulin, insulin-responsive tissues fail to take up and store glucose, amino acids, and lipids, despite the high circulating plasma levels of these fuels. To make the situation worse, the unopposed action of the counter-regulatory hormones, primarily glucagon, induces a starvation-like response. Glycogenolysis and gluconeogenesis proceed unchecked, further contributing to the high blood glucose concentration. Although blood glucose levels are elevated, a lack of insulin prevents glucose uptake into muscle and fat. This stimulates muscle proteolysis and adipose lipolysis, which provide additional precursors for gluconeogenesis, further exacerbating blood glucose levels. The process of fatty acids break down also generates ketones for export as ketone bodies that could be used as fuel by the brain. These ketones equilibrate into β-hydroxybutyrate and acetoacetate, and as the concentration of these metabolic acids increase, they deplete serum bicarbonate, leading to a state of metabolic acidosis called diabetic ketoacidosis (DKA). DKA is a serious, potentially life-threatening medical emergency that requires immediate aggressive treatment and is often the precipitating event that leads to a diagnosis of type 1 diabetes.

Type 1 diabetes has traditionally been diagnosed based on clinical catabolic symptoms suggestive of insulin deficiency: polyuria, polydipsia, weight loss, and marked hyperglycemia that is nonresponsive to oral agents. DKA may be present acutely or become the first manifestation that leads to a diagnosis of type 1 diabetes (Imam, 2012).

Tremendous variability exists in the initial presentation of type 1 diabetes in youth and adults: whereas children often present acutely, with severe symptoms of polyuria, polydipsia, and ketonemia; in adults, the disease presents with a more gradual onset, with a clinical presentation that may initially appear consistent with type 2 diabetes (Chiang, 2014).

Growing evidence suggests that impaired central tolerance to selected autoantigens is the earliest event in type 1 diabetes. Studies of the pathogenic mechanism of type 1 diabetes have identified several islet autoantigens, including insulin/proinsulin, glutamic acid decarboxylase (GAD65), the tyrosine phosphatase-like protein IA-2, the islet-specific glucose-6-phosphatase catalytic subunit-related protein (IGRP) and the cation efflux transporter ZnT8. Many of these autoantigens are diagnostic and predictive markers widely employed as screening tools (Vehik et al., 2011). Studies evaluating children at risk for developing type 1 diabetes have shown that the presence of more than two autoantibodies was associated with a nearly 70% risk for disease development within 10 years and 84% within 15 years (Ziegler et al., 2013). One and usually more of these autoantigens are present in 85-90% of individuals when fasting hyperglycemia is initially detected (American Diabetes, 2013). Also, the disease has strong human leukocyte antigen (HLA) associations. Genetic variants in the highly polymorphic HLA on chromosome 6p21.3 can lead to functional differences in how fragments of proteins are presented to the immune system. In this regard, the HLA DR4-DQ8 and/or DR3-DQ2 genes are positively linked to type 1 diabetes, while the DR2-DQB1*0602 allele is negatively associated. The HLA class II DQB*0302 on the DR4 haplotype and DQB1*0201 on the DR3 haplotype are generally considered the principal susceptibility

markers (Rubio-Cabezas and Argente, 2008). Type 1 diabetes has a family predilection and family members have higher risk of developing the disease compared to the general population, and the risk increases with the degree of genetic identity with the proband (Bonifacio and Ziegler, 2010). Despite the critical role of autoimmunity, growing evidence has shown that additional factors, including viruses (in particular enteroviruses) and environmental factors, can also contribute to the disease pathogenesis (Pugliese, 2013). Experimental evidence suggests that enteroviruses can infect and damage β-cells and induce expression of HLA class I antigens and α-interferon, which could amplify inflammation and provide a link to the triggering of islet autoimmunity (Dotta et al., 2007; Foulis et al., 1987).

Despite active research unveiling its pathogenesis, type 1 diabetes has no cure. However, it can be managed with proper treatment. The Diabetes Control and Complications Trail (DCCT) clearly showed that intensive insulin therapy, defined as three or more injections of insulin per day or continuous subcutaneous insulin infusion, was a key part of improved glycemia and better outcomes (1993a). A number of rapid-acting and long-acting insulin analogs have been developed to avoid side effects associated with the use of human insulin, such as hypoglycemia, while offering considerable glycemia improving effects in people with type 1 diabetes (Rodbard et al., 2014). In addition to intensive insulin supplementation, current experimental therapy trails also focus on the prevention of disease development, preservation of remaining β-cells, and replacement of β-cells (Chiang, 2014). Whereas pancreas transplantation is now accepted as a proven therapy for patients that require both kidney and pancreas transplant (Fioretto et al., 1998; Gruessner, 2011), ongoing trails that focus on efforts to

delay or prevent disease onset have been largely disappointing. A variety of different immuno-modulatory and immuno-suppressive agents have been evaluated in patients with recent-onset type 1 diabetes, but the results have been modest at best. Promising new agents and combinations of drugs or cell-based therapies are still being investigated in an effort to safely and effectively modulate the autoimmune response (Peters AL, 2013).

Type 2 Diabetes Mellitus

Type 2 diabetes mellitus, also known as the noninsulin-dependent diabetes mellitus (NIDDM) or adult-onset diabetes, is now the most prevalent form of diabetes. The World Health Organization (WHO) estimates that 90-95% of people around the world suffer from type 2 diabetes (WHO, 2013b). More than 20 million adults in the US alone are reported to have type 2 diabetes (CDC, 2014), and the number is still on the rise. Unlike type 1 diabetes, the pathogenesis of type 2 diabetes does not involve autoimmune destruction of pancreatic β-cells. Thus, type 2 diabetes is not associated with direct lack of insulin. Rather, it is due to the body's inability to respond properly to normal or even enhanced levels of insulin, creating a situation of relative insulin insufficiency, which is termed as insulin resistance.

Type 2 diabetes has a multifactorial pathogenesis in which interactions between genetic and environmental factors result in the development of insulin resistance and β-cell dysfunction (Figure 1.1-1) (Stumvoll et al., 2005). Insulin resistance, which is the hall mark of type 2 diabetes, is strongly associated with obesity and physical inactivity. Obesity is almost inevitably present in the majority of type 2 diabetes patients and responsible for the rising trend of the disease not only in adults but also in children and

teenagers (Engelgau et al., 2004). Several factors are proposed to link obesity to insulin resistance, which include free fatty acids (FFA) and tumor necrosis factor-α (TNF-α). In fact, it has been suggested that elevated levels of FFA and inflammatory cytokines released by expanded adipose tissue adversely affect the insulin signaling cascade (Boden and Shulman, 2002). FFA inhibit insulin-stimulated glucose uptake and glycogen synthesis in skeletal muscle and stimulate gluconeogenesis in liver (Boden and Shulman, 2002), whereas TNF-α enhances adipocyte lipolysis, further increasing FFA, and at the same time elicits negative effects on insulin signaling itself (Hotamisligil, 2000). Abnormally activated cellular kinases, including atypical protein kinase C (PKC) isoforms also accompanies increases in the levels of FFA and cytokines. These events can activate the inflammatory kinases, inhibitor of κB kinase (IKK) and c-jun N-terminal kinase (JNK), which together decrease signaling through insulin receptor substrate-1 (IRS-1) (Gao et al., 2004; Griffin et al., 1999; Itani et al., 2002).

The second and equally important pathogenic factor is a decline in β-cell function, which is found in about 50% of patients at the time of diagnosis (DeFronzo, 2004; Stumvoll et al., 2005). Even before the onset of overt hyperglycemia, pancreatic β-cell dysfunction and secretory defects have been shown, for example in individuals with IGT and IFG (van Haeften et al., 2002). A number of different hypothesis have been proposed to explain the development of β-cell dysfunction in type 2 diabetes. Insulin insensitivity appears as an early phenomenon in the course of type 2 diabetes, and to compensate for the increase demand of insulin due to insulin resistance, increased insulin production and secretion by β-cells is required. Over a prolonged period of time, the increased demand can ultimately lead to β-cell exhaustion and dysfunction (DeFronzo et al., 1992). In

addition, hyperglycemia itself can induce irreversible damages to cellular components of insulin production over time, which is referred to as “glucotoxicity” (Robertson et al., 2003; Yki-Jarvinen, 1992). During oxidative glucose metabolism, reactive oxygen species (ROS) are produced as an inevitable byproduct of mitochondrial respiration. Whereas under normal conditions, the amount of ROS produced in β-cells can be effectively detoxified by catalase and superoxide dismutase, hyperglycemia leads to a substantial increase in the amounts of ROS and subsequent damage to cellular components (Robertson et al., 2003; Yki-Jarvinen, 1992). The “lipotoxicity” theory suggests that chronically elevated FFA may exert a direct toxic effect on pancreatic cells by increasing the rate of nitric oxide formation, yet providing another explanation for the development of β-cell dysfunction in type 2 diabetes (McGarry and Dobbins, 1999; Unger, 1995; Unger and Zhou, 2001).

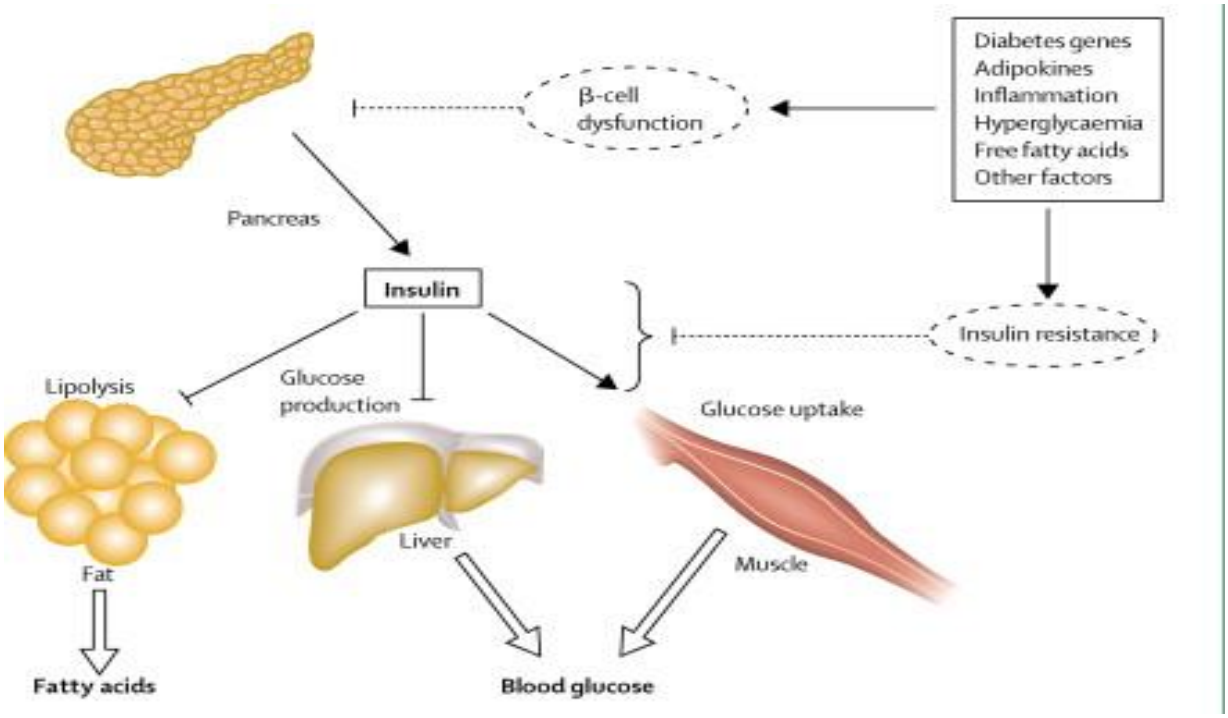

Figure 1.1-1: Pathophysiology of hyperglycemia and increased circulating FFA in type 2 diabetes.

Under normal circumstance, insulin secretion from the pancreas reduces glucose output by the liver, enhances glucose uptake by skeletal muscle, and suppresses FFA release from fat tissue. The various factors shown that contribute to the pathogenesis of type 2 diabetes affect both insulin secretion (β-cell function) and insulin action. The onset of insulin resistance, together with the subsequent β-cell dysfunction will reduce insulin signaling in its target tissues, leading to increased circulating FFA and hyperglycemia. The raised level of plasma glucose and FFA further worsens the condition of insulin resistance, and β-cell destruction through glucotoxicity and lipotoxicity. *(adapted from Stumvoll et al., 2005)*

Although the triggering pathogenic factors of type 2 diabetes comprise mainly environmental elements, genetic elements are also involved. Positive family history confers a 2-4 fold increased risk for type 2 diabetes, and 15-25% of the first-degree relatives of patients with type 2 diabetes develop IGT or diabetes (Pierce et al., 1995). Though there is little doubt that inherited factors predispose to an increased risk of developing type 2 diabetes, the genes involved remain largely elusive. For example,

polymorphisms in IRS-1 (Cocozza et al., 1992; O'Rahilly et al., 1991), the β3 adrenergic receptor (Lee et al., 2006), the insulin-sensitive glucose transporter (GLUT)-4 (Kusari et al., 1991) and a zinc transporter (*SLC30A8* encoded) exclusively expressed on insulin secretory vesicles (Sladek et al., 2007) have been detected in certain sub-groups of type 2 diabetes patients, but this initial association was not replicated in subsequent analysis. Currently, the most robust candidate variant is the highly prevalent Pro12A1a polymorphism in peroxisome proliferator-activated receptor γ (PPARγ) (Lohmueller et al., 2003).

Type 2 diabetes frequently goes undiagnosed for many years as the disorder develops gradually and is often asymptomatic at earlier stages. It is frequently diagnosed either by elevated blood glucose levels in routine screening tests or after the disease has become severe enough to cause diabetic complications. Several risk factors have been identified, including age, sex, obesity and central obesity, low physical activity, smoking, low fiber and high saturated fat diet, ethnicity, family history, history of gestational diabetes mellitus, history of the nondiabetic elevation of fasting or 2h glucose, elevated blood pressure, dyslipidemia, and different drug treatments (diuretics, unselected β-blockers, *etc*.) (Unwin et al., 2010).

As insulin resistance plays a fundamental role in the disease pathogenesis, one intervention for type 2 diabetes is to use therapeutic agents that improve tissue insulin sensitivity. Drugs that enhance insulin sensitivity are primarily the thiazolidinediones, which are PPARγ agonists and can alter adipose metabolism and distribution (Hevener et al., 2001; Lebovitz and Banerji, 2001). The thiazolidinediones have been shown to not only reduce glycemia, but also enhance vascular function, ameliorate dyslipidemia and

inflammatory milieu of type 2 diabetes (Yki-Jarvinen, 2004). Metformin has been shown effective in reducing glycemia as well as improving cardiovascular functions through reduction of hepatic glucose output (Bailey and Turner, 1996; Cusi et al., 1996; Mamputu et al., 2003), since it works independently of the pancreas it has less robust effects on insulin resistance. Sulfonylurea derivatives are insulin secretion enhancers, which work through closing the potassium channels in β-cells. These drugs have been shown effective in the control of blood glucose, as well as reducing the occurrence of microvascular and macrovascular complications of type 2 diabetes (1998b). Glucagon-like peptide-1 (GLP-1) is a gastrointestinal hormone, and has important effects on several of the pathophysiological features of type 2 diabetes, including potentiation of insulin secretion and suppression of glucagon secretion. Thus, GLP-1 agonists and mimetics serve as insulin secretagogues in the treatment of type 2 diabetes (Knudsen, 2004; Lund et al., 2014). As some oral insulin sensitizers are ineffective without adequate amounts of insulin, exogenous insulin supplementation may also be necessary to achieve glycemic control in type 2 diabetes (Stumvoll et al., 2005).

Gestational and Other Specific Types of Diabetes Mellitus

Gestational diabetes mellitus is the third main form of diabetes and has been defined as any degree of glucose intolerance with onset or first recognition during pregnancy (American Diabetes, 2013). The International Diabetes Federation (IDF) estimates that 21.4 million or 16.8% of live births to women in 2013 have hyperglycemia in pregnancy (Linnenkamp et al., 2014). According to a 2014 analysis by the CDC, the prevalence of gestational diabetes in the US is as high as 9.2%. The condition arises as the action of insulin is blocked, probably by hormones produced by the placenta, and can lead to

serious health risks to the mother and infants and increases the risk for developing type 2 diabetes later in life. Gestational diabetes is usually asymptomatic, and formal systemic testing for gestational diabetes is normally performed between 24 and 48 weeks of pregnancy, with diagnostic criteria same as with other types of diabetes. Re-evaluation of blood glucose is required for women diagnosed with gestational diabetes six weeks or more after delivery.

Other specific sub-types of diabetes are associated with genetic defects of β-cell function or insulin action. The former is referred to as maturity-onset diabetes of the young (MODY), and is characterized by impaired insulin secretion with minimal or no defects in insulin action. Common forms of MODY are due to mutations in the genes for hepatocyte nuclear transcription factor (HNF) 4-α (MODY-1), glucokinase (MODY-2), HNF1-α (MODY-3) and insulin promoter factor-1 (MODY-4). The latter one is mostly caused by mutations in the insulin receptor. Leprechaunism and Rabson-Mendenhall syndrome are two pediatric syndromes with mutations in the insulin receptor gene that cause subsequent alterations in insulin receptor function and extreme insulin resistance. Other specific causes of diabetes involve endocrinopathies, diseases of the exocrine pancreas and usage of drugs such as glucocorticoids (American Diabetes, 2013).

1.1.4. Insulin Signaling in Diabetes Mellitus

Insulin is the most potent physiological anabolic hormone known and is essential for appropriate tissue development, growth, and maintenance of glucose homeostasis. It serves as the primary regulator of blood glucose concentration by increasing glucose uptake in muscle and fat, and inhibiting hepatic glucose production. In addition, insulin stimulates cell growth and differentiation, promotes the storage of substrates by

stimulating lipogenesis, glycogen and protein synthesis and inhibiting lipolysis, glycogenolysis and protein breakdown (Chang et al., 2004; Saltiel and Kahn, 2001). Dysregulation of these processes due to insulin deficiency or resistance is a fundamental contributor to the pathogenesis of diabetes mellitus.

Insulin Production and Secretion

Insulin is exclusively produced by pancreatic β-cells, which are located in the pancreas in clusters known as the islets of Langerhans. The mature insulin molecule is a 51-amino acid protein composed of two polypeptide chains designated as A and B that are linked by two disulfide bridges. There is an additional intramolecular disulfide bond in the A chain. Insulin is initially synthesized as preproinsulin on the ribosomes of the rough endoplasmic reticulum (ER), and is rapidly transferred to and sequestered within the ER. Following synthesis, the signal sequence on the N-terminus of preproinsulin is rapidly cleaved enzymatically to form proinsulin, which contains the insulin A and B chains linked by the connecting peptide or C-peptide (Dodson and Steiner, 1998). The C-peptide ensures the efficient folding of the proinsulin molecule and the formation of its three intra-chain disulfide bonds in proinsulin. Once folding and disulfide bond formation has been accomplished, proinsulin is transferred in small vesicles to the Golgi apparatus, where it is packaged into secretory granules located close to the cell membrane. As the granules mature, proteases split proinsulin into equal amounts of insulin and C-peptide, allowing the insulin molecule to assume its active configuration (Steiner et al., 2009). Importantly, C-peptide remains intact and is stored and released during active secretion together with insulin, which makes it an independent indicator of insulin synthesis and secretion in clinical applications (Brandenburg, 2008; Steiner et al., 1969).

Insulin secretion by β-cells is stimulated in response to increased circulating levels of glucose and amino acids after a meal. Type 2 glucose transporter (GLUT-2), which is an insulin-independent glucose transporter with low substrate affinity, mediates the entry of glucose into β-cells. Glucose is phosphorylated to glucose-6-phosphate (G6P) by the rate-limiting enzyme glucokinase and thus started down the glycolytic pathway (Matschinsky et al., 1993). This modified glucose becomes effectively trapped within the β-cells and is further metabolized in the mitochondria to produce ATP. The increased ATP/ADP ratio causes the ATP-gated potassium (K^+/ATP) channels in the plasma membrane to close, preventing K^+ efflux. The ensuing rise in positive charge due to the increased concentration of K^+ ions leads to depolarization of the cell. The net effect is the activation of voltage-gated calcium (Ca^{2+}) channels, which transport Ca^{2+} into the cell. The brisk increase in intracellular Ca^{2+} concentrations triggers exocytosis of the insulin-storing granules. The ultimate result is the export of insulin from β-cells and its diffusion into nearby blood vessels (Koster et al., 2000). In contrast, under conditions of relatively low extracellular glucose concentrations, the β-cell has a low ATP/ADP ratio. In this case, the K^+/ATP channels remain open, which prevents Ca^{2+} influx and subsequent insulin secretion.

Insulin Signaling through the Insulin Receptor

Insulin elicits its effects by binding to the receptors on the surface of target cells (Figure 1.1-2). Although virtually all tissues express insulin receptors, the energy-storing tissues (liver, muscle, and adipose) express much higher levels of insulin receptor and thus constitute the main insulin target tissues. The insulin receptor is a tetrameric protein consisting of four disulfide-linked subunits. It is comprised of two extracellular α

subunits and two β subunits. The β subunits function as allosteric enzymes whose intrinsic tyrosine kinase activity is inhibited by the α subunits. The binding of insulin to the α subunit leads to derepression of the kinase activity in the β subunit, resulting in "autophosphorylation" of tyrosine on the nearby β subunit and a conformational change that further increases kinase activity (Patti and Kahn, 1998). Activation of the tyrosine kinase of the insulin receptor results in phosphorylation of several other intracellular proteins, most importantly, four members of the insulin receptor substrates (IRS) family (White, 1998). Other substrates include Gab-1, $p60^{dok}$, Cbl, APS and isoforms of Shc (Pessin and Saltiel, 2000). In response to insulin, these substrate proteins are recruited to the phosphorylated insulin receptor through the phosphotyrosine binding (PTB) domains, and are phosphorylated at tyrosine residues (Gual et al., 2005; Sasaoka and Kobayashi, 2000). The phosphorylated tyrosine in these substrates then act as docking sites to recruit a series of Src-homology-2 (SH2) domain containing signal transducers, including the phosphatidylinositol 3-kinase (PI3-K) (White, 2002).

The first step by which insulin increases energy storage or utilization is through regulating transport of glucose into the cell, mediated by the type 4 glucose transporter (GLUT-4). GLUT-4 is found in vesicles that slowly cycle between the plasma membrane and intracellular stores within the cell. Insulin increases glucose uptake in fat and muscle cells by stimulating GLUT-4 vesicle exocytosis, and by slightly attenuating the rate of its internalization (Chang et al., 2004). PI3-K plays a pivotal role in insulin-stimulated glucose uptake and GLUT-4 translocation (Shepherd et al., 1995). PI3-K interacts with tyrosine-phosphorylated IRS through the SH2 domains on its p85 regulatory subunit, leading to the activation and translocation of the enzyme to the plasma membrane, where

it catalyzes the phosphorylation of phosphatidylinositols at 3' position of the sugar alcohol, typically generating phosphatidylinositol 3,4 bis-phosphate (PIP_2) and phosphatidylinositol 3,4,5-tris-phosphate (PIP_3) (Lietzke et al., 2000). Inhibition of PI3-K with pharmacological inhibitors or overexpression of dominant interfering forms of PI3-K blocks insulin-stimulated GLUT-4 translocation and glucose uptake. Conversely, overexpression of constitutively active forms of PI3-K partially mimics insulin action (Martin et al., 1996; Okada et al., 1994; Sharma et al., 1998). Insulin-stimulated increase in PIP_3 leads to the recruitment and/or activation of a variety of pleckstrin homology (PH) domain-containing signaling molecules, enzymes, as well as cytoskeletal proteins (Lietzke et al., 2000). PIP_3 plays a direct role in the recruitment of the Ser/Thr kinases PDK1 and Akt to the plasma membrane via their PH domain (Corvera and Czech, 1998). PDK1 then phosphorylates and activates Akt and other downstream kinases including atypical protein kinases C (PKC) λ and ζ (Mora et al., 2004). PKC λ and PKCζ activity seems to be essential for insulin-stimulated glucose transport (Kohn et al., 1998; Kohn et al., 1996).

Despite the important role for the PI3-K pathway, activation of this pathway alone is not sufficient for insulin-stimulated glucose uptake. For example, platelet-derived growth factor (PDGF) and interleukin-4 also stimulate PI3-K activity but have no effect on either GLUT-4 translocation or glucose uptake (Isakoff et al., 1995; Wiese et al., 1995). Thus, other signaling pathways seem to be required for insulin-stimulated glucose uptake in addition to the PI3-K pathway (Figure 1.1-2) (Saltiel and Kahn, 2001). Studies suggest that this second pathway is localized in lipid raft domains, and seems to involve tyrosine phosphorylation of the Cbl proto-oncogene (Ribon and Saltiel, 1997). Activation of the

insulin receptor located in the lipid raft domain recruits Cbl to the phosphorylated insulin receptor adapter protein APS (Hu et al., 2003), and subsequently stimulates the tyrosine phosphorylation of Cbl (Liu et al., 2002). The Cbl associated protein (CAP) is an adapter protein containing three SH3 domains in its C-terminus and a sorbin homology (SoHo) domain (Kimura et al., 2001). CAP binds to the proline-rich sequences in Cbl through the SH3 domains (Ribon et al., 1998), and is recruited to the insulin receptor-APS complex together with Cbl. Upon recruitment to the insulin receptor, CAP interacts with the lipid raft domain protein flotillin via its SoHo domain, which is required for insulin-stimulated glucose uptake and GLUT-4 translocation (Baumann et al., 2000; Kimura et al., 2001). Tyrosine-phosphorylated Cbl interacts with the SH2/SH3-containing adapter protein CrkII, recruiting CrkII together with the nuclear exchange factor C3G to the lipid raft domain (Knudsen et al., 1994; Ribon et al., 1996). C3G can catalyze the activation of the small G protein TC10 in the lipid rafts, which provides a second signal to GLUT-4 translocation that functions in parallel with the PI3-K pathway (Chiang et al., 2001).

Once glucose is transported into the cells, insulin stimulates glycogenesis, lipogenesis and protein synthesis, and inhibits glycogenolysis, lipolysis and protein breakdown primarily through the PI3-K/Akt pathway. In muscle tissues, insulin stimulates glycogen synthesis by dephosphorylation and activation of glycogen synthase, which is done through inhibition of kinases such as PKA or glycogen synthase kinase (GSK)-3β (Cross et al., 1995) and activation of protein phosphatase 1 (PP1) (Brady et al., 1997). In adipose tissues, insulin promotes lipid synthesis and inhibits lipolysis through increased expression of the transcription factor steroid regulatory element-binding protein (SREBP)-1c, which regulates the expression of lipogenic genes (Shimomura et al., 1999).

Insulin activates protein synthesis by activating components of the translational machinery including eukaryotic initiation factors (eIFs) and eukaryotic elongation factors (eEFs) (Proud, 2006). In the liver, insulin inhibits gluconeogenesis and glycogenolysis, primarily through a direct effect on the activities of metabolic enzymes via phosphorylation and dephosphorylation and also regulation of gene expression of hepatic enzymes (Pilkis and Granner, 1992).

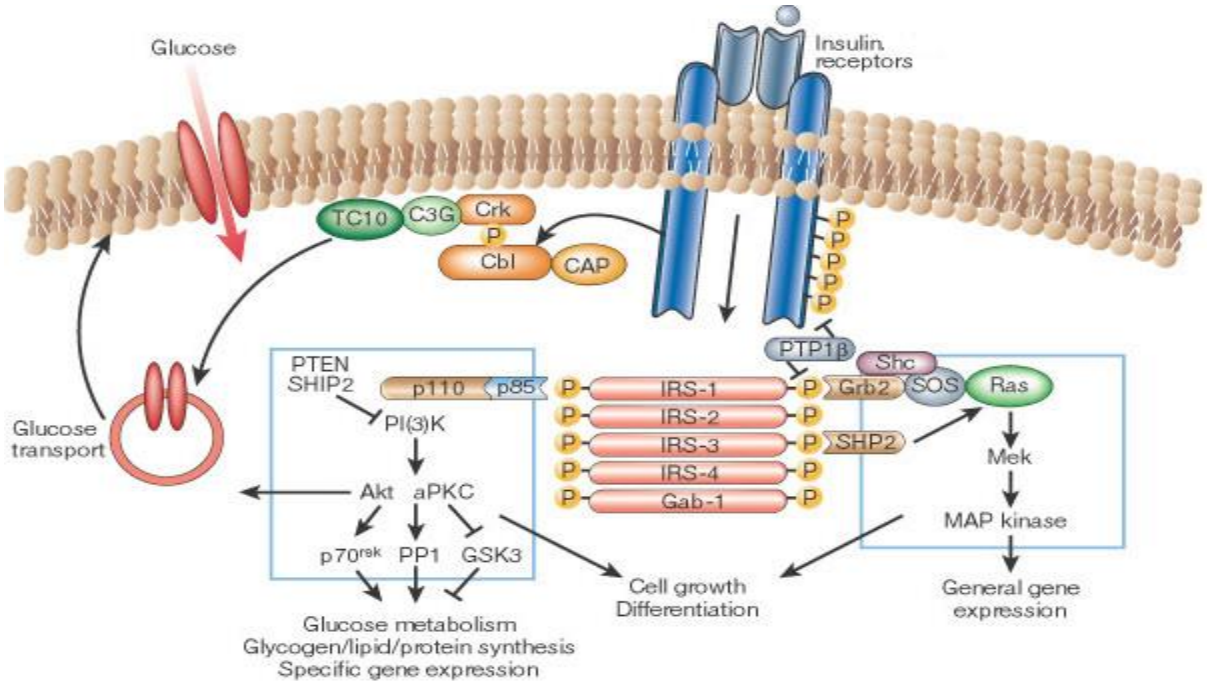

Figure 1.1-2: Signaling transduction in insulin action.

The insulin receptor is a tyrosine kinase that undergoes autophosphorylation, and catalyzes the phosphorylation of cellular proteins such as members of the IRS family, Shc and Cbl. Upon tyrosine phosphorylation, these proteins interact with signaling molecules through their SH2 domains, resulting in a diverse series of signaling pathways, including activation of PI3-K and downstream PIP_3-dependent protein kinases, Ras and the MAP kinase cascade, Cbl/CAP and the activation of TC10. These pathways act in a concerted fashion to coordinate vesicle trafficking, protein synthesis, enzyme activation and inactivation, and gene expression, which together regulate cellular glucose, lipid and protein metabolism. *(adapted from Saltiel and Kahn, 2001)*

In addition to its anabolic actions, insulin also promotes mitogenesis by stimulating the mitogen-activated protein kinase (MAPK); also referred to as the extracellular

regulated kinase (ERK). This pathway initiates with the tyrosine phosphorylation of IRS proteins and/or Shc, which in turn interact with Grb2, recruiting the Son-of-sevenless (SOS) exchange protein to the plasma membrane for the activation of Ras. Stimulation of the tyrosine phosphatase SHP2 through its interaction with receptor substrates such as Gab-1 or IRS-1/2 is also required for the activation of Ras. Upon activation, Ras stimulates a serine kinase cascade through the stepwise activation of Raf, MEK and ERK, which is essential for cellular proliferation and differentiation (Boulton et al., 1991) (Figure 1.1-2).

Upon dissociation of insulin, both the insulin receptor and its substrates undergo a rapid dephosphorylation mediated by protein tyrosine phosphatases (PTPase). A number of PTPase have been identified to dephosphorylate the insulin receptor *in vitro*, some of which are expressed in insulin-responsive cells or upregulated under states of insulin resistance (Drake and Posner, 1998). The cytoplasmic phosphatase PTP1B is important in dampening insulin signaling since its genetic deletion leads to increased tyrosine phosphorylation of the insulin receptor and IRS proteins and enhanced insulin sensitivity (Elchebly et al., 1999). Lipid phosphatases, such as PTEN (Maehama and Dixon, 1999) and SHIP2 (Vollenweider et al., 1999) may also attenuate insulin signaling through dephosphorylation of phosphatidylinositol polyphosphates. Substantial evidence has revealed a reduction in the autophosphorylation of insulin receptor as well as the tyrosine phosphorylation of its substrates in patients with type 2 diabetes, which subsequently leads to reduced PI3-K activity (Morino et al., 2006; Pessin and Saltiel, 2000). Other negative regulators of insulin signaling include serine phosphorylation of the insulin receptor and IRS proteins, which likely inhibits insulin signaling through decreasing

insulin-stimulated tyrosine phosphorylation (Hotamisligil et al., 1996) and promoting interaction with 14-3-3 proteins (Craparo et al., 1997). Several kinases have been implicated in this process, including PI3-K, Akt, GSK-3 and mammalian target of rapamycin (mTOR) (Saltiel and Kahn, 2001). For example, Ser312, a residue located close to the IRS-1 PTB domain, has been shown to be phosphorylated by JNK, IKKβ and mTOR. Phosphorylation of this serine residue impairs IRS-1 binding to the activated insulin receptor, and contributes to onset of insulin resistance (Aguirre et al., 2002; Carlson et al., 2004; Gao et al., 2002). In addition, phosphorylation of IRS-1 serine residues that locate in proximity to the SH2 domain binding motif, for example Ser636, negatively modulates the binding of PI3-K to IRS-1, further abolishing the downstream signaling (Ozes et al., 2001).

As discussed above, the insulin signaling system plays an important role in many physiological processes, including carbohydrate, lipid and protein metabolism, cellular growth, differentiation and survival. Systematic interactions between the insulin receptor and its substrates, as well as interactions between downstream signaling molecules are crucial for the maintenance of insulin-stimulated signal transduction. Dysregulation of insulin signaling, either due to a lack of insulin production or insulin resistance, leads to onset of a cohort of systemic disorders including impaired glucose tolerance, dyslipidemia and overt diabetes. Thus, halting the loss of insulin-producing β cells and/or increasing insulin sensitivity is a key tactic for contending with these metabolic disorders and the associated complications.

1.1.5. Complications of Diabetes Mellitus

Long-term diabetes increases the likelihood of developing secondary damage to numerous systems, which are the major sources of morbidity and mortality in both type 1 and type 2 diabetes. It is recognized that until a cure for the worldwide diabetes epidemic is realized, it is also necessary to address approaches that delay the onset of diabetic complications. Generally, the injurious effects of hyperglycemia are separated into macrovascular complications (due to damage to larger blood vessels) and microvascular complications (due to damage to small blood vessels). Macrovascular complications include atherosclerosis, coronary artery disease and cerebrovascular disease, such as stroke. Microvascular complications include diabetic retinopathy, diabetic nephropathy and diabetic neuropathy (Mattila and de Boer, 2010).

Macrovascular Complications

Both type 1 and type 2 diabetes have a largely irreversible and devastating effect on small and large blood vessels, leading to vascular injuries and subsequently, macrovascular complications of diabetes (Holman et al., 2008; Nathan et al., 2005). Common consequences of vascular injury, such as hypertension, altered vascular permeability and ischemia, can also contribute to other diabetic complications. Macrovascular complications of diabetes affect many organs, and can cause substantial morbidity and early mortality, with cardiovascular disease and stroke being the leading causes of mortality in diabetic patients (Dale et al., 2008; Nathan et al., 2005). Approximately 71% of adults with diabetes also have hypertension and 65% have high cholesterol. The risk of having a stroke is 1.5 times higher in diabetic patients and the heart disease death rate is about 1.7 times higher than people without diabetes.

Hyperglycemia and dyslipidemia, along with many glucose-driven pathways, have been shown as key players in contributing to these vascular co-morbidities. Oxidative stress and inflammation have been heightened as central pathogenic mechanisms for these marcovascular complications, as they markedly alter gene expression patterns in the vasculature, shifting the balance towards an increased pro-inflammatory and thrombogenic potential (Calcutt et al., 2009). Studies in type 1 diabetes have shown that intensive glucose control is associated with a 42% risk reduction in all cardiovascular events and a 57% reduction in the risk of nonfatal myocardial infarction (MI), stroke, or death from cardiovascular diseases (CVD) (Nathan et al., 2005). Though there has not been a large, controlled study showing decreases in macrovascular disease from improved glycemic control in type 2 diabetes, modification of other elements of the metabolic syndrome, such as lowering blood pressure, has been shown to significantly decrease the risk of cardiovascular events (1998a). The increased understanding towards mechanisms underlying these diabetes-induced complications have led to clinical trials investigating antagonism of various glucose-driven pathways, including the polyol pathway, activation of PKC isoforms, accumulation of advanced glycation endproducts (AGEs) and oxidative stress (Joy et al., 2005; Kass et al., 2001; Stirban et al., 2006; Suzen and Buyukbingol, 2003). Agents that suppress inflammation and adaptive immune mechanisms, such as statins and PPAR agonists, have also been considered relevant to the treatment of vascular diseases in diabetes (Ludwig and Shen, 2006; Panunti and Fonseca, 2006). As many mechanisms may synergize to cause vascular injuries in diabetes, therapies that target various components in disease pathogenesis may also be beneficial.

Diabetic Retinopathy

Diabetic retinopathy is the leading cause of blindness in persons 25-74 years old in the US. The progression of diabetic retinopathy can be divided into two stages: non-proliferative diabetic retinopathy (NPDR) and proliferative diabetic neuropathy (PDR). In the initial stages of diabetic retinopathy, patients are generally asymptomatic. In the more advanced stages of the disease patients may experience symptoms that include floaters, blurred vision, distortion and progressive visual acuity loss (Bhavsar, 2014). The clinical signs of diabetic retinopathy include a range of retinal lesions and abnormalities that indicate vascular damage (capillary microaneurysms, capillary degeneration, increased vascular permeability and new vessel formation) and death or dysfunction of the neural retina ('cotton wool spots', alterations in retinal electrophysiology and loss of color or hue discrimination) (Frank, 2004).

Approximately 700,000 people in the US have proliferative diabetic retinopathy (PDR), with an annual incidence of 65,000 (Bhavsar, 2014; Zhang et al., 2010b). Diabetic retinopathy occurs in all forms of diabetes, and its development depends on the duration and severity of diabetes, as is the case with all diabetes-specific complications. Other risk factors for diabetic retinopathy include hypertension, hyperlipidemia, and most importantly, hyperglycemia (Crawford et al., 2009). The disease takes years to develop, and almost all patients with type 1 and type 2 diabetes will to some extent develop retinopathy after 20 years of disease (Kempen et al., 2004; Roy et al., 2004). In patients with type 1 diabetes, no clinically significant signs of retinopathy can be seen in the first 5 years after the initial diagnosis of diabetes. After 10-15 years, 25-50% of patients show some signs of retinopathy, and the prevalence increases to 75-95% after 15 years and

approaches 100% after 30 years of diabetes. PDR is rare within the first decade of type 1 diabetes diagnosis but increases to 14-17% by 15 years, rising steadily thereafter. In patients with type 2 diabetes, the incidence of diabetic retinopathy increases with the disease duration; 23% have non-proliferative diabetic retinopathy (NPDR) after 11-13 years, 41% have NPDR after 14-16 years, and 60% have NPDR after 16 years (Bhavsar, 2014).

Although studies have clearly shown that the development of diabetic retinopathy is tightly associated with poor glycemic control, achievement of better glycemic control does not promise reversion or immediately halt disease progression (1993a; Engerman and Kern, 1987). Indeed, co-morbidities that commonly parallel with hyperglycemia, such as hypertension and dyslipidemia, can influence the progression rate of retinopathy (1998a; Barile et al., 2005). Thus, tight control of blood glucose, blood pressure and cholesterol levels are essential for the prevention of diabetic retinopathy. Treatment for diabetic retinopathy varies with the stage of the disease and is directed towards slowing or halting the progression of the disease. In the early stages of NPDR, treatment other than regular monitoring may not be required. With progression of the disease, leakage of fluid from blood vessels can lead to macular edema, under which condition laser treatment (photocoagulation) is used to stop the leakage of blood and fluid into the retina. When blood vessel growth is more widespread throughout the retina, as in PDR, a pattern of scattered laser burns is conducted to help shrink the abnormal blood vessels (Institute, 2014). In addition to laser surgeries, a number of potential therapies, ranging from pan-complication therapies (aldose reductase inhibitors and PKC-β inhibitors) to retinopathy-specific strategies (anti-VEGF agents), have been reported to inhibit diabetes-induced

degeneration of retinal capillaries and neurons and increase in retinal vascular permeability in animals (Dorrell et al., 2007; Kern, 2007). However, approved pharmacologic treatments in humans are limited to several anti-VEGF agents.

Diabetic Nephropathy

Diabetic nephropathy is the leading cause of renal failure, and it has become the most common single cause of end-stage renal disease (ESRD) in the Western world (Gilbertson et al., 2005). In the US, diabetic nephropathy accounts for about 40% of new cases of ESRD. About 20-30% of patients with type 1 and type 2 diabetes develop evidence of nephropathy. Whereas diabetic nephropathy rarely develops in the first decade of type 1 diabetes, approximately 3% of newly diagnosed patients with type 2 diabetes have overt nephropathy. The peak incidence of nephropathy is usually found in people who have had diabetes for 10-20 years, after which the rate progressively declines. Though in type 2 diabetes, a considerably smaller fraction of nephropathy cases would progress to ESRD, such patients constitute over half of the diabetic patients currently requiring dialysis because of the greater prevalence of type 2 diabetes (Batuman, 2014; Molitch et al., 2004).

Diabetic nephropathy is defined by proteinuria > 300 mg in 24 hours in the setting of diabetes, followed by a subsequent decline in glomerular filtration rate and ultimate progression to azotemia and uremia, which is fatal if left untreated (Mogensen et al., 1983). The onset of overt proteinuria is preceded by microalbuminuria, which is characterized by the appearance of low but abnormal levels (30-299 mg / 24 hours) of albumin in the urine, and patients with microalbuminuria are referred to as having

incipient nephropathy. Without intervention, patients of both type 1 and type 2 diabetes with microalbuminuria typically progress to overt diabetic nephropathy.

Like the other microvascular diabetic complications, there is strong association between glycemic control and the risk of developing nephropathy, which makes tight glycemic control the initial prevention and treatment of diabetic nephropathy (1993a). Another main risk factor for nephropathy is hypertension. Hypertension has an interdependent relationship with nephropathy since the onset of nephropathy often leads to a further increase in the blood pressure of diabetic patients (1993b). Insight into the molecular and biochemical mechanisms for diabetes-induced renal lesions revealed several potential therapeutic targets for treating diabetic nephropathy. Glucose-dependent pathways, such as advanced glycation, have been shown to be involved in disease pathogenesis both through the disruption of vasoactive hormone pathways, and through activation of the receptor for AGEs (RAGE), PKC, MAPK and angiotensin II (AT2) (1993b; Wendt et al., 2003). Despite ongoing research on disease mechanisms and potential therapies, the drugs currently used to treat diabetic nephropathy are mainly anti-hypertensive agents. Drugs that interrupt the renin-angiotensin system (RAS), including angiotensin-converting enzyme (ACE) inhibitors and AT2 receptor antagonists, have been incorporated into most national and international treatment guidelines and are currently the first-line treatments for diabetic nephropathy (Molitch et al., 2004).

1.2. Diabetic Neuropathy

Diabetic neuropathy is the most common and intractable complication of diabetes, affecting about 60-70% of patients with type 1 and type 2 diabetes (Veves et al., 2008). There is increasing evidence that pre-diabetic conditions are also associated with some

forms of neuropathy (Singleton et al., 2003). Recognized by the ADA as "the presence of signs of peripheral nerve dysfunction in people with diabetes after the exclusion of other causes" (American Diabetes, 2007), diabetic neuropathy has become the most prevalent neuropathy in the western world. Diabetic neuropathy can result in pain, decreased motility, and foot ulceration and is the leading cause of non-traumatic lower-limb amputations in the US, accounting for about 60% cases among people aged 20 years or older. Economically, diabetic neuropathy constitutes a huge burden on the healthcare system, with an estimate annual cost of up to $13.7 billion (Gordois et al., 2003). Also about one-third of the direct medical cost of diabetes may be attributed to diabetic neuropathy and its complications (*e.g.* foot ulceration) (Carls et al., 2011).

1.2.1. Classification and Clinical Manifestations

Diabetic neuropathy is a descriptive term that encompasses a spectrum of clinical and subclinical syndromes that affect different parts of the nervous system and present with diverse clinical manifestations. Diabetic patients may have only one type of neuropathy or develop different combinations of neuropathies. Different forms of diabetic neuropathy can be classified in terms of their anatomical distribution (*e.g.*, proximal or distal, symmetric or asymmetric, focal or diffuse), clinical course (*e.g.*, acute or chronic) and characteristic features (*e.g.*, painful or insensate, sensory, motor, or autonomic). Table 1.2-1 lists the major types of diabetic neuropathy which are classified into diffuse and focal neuropathies (Boulton et al., 2005; Edwards et al., 2008). The diffuse neuropathies are common, usually chronic and progressive. In contrast, the focal neuropathies are less common, usually acute in onset, and often self-limited. The patterns

of nerve injuries in diabetic neuropathy are illustrated in figure 1.2-1 (Callaghan et al., 2012a).

Table 1.2-1: Classification of Diabetic Neuropathy

Diffuse neuropathy	**Focal neuropathy**
Distal symmetrical sensorimotor polyneuropathy (DPN)	Mononeuropathy
-Small fiber	Mononeuropathy multiplex
-Large fiber	Plexopathy
-Mixed	Radiculopathy
Diabetic autonomic neuropathy (DAN)	Cranial neuropathy
-Abnormal pupillary function	
-Sudomotor dysfunction	
-Genitourinary	
-Gastrointestinal	
-Cardiovascular	
-Hypoglycemia unawareness	

(modified from Boulton et al., 2005; Edwards et al., 2008)

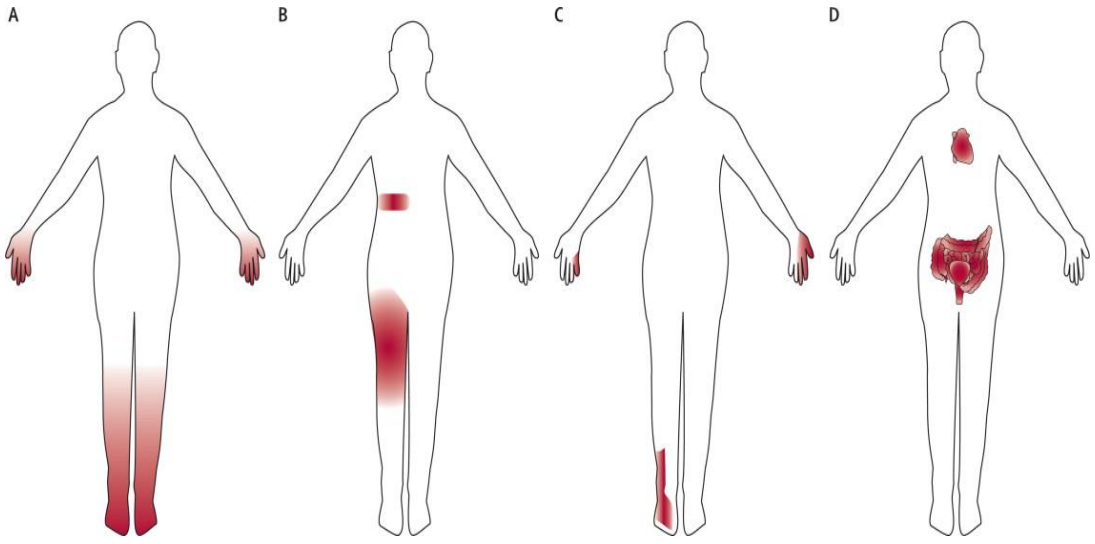

Figure 1.2-1: Patterns of Nerve Injuries in Diabetic Neuropathy.

The patterns of nerve injuries are illustrated as follow. The affected areas in different categories are indicated with red shading. (A) Distal symmetrical sensorimotor polyneuropathy (DPN) and small-fiber predominant neuropathy; (B) plexopathy and radiculopathy; (C) mononeuropathy and mononeuropathy multiplex; and (D) autonomic neuropathy (DAN). Among

them, DPN (A) and DAN (D) are diffuse neuropathies, and they normally progress with increasing duration and severity of diabetes. Plexopathy, radiculopathy (B), mononeuropathy and mononeuropathy multiplex (C) are focal neuropathies. Diabetic plexopathy can be responsive to immunotherapy and, in contrast to most nerve injury in patients with diabetes, usually improves with time. *(adapted from Callaghan et al., 2012a)*

Distal Symmetrical Sensorimotor Polyneuropathy

Distal symmetrical sensorimotor polyneuropathy (DPN) is the most common subtype of diabetic neuropathy, with up to 50% of patients experiencing symptoms such as numbness, tingling, pain, or weakness. These symptoms appear first in the distal portions of the extremities and progress gradually to the more proximal part of the body in a "stocking-glove" distribution with increasing duration and severity of diabetes. The prevalence of DPN increases with age in both type 1 and type 2 diabetes, and tends to be more common in patients with type 2 diabetes. Height is another risk factor for DPN, implicating the distant-dependent pathology of DPN. Other suggested risk factors for DPN include hypertension, low plasma insulin levels, other microvascular diabetic complications, smoking and excessive alcohol use (Edwards et al., 2008).

The symptoms of DPN are associated with many downstream effects that greatly affect quality of life for patients. One determinant factor of the signs and symptoms of DPN is the fiber type involved. Large-fiber involvement results in impaired proprioception and light touch, while small-fiber involvement results in impaired pain and temperature perception (Edwards et al., 2008). Neuropathic pain is one of the most disabling symptoms in patients with DPN. Patients experience frequent burning pain, electrical or stabbing sensations, paresthesia, hyperesthesia, and deep aching pain, which typically worsen at night. Allodynia (painful sensations to innocuous stimuli) and hyperalgesia (increased sensitivity to painful stimuli) are also common symptoms for

DPN (Boulton et al., 2005). DPN-associated numbness often causes balance problems, which makes it one of three main risk factors for falls in patients with diabetes (Agrawal et al., 2010). Additionally, patients with severe DPN are at risk of ulcerations, neuroarthropathy (Charcot's joints) and lower-extremity amputations, with 15% developing an ulcer during the course of their disease (Gordois et al., 2003). With disease progression, distal weakness might occur in the most severe cases (Edwards et al., 2008).

As up to half of the patients may be asymptomatic, the diagnosis of DPN can only be made after a careful clinical examination. All patients with diabetes should be screened annually for DPN by examining pinprick, temperature, and vibration perception (using a 128-Hz tuning fork), 10-g monofilament pressure sensation at the distal halluces, and ankle reflexes. Combinations of more than one test have >87% sensitivity for the detection of DPN. Loss of 10-g monofilament perception and reduced vibration perception provide good prediction for foot ulcers. The feet should be examined for ulcers, calluses and deformities, and footwear should be inspected. Different scoring systems have been developed for monitoring progression or response to intervention in clinical trials. As the definition of diabetic neuropathy is defined by “the presence of signs of peripheral nerve dysfunction in people with diabetes after the exclusion of other causes”, the diagnosis of DPN should involve the exclusion of other non-diabetic causes, which include chronic inflammatory demyelinating polyneuropathy (CIDP), B12 deficiency, hypothyroidism, and uremia. A combination of typical symptomatology and distal sensory loss with absent reflexes, or the signs in the absence of symptoms, is highly suggestive of DPN (Boulton et al., 2005).

Nerve conduction (NC) studies, which include motor nerve conduction, F response and sensory nerve conduction, can be used to quantify the degree of nerve injury in DPN. Though the electrodiagnostic studies are not required for the diagnosis of DPN, they are recommended to monitor disease progression in clinical research protocols. Abnormal nerve conduction velocities appears to be the first objective quantitative indication of the condition (Tesfaye et al., 2010). Table 1.2-2 lists the stages of DPN severity, using NC as a quantitative indicator (Dyck, 1988).

Table 1.2-2: Stages of severity of DPN.

Grade 0	No abnormality of NC, *e.g.*, Σ 5 NC normal deviates < 95th percentile or another suitable NC criterion.
Grade 1a	Abnormality of NC, *e.g.*, Σ 5 NC normal deviates ≥ 95th percentile without symptoms or signs.
Grade 1b	NC abnormality of stage 1a plus neurologic signs typical of DPN but without neuropathy symptoms.
Grade 2a	NC abnormality of stage 1a with or without signs (but if present, < 2b) and with typical neuropathic symptoms.
Grade 2b	NC abnormality of stage 1a, a moderate degree of weakness (*i.e.*, 50%) of ankle dorsiflexion with or without neuropathy symptoms.

(modified from Dyck, 1988)

Diabetic Autonomic Neuropathy

Diabetic autonomic neuropathy (DAN) is the other form of diffuse diabetic neuropathy, and it often accompanies DPN. DAN can impair any sympathetic or parasympathetic autonomic function, resulting in significant morbidity and mortality in patients with diabetes, in fact, the mortality rate in patients with DAN is twice of the rate in patients without DAN (Soedamah-Muthu et al., 2008). The clinical manifestations of DAN is listed in table 1.2-3, which mainly include resting tachycardia, exercise intolerance, orthostatic hypotension, constipation, gastroparesis, erectile dysfunction, sudomotor dysfunction, impaired neurovascular function and hypoglycemic autonomic failure (Boulton et al., 2005; Edwards et al., 2008). Many of the clinical symptoms of DAN are common and may be associated with causes other than diabetic neuropathy. Thus, a non-diabetes related etiology for the specific symptoms presented by a diabetic patient must be ruled out for the proper diagnosis and treatment of DAN.

Table 1.2-3: Clinical manifestation of diabetic autonomic neuropathy.

Cardiovascular -Resting tachycardia -Exercise intolerance -Orthostatic hypotension -Silent myocardial ischemia	**Sudomotor** -Anhidrosis -Heat intolerance -Gustatory sweating -Dry skin
Gastrointestinal -Esophageal dysmotility -Gastroparesis -Constipation -Diarrhea, fecal incontinence	**Genitourinary** -Neurogenic bladder -Erectile dysfunction -Retrograde ejaculation -Female sexual dysfunction
Pupillary -Decreased dark-adapted pupil diameter	

(modified from Boulton et al., 2005; Edwards et al., 2008)

Other Types of Neuropathies

A focal neuropathy reflects damage to single (mononeuropathy) or multiple peripheral nerves (mononeuropathy multiplex), cranial nerves, regions of the brachial or lumbosacral plexuses (plexopathy), or the nerve roots (radiculopathy). The occurrence of focal neuropathy is far less common than DPN and DAN, and it affects mostly older diabetic patients. Focal neuropathies may have a sudden onset and sometimes improve on their own within 6 to 8 weeks (Edwards et al., 2008).

Although poor glucose control is associated with an increased risk of neuropathy, intensive treatment of diabetes can also cause neuropathy. Treatment-induced neuropathy can occur after any quick establishment of glucose control, with insulin treatment being the most common trigger. It often presents as acute pain, and may have autonomic involvement, which can improve significantly with time (Gibbons and Freeman, 2010).

1.2.2. Animal Models of Diabetic Peripheral Neuropathy

Animal models provide a valuable resource to study the pathogenesis as well as potential treatment of diabetic peripheral neuropathy (DPN). There are a number of

rodent models available to study DPN in both type 1 and type 2 diabetes. Though in early studies of diabetes it was difficult to establish neuropathic changes in animal models, technical advances have enabled the identification of biochemical, electrophysiological, and morphological changes that contribute to the etiology of DPN and its progression. In rat models, DPN initially presents with an acute metabolic phase featuring nerve conduction velocity (NCV) slowing and hyperalgesia that are usually reversible. With increasing duration of diabetes, more severe functional abnormalities develop in concert with progressive structural changes in the nerve, which is less amenable to metabolic interventions.

Type 1 Diabetes Models

Streptozotocin (STZ), a glucosamine-nitrosourea compound that is particularly toxic to the insulin producing pancreatic β-cells, is widely used to induce type 1 diabetes in experimental animals. There are clear advantages to using STZ diabetic animal models, with its relative inexpensiveness and the availability of a considerable body of published data. To date, the STZ diabetic rat has been the most commonly used model to study DPN. Diabetes is induced by a single dose of 40-80 mg STZ/kg body weight through intraperitoneal (IP) or intravenous (IV) injection. Fasting plasma glucose is measured one week after injection, and diabetes is usually defined by blood glucose concentrations of 15 mM (270 mg/dL) or greater. Depending on the aspect of neuropathy under investigation, the duration of diabetes can be as little as 2-4 weeks for symptoms of allodynia and NCV slowing, while longer durations (at least 8-16 weeks) are required for the presentation of structural features of neuropathy.

STZ can also be used to induce diabetes in both inbred (C57/Bl6 and CD1) and outbred (Swiss Webster) mouse strains, administered either at a single high dose in the 150-200 mg/kg range, or at lower doses given over consecutive days such as 90+90, 85+70+55, or 100+40+40 mg/kg. Mouse models are limited in studies of neuropathy due to size constrains, which can preclude certain examination techniques. However, one advantage for phenotyping neuropathy in the mouse is that diabetes can be induced in a wide range of genetically modified strains to highlight specific pathogenic mechanisms and treatments. In these diabetic mice, NCV slowing, impaired responses to sensory stimuli, and intraepidermal nerve fiber (IENF) loss occur within 2-8weeks of diabetes, whereas distal nerve fiber loss, axonal atrophy and myelin thinning have been reported to occur after many months of diabetes (Biessels et al., 2014).

Genetic models of type 1 diabetes include the BB/Wor-rat, the non-obese diabetic (NOD) mouse and the Akita mouse. The diabetes prone BB/Wor rats, which lack T lymphocytes that express the RT6 alloantigen, spontaneously develop type 1 diabetes, whereas the diabetes resistant BB/Wor rats serve as controls (Nakhooda et al., 1978). These diabetic rats develop NCV deficits after 2 weeks of diabetes, and sural nerve fiber loss and structural pathology have been reported by 4 months. Though this model has a clear advantage for its close resemblance to human type 1 diabetes, extensive application of this model has been limited due to the high cost and maintenance need. There is currently little consistent information on the development of neuropathy in NOD and Akita mice, which also spontaneously develop type 1 diabetes. Similar to the BB/Wor rats, these mice are expensive to maintain since daily insulin supplementation are frequently required for survival (Biessels et al., 2014).

Type 2 Diabetes Models

Genetic rat models of impaired glucose tolerance and type 2 diabetes include the Zucker fatty (ZF) and Zucker Diabetic Fatty (ZDF) rat, which exhibit leptin receptor deficiency. Whereas the ZF rat harboring a missense mutation in the leptin receptor (Lepr) gene develops obesity without diabetes, the ZDF rat derived from the ZF strain exhibit obesity which progress to overt diabetes at 8-10 weeks of age. Increases in hyperinsulinemia and hyperlipidemia parallel the progression through pre-diabetes (ZF) to overt diabetes (ZDF) in these animals, with the appearance of hypertension later in the disease course. These animals develop neuropathic symptoms including NCV slowing, mechanical allodynia and IENF loss. Similar to genetic rat models of type 1 diabetes, the primary disadvantages of the ZDF rats are the high cost, the need for close attention and maintenance, and high mortality after 4-6 months of diabetes.

Mouse models for type 2 diabetes used in the study of DPN include the db/db mouse (lepr mutation) and the ob/ob mouse (leptin mutation). Both models develop diabetes at 4-6 weeks of age with concurrent onset of hyperinsulinmia and hyperlipidemia. NCV slowing and behavioral deficits are established with 4–8 weeks of diabetes, IENF loss and structural abnormalities of the sural nerve are also reported at late stages of the disease. Whereas both db/db and ob/ob mice are available on the C57 BKLS and Bl/6 J backgrounds and develop symptoms of type 2 diabetes similarly, there is growing recognition that the development of neuropathic symptoms might be background specific (Biessels et al., 2014).

In addition to the genetic models of type 2 diabetes, feeding a high fat diet (HFD) has also been used to induce a type 2 diabetes. Additional, a HFD can promote a pre-

diabetic state and metabolic syndromes that may contribute to DPN in the absence of overt diabetes due to insulin resistance and dyslipidemia. Rodents fed with a HFD have been reported to develop symptoms of neuropathy such as NCV deficits, altered response to sensory stimuli and IENF loss (Guilford et al., 2011; Xu et al., 2014).

1.2.3. Pathogenesis of Diabetic Peripheral Neuropathy

Despite the high prevalence of DPN in both type 1 and type 2 diabetic patients, the disease etiology remains largely unknown. Hyperglycemia, as the fundamental cause for diabetic mellitus, clearly plays a critical role in the pathogenesis of DPN. Various glucose-driven metabolic pathways, including the polyol pathway, formation of advanced glycation end-products (AGEs), abnormal activation of PKC isoforms, oxidative stress and mitochondrial dysfunction have all been shown to be involved in peripheral nerve dysfunction in diabetic patients. In addition, factors other than hyperglycemia also seem to be involved in the development of DPN, especially in type 2 diabetes, since tight glycemic control is more effective in risk reduction of DPN in patients with type 1 rather than type 2 diabetes. In this regard, recent findings suggest that obesity, hypertension, dyslipidemia, inflammation and insulin resistance contribute to DPN in type 2 diabetes to an equal, if not greater degree compared with hyperglycemia (Callaghan et al., 2012b).

The Polyol Pathway

The polyol pathway of glucose metabolism consists of two tandem reactions. First, aldose reductase (AR) utilizes NADPH to reduce glucose to sorbitol and $NADP^+$. Sorbitol dehydrogenase (SDH) then utilizes NAD^+ to oxidize sorbitol into fructose and NADH (Oates, 2008). Under diabetic conditions, the polyol pathway is activated by hyperglycemia primarily through mass action since glycolytic capacity is saturated. The

excess glucose is then available for shunting into the polyol pathway resulting in an increase in intracellular sorbitol. An increase in sorbitol contributes to a relative intracellular hypertonic state and a compensatory efflux of other osmolytes such as myo-inositol and taurine (Edwards et al., 2008). Though this increase in intracellular osmolarity has been proposed as one of the mechanisms involved in the pathogenesis of diabetic complications, this may not be the case for diabetic neuropathy (Oates, 2002; Oates, 2008), since sorbitol levels have been reported to be comparatively modest in diabetic nerves (Clements, 1986). Also, certain pharmacological agents robustly raise peripheral nerve sorbitol, fructose, and myo-inositol, yet do not cause detectable impairment of peripheral nerve function (Oates, 2002).

Ironically, evidence that AR plays a key pathogenic role in diabetic neuropathy has continued to mount. Diabetic mice overexpressing AR have accelerated nerve dysfunction and damage, which could be prevented by the treatment with the AR inhibitor WAY121-509 (Yagihashi et al., 2001). In contrast, AR-deficient mice exhibit strong protection of nerve function under diabetic conditions (Ho et al., 2006). Human diabetics with "high AR expression" alleles show a faster loss of maximum pupillary constriction velocity, an indicator of autonomic neuropathy, while those with "low AR expression" alleles have a slower loss in plantar heat sensitivity, an indicator of sensory neuropathy (Oates, 2008). This suggests that there must be other mechanisms linking the polyol pathway to the pathogenesis of diabetic neuropathy, and numerous studies suggest this alternative mechanism to be oxidative stress. The polyol pathway contributes to oxidative stress through the interdependence of many key biochemical pathways involved in glucose metabolism that form a network linked via the $NADPH/NADP^+$ and

NADH/NAD^+ cofactor systems (Oates, 2008). Increased flux through the polyol pathway consumes NADPH, which is needed for the regeneration of a major cellular antioxidant, reduced glutathione (GSH), thus weakening the cell's capacity to defend against oxidants. Chronic elevation of the NADH/NAD^+ ratio can lead to the synthesis of diacylglycerol (DAG), a well-known activator of PKC. PKC activation can increase superoxide production and oxidative stress via elevated NAD(P)H oxidase activity and mitochondrial metabolism. Furthermore, the polyol pathway generates fructose, a 10-times more potent glycation agent than glucose, contributing to the formation of advanced glycation end-products. Similar to PKC, AGE production can also generate oxidative stress through interacting with the receptor for AGEs (RAGE) (Obrosova, 2005).

The Advanced Glycation Endproducts Pathway

The formation of early glycation adducts and AGEs results from the non-enzymatic reactions of glucose, oxaldehydes and other saccharide derivatives with proteins, nucleotides and lipids. However, other reducing sugars such as fructose and fructose-3-phosphate, which are also formed under hyperglycemia conditions, undergo non-enzymatic glycation at a faster rate compared with glucose (Ahmed, 2005; Szwergold et al., 1990). Emerging data from animal and clinical studies suggest the role of AGEs in the pathogenesis of diabetic neuropathy. The accumulation of AGEs is considered detrimental mainly in two ways. Firstly, the glycation of proteins alters their function and cellular transport and causes abnormal interactions with other matrix proteins, eventually leading to functional and structural abnormalities in diabetic peripheral nerves. Secondly, accumulation of extracellular protein AGEs can activate RAGE (Ramasamy et al., 2007), which subsequently activates the transcription factor nuclear factor kappa B (NF-κB)

(Ramasamy et al., 2005) and induces oxidative stress through NAD(P)H oxidase activity (Vincent et al., 2007).

Evidence for accumulation of fructosyl-lysine and AGEs in peripheral nerve of STZ-diabetic rats has been provided using liquid chromatography with tandem MS detection (Karachalias et al., 2003). Furthermore, myelin components in the peripheral nervous system have been shown to be subject to non-enzymatic glycation in diabetic rodent studies (Vlassara et al., 1983). It has been suggested that AGE-modified peripheral nerve myelin is susceptible to phagocytosis by macrophages and that this stimulates macrophages to secrete proteases, which may contribute to demyelination in diabetic neuropathy (Vlassara et al., 1985). Also likely to undergo glycation during diabetes are major axonal cytoskeletal proteins such as tubulin, neurofilament, and actin, which are central to the maintenance of axonal function and structure (Cullum et al., 1991; Pekiner et al., 1993; Ryle et al., 1997; Williams et al., 1982). The glycation of these cytoskeletal proteins may alter the structural and functional properties of the axon, thereby leading to axonal atrophy and degeneration, as well as slowing axonal transport (Sugimoto et al., 2008). The ability of peripheral nerve to regenerate might also be impaired by glycation of extracellular matrix proteins. The glycation of two major components of basal lamina, collagen type IV and laminin, has been shown to reduce neurite outgrowth in dorsal root ganglion (DRG) neurons obtained from neonatal rats (Luo et al., 2002) and young adult mice (Ozturk et al., 2006). These data suggest that the accumulation of AGEs in peripheral nerves contributes to segmental demyelination, axonal degeneration, and diminished regeneration of neurons, which are important pathophysiological features of diabetic neuropathy.

RAGE, a multi-ligand member of the immunoglobulin superfamily of cell surface molecules (Stern et al., 2002), has also been implicated in the pathogenesis of diabetic neuropathy. Ligation of RAGE by its ligands can upregulate receptor expression and trigger a spiral of cellular perturbations due to sustained RAGE-mediated signaling (Stern et al., 2002). In support of this view, a dramatic and cumulative rise in RAGE mRNA and protein expression has been found in peripheral epidermal axons, sural axons, Schwann cells, and sensory neurons within DRG, which correlates with progressive electrophysiological and structural abnormalities in STZ-diabetic mice with neuropathy (Toth et al., 2008). The activation of RAGE can result in a burst of ROS, caspase-3 activation, and nuclear DNA degradation in the DRG neurons from embryonic rat. All of these abnormalities were prevented by treatment with the antioxidant α-lipoic acid (Vincent et al., 2007), suggesting a role for RAGE activation in the generation of oxidative stress. Human sural nerve biopsy studies have revealed the co-localization of RAGE ligands, RAGE and NF-κB in the perineurium, as well as in the endoneurial and epineurial vessels of patients with diabetic neuropathy (Haslbeck et al., 2007). A similar localization is also found in patients with IGT-related peripheral neuropathy (Haslbeck et al., 2005), implicating the involvement of AGE/RAGE/NF-κB signaling pathway in the etiology of DPN. This relationship is further consolidated by the recently generated $RAGE^{-/-}$ mice which displayed diminished upregulation of peripheral nerve NF-κB and NF-κB-dependent proinflammatory gene expression. The absence of NF-κB activation partially protected the mice from a diabetes-associated loss of pain perception (Bierhaus et al., 2004a). Curiously, the activation of RAGE also mediates neurite outgrowth and

cell survival through NF-κB (Huttunen et al., 2000), but whether this has any physiological significance for slowing the onset of DPN is unclear.

The Protein Kinase C Pathway

Protein kinase C (PKC) comprises a superfamily of isoenzymes that play a key role in many cellular functions, and is involved in numerous signal transduction pathways (Newton, 2003). Increased production of PKC, especially the PKCβ isoform, has been implicated in the pathogenesis of diabetic complications, as it is associated with overexpression of vascular endothelial growth factor (VEGF), plasminogen activator inhibitor-1 (PAI-1), NF-κB, and transforming growth factor-β (TGF-β) (Das Evcimen and King, 2007).

The activation of PKC in hyperglycemic or diabetic environment has been suggested to associate with elevated levels of the well-known PKC activator diacylglycerol (DAG). Chronic hyperglycemia leads to an increase in the glycolytic intermediate dihydroxyacetone phosphate, which when reduced to glycerol-3-phosphate, contributes to the enhanced *de novo* synthesis of DAG (Xia et al., 1994). An increase in NADH level due to activation of polyol synthesis also leads to DAG synthesis from dihydroxyacetone phosphate (Thomas et al., 1994). Steadily accumulating evidence has strongly linked retinal, renal, and cardiovascular complications of diabetes with elevations in DAG levels as well as an increase in both PKC activation and activity (Idris et al., 2001; Ways and Sheetz, 2000). However, the exact role of PKC activity in diabetic neuropathy is yet to be established. Despite the beneficial effects of various PKC inhibitors in ameliorating diabetes-induced deficits in the peripheral nerves (Cameron et al., 1999; Nakamura et al., 1999; Sasase et al., 2005), PKC activity has been reported to be decreased (Kim et al.,

1991), unchanged (Cameron et al., 1999), or increased (Kishi et al., 1999), with no consistent change in DAG levels (Ido et al., 1994) in diabetic rat nerve. Considering the role of PKC in altering vasoconstriction and capillary permeability, causing angiogenesis, basement membrane thickening, and endothelial proliferation, the contribution of this pathway to diabetic neuropathy is likely through its effects on vascular blood flow and microvascular disease rather than directly on neuronal cells. Other studies suggest that the deleterious role of PKC activation in the nerves might be isoform-specific: in diabetic rats, there is a trend towards decreased expression of PKCα, an isoform that is primarily expressed in the Schwann cells, and intensified expression of PKCβII, an isoform that localizes in the axons of nerve fibers, macrophages and the wall of endoneurial microvessels (Mizukami et al., 2011). Whereas increased PKCβII expression and activity is consistent with other diabetic complications, the unique decrease in PKCα level might be related to the decrease of Schwann cell proliferation under hyperglycemic conditions. Decreased proliferative potential of Schwann cells might be an underlying mechanism for the slowing of Schwann cell regeneration in glucose stressed cells, which likely contributes to segmental demyelination manifested in human diabetic neuropathy(Kamiya et al., 2003).

Oxidative Stress

Oxidative stress occurs in a cellular system when the production of free radicals exceeds the antioxidant capacity of the system. An imbalance between the production and neutralization of reactive oxygen species (ROS) is a well-recognized mechanism in the pathogenesis of diabetic neuropathy and may be a central biochemical mechanism in disease progression.

Several free radical species, including superoxide (O_2^-) and nitric oxide (NO), are produced in the body under normal conditions to perform specific functions. While the presence of these free radicals is essential for normal physiology, their overproduction during metabolic dysfunction leads to cellular injury. In addition to their distinct roles in inhibiting protein/enzyme activity, the combination of the relatively inert O_2^- and NO forms peroxynitrite, a highly reactive ROS which attacks proteins, DNA and lipids (Vincent et al., 2004b).

The presence of oxidative stress in diabetic peripheral nerves has been demonstrated by the identification of various biomarkers of ROS-induced injury, including accumulation of free lipid peroxidation products, increased GSSH/GSH ratio, GSH depletion, downregulated superoxide dismutase (SOD) activity, decreased catalase, decreased total quinone reductase activities, depletion of ascorbate and taurine, and an increase in the dehydroascorbate/ascorbate ratio (Cheng and Zochodne, 2003; Obrosova et al., 2001; Stevens et al., 2000). Accumulation of nitrotyrosine, which is the marker of peroxynitrite-induced protein nitration, has been documented in peripheral nerve, spinal cord, vasa nervorum and DRG in both type 1 and type 2 diabetes rodent models (Cheng and Zochodne, 2003; Drel et al., 2007; Obrosova et al., 2007a; Obrosova et al., 2005b; Vareniuk et al., 2007).

Oxidative stress can be deleterious in several ways and oxidative damage of DNA is known to promote apoptosis (Harrison et al., 2005). Lipid peroxides are the end products of lipid peroxidation that can be toxic to a cell and require removal by GSH (Mylonas and Kouretas, 1999). Lastly, accumulation of proteins that have undergone peroxidation or nitrosylation can overload the cell's ability to recycle them and induce cellular

dysfunction (Berlett and Stadtman, 1997). Combined with the efficacy of various antioxidants in improving NCV and ameliorating deficits in nerve blood flow (Obrosova et al., 2001; Stevens et al., 2000), these data clearly support a role of oxidative damage in the peripheral nerve as a major contributor to diabetic neuropathy.

The generation of oxidative stress not only causes damage to the cells through free radical attack, but also through induction of other cellular pathways. Poly(ADP-ribose) polymerase (PARP) is one of the downstream effectors of enhanced oxidative stress in diabetic neuropathy. The nuclear and mitochondrial poly(ADP-ribose) polymerases are closely associated with oxidative-nitrosative stress. Free radicals and peroxynitrite can induce DNA strand breakage, activating PARP, which in turn further intensifies oxidative stress (Obrosova et al., 2005a). Activated PARP cleaves NAD^+ to nicotinamide and ADP-ribose, which can ADP-ribosylate nuclear proteins and PARP itself. Formation of poly(ADP-ribosyl)ated protein polymers plays an important role in the pathogenesis of DPN (Jagtap and Szabo, 2005). For example, poly(ADP-ribosyl)ation of glyceraldehyde 3-phosphate dehydrogenase (GAPDH) diverts glycolytic flux towards the polyol pathway, contributing to diabetic complications (Obrosova et al., 2004). The PARP activation has been shown in the peripheral nerve, vasa nervorum, and DRG neuron of STZ diabetic rats (Li et al., 2004; Obrosova et al., 2007a; Obrosova et al., 2004), STZ-diabetic mice (Drel et al., 2007), ob/ob mice (Vareniuk et al., 2007), and HFD-fed mice (Obrosova et al., 2007b). Furthermore, activation of the PARP pathway depletes NAD^+, a factor for glycolysis and the tricarboxylic acid (TCA) cycle, which could ultimately lead to an energy failure in the cells (Obrosova et al., 2004). Also, PARP activation affects gene transcription mainly through NF-κB, which leads to increased expression of

inflammatory genes (Ha et al., 2002). In support of the important role of PARP, PARP-deficient mice were protected from both diabetes- and galactose-induced motor and sensory nerve conduction slowing and nerve energy failure. In addition, two structurally unrelated PARP inhibitors, 3-aminobenzamide and 1, 5-isoquinolinediol have been shown to reverse established nerve blood flow and conduction deficits and energy failure in STZ-induced diabetic rats (Obrosova et al., 2004).

Another pathway that is indicated as a downstream effector of oxidative stress is the activation of MAPK (Torres and Forman, 2003). High glucose has been shown to activate JNK and p38 MAPK in cultured adult DRG neurons, whereas oxidative stress has been shown to activate ERK and p38 MAPK and cause damage to the cells (Purves et al., 2001). In addition, ERK, p38 MAPK and JNK are found activated in DRG neurons of STZ-diabetic rats. JNK activation and increases in total levels of p38 and JNK are also observed in sural nerve of type 1 and 2 diabetes patients (Purves et al., 2001; Tomlinson and Gardiner, 2008). It is proposed that elevated MAPK activity in diabetic nerves is associated with increased neurofilament phosphorylation, which is a contributor to the distal sensory axonopathy in diabetes (Fernyhough et al., 1999). Furthermore, the potency of a p38 MAPK inhibitor to correct motor and sensory nerve conduction velocity (MNCV and SNCV) deficits in STZ-diabetic rats also implicates a role of MAPK activation in motor and sensory nerve dysfunction (Price et al., 2004).

Mitochondrial Dysfunction

As the most important organelle in controlling the bioenergetic status of cells, mitochondria have been shown to play a crucial role in the development of diabetic neuropathy (Sivitz and Yorek, 2010). Failure of the mitochondria to synthesize adequate

ATP for high energy requiring axonal functions such as excitation, axonal transport and growth cone motility is suggested to be one prime trigger of peripheral nerve degeneration.

In eukaryotes, mitochondrial oxidative phosphorylation is the major ATP synthetic pathway. Upon uptake into cells, glucose is metabolized through the TCA cycle, generating electron donors such as NADH and $FADH_2$. The electrons then travel through the electron transport chain (complex I-IV) located in the inner mitochondria membrane for the reduction of molecular oxygen (O_2) to water. While the majority of O_2 is reduced to water at complex IV, 1-4% of the O_2 is incompletely reduced to O_2^- mainly at complexes I and III. The O_2^- produced is trapped in the intermembrane space or matrix of the mitochondria as it cannot readily diffuse across mitochondrial membranes (Figueroa-Romero et al., 2008). The conversion of O_2^- to H_2O_2 by the mitochondrial isoform of the enzyme superoxide dismutase (SOD) facilitates the permeation of ROS across the mitochondrial membrane. H_2O_2 could then be reduced enzymatically to water and O_2 by other enzymes both inside and outside the mitochondria (Brownlee, 2005).

In normal cells, ROS accounts for a tiny proportion of the products of the electron transport chain, and can be scavenged efficiently by innate antioxidants. However, as proposed by Brownlee *et al.*, under diabetic conditions, high glucose in tissues susceptible to diabetic complications leads to an increased supply of NADH in the mitochondria, the subsequent increase in electron availability and/or saturation may cause enhanced production of superoxide radicals in the proximal part of the electron transport chain (Nishikawa et al., 2000a). Though this mechanism might be true in cultured endothelial cells where high glucose drives excessive electron donation to the electron

transport chain in mitochondria resulting in the hyperpolarization of mitochondrial inner membrane and elevated production of ROS (Nishikawa et al., 2000a; Nishikawa et al., 2000b), its validity remains unclear for sensory neurons. The work from many distinct research groups have shown depolarized mitochondrial inner membrane potential in adult sensory neurons from STZ-diabetic rats (Huang et al., 2003; Huang et al., 2005; Srinivasan et al., 2000), as well as high glucose-treated embryonic sensory neurons (Russell et al., 2002), which is contradictory to the mechanism proposed by Brownlee *et al*. (Brownlee, 2005). In cultured embryonic DRG neurons, high glucose treatment induced a rapid increase in mitochondrial membrane potential that peaked at 3h, followed by a subsequent decrease. After 24h of hyperglycemia, the mitochondrial membrane potential of hyperglycemically stressed neurons was lower than control neurons (Russell et al., 2002; Vincent et al., 2004a). Thus, one plausible illustration for the depolarization of mitochondrial membrane potential is that the DRG neurons might have undergone a state of hyperpolarization in membrane potential at the initial stage of diabetes, which initiates the serial oxidative damage, resulting in mitochondrial depolarization at later stages. Hence, as a contributor rather than a consequence of peripheral neuropathy, the mitochondrial hyperpolarization is beyond detection in animals that already have significant signs of diabetic neuropathy.

DRG neurons are uniquely susceptible to damage by hyperglycemia because they have long, mitochondria-rich axons that directly access the nerve blood supply (Leinninger et al., 2006b). Consequently, axonal mitochondrial are acutely exposed to the hyperglycemic environment in diabetic conditions, and as the sites of increased ROS production, are early targets of oxidative damage. In diabetic nerves, mitochondria appear

swollen, structurally disrupted or, in some cases, as an abundant population of smaller-than-normal organelles (Bach et al., 2005; Bach et al., 2003). It has also been shown that in cultured primary DRG neurons, high glucose treatment induced a rise in ROS production, and corresponding mitochondrial swelling, loss of mitochondrial membrane potential, depletion of ATP and apoptosis (Russell et al., 2002; Vincent et al., 2005).

Mitochondrial DNA (mtDNA), which encodes genes that are involved in local mitochondrial protein synthesis, is also susceptible to oxidative damage (Leinninger et al., 2006b). Increased ROS destabilizes mtDNA and prevents cAMP responsive element binding protein (CREB)-mediated transcription in mitochondria, thereby inhibiting production of proteins that are critical to mitochondrial function (Ryu et al., 2005). Many proteins involved in mitochondrial function, including complexes I-III, are exquisitely sensitive to ROS-induced inhibition of activity (Brown, 1999). In addition, oxidative stress has been implicated in the inhibition of mitochondrial import of preproteins (Wright et al., 2001), the presence of which are essential for normal mitochondrial function.

Other signaling pathways that result in localized mitochondrial destruction have also been proposed as underlying mechanisms for mitochondrial dysfunction in DPN. For example, in times of stress, ATP depletion stimulates dynamin-related protein 1 (Drp1) translocation from cytosol to the mitochondria to increase mitochondrial fission, presumably to increase mitochondrial number and distribute energy throughout the cell. Though increased fission might provide an immediate relief for the cellular energy crisis, long-term imbalance between mitochondrial fission and fusion leads to the production of small, damaged mitochondria (Arnoult et al., 2005). In this regard, increased levels of

Drp1 have been found in *in vitro* and *in vivo* models of diabetic neuropathy (Leinninger et al., 2006a). Through gene array and proteomic studies, reduced expression of oxidative phosphorylation genes have been found in type 2 diabetes (Mootha et al., 2003), decreased expression of the transcriptional regulator nuclear respiratory factor 1 (NRF-1) and peroxisome proliferator-activated receptor- γ coactivator 1α (PGC-1α) has also been observed in pre-diabetic and diabetic tissues (Patti et al., 2003). Some groups discovered significantly decreased phosphorylation of AMP-activated protein kinase (AMPK) and decreased expression of PGC-1α in DRG neurons from STZ-diabetic Swiss Webster mice (Chowdhury et al., 2011), suggesting the role of these upstream regulators of mitochondrial biogenesis in mitochondrial dysfunction and subsequent deficits in nerve function.

Impaired Neurotrophic Support

Neurotrophic/growth factors are essential for the growth and survival of neurons. A variety of neurotrophic and growth factors secreted by target tissues, Schwann cells, and neurons themselves support nerve regeneration after injury. Dysregulation of neurotrophic factors, including insulin, insulin-like growth factor (IGF), nerve growth factor (NGF) and neurotrophin 3 (NT-3), have been implicated to contribute to segmental demyelination, axon atrophy or loss, slowed NCV, and impaired retrograde transport in DPN (Apfel, 1999). In fact, the expression levels of multiple neurotrophins have been found to be decreased in diabetic animals. In addition, many of the neuronal abnormalities of DPN can be duplicated by genetic depletion of specific neurotrophins, their receptors or binding proteins, further consolidating an important role for

dysregulated neurotrophic support in the pathogenesis of DPN (Pittenger and Vinik, 2003).

The impact of neurotrophic factors is often selective. The relationship of different nerve fiber types, the modalities served, and the neurotrophins targeting them is illustrated in Figure 1.2-2 (Pittenger and Vinik, 2003). Neurotrophins exert their effects through binding to two classes of receptors: the trk family of receptor tyrosine kinases (trk A, trk B, trk C) and the low-affinity receptor p75. Functional binding of neurotrophins to trks largely mediates the signal transduction and biological functions of neurotrophins, including neuronal survival and differentiation, cytoskeletal changes, and synaptic plasticity. In contrast, p75 has been shown to act as a modifier for trks. It has also been shown that p75 is widely expressed in non-neuronal tissues, such as Schwann cells, where its expression increases following nerve injury. NGF activity is specifically associated with activation of p75 and/or trk A, with concomitant effects on small sensory and autonomic nerve fibers. In contrast, the activity of trk C mediated NT-3 signaling is essential for large nerve fiber function, whereas BDNF, NT-4 and NT-5 exert their effects on medium-sized fibers through trk B receptor (Glass and Yancopoulos, 1993).

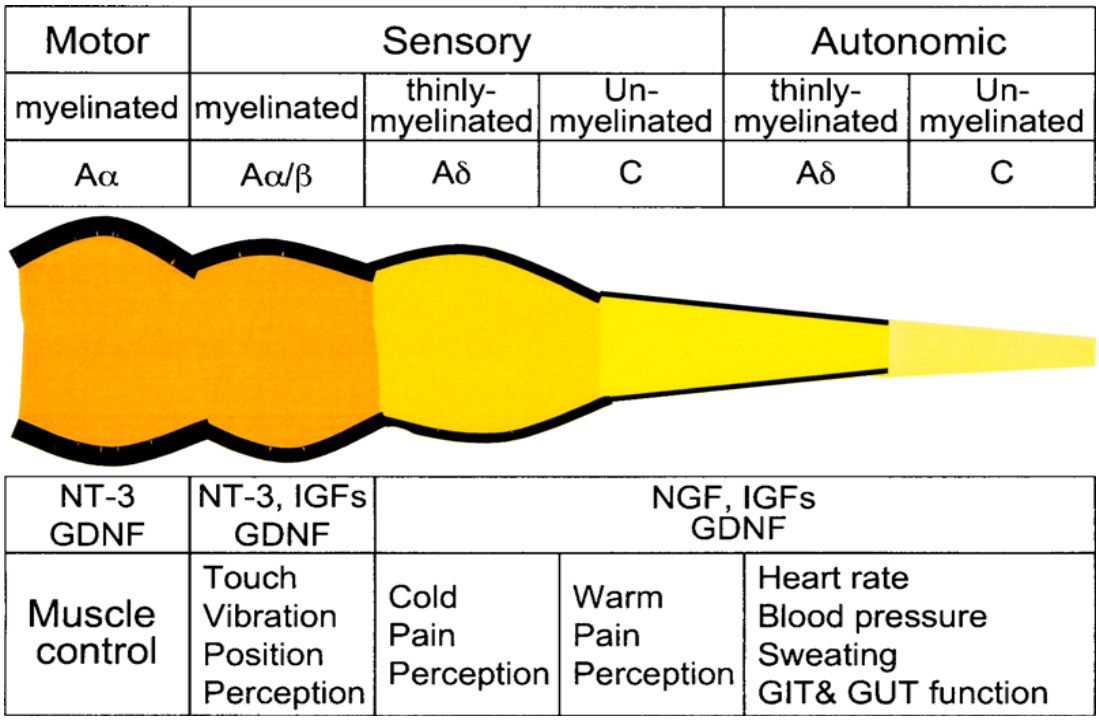

Figure 1.2-2: Schematic illustration of the peripheral nervous system, nerve fiber types, and the potential growth factors responsible for the integrity of the different fiber types.

A nerve fiber is a threadlike extension of a nerve cell and consists of an axon and myelin sheath (if present). In the peripheral nervous system, myelin is formed by Schwann cells, which can also make a thin covering for an axon without formation of myelin. There are three types of nerve fibers in a mixed nerve which include motor nerve fibers, sensory nerve fibers, and autonomic nerve fibers. Individual nerve fibers vary widely in diameter and also may be myelinated or unmyelinated, which enable them to carry out different functions: the Aα nerve fibers are large in diameter and involved in muscle control; the Aβ fibers mainly carry sensory information related to touch, pressure, vibration and joint position; the Aδ fibers carry information related to sharp pain, very light touch and cold sensation; and the unmyelinated C fibers are mainly involved in sensations of dull, aching, burning pain and temperature. *(adapted from Pittenger and Vinik, 2003)*

Nerve growth factor (NGF) is the most extensively investigated neurotrophin as a possible contributor to the development of DPN. Both sensory neurons and sympathetic neurons are dependent on NGF for development, maintenance and survival (Calcutt et al., 1990; Rich et al., 1987). NGF levels, as well as its retrograde transport which is required for its neurotrophic effects, have been shown diminished in multiple diabetic models (Hellweg et al., 1994). The reduced NGF levels in STZ-induced diabetic rats could be

restored by allogenic islet transplantation, implicating the effect of hyperglycemia and/or insulin deficiency on growth factor levels (Hellweg et al., 1991). The expression of the low-affinity receptor for NGF, p75, has also been found reduced in STZ-diabetic rats, leading to impaired NGF signaling in the neurons (Schmidt et al., 2000). Knockout of p75 was found to result in loss of small sensory ganglia, with decreased pain perception and cutaneous innervation. NGF treatment prevented diabetes-related reduction in pain sensation, as well as the levels of calcitonin gene related peptide (CGRP) and substance P (SP) in sensory ganglia of diabetic animals (Apfel et al., 1998; Diemel et al., 1994). Similar to NGF, the expression of IGF-I and II are also down-regulated under diabetic conditions and could be reversed by insulin treatment (Migdalis et al., 1995; Wuarin et al., 1994). Intrathecal delivery of low doses of insulin (at levels insufficient to reduce hyperglycemia) and IGF-I were associated with reversal of motor and sensory nerve conduction deficits in diabetic rats. In addition, insulin and IGF-I both reversed atrophy in myelinated sensory axons within the sural nerve (Brussee et al., 2004). Though NGF and IGF both yielded encouraging results in animal studies, only recombinant NGF has been tested in phase III clinical trials in humans, and it did not demonstrate major benefits.

Inflammation

Recent studies have shown that inflammation also plays a determinant role in the development of microvascular diabetic complications (Navarro and Mora, 2005). Higher levels of inflammatory agents, including C-reactive protein and TNF-α have been found in the blood of diabetic patients, which correlate with the incidence of neuropathy (Gonzalez-Clemente et al., 2005; Herder et al., 2009). Multiple glucose-driven pathways,

including AGE/RAGE, PKC, PARP and oxidative stress, have been shown to activate NF-κB and transcription of a series of inflammatory and immune mediators. Activated NF-κB has been identified in perineurium, epineurial vessels and endoneurium of sural nerve biopsies of diabetic patients (Bierhaus et al., 2004b). Secondary effectors of the NF-κB pathway, including inducible nitric oxide synthase (iNOS), cyclooxygenase-2 (COX-2), TNF-α, endothelin-1 and cell adhesion molecules, have been shown to be upregulated under diabetic conditions, which also contribute to the pathogenesis of DPN (Ha et al., 2002). In addition, enhanced NF-κB activation downregulates the NRF-2 pathway, thus indirectly weakens the antioxidant defense through suppressing the expression of antioxidant genes (Ganesh Yerra et al., 2013). The upregulated inflammatory response drives a feed-forward loop since enhanced NF-κB activity increases TNF-α and COX-2 production, which can stimulate ROS and prostaglandin E2 (PGE2) production and further activate NF-κB (Williams and Nadler, 2007). Chronic hyperglycemia-induced inflammation also affects peripheral nerve function through extensive infiltration of monocyte, macrophages and modest infiltration of granulocytes from the blood circulation (Wang et al., 2006). Cytokines induced by NF-κB activation in endothelial cells, Schwann cells and neurons leads to macrophage recruitment to the diabetic nerves, which results in damaged myelin sheath, increased nerve excitability, impaired nerve regeneration and the onset of DPN (Conti et al., 2002; Yamagishi et al., 2008).

Given the important role of neuroinflammation in the pathogenesis of DPN, it is not surprising that inhibition of NF-κB with an IκB protease inhibitor is effective at correcting nerve conduction and nerve blood flow deficits in STZ-induced diabetic rats

(Cameron and Cotter, 2008). The various downstream effectors of NF-κB have also been extensively studied in experimental diabetics. Chemical and genetic inhibition of COX-2 has shown effectiveness in preventing nerve conduction and endoneurial nutritive blood flow deficits, peripheral nerve oxidative damage and inflammation in diabetic animals (Kellogg et al., 2007; Pop-Busui et al., 2002). Blockade of receptors for endothelin-1, which is a powerful vasoconstrictor that is upregulated in diabetes, normalized nerve blood flow, motor and sensory NCV, and mechanical hyperalgesia in diabetic rats (Cameron and Cotter, 1996). 12/15-lipoxygenase (12/15-LO) is an important member of the lipoxygenase family that produces pro-inflammatory substances such as the hydroxyeicosatetraenoic acids (HETEs). In diabetic mice, 12/15-LO inhibition reversed motor and sensory NCV deficits and mechanical allodynia, but had no effects on thermal hypoalgesia. 12/15-LO$^{-/-}$ mice were more resistant to the development of DPN in both type 1 (STZ-induced) and type 2 (HFD-induced) diabetic models (Obrosova, 2009).

1.2.4. Current Therapeutic Strategies for Diabetic Peripheral Neuropathy

Treatment of DPN has been largely directed at control of symptoms rather than targeting the underlying pathogenic mechanisms with the exception of glycemic control. Despite increasing understanding towards the etiology of DPN, to date, tight and stable glycemic control remains to be the only proven effective pathogenic treatment for DPN. The DCCT and the Epidemiology of Diabetes Interventions and Complications (EDIC) follow-up study clearly demonstrate that intensive glycemic control implemented early in the course of diabetes effectively delays development of DPN in patients with type 1 diabetes (Albers et al., 2010; Wolffenbuttel, 1993). Compared with type 1 diabetes, the beneficial effects of glycemic control on DPN in patients with type 2 diabetes are less

definitive. In several randomized controlled trials of patients with type 2 diabetes, only a modest reduction in neuropathy was observed in patients receiving intensive glucose control (Callaghan et al., 2012a). Whereas some studies suggest that intensive glycemic control in type 2 diabetes patients is most beneficial if implemented early in the disease when patients have fewer microvascular complications (Ismail-Beigi et al., 2010; Ohkubo et al., 1995), other studies failed to confirm this finding (Azad et al., 1999). Interestingly, the Bypass Angioplasty Revascularization Intervention 2 Diabetes trial reported that specific glucose-lowering strategies and medications have different effects on DPN prevention in type 2 diabetes (Pop-Busui et al., 2013). In addition to tight glycemic control, diet and exercise lifestyle interventions, have also shown some promise in reversing neuropathic symptoms in patients with IGT (Smith et al., 2006) and type 2 diabetes (Kluding et al., 2012).

Attempts to treat DPN through targeting other proposed pathogenic mechanisms include aldose reductase inhibitors, antioxidants, recombinant nerve growth factor, and acetylcarnitine, all of which have shown efficacy in animal models but failed in clinical trials. Some mechanistic treatments are currently undergoing evaluation, the most promising one among which is the ROS scavenger α-lipoic acid. Several trials have associated α-lipoic acid with reduced neuropathic symptoms of DPN, although no significant differences were identified for primary end points, NCV results, or quantitative sensory testing (Ziegler et al., 2006; Ziegler et al., 2004). Other agents currently under investigation include C-peptide and Actovegin. Beneficial effects of C-peptide on measures of DPN in patients with type 1 diabetes have been reported by several small clinical studies. A Phase III clinical trial evaluating the effects of

PEGylated C-peptide in type 1 diabetes patients with mild to moderate DPN is ongoing (Ekberg et al., 2003; Ekberg et al., 2007). Actovegin is a deproteinized hemoderivative mixture of low molecular weight compounds produced from calf blood that is thought to stimulate oxygen utilization, cellular energy metabolism, glucose transport, and glucose oxidation. A randomized trial of patients with DPN in type 2 diabetes has shown that Actovegin improved neuropathic symptoms, vibration perception threshold, and sensory function (Ziegler et al., 2009), but it has not received broad medical acceptance.

One confounding factor in identifying effective treatments for DPN is that the contribution of various pathogenic pathways differs between individuals and does not occur with temporal and/or biochemical uniformity. Thus, before the identification of a uniform target in the disease pathogenesis, combinatorial therapies targeting multiple glucose-driven insults may be the best approach to control DPN in addition to good glycemic control. On the other hand, reinforcing endogenous cytoprotective mechanisms has appeared as an innovative strategy to help counteract glucotoxicity and manage DPN. Pharmacological modulation of heat shock proteins (HSPs) has shown great benefits in ameliorating peripheral nerve dysfunction, iENF loss and mitochondrial dysfunction in STZ-diabetic mice (Urban et al., 2010; Urban et al., 2012b).

1.3. Heat Shock Proteins

1.3.1. Overview of Heat Shock Proteins

The heat shock proteins (HSPs) were initially identified as gene products whose expression is induced by heat or other stresses. However, research over the past several decades has gradually revealed their roles as molecular chaperones which are involved in diverse cellular activities, even in unstressed cells. These HSPs, along with their close

relatives and molecular partners, play essential roles in protein folding, assembly, intracellular localization, secretion, regulation, and degradation. Dysregulation of these activities have been implicated in numerous human diseases (Feder and Hofmann, 1999; Thomas et al., 1995).

HSPs are among the most highly conserved proteins in existence, and function as heavy duty molecular machines that operate on a wide range of substrates found in all cellular compartments. Through interaction with other proteins, they minimize inappropriate protein interactions, and thus reduce the probability of protein aggregation. Though not all HSPs are stress-inducible, the stress-inducible HSPs respond to a wide variety of stresses, including temperature, cellular energy depletion, extreme concentrations of ions, osmolytes, gases, and various toxic substances. A common feature of these stresses is that they result in the accumulation of non-native proteins, which is consistent with the role of HSPs as molecular chaperones to help folding, unfolding or disposing denatured proteins. HSPs preferentially bind to proteins that are in their non-native conformations, either because the peptides have not yet been fully synthesized, folded, assembled, localized to the proper cellular compartment, or have undergone some level of protein-denaturation. HSPs normally function as complexes of several different chaperones, co-chaperones, and/or nucleotide exchange factors. Many chaperones are ATP-dependent, and utilize cycles of ATP binding and hydrolysis to assist the folding or unfolding of non-native polypeptides (Feder and Hofmann, 1999; Lindquist and Craig, 1988).

Heat Shock Response and the Heat Shock Factors

Cells respond to protein-denaturing stresses by induction of HSPs, and this process is termed as heat shock response (HSR). This response is universal, as it has been observed in organisms from eubacteria to archebacteria, from plants to mammals. Despite the existence of several mechanisms to regulate the abundance of cytosolic and nuclear chaperones, the induction of HSPs is largely mediated by transcription factors termed "heat shock factors" (HSFs). In response to various proteotoxic stresses, HSFs bind to a highly conserved short DNA sequence known as the heat shock element (HSE) to mediate the transcription of heat shock genes (Sorger, 1991).

Several members of the HSF family (*i.e.*, murine and human HSF1, 2, and 4 and a unique avian HSF3) have been identified (Pirkkala et al., 2001). HSF1 functions as the major transcription factor that can be activated by a diverse range of stresses in most vertebrates, whereas HSF3, has been shown to be a heat responsive transcription factor. In contrast, HSF2 is only activated under developmentally related stress conditions; and the most recently identified mammalian HSF, HSF4, is expressed in a tissue-specific manner and required for proper eye development (Anckar and Sistonen, 2007).

Although different HSFs play distinct biological roles, they share a highly conserved structure, with the N-terminal helix-turn-helix DNA binding domain (DBD) being the most conserved functional domain. HSFs bind to DNA as trimers, in which the concurrent binding of all DBDs to the pentameric nGAAn sequences (n denotes less strongly conserved nucleotides that nevertheless may be involved in important DNA-protein interactions) within the HSEs on the promoter region of HSP genes is required for stable binding (Sorger, 1991). A long, interrupted, hydrophobic repeat sequence (HR-A/B)

that is situated adjacent to the DBD is required for activation-induced trimerization of HSFs. In contrast, an additional hydrophobic repeat sequence (HR-C) which locates near the C-terminus of the protein has been suggested to negatively regulate HSF trimerization (Pirkkala et al., 2001; Voellmy and Boellmann, 2007). Human HSF4 lacks the HR-C, which explains its constitutive trimerization and DNA binding activity. The transactivation domain is positioned at the extreme C-terminus of most HSFs, and is responsible for the responsiveness to stress stimuli (Akerfelt et al., 2010).

In vertebrates, HSF1 has been identified as the HSF that mediates stress-induced heat shock gene expression in response to environmental, as well as physiological stressors. HSF1 mainly exists as transcriptionally inactive monomers in the nucleoplasm or the cytosol under normal growth conditions, and its activity is largely mediated post-translationally (Figure 1.3-1). One common feature of the diverse signals that regulate HSF1 activity is that it responds to the accumulation of non-native proteins. This has led to a widely accepted model in which the elevated level of mis-folded protein liberates HSF1 from HSPs to allow HSF1 to be converted into its active state. HSF1 interacts with multiple HSPs at different phases of its activation cycle, and Hsp90 is a key negative regulator of HSF1 activity. Reduced levels of Hsp90 have been demonstrated to induce HSF1 activation *in vitro*. Similarly, low levels of geldanamycin, which binds to the ATP-binding pocket of Hsp90 and specifically inhibits its activity, has been shown to activate HSF1 and induce the HSR *in vivo* (Zou et al., 1998). In contrast, Hsp70 and the co-chaperone Hsp40 (also known as DNAJB1) interacts with the activated HSF1 trimers, thereby suppressing its activity by inhibiting its transactivation capacity (Shi et al., 1998).

The activation-attenuation mechanism of HSF1 is multifaceted and also involves extensive post-translational modifications, including acetylation, phosphorylation and SUMOylation (Figure 1.3-1) (Akerfelt et al., 2010). HSF1 exists as a phosphoprotein even under unstressed conditions. As revealed by mass spectrometry and phosphopeptide mapping analysis, at least 12 serine residues are phosphorylated (Guettouche et al., 2005), among which stress-inducible phosphorylation of Ser230 and Ser326 in the regulatory domain contributes to the transactivation function of HSF1 (Guettouche et al., 2005; Holmberg et al., 2001). In addition, phosphorylation mediated SUMOylation on a single lysine residue in the regulatory domain occurs rapidly and transiently upon exposure to heat shock: phosphorylation of Ser303 is required for the conjugation of SUMO (small ubiquitin-like modifier) to Lys298 (Hietakangas et al., 2003). Though SUMOylation could positively modulate HSF1 activity under moderate stress conditions, the kinetics of phosphorylation-dependent SUMOylation of HSF1 correlates inversely with the severity of heat stress (Hietakangas et al., 2006). Thus, the mechanisms through which SUMO modification regulates the activity of HSF1, and the functional relationship between SUMOylation and other post-translational modifications of HSF1 are the subject of future studies.

In contrast to phosphorylation and SUMOylation of HSF1 which occur rapidly upon heat shock, acetylation is delayed and coincides with the attenuation phase of the HSF1 activation cycle. The acetylation of HSF1 is regulated by the balance between acetylation by p300-CBP (CREB-binding protein) and deacetylation by the NAD^+-dependent sirtuin, SIRT1. During the activation phase, SIRT1 maintains HSF1 in a state that is competent for DNA binding, whereas during the attenuation phase, the effect of p300-CBP overrides

and diminishes the DNA binding activity of HSF1. In accordance with this theory, increased expression and activity of SIRT1 has been found to enhance the DNA-binding activity of HSF1 at the human Hsp70.1 promoter. In contrast, downregulation of SIRT1 enhances the acetylation of HSF1 and attenuates its DNA-binding without affecting the formation of HSF1 trimers (Westerheide et al., 2009). The acetylation of HSF1, together with feedback regulation by increased levels of HSPs (*e.g.*, Hsp70-Hsp40 complex) mediates the attenuation phase of the HSF1 activation cycle and ensures proper functioning of HSF1.

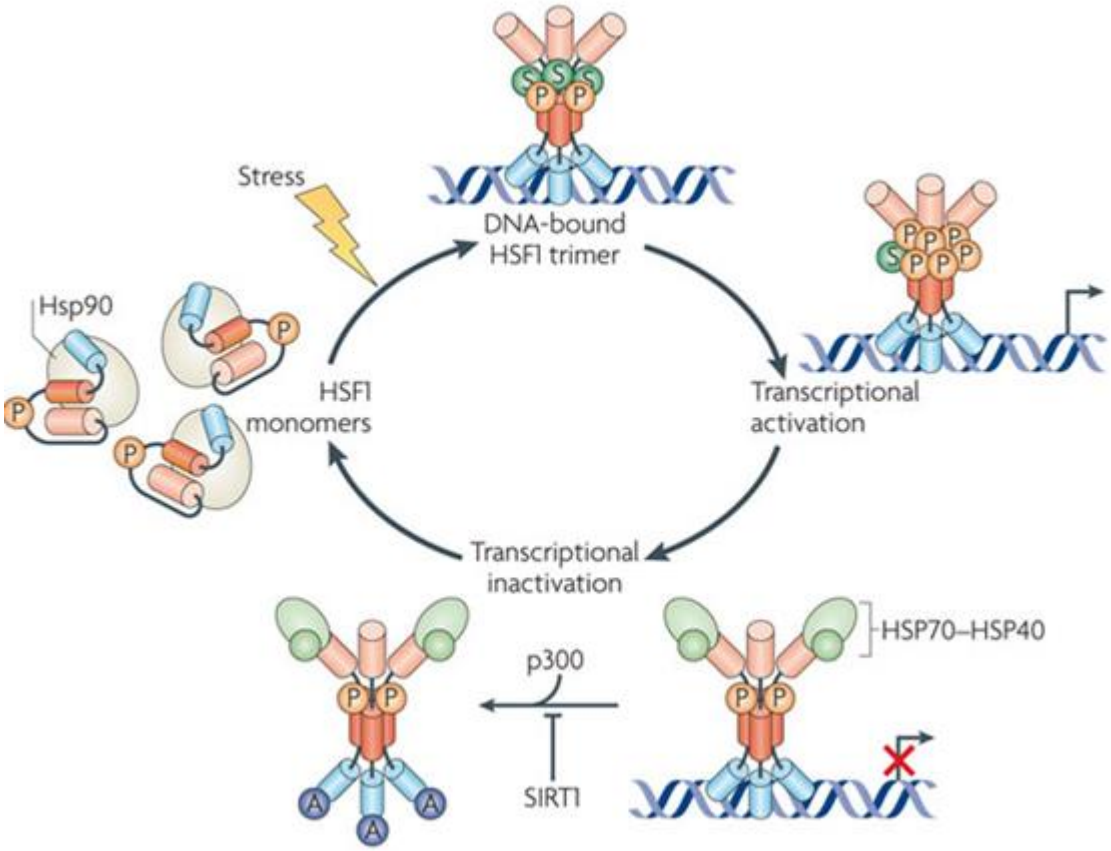

Figure 1.3-1: The activation cycle of HSF1.

In the resting state, HSF1 exists as a monomer and interacts with Hsp90 as a phosphoprotein. Upon cellular stresses, HSFl dissociates from Hsp90 and acquires DNA-binding activity through a monomer-to-trimer transition and binds to the HSE in HSP genes. Several posttranslational modifications, such as phosphorylation and SUMOylation, are involved in regulating the

transactivation capacity of HSF1. The transcriptional activity of HSF1 is abrogated during the attenuation phase, which involves two regulatory steps: negative feedback from the Hsp70-Hsp40 complex, which represses the transactivation activity of DNA-bound HSF1; and acetylation of Lys80 in the DBD of HSF1, which inhibits its DNA binding activity. The acetylation of HSF1 is mediated by p300–CBP, whereas the sirtuin SIRT1 negatively regulates the attenuation phase of the HSR by preventing HSF1 acetylation. *(adapted from Akerfelt et al., 2010)*

Classification of Heat Shock Proteins

HSPs can be assigned into different families on the basis of their molecular weights: Hsp110, Hsp100, Hsp90, Hsp70, Hsp60, Hsp40, Hsp10, and small HSP families. In eukaryotes, these families comprise multiple members that differ in inducibility, intracellular localization, and function. Among these HSP families, members of the Hsp70 and Hsp90 function as the main chaperones that determine the destiny of proteins and integrate signaling functions (Saibil, 2013).

a. Hsp70 Family

The Hsp70 family of proteins is the most abundant HSPs that exists as many paralogues in different cellular compartments. They are also highly conserved across species, demonstrating a 60–80% base identity among eukaryotic cells (Kregel, 2002). The human Hsp70 family comprises at least eight members that differ from each other by amino acid sequences, expression levels and sub-cellular localizations (Table 1.3-1) (Daugaard et al., 2007). Most Hsp70 family members reside in the cytosol and nucleus except for Hsp70-5 (also known as Bip, Grp78) and Hsp70-9 (also known as Grp75, mtHsp70, Mortalin) which are confined in the lumen of the ER and the matrix of the mitochondrial, respectively. These Hsp70 proteins share a highly conserved domain structure consisting of an ATPase domain, a middle region with protease sensitive sites, a substrate binding domain, and a C-terminal region containing an EEVD-motif enabling

the proteins to bind co-chaperones and other HSPs (Tavaria et al., 1996). The members that have special localizations also possess a signal sequence in their N-terminus, ensuring their translocation to the proper cellular compartments.

Table 1.3-1: The human HSP70 family.

Protein, Alternative Names	Gene Symbol	Cellular Localization	Stress-induced
Hsp70-1a, Hsp70, Hsp72, Hsp70-1	HSPA1A	Cytosol, Nucleus, Lysosomes	Yes
Hsp70-1b, Hsp70, Hsp72, Hsp70-1	HSPA1B	Cytosol, Nucleus, Lysosomes	Yes
Hsp70-1t, Hsp70-hom	HSPA1L	Cytosol, Nucleus	No
Hsp70-2, Hsp70-3, HspA2	HSPA2	Cytosol, Nucleus	No
Hsp70-5, Bip, Grp78	HSP70A5	ER	No
Hsp70-6, Hsp70B	HSP70A6	Cytosol, Nucleus	Yes
Hsc70, Hsp70-8, Hsp73	HSPA8	Cytosol, Nucleus	No
Hsp70-9, Grp75, mtHsp70, Mortalin	HSPA9	Mitochondria	No

(modified from Daugaard et al., 2007)

The Hsp70 proteins are associated with a wide variety of cellular activities. The Hsp70 system coordinates cellular functions by directing substrates for unfolding, disaggregation, refolding or degradation, and it is also an important component of the organelle translocation system. Monomeric Hsp70 recognizes short hydrophobic peptide segments such as those exposed in nascent polypeptide chains. The binding of a polypeptide chain to Hsp70 prevents mis-folding and aggregation and maintains the substrate in an unfolded state for its subsequent folding/refolding or translocation to a cellular compartment (Saibil, 2013). The nucleotide binding state of the ATPase domain determines the opening and closing of the substrate binding domain: ATP binding leads to substrate binding and ATP hydrolysis leads to substrate release. Two co-chaperones, Hsp40 and a nuclear exchange factor (NEF) (Hsp110 in eukaryotic cells), act together with Hsp70 to facilitate protein folding. Hsp40 serves as the primary substrate recruiter

and stimulates the Hsp70 ATPase activity, and the NEF opens up the nucleotide cleft for nucleotide exchange (Jiang et al., 2007; Polier et al., 2008).

Among the Hsp70 protein family, Hsp70-5 and Hsp70-9, facilitate chaperone-dependent transport and folding of proteins targeted for the ER and mitochondria, respectively. The rest of the Hsp70 proteins can be divided into constitutively present and stress-inducible forms, with the constitutive Hsp70s essential for basic housekeeping functions. The stress-inducible Hsp70-1 functions as the major chaperone that enables the cell to cope with aggregation of denatured proteins during and following cellular stress: mice lacking Hap70.1 and Hsp70.3 (the murine homologues of human Hsp70-1a and -1b) are more susceptible to stress, but develop normally under unstressed conditions (Hunt et al., 2004; Singleton and Wischmeyer, 2006). In contrast, knockout of Hsp70-2 in mice leads to developmental defects in spermatogenesis (Dix et al., 1996), and Hsc70 appears to be absolutely essential for cell viability (Florin et al., 2004).

b. Hsp90 Family

Hsp90 is another highly abundant molecular chaperone that accounts for 1–2% of cellular proteins under normal growth conditions. Unlike Hsp70 which is essential for nascent protein folding, most of the known substrates for eukaryotic cytosolic Hsp90 are signal transduction proteins, making it a cellular signaling hub for many pathways (Xu and Lindquist, 1993). At a molecular level, Hsp90 binds to substrate proteins that are in a near native state and acts at a late stage of folding through maturation and conformational maintenance of its client proteins. The Hsp90 family comprises mainly the cytosolic Hsp90 (termed variously Hsp90α and β in humans), the ER-specific Grp94, and Hsp75/TRAP1 which localizes in the mitochondrial matrix (Young et al., 2001). Hsp90

exists constitutively as homodimers and consists of an N-terminal domain that serves as the binding site for ATP, a middle segment that is essential for client protein binding, and a C-terminal homodimerization domain (Saibil, 2013). Hsp90 also dimerizes transiently through its N-terminal ATPase domain upon ATP binding. This enables the ATP-bound Hsp90 to bind stably with substrate polypeptides while hydrolysis of ATP releases the substrate by opening up the Hsp90 dimer (Young et al., 2001).

The activity of Hsp90 is modulated by a variety of co-chaperone proteins, most of which interact via a tetratricopeptide repeat (TPR) motif with the C-terminal EEVD motif of Hsp90. These co-chaperones, together with Hsp90 and Hsp70, arrange into a functional multi-chaperone complex that plays an essential role in cellular proteome maintenance *in vivo*. For example, Hsp70-Hsp90 Organizing Protein (HOP) is a multi-TPR domain containing protein that recruits Hsp70 to Hsp90, thus creating a complex for substrate handover (Chen and Smith, 1998). On the other hand, C terminus of Hsc70-Interacting Protein (CHIP) is a single TPR domain-containing co-chaperone that links Hsp90 to the ubiquitination apparatus, thereby controlling protein degradation through the proteasome (Connell et al., 2001).

Though Hsp90 displays substrate specificity during normal cell developmental processes, under stress conditions such as heat shock, Hsp90 contributes more generally to the refolding of denatured proteins (Nathan et al., 1997). The exact structural features recognized by Hsp90 are yet to be established, however, denatured proteins do seem to share a similar character with signaling proteins as they all possess some degree of structural flexibility, either intrinsically or induced by stress (Young et al., 2001). Thus,

interactions of substrate proteins with Hsp90 likely arise from structural properties at the molecular level rather than via a specific biological function.

1.3.2. Heat Shock Proteins in Diabetic Peripheral Neuropathy

The profound role of HSPs in cellular protection and recovery has led to the idea of treating protein mis-folding diseases through chaperone induction. In diabetes, chronic hyperglycemia imposes glucotoxicity and causes changes in metabolic fluxes that are metabolically stressful and ultimately detrimental to cells. Although the progression of DPN seems unrelated to the accumulation of any one specific mis-folded or aggregated protein, hyperglycemia can increase oxidative modification of amino acids, which can lead to damaged protein structure, impaired protein folding, decreased refolding of damaged proteins and increased protein aggregation. In this regard, it has been reported that proteins associated with mitochondrial dysfunction, oxidative phosphorylation, ubiquinone biosynthesis, and the citric acid cycle were downregulated in the DRG of 22-week-old STZ-diabetic rats, corresponding to the development of mitochondrial dysfunction (Akude et al., 2011). In the well-characterized leptin receptor deficient (db/db) mice, oxidative stress induces carbonylation and misfolding of sciatic nerve/myelin proteins, which may have important implications in deficits of myelin integrity and nerve conduction in peripheral neuropathies (Hamilton et al., 2013).

Many pathological states, including diabetes, neurodegenerative diseases and the aging process, are characterized by dysregulation of the HSR, which has a pathogenic role in either initiating or worsening the diseases. Thus, the vulnerability of postmitotic neurons to stress-induced protein denaturation might be associated with decreased expression of molecular chaperones in diabetic tissues. Indeed, 10-month of diabetes

markedly reduced Hsp70 levels in DRG from the spontaneously diabetic BB/Worcester rats, a model of type 1 diabetes (Kamiya et al., 2006). In contrast, 4-month of diabetes increased Hsp27 and Hsp70 in DRG of BB/Worcester rats (Kamiya et al., 2005). It is conceivable that chaperone expression varies as degeneration of peripheral nerves progresses. Whereas the level of endogenous chaperones may be sufficient to counter early glycemic insults, increased chaperone expression may represent a cytoprotective response as the disease progresses. However, this response may be eventually overwhelmed by the excessive metabolic disturbances associated with chronic hyperglycemia.

Studies of the role of HSPs in the pathogenesis and treatment of metabolic diseases have been ongoing for decades. It has been reported that the expression of Hsp72 was decreased in both type 1 and type 2 diabetes patients (Bruce et al., 2003; Strokov et al., 2000). This may contribute to diabetes since glucose metabolism could be improved by Hsp72 restoration through overexpression of the protein, administration of pharmacological inducers or long-term mild hyperthermia (Kondo et al., 2011). In a clinical study using α-lipoic acid for the treatment and prevention of diabetic polyneuropathy, it has been shown that induction of Hsp72 seem to be essential for the effectiveness of α-lipoic acid treatment in reversing clinical and electrophysiological manifestations of DPN (Strokov et al., 2000). The important role for Hsp72 in neuroprotection is also implicated in a study where the degree of protection provided by a pre-conditioning stress closely correlated with the amount of Hsp72 it induced in the DRG neurons (Amin et al., 1995). That being said, reinforcing the HSR in sensory neurons seems to be a probable approach for the management of DPN.

1.3.3. Inhibiting Hsp90 as a Novel Therapeutic Strategy against Diabetic Peripheral Neuropathy

The most widely characterized pharmacological inducer of the HSR are Hsp90 inhibitors. In unstressed cells, the activity of HSF-1 is under tight negative regulation by the Hsp90 and release of HSF-1 represents a crucial step in its activation during stress conditions. As many of the Hsp90 client proteins are involved in signal transduction pathways associated with cellular growth, differentiation and survival, inhibition of Hsp90 was initially investigated for treatment of cancer (Peterson and Blagg, 2009). The best characterized Hsp90 inhibitors, geldanamycin (GDA) and its derivative 17-allylamino-17-demethoxygeldanamycin (17-AAG), function through competitive interaction with the N-terminal ATP-binding site of Hsp90, and thus disrupt the ATP-dependent interaction of Hsp90 with its client proteins (Roe et al., 1999). One important aspect of these N-terminal Hsp90 inhibitors in cancer therapy is that they preferentially inhibit Hsp90 and induce client protein degradation in malignant versus normal cells (Luo et al., 2008). The selectivity of Hsp90 inhibition in malignant cells is likely conferred by the enhanced expression of Hsp90 in malignant tumor cells to accommodate their high metabolic requirements (Chiosis et al., 2003). However, the application of these Hsp90 inhibitors in cancer treatment has been hampered as induction of client protein degradation and cytotoxicity can occur at drug concentrations that also induce the cytoprotective HSR. In this regard, N-terminal Hsp90 inhibitors have been shown to decrease τ protein aggregation in Alzheimer's disease models (Dickey et al., 2007) and improve motor function in spinal and bulbar muscular atrophy (Waza et al., 2005). Thereby, the existing problem is how to dissociate the cytotoxic and cytoprotective

effects of Hsp90 inhibition, enabling Hsp90 inhibitors to be used as both chemotherapeutic and neuroprotective agents.

The 12-kDa C-terminal domain of Hsp90 is responsible for its homodimerization, as well as coordinating interactions with Hsp90 partner proteins. The C-terminal domain also contains a putative nucleotide-binding site, which facilitates nucleotide exchange at the N-terminus (Soti et al., 2003). Thus, targeting the C-terminus of Hsp90 seems to be another feasible strategy for the inhibition of Hsp90 activity. Indeed, coumarin antibiotics such as novobiocin and chlorobiocin, disrupt Hsp90 function through binding to the C-terminal region of the protein (Marcu et al., 2000). However, as with the N-terminal Hsp90 inhibitors, novobiocin also promotes client protein degradation and induces a HSR at similar drug concentrations. Thus, systematic modification of novobiocin was undertaken to identify structure-activity relationships that yield high-affinity C-terminal analogues that could diverge client protein degradation from Hsp70 induction. As a result, KU-32 (N-(Farmer et al., 2012b 5R)-3, 4-dihydroxy-5-methoxy-6, 6-dimethyl-tetrahydro-2H-pyran-2-yloxy]-8-methyl-2-oxo-2H-chromen-3-yl) acetamide) was identified as a lead compound that exhibits at least a 500-fold divergence of client protein degradation from induction of Hsp70 (Figure 1.3-2) (Urban et al., 2010). This divergence provides an excellent therapeutic window for treating neurodegenerative disease without inducing cytotoxicity. In support of its cytoprotective property, KU-32 has been shown to protect against neuronal death induced by amyloid β-peptide and glucotoxicity (Ansar et al., 2007; Kusuma et al., 2012). Moreover, weekly administration of 20mg/kg KU-32 to STZ-diabetic mice reversed multiple clinical indices of DPN, including mechanical and thermal hypoalgesia and deficits in motor and sensory NCV. Further supporting an

essential role of Hsp70 in neuroprotection, mice with genetic ablation of the stress-inducible Hsp70 (Hsp70.1 and Hsp70.3) failed to respond to KU-32 despite the development of similar diabetes-associated neuronal deficits as compared to wild type (WT) mice. Of note, the neuroprotective effects of KU-32 in WT diabetic mice are not accompanied by significant alternation of metabolic parameters, despite the apparent effects on increasing insulin secretion and survival of isolated human pancreatic islets (Farmer et al., 2012a). *In vitro* assessments of primary sensory neurons indicate that KU-32 protects unmyelinated and myelinated neuronal cultures against DPN-associated neuropathic changes. To be more specific, KU-32 dose-dependently prevented neuregulin-1 (NRG1)-induced myelin degeneration in myelinated sensory neuron/Schwann cell co-cultures in an Hsp70-dependent manner, indicating a chaperone-mediated intervention of aberrant growth factor signaling (Li et al., 2012; Urban et al., 2010). In addition, KU-32 has been shown to decrease mitochondrial superoxide levels and significantly enhance respiratory activity in hyperglycemically stressed rat embryonic sensory neurons, which correlated with increased translation of Mn superoxide dismutase (MnSOD) and several cytosolic and mitochondrial chaperones (Zhang et al., 2012).

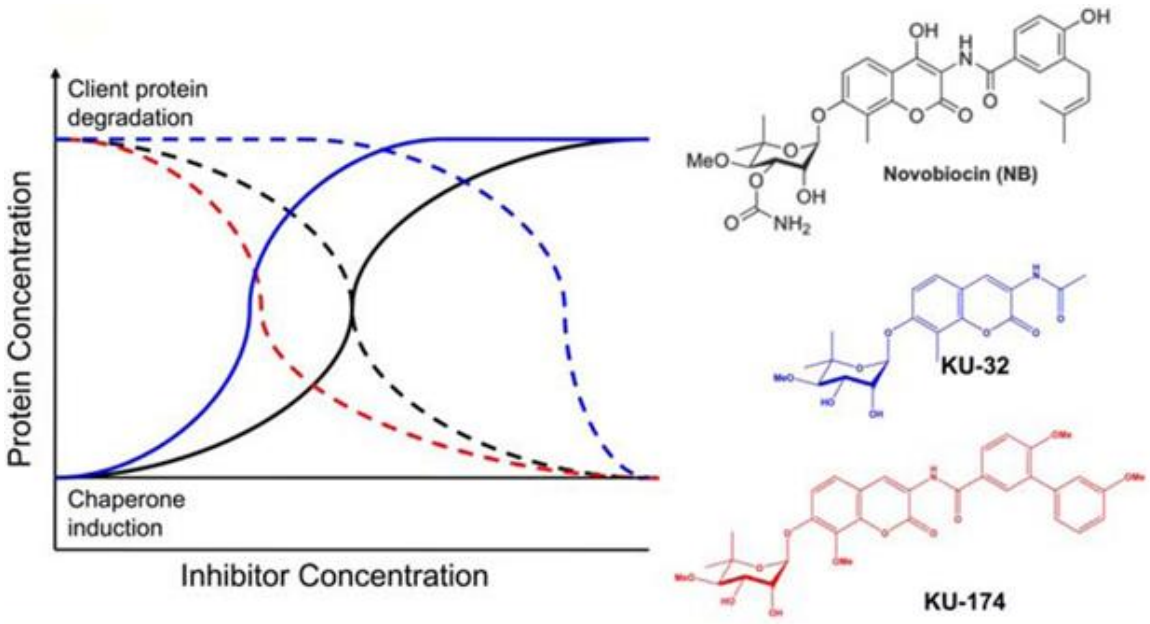

Figure 1.3-2: Structure-activity relationships of novobiocin analogs.

Structure of novobiocin analogues and the schematic representation of dose effects in client protein degradation (dotted lines) and chaperone induction (solid lines) for novobiocin (black), KU-32 (blue) and KU-174 (red). *(adapted from Urban et al., 2010)*

As discussed previously, mitochondrial dysfunction plays an essential role in the pathogenesis of DPN. Although the mechanisms underlying the protective effect of KU-32 in antagonizing the proneuropathic action of the established biochemical mediators of DPN remains unclear, induction of Hsp70 improves mitochondrial function in the sensory neurons of diabetic mice (Urban et al., 2012b). Several lines of evidence have implicated a role for Hsp70 in the maintenance of multiple aspects of mitochondrial function. For example, the cytosolic Hsp70 plays an important role in the biogenesis as well as the proper translocation of mitochondrial protein into the mitochondrial matrix through the outer mitochondrial membrane import receptor, Tom70 (Stuart et al., 1994; Young et al., 2003). Likewise, induction of Hsp70 is essential to maintain normal mitochondrial function under stress conditions. In this regard, overexpression of Hsp70 in

astrocytes increased mitochondrial function and decreased neuronal injury after basal forebrain ischemia (Xu et al., 2010). Additionally, upregulation of Hsp70 protected against ischemia-reperfusion injury in heart tissue through improving mitochondrial function (Jayakumar et al., 2001). Consistent with this theory, KU-32 has been shown to decrease mitochondrial superoxide levels and improve mitochondrial bioenergetics (mtBE) in hyperglycemically stressed primary neurons (Zhang et al., 2012). Thus, in the current study, we sought to determine whether the effect of KU-32 to correct the clinical deficits associated with DPN relied on an improvement in mtBE in sensory neurons. Also, using animal models of both type 1 and type 2 diabetes, we sought to determine whether deficits in mtBE show a similar relationship to the temporal onset of sensory hypoalgesia in models of type 1 and type 2 diabetes and ascertain if KU-32 improves mtBE and reverses DPN in an Hsp70-dependent manner.

Chapter 2: Heat Shock Protein 70 is Necessary to Improve Mitochondrial Bioenergetics and Reverse Diabetic Sensory Neuropathy Following KU-32 Therapy

Portions of this chapter are directly exerted from the following publication:

Ma J, Farmer KL, Pan P, Urban MJ, Zhao H, Blagg BS, et al. Heat shock protein 70 is necessary to improve mitochondrial bioenergetics and reverse diabetic sensory neuropathy following KU-32 therapy. The Journal of pharmacology and experimental therapeutics 2014; 348: 281-92.

Abstract

Impaired neuronal mitochondrial bioenergetics contributes to the pathophysiologic progression of diabetic peripheral neuropathy (DPN) and may be a focal point for disease management. We have demonstrated that modulating Hsp90 and Hsp70 with the small-molecule drug KU-32 ameliorates psychosensory, electrophysiologic, morphologic, and bioenergetic deficits of DPN in animal models of type 1 diabetes. The current study used mouse models of type 1 and type 2 diabetes to determine the relationship of changes in sensory neuron mitochondrial bioenergetics to the onset of and recovery from DPN. The onset of DPN showed a tight temporal correlation with a decrease in mitochondrial bioenergetics in a genetic model of type 2 diabetes. In contrast, sensory hypoalgesia developed 10 weeks before the occurrence of significant declines in sensory neuron mitochondrial bioenergetics in the type 1 model. KU-32 therapy improved mitochondrial bioenergetics in both the type 1 and type 2 models, and this tightly correlated with a decrease in DPN. Mechanistically, improved mitochondrial function following KU-32 therapy required Hsp70, since the drug was ineffective in diabetic Hsp70 knockout mice. Our data indicate that changes in mitochondrial bioenergetics may rapidly contribute to

nerve dysfunction in type 2 diabetes, but not type 1 diabetes, and that modulating Hsp70 offers an effective approach toward correcting sensory neuron bioenergetic deficits and DPN in both type 1 and type 2 diabetes.

2.1. Introduction

Diabetic peripheral neuropathy (DPN) is experienced by a majority of patients with type 1 or type 2 diabetes (Callaghan et al., 2012a). The development of DPN is associated with a small-fiber neuropathy resulting from dysfunction of unmyelinated or thinly myelinated sensory fibers and the gradual degeneration of larger myelinated fibers. Although numerous pathologic mechanisms contribute to DPN (Urban et al., 2010), altered mitochondrial bioenergetics (mtBE) may be a central facilitator in its development (Fernyhough et al., 2010). For example, mitochondrial function is impaired in adult sensory neurons or dorsal root ganglia isolated from diabetic rats (Akude et al., 2011; Chowdhury et al., 2010; Huang et al., 2003). Additionally, in-depth bioenergetic analysis of adult sensory neurons isolated from models of type 1 diabetic mice (Urban et al., 2012b) or rats (Chowdhury et al., 2012) found substantive decreases in mtBE. However, since the etiologic development of DPN in type 1 and type 2 diabetes does not necessarily share identical mechanisms, it is unclear whether deficits in mtBE may have a kinetically similar relationship to the onset of sensory hypoalgesia that is symptomatic of DPN. Moreover, the efficacy of interventional therapies is also not identical in patients with type 1 versus type 2 diabetes. For example, tight control of blood glucose more effectively ameliorates DPN in patients with type 1 diabetes (Callaghan et al., 2012a). Similarly, enalapril improved nerve blood flow and electrophysiology in a type 1 diabetic rat model (Coppey et al., 2006), but had modest effects in diabetic Zucker fatty rats, a

type 2 model (Oltman et al., 2008). These results underscore that an effective therapy for DPN should be equally efficacious regardless of the underlying diabetic phenotype. To this end, we have been exploring the potential of pharmacologically manipulating molecular chaperones for treating DPN.

Hsp90 and Hsp70 are molecular chaperones that are critical for folding nascent proteins into their biologically active conformations (Evans et al., 2010). Hsp90 contains N- and C-terminal ATP-binding domains and has intrinsic ATPase activity. Because pharmacologic agents that inhibit the N- or C-terminal ATPase activity can prevent protein folding, inhibiting Hsp90 is an attractive target for treating malignancies, as many oncoproteins require Hsp90 for proper folding (Peterson and Blagg, 2009). However, Hsp90 also binds the transcription factor, heat shock factor 1. Upon exposure to Hsp90 inhibitors, heat shock factor 1 dissociates from Hsp90, translocates to the nucleus, and upregulates a heat shock response that promotes synthesis of cytoprotective antioxidant genes and chaperones, such as Hsp70. This response can antagonize the desired goal of cytotoxicity in treating cancers. On the other hand, inducing the heat shock response can increase molecular chaperones and decrease misfolded protein aggregates. Thus, stimulating this aspect of Hsp90 biology may have utility for treating neurodegenerative diseases (Morimoto, 2011; Zhao et al., 2012). However, developing an effective Hsp90 inhibitor for treating neurodegeneration requires establishing a therapeutic window that leads to upregulation of cytoprotective chaperones, such as Hsp70, in the absence of client protein degradation that can antagonize the protective heat shock response.

Novobiocin is the prototypic ligand that binds to the C-terminal site of Hsp90, and systematic modification of novobiocin identified KU-32 (Figure 2.1-1A) as a

neuroprotective lead compound that exhibits a 500-fold divergence of Hsp70 induction from client protein degradation (Urban et al., 2010). This divergence provides an excellent therapeutic window to promote neuroprotection in the absence of toxicity; weekly administration of KU-32 reversed psychosensory, electrophysiologic, bioenergetic, and morphologic indices of DPN in diabetic mice (Urban et al., 2012a; Urban et al., 2010). Mechanistically, KU-32 binds Hsp90 directly (Matts et al., 2011), but the drug's neuroprotective efficacy depends upon the downstream action of Hsp70 (Li et al., 2012; Urban et al., 2010).

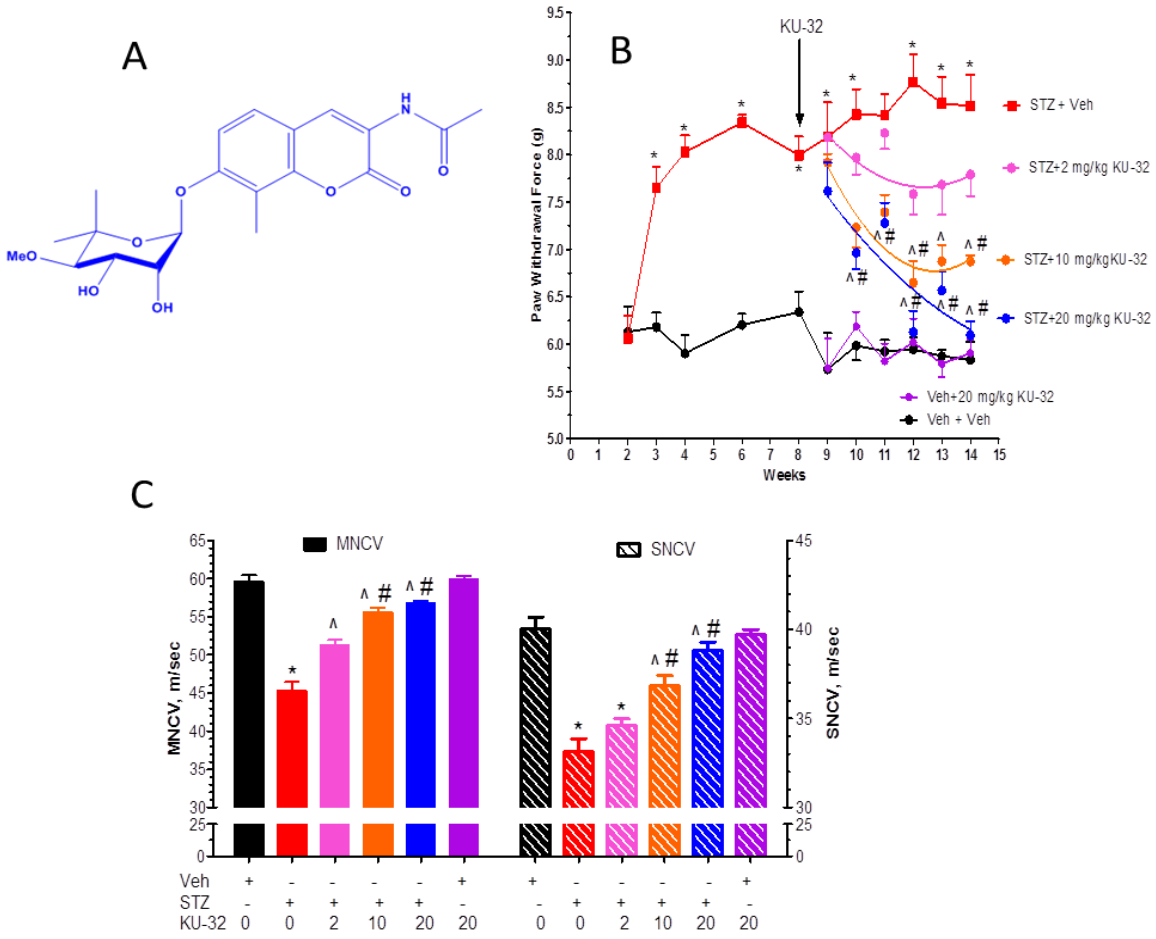

Figure 2.1-1: Dose response of KU-32 in improving mechanical hypoalgesia and NCV deficits in diabetic Swiss Webster mice.

(A) Structure of KU-32. (B) Swiss Webster mice were rendered diabetic with STZ and mechanical sensitivity was assessed at the indicated weeks. After 8 weeks of diabetes, mice were treated once per week with 2, 10, or 20 mg/kg KU-32 for 6 weeks and mechanical sensitivity measured weekly. One group of nondiabetic mice was treated with only 20 mg/kg KU-32 as a control. *P < 0.05 versus time-matched vehicle (Veh) + Veh; ^P < 0.05 versus time-matched STZ + Veh; #P < 0.05 versus time-matched STZ+ 2 mg/kg KU-32. (C) Effect of 6 weeks of KU-32 therapy on MNCV and SNCV. *P < 0.05 versus Veh + Veh; ^P < 0.05 versus STZ + Veh; #P < 0.05 versus STZ + 2 mg/kg KU-32.

The current study sought to determine whether deficits in mtBE in models of type 1 and type 2 diabetes show a similar relationship to the temporal onset of sensory hypoalgesia and ascertain if KU-32 improves mtBE and reverses DPN in an Hsp70-dependent manner. Our results indicate that the development of a sensory hypoalgesia preceded substantial changes in mtBE in type 1 diabetic mice. In contrast, the onset of mitochondrial dysfunction and sensory hypoalgesia were tightly correlated in type 2 diabetic mice. KU-32 improved the bioenergetic profile of sensory neurons in an Hsp70-dependent manner and effectively reversed insensate DPN in both diabetic models. These data provide novel insight into the role of mitochondrial dysfunction in the onset of insensate DPN and indicate that Hsp70 can have beneficial effects on mtBE.

2.2. Materials and Methods

Streptozotocin (STZ), carbonylcyanide-4-(trifluoromethoxy)-phenylhydrazone (FCCP), oligomycin, rotenone, antimycin A, Percoll, and poly(DL)ornithine were obtained from Sigma-Aldrich (St. Louis, MO). KU-32, [N-(7-((2R,3R,4S,5R)-3,4-dihydroxy-5-methoxy-6,6-dimethyl-tetrahydro-2H-pyran-2-yloxy)-8-methyl-2-oxo-2H-chromen-3-yl)acetamide] and trideutero KU-32 were synthesized and structural purity (>95%) verified as described previously (Huang and Blagg, 2007). Collagenase and laminin were purchased from Gibco/Invitrogen (Carlsbad, CA).

Animals

Male and female wild-type (WT) C57Bl/6 and Hsp70.1/70.3 double knockout (KO) mice on a C57Bl/6 background (Hsp70 KO) were used in the study and obtained from in-house breeding colonies (Urban et al., 2010). Male Swiss Webster mice were purchased from Harlan Laboratories (Indianapolis, IN). As a model of type 1 diabetes, 8-week-old

male and female mice were fasted for 6 hours and rendered diabetic with an intraperitoneal injection of STZ (100 mg/kg) given on two consecutive days. One week after the second injection, mice were fasted as above, blood was obtained from the tail vein, and animals with fasting blood glucose (FBG) ≥ 290 mg/dl (16 mM) were deemed diabetic.

To model type 2 diabetes, heterozygous BKS.Cg-Dock7m$^{+/+}$ Lepr^{db}/J mice were acquired from The Jackson Laboratory (Bar Harbor, ME) to generate animals homozygous (Lepr$^{db/db}$) for the lepr mutation. Heterozygous (Lepr$^{db/+}$) mice served as controls. At ~4–6 weeks of age, the Lepr$^{db/db}$ mice became identifiably obese and exhibited elevated FBG compared with their heterozygous littermates. Similar numbers of male and female animals between the genotypes were enrolled in the study when they were 8 weeks old.

All animals were maintained on a 12-hour light/dark cycle with ad libitum access to water and Purina 5001 rodent chow. Preliminary dose-response studies indicated that after 8 weeks of diabetes, once a week dosing of 20 mg/kg KU-32 administered intraperitoneally in 0.2 ml of 0.1 M Captisol (β-cyclodextrin sulfobutylethers; CyDex Pharmaceuticals, Lenexa, KS) gave maximal recovery of mechanical hypoalgesia (Figure 2.1-1B) and nerve conduction velocity deficits (Figure 2.1-1C). All subsequent studies were performed using a once per week 20 mg/kg dosing of the drug. At the termination of each study and prior to sacrifice of the animals, FBG and hemoglobin A1c levels (A1c Now+) were determined. All animal procedures were performed in accordance with protocols approved by the Institutional Animal Care and Use Committee and in

compliance with standards and regulations for the care and use of laboratory rodents set by the National Institutes of Health.

Psychosensory and Electrophysiologic Analyses

Mechanical sensitivity was assessed in $Lepr^{db/db}$ mice using a nylon Semmes-Weinstein von Frey monofilament (Stoelting, Wood Dale, IL). The filament that possesses a buckling force of 1.4g was applied to the plantar surface of the right and left hind paw. A positive response was recorded after lifting or flinching of the animal's paw. This procedure consisted of six trials, which alternated between right and left hind paws. The percent response was obtained by determining the number of withdrawals in response to 12 separate monofilament applications (Jack et al., 2011). Alternatively, mechanical sensitivity was assessed in the type 1 animal models using a Dynamic Plantar Aesthesiometer (Stoelting Inc.) fitted with a stiff monofilament that was applied to the plantar surface at an upward force of 10g in the Swiss Webster mice or 8g for the C57Bl/6 and Hsp70 KO mice. Thermal sensitivity was assessed by paw withdrawal latency to a ramping, focal heat using a Hargreaves Analgesiometer (Stoelting Inc.) (Urban et al., 2010). Responses from each animal were measured four times on alternate feet and averaged. Sensory assessments were performed once a week at approximately the same time of day. In animals treated with KU-32, sensory measures were taken 1 week after drug administration. At select time points, animals were anesthetized prior to measuring motor and sensory nerve conduction velocities (MNCV and SNCV, respectively) as previously described (McGuire et al., 2009). Animals were then euthanized prior to tissue collection.

Isolation of Adult Sensory Neurons

Adult sensory neurons were isolated from L_4–L_6 dorsal root ganglia (DRG) of three to five mice per treatment with minor modifications (Delree et al., 1989; Urban et al., 2012b). After removing connective tissue and trimming, the cleaned ganglia were maintained in 1 ml of serum-free Ham's F10 medium at 37°C and dissociated with 1 ml of 1.25% collagenase for 45 minutes, followed by a secondary digestion with 1 ml of 2% trypsin for 30 minutes. Cells were isolated by centrifugation at 1000 × g for 5 minutes, and the pellet was further dissociated by triturating in F10 medium with a fire-polished glass pipette. The cell suspension was layered on a 10-ml gradient of sterile iso-osmotic Percoll and centrifuged at 800g for 20 minutes. The cell pellet was resuspended in fresh F10 medium, passed through a 40-μm nylon mesh (Mt. Baker Bio, Everett, WA), and the filter washed with 5 ml of serum-free medium. The cells in the filtrate were recovered by centrifugation and resuspended in maintenance medium: Ham's F10 medium (6.1 mM glucose) containing 50 ng/ml nerve growth factor and 1 ng/ml neurotrophin 3 and N2 supplement without insulin (Invitrogen, Carlsbad, CA). Neurons were plated onto poly(DL)ornithine (0.5 mg/ml overnight)/laminin (2 mg/ml for 3 hours)–coated 96-well plates at 5000–8000 cells per well. Neurons from control and diabetic animals were incubated in maintenance medium for 1 day prior to use in the bioenergetic analysis on day 2 in vitro.

Mitochondrial Bioenergetic Assessment

Oxygen consumption rate (OCR) was assessed in intact lumbar DRG sensory neurons using an XF96 Extracellular Flux Analyzer (Seahorse Biosciences, North Billerica, MA). The maintenance medium was changed 1 hour before starting the assay to

unbuffered Dulbecco's modified Eagle's medium supplemented with 1 mM pyruvate and 5.5 mM D-glucose and the cells incubated at 37 ℃. The plate was introduced into the XF96 analyzer, a 3-minute mix cycle used to oxygenate the medium, and respiration was assessed in a 4-minute measurement cycle. As a general description of a mitochondrial stress assay, the initial rates provide a measure of the basal OCR prior to assessing mitochondrial dysfunction using respiratory chain poisons (Brand and Nicholls, 2011). The portion of basal OCR that is coupled to ATP synthesis was estimated by the decrease in OCR following addition of the ATP synthase inhibitor, oligomycin (1 μg/ml). The residual OCR that persists after oligomycin treatment is from uncoupled respiration (proton leak). Next, maximal respiratory capacity (MRC) was assessed following dissipation of the proton gradient across the inner mitochondrial membrane with the protonophore FCCP (1 μM). Non-mitochondrial respiration was then assessed by coinjection of 1 μM rotenone or rotenone + 1 μM antimycin A.

After the respiratory measures, the cells were harvested and OCR values were normalized to the total protein content of each well. ATP-linked respiration, proton leak, maximal respiratory capacity, spare respiratory capacity, and respiratory control ratio were determined as described previously (Brand and Nicholls, 2011; Chowdhury et al., 2012).

In Vivo Pharmacokinetics

Mice were fasted for 4 hours and Captisol or 20 mg/kg KU-32 given via oral gavage. After 1 hour, food was given ad libitum, the animals sacrificed at the indicated time, and lumbar dorsal root ganglia, sciatic nerve, and plantar foot pads harvested and rapidly frozen on dry ice. Tissues were minced, homogenized in water by sonication (25 mg/g

water), and spiked with 50 ng/ml trideutero KU-32 as the internal standard. The homogenate was extracted with 1 ml of t-butyl methyl ether and centrifuged. An aliquot (0.95 ml) of the supernatant was recovered and evaporated to dryness, and the resulting residue was resuspended in 0.05 ml of 20% CH_3CN. After a second centrifugation, 0.045 ml was transferred to autosampler vials. Chromatographic separation was performed using a 5-micron Agilent Zorbax SB C18 column (2.1 × 50 mm; Santa Clara, CA) and a linear gradient of CH3CN:H2O:formic acid (5:95:0.1) to CH3CN:H2O:formic acid (95:5.0:0.1) at a flow rate of 0.30 ml/min. The effluent was introduced to a Sciex API3200 Linear Ion Trap detector (Framingham, MA) using turbo ion spray in the positive ion mode. Linear calibration curves were constructed in each tissue matrix over a range of 0–1000 ng/ml, and analyte recoveries ranged from 65% to 75%.

Mitochondrial Copy Number

Real-time polymerase chain reaction (PCR) was used to measure mitochondrial copy number using primers for murine cytochrome b, cytochrome c oxidase subunit II (COII, mitochondrial genes), and β-actin (nuclear gene) (Santos et al., 2011). Forward and reverse primer sequences for mouse cytochrome b were 5'-GCAACCTTGACCCGATTCTTCGC-3' and 5'-TGAACGATTGCTAGGGCCGCG-3'. Forward and reverse primer sequences for mouse COII were 5'-ATTGCCCTCCCCT-CTCTACGCA-3' and 5'-CGTAGCTTCAG-TATCATTGGTGCCC-3'. PCR was performed using 25–50 ng of genomic DNA, 200 nM concentration of each primer, and the SYBR Green PCR master mix from Applied Biosystems (Grand Island, NY). Products were amplified following DNA denaturation at 95 ℃ for 5 minutes followed by 35 cycles at 95 ℃ for 15s, 62 ℃ for 30s, 72 ℃ for 30s, and a final extension at 72 ℃ for 5

minutes. Melting curve analysis and gel electrophoresis verified the specific amplification of the expected product. Differences in gene expression were determined after normalization to β-actin using the ΔΔC(T) method.

Statistical Analysis

Student's t tests, one-way analysis of variance (ANOVA), and repeated measures one-way ANOVA were applied for between-group comparisons. Post hoc analyses were conducted using Tukey's test, and nonparametric data were analyzed with a Kruskal-Wallis and Dunn's test. All data are presented as mean ± S.E.M.

2.3. Results

2.3.1. KU-32 Reverses DPN in Lepr$^{db/db}$ Mice

Beginning at 8 weeks of age, FBG, body weight, and psychosensory measures were assessed weekly in the Lepr$^{db/db}$ and Lepr^{db+} mice. Each genotype was subdivided into two groups at 10 weeks of age and given a weekly injection of KU-32 or Captisol for up to 8 weeks (Figure 2.3-1A). After 4 weeks of drug therapy, a subgroup of the KU-32-treated Lepr$^{db/db}$ mice was administered Captisol for the final 4 weeks to investigate the effects of drug withdrawal. To examine the effect of diabetes and drug treatment on mitochondrial bioenergetic (mtBE), sensory neurons were isolated from five mice prior to drug treatment and at 4 and 8 weeks after administering KU-32.

Consistent with the onset of type 2 diabetes, the Lepr$^{db/db}$ mice showed significant increases in total body weight and FBG and at 18 weeks of age had elevated glycated hemoglobin levels compared with aged-matched Lepr$^{db/+}$ mice (Table 2.3-1). However, treatment with KU-32 did not affect any of these parameters in either genotype, nor did it

improve glucose disposal following a 3-hour glucose tolerance test (6-hour fast and 0.5-g glucose given intraperitoneally; data not shown).

By 8 weeks of age, the $Lepr^{db/db}$ mice showed a significantly lower percent withdrawal response to a von Frey hair indicative of a mechanical hypoalgesia (Figure 2.3-1B). In agreement with a prior study (Wright et al., 2007), the $Lepr^{db/db}$ mice did not develop a thermal hypoalgesia (Table 2.3-1) and did not show a significant decrease in intra-epidermal nerve fiber density in the foot pad at 18 weeks of age (data not shown). Weekly administration of KU-32 significantly improved mechanical sensitivity in the $Lepr^{db/db}$ mice, but had no effect on the $Lepr^{db/+}$ mice. MNCV and SNCV decreased significantly in the untreated 18-week-old $Lepr^{db/db}$ mice, and KU-32 therapy improved these electrophysiologic deficits (Figure 2.3-1C).

After 4 weeks of KU-32 therapy, drug withdrawal led to a gradual redevelopment of the mechanical hypoalgesia. In contrast, MNCV and SNCV rates remained similar to those observed in the $Lepr^{db/db}$ mice that received the drug continuously. Although the reason for this distinction is unclear, it is not related to differences in the rate of drug clearance since pharmacokinetic analysis showed that KU-32 is rapidly distributed to and quickly cleared from dorsal root ganglia, sciatic nerve, and plantar foot pads, with a half-life of 1.5–2 hours (Figure 2.3-1D).

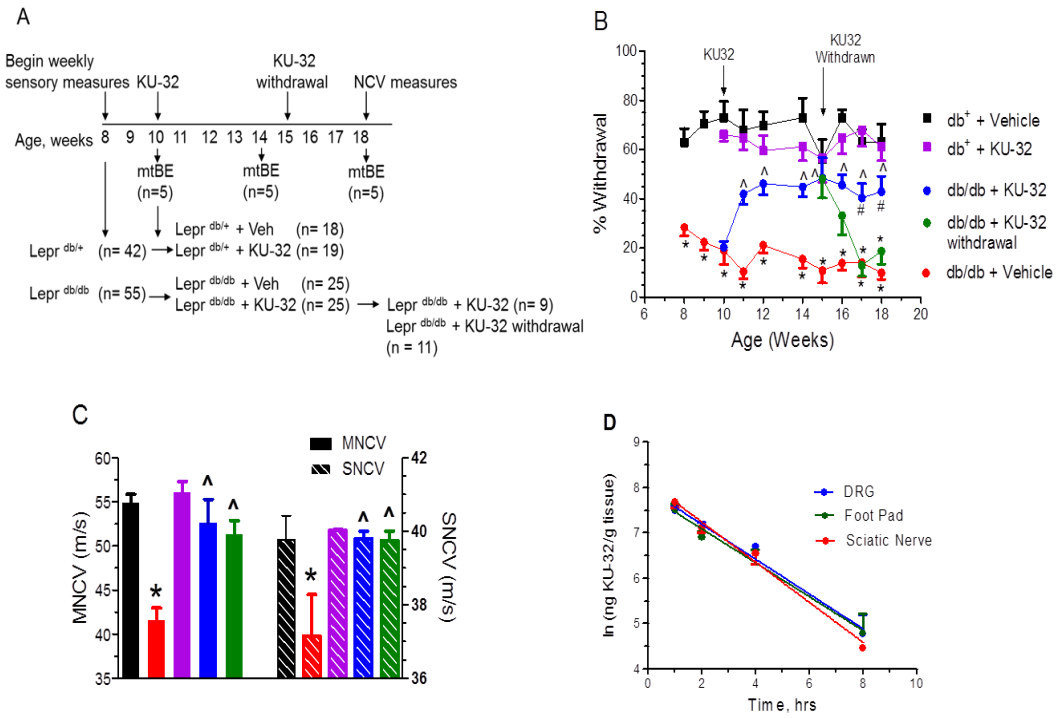

Figure 2.3-1: KU-32 improves mechanical hypoalgesia and NCV deficits in Lepr$^{db/db}$ mice.

(A) Scheme of the study design using the Lepr$^{db/db}$ and Lepr$^{db/+}$ mice. (B) Mechanical hypoalgesia was assessed in the Lepr$^{db/db}$ and Lepr$^{db/+}$ mice at the indicated age and weekly KU-32 therapy initiated at 10 weeks of age. KU-32 was then withdrawn in a subgroup of these mice after 4 weeks of treatment. *, $p < 0.05$ versus time-matched Lepr$^{db/+}$ + vehicle (Veh); ^, $p < 0.05$ versus Lepr$^{db/db}$ + Veh; # =, $p < 0.05$ versus Lepr$^{db/db}$ + KU-32 withdrawal. (C) The effect of genotype and treatments on MNCV (solid bars) and SNCV (striped bars) at 18 weeks. Group colors are the same as indicated in (B). *, $p < 0.05$ versus time-matched Lepr$^{db/+}$; ^, $p < 0.05$ versus Lepr$^{db/db}$ + Veh. (D) Pharmacokinetic analysis of KU-32 uptake in DRG, sciatic nerve, and foot pad.

Table 2.3-1: Weight, FBG, HbA1c, and thermal latencies of Lepr$^{db/+}$ and Lepr$^{db/db}$ mice.

Week	Group	Weight g	*n*	FBG mg/dl	*n*	HbA1c %(mmol/mol)[a]	Latency[b] sec	*n*
10	*db*$^+$ + Veh	24.8 ± 1.2	5	135 ± 45	5	—	3.5 ± 0.8	5
	db$^+$ + KU-32	24.0 ± 2.1	5	144 ± 14	5	—	4.9 ± 1.4	5
	db/*db* + Veh	46.6 ± 2.7*	5	317 ± 108*	12	—	4.3 ± 0.3	7
	db/*db* + KU-32	42.1 ± 4.0*	10	357 ± 111*	23	—	4.3 ± 0.6	15
12	*db*$^+$ + Veh	25.0 ± 3.6	20	124 ± 17	5	—	4.5 ± 1.3	5
	db$^+$ + KU-32	26.1 ± 3.4	22	129 ± 20	5	—	4.4 ± 0.8	5
	db/*db* + Veh	46.5 ± 5.3*	18	478 ± 98*	18	—	4.9 ± 0.7	7
	db/*db* + KU-32	45.7 ± 4.0*	37	475 ± 102*	37	—	4.2 ± 0.7	15
14	*db*$^+$ + Veh	25.8 ± 3.6	20	130 ± 21	10	—	4.5 ± 0.9	5
	db$^+$ + KU-32	26.8 ± 3.4	22	118 ± 36	9	—	4.8 ± 0.9	5
	db/*db* + Veh	48.7 ± 5.6*	18	496 ± 70*	18	—	5.2 ± 0.9	7
	db/*db* + KU-32	48.4 ± 4.8*	37	518 ± 89*	37	—	4.4 ± 0.9	15
16	*db*$^+$ + Veh	27.8 ± 4.7	10	139 ± 26	5	—	5 ± 0.7	5
	db$^+$ + KU-32	26.8 ± 3.0	8	144 ± 29	5	—	5.2 ± 1.4	5
	db/*db* + Veh	49.1 ± 5.0*	10	533 ± 61*	13	—	4.9 ± 0.9	7
	db/*db* + KU-32	49.4 ± 6.5*	12	506 ± 103*	13	—	4.9 ± 0.9	8
	db/*db* + KU-32 withdrawal	50.6 ± 7.0*	11	501 ± 73*	16	—	5.5 ± 1.0	7
18	*db*$^+$ + Veh	28.0 ± 5.0	10	122 ± 17	5	4.3 ± 0.1 (23 ± 1.1)	5.2 ± 0.6	5
	db$^+$ + KU-32	26.9 ± 3.6	8	137 ± 33	5	4.4 ± 0.1 (24 ± 1.1)	4.8 ± 0.2	5
	db/*db* + Veh	48.8 ± 5.8*	10	499 ± 78*	10	10.8 ± 0.5* (95 ± 5.6)	4.9 ± 0.7	6
	db/*db* + KU-32	50.1 ± 8.2*	12	504 ± 90*	12	10.3 ± 0.4* (89 ± 4.6)	5.5 ± 1.3	8
	db/*db* + KU-32 withdrawal	51.4 ± 8.4*	11	495 ± 54*	11	10.5 ± 0.4* (91 ± 4.2)	5.4 ± 0.6	7

Veh, vehicle.

[a] mmol of HbA1c/mol of hemoglobin.

[b] Paw withdrawal latency to thermal stimuli.

* $p < 0.05$ versus db$^+$ + Veh.

2.3.2. Diabetes-Induced Hypoalgesia Coincides with Decreased Mitochondrial Function in Lepr$^{db/db}$ Mice

The L_4–L_6 lumbar ganglia provide the cell bodies for the motor and sensory fibers that are affected in DPN and whose physiology was improved by KU-32. To determine whether the improvement in psychosensory function and NCV was associated with a change in mtBE, sensory neurons were isolated from these ganglia at 6, 8, 10, 14, and 18 weeks of age. The neurons were cultured in vitro for 2 days and the OCR was determined for 2 hours in the intact cells (Zhang et al., 2012).

At 6 weeks of age, Lepr$^{db/db}$ mice showed a modest decline in maximal respiratory capacity and spare respiratory capacity (SRC), but these parameters were significantly decreased by 8 weeks (Figure 2.3-2A) and 10 weeks (Figure 2.3-2B) of age. To gain broader insight into the effect of diabetes on cellular respiration, the ATP-linked OCR, proton leak, SRC, and nonmitochondrial OCR were expressed as a percent of the MRC (Figure 2.3-2B). At 10 weeks of age, Lepr$^{db/db}$ showed a significant decrease in SRC and an increase in proton leak, ATP-linked OCR, and nonmitochondrial respiration, consistent with an overall alteration in mtBE.

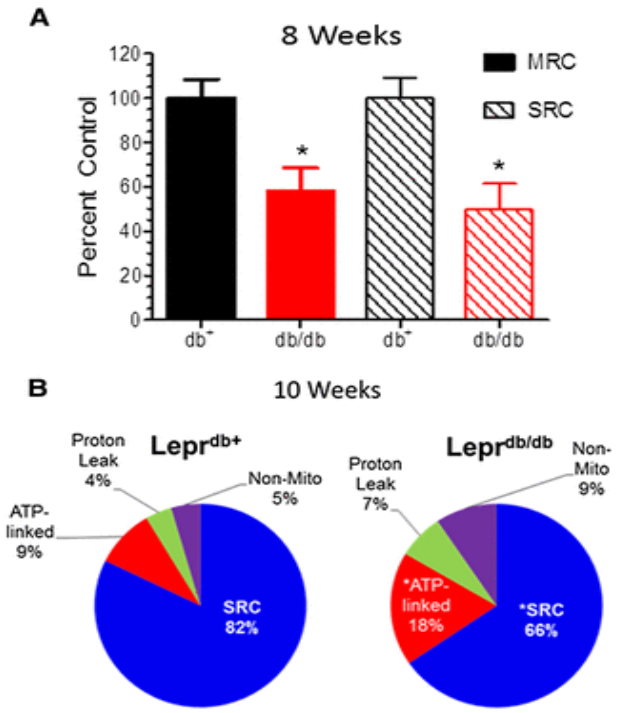

Figure 2.3-2: Deficits in mitochondrial bioenergetics in Lepr$^{db/db}$ mice correlate with the development of mechanical hypoalgesia.

Sensory neurons were obtained from 8–10-week-old Lepr$^{db/db}$ and Lepr$^{db/+}$ mice, cultured for 2 days, and mtBE assessed using an XF96 Extracellular Flux Analyzer. (A) MRC and SRC are significantly decreased in 8-week-old Lepr$^{db/db}$ mice compared with age-matched Lepr$^{db/+}$ mice. Respiratory parameters are expressed as the percent of control using values from the Lepr$^{db/+}$ mice. (B) Ten-week-old Lepr$^{db/db}$ mice have a significant decrease in SRC and an increase in ATP-linked and nonmitochondrial respiration compared with age-matched Lepr$^{db/+}$ mice. *, $p < 0.05$ versus Lepr$^{db/+}$ + vehicle (Veh). Respiratory parameters are expressed as the percent of the MRC in each genotype.

2.3.3. KU-32 Therapy Improves mtBE and Sensory Hypoalgesia in Lepr$^{db/db}$ Mice

Deficits in mtBE worsened by 14 weeks of age (Figure 2.3-3, A and B) and while the extent of ATP-linked and nonmitochondrial respiration increased, SRC declined between 10 and 14 weeks of age (compare Figures 2.3-2B and 2.3-3B). The respiratory control ratio (RCR) is an indication that the mitochondria have a high capacity for substrate oxidation and ATP synthesis and a low proton leak (Brand and Nicholls, 2011). At 14 weeks of age, diabetes decreased the RCR from 14.8 ± 1.6 in the Lepr$^{db/+}$ mice to 6.8 ± 0.03 in the untreated Lepr$^{db/db}$ animals. Lepr$^{db/db}$ animals treated for 4 weeks with KU-32 showed a significant improvement in MRC and SRC, and the RCR increased to 12.5 ± 0.5 versus untreated Lepr$^{db/db}$ animals, suggesting that modulating molecular chaperones increased the capacity for mitochondrial substrate oxidation.

Not surprisingly, MRC and SRC remained significantly impaired in the 18-week-old Lepr$^{db/db}$ animals compared with the Lepr$^{db/+}$ mice, and continued therapy with KU-32 improved MRC and SRC, but not really beyond levels observed after 4 weeks of drug administration (Figure 2.3-3, C and D). However, KU-32 therapy exerted a prolonged effect on neuronal mitochondrial function because the improvement in SRC promoted by 4 weeks of KU-32 therapy (Figure 2.3-3B) was maintained 4 weeks after drug administration was terminated (Figure 2.3-3D). This result was similar to the continued increase in nerve electrophysiology that was observed 4 weeks after drug withdrawal.

Lastly, to determine whether the improved bioenergetics might be due to an increase in mitochondrial biogenesis, the levels of cytochrome b and cytochrome c oxidase subunit II (mitochondrial genes) in the DRG from the 18-week-old mice were assessed by quantitative PCR and normalized to the nuclear gene, β-actin (Santos et al., 2011). The

expression of both genes was expressed as the fold of the level present in vehicle-treated $Lepr^{db/+}$ mice. However, no differences were observed in the untreated (1.01 ± 0.08, $n = 3$) or KU-32 treated (0.98 ± 0.06, $n = 4$) $Lepr^{db/db}$ mice.

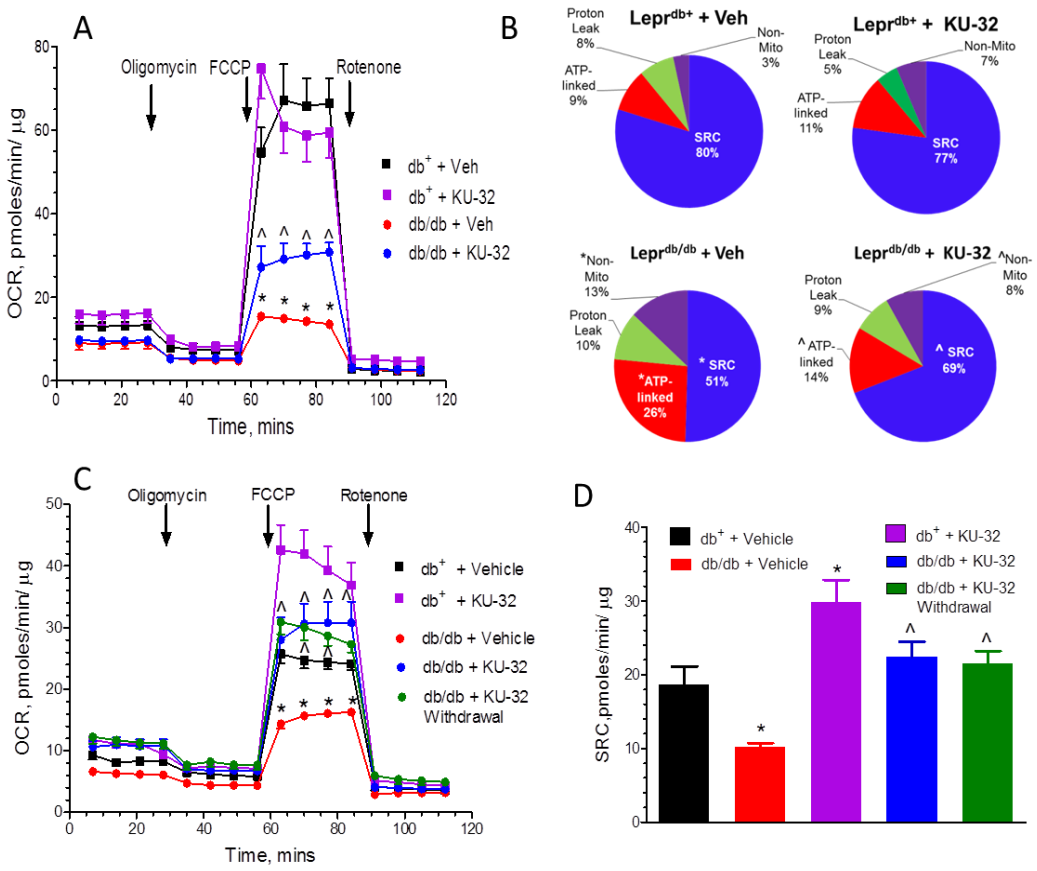

Figure 2.3-3: KU-32 improves mitochondrial bioenergetics in Lepr$^{db/db}$ mice.

Sensory neurons were obtained from 14- (A and B) or 18-week- (C and D) old Lepr$^{db/db}$ and Lepr$^{db/+}$ mice treated with KU-32 or Captisol and prepared for bioenergetic analysis. (A) MRC was significantly impaired in untreated Lepr$^{db/db}$ compared with age-matched Lepr$^{db/+}$ mice, and this deficit was significantly improved by KU-32 treatment. (B) Fourteen-week-old Lepr$^{db/db}$ mice have a significant decrease in SRC and an increase in ATP-linked and nonmitochondrial respiration compared with age-matched Lepr$^{db/+}$ mice, and these parameters were significantly improved by KU-32 therapy. (C) At 18 weeks of age MRC remained significantly impaired in the Lepr$^{db/db}$ compared with age-matched Lepr$^{db/+}$ mice. However, MRC was essentially unchanged from 14-week-old untreated Lepr$^{db/db}$. (D) MRC and SRC remained significantly improved in KU-32 treated Lepr$^{db/db}$ mice regardless of whether the drug was give continuously or withdrawn for the final 4 weeks of the study. In (A–D), *, $p < 0.05$ versus Lepr$^{db/+}$ + vehicle (Veh); ^, $p < 0.05$ versus Lepr$^{db/db}$ + Veh.

2.3.4. Diabetes-Induced Hypoalgesia Precedes Decreased Mitochondrial Function in a Model of Type 1 Diabetes

Because it is unclear whether changes in mtBE and sensory function follow similar patterns in type 1 and type 2 diabetes, this was examined using Swiss Webster mice rendered diabetic with STZ (Table 2.3-2). By 12 weeks of diabetes, the mice developed a significant mechanical (Figure 2.3-4A) and thermal (Figure 2.3-5A) hypoalgesia. However, these early sensory deficits were not associated with a significant impairment in mitochondrial respiration since SRC was significantly impaired only after 16 weeks of diabetes (Figure 2.3-4B).

To determine whether improved sensory function following treatment with KU-32 was linked to an improvement in mtBE, drug therapy was initiated at week 17, and sensory neurons were harvested 1, 3, and 5 weeks after drug administration. Prior to drug treatment, the mice showed significant decreases in nerve conduction velocities (Figure 2.3-5B) along with the thermal and mechanical hypoalgesia. Although 1 week of KU-32 administration did not increase the diabetes-induced decline in mitochondrial respiration, continued treatment revealed a tight temporal correlation between an improved SRC (Figure 2.3-4B) and recovery from the mechanical hypoalgesia (Figure 2.3-4C), MNCV (Figure 2.3-4D), and SNCV deficits (Figure 2.3-5C).

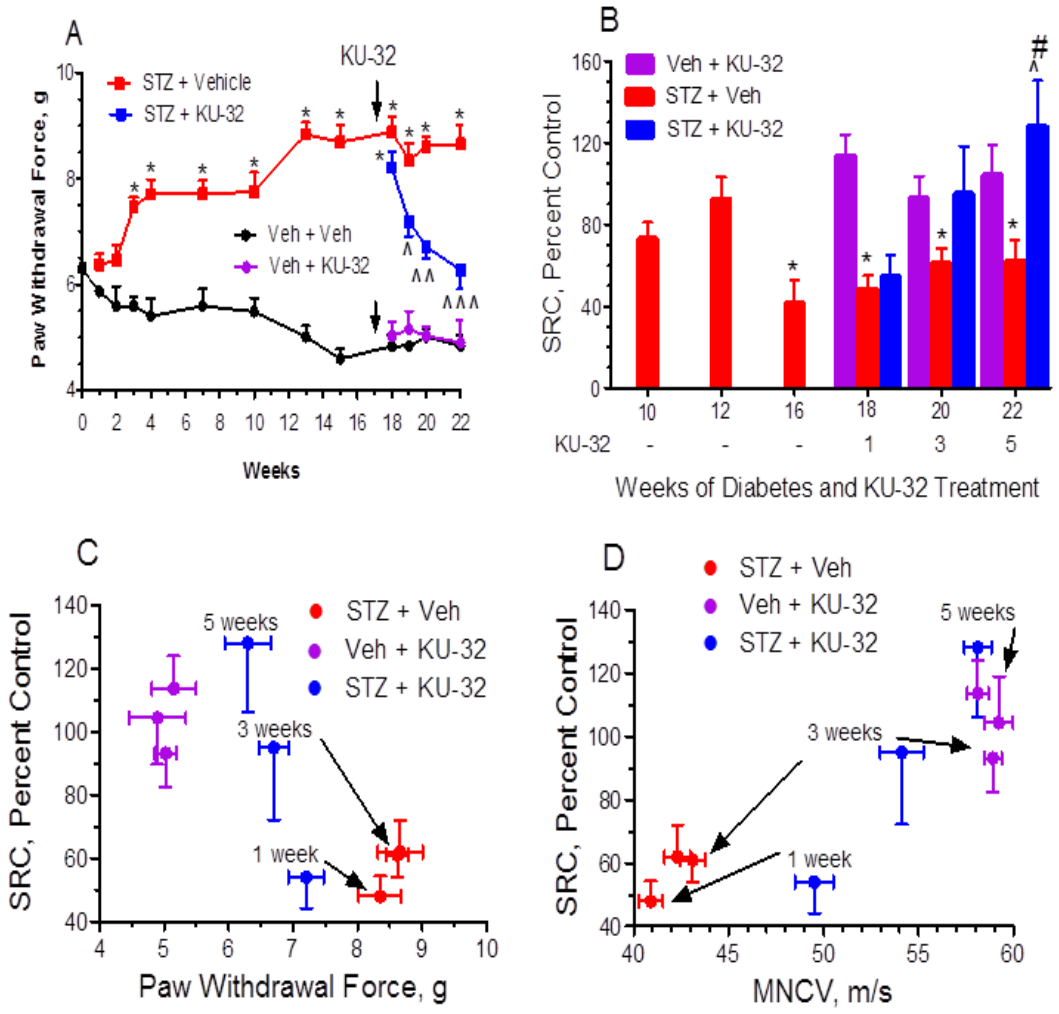

Figure 2.3-4: Sensory hypoalgesia precedes the onset of mitochondrial bioenergetics deficits in a type 1 model of diabetes.

Swiss Webster mice were rendered diabetic with STZ, mechanical sensitivity measured at the indicated weeks, and sensory neurons isolated after 10, 12, and 16 weeks of diabetes to assess mitochondrial function. After 17 weeks of diabetes, KU-32 was given weekly and sensory neurons isolated 1, 3, and 5 weeks after drug administration to assess mitochondrial function. (A) Diabetes induced a mechanical hypoalgesia that was maximal after 13 weeks and was reversed by KU-32 treatment. *, $p < 0.05$ versus time-matched vehicle (Veh) + Veh; ^, $p < 0.05$; ^^, $p < 0.01$; ^^^, $p < 0.001$, versus time-matched STZ + Veh for all p values. (B) SRC was significantly decreased after 16 weeks of diabetes, and initiation of KU-32 therapy led to a time-dependent recovery of SRC that correlated with improvements in mechanical hypoalgesia (C) and MNCV (D). *, $p < 0.05$ versus Veh + Veh; ^, $p < 0.05$ versus STZ + Veh; #, $p < 0.05$ versus STZ + 1 week KU-32.

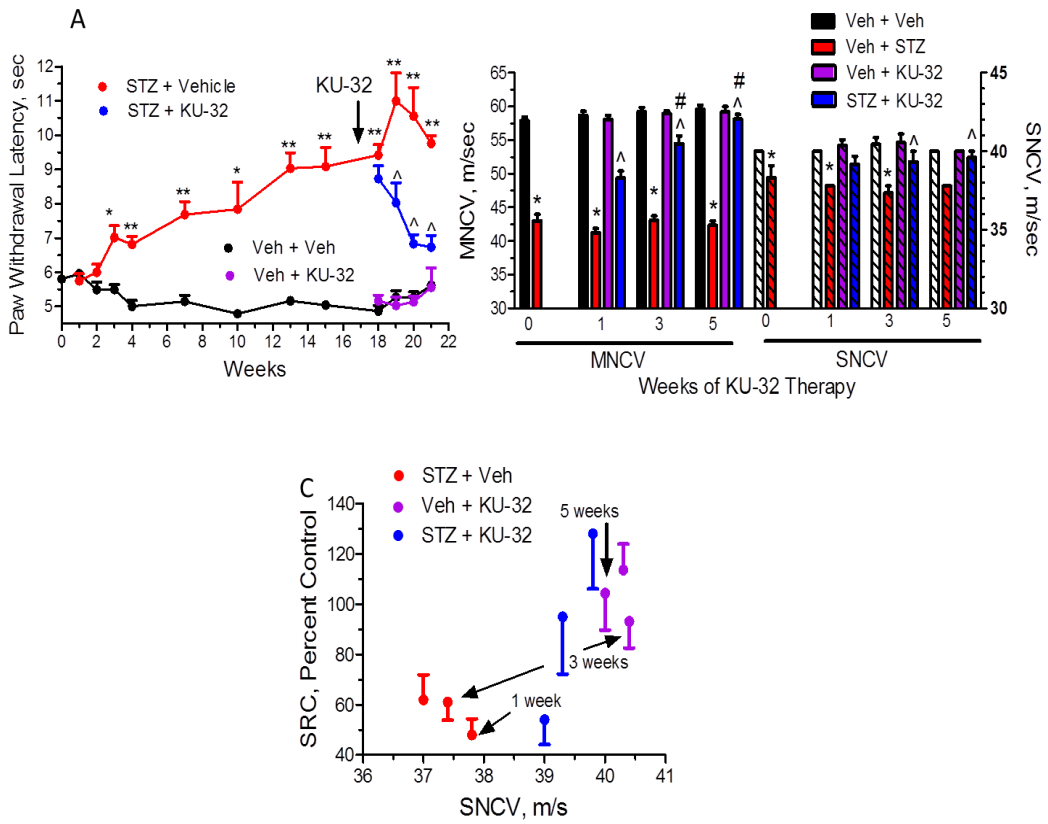

Figure 2.3-5: Effect of Diabetes and KU-32 Therapy on Thermal Hypoalgesia, NCV and Mitochondrial Bioenergetics.

Swiss Webster mice were rendered diabetic with STZ and thermal sensitivity assessed at the indicated weeks. After 17 weeks of diabetes, KU-32 was given weekly and at 1, 3 and 5 weeks after drug administration, NCV was measured and sensory neurons were isolated to assess mitochondrial bioenergetics. A) Diabetes induced a thermal hypoalgesia that was reversed by KU-32 treatment. *, $p < 0.05$, **, $p < 0.01$ vs time-matched Veh + Veh; ^, $p < 0.05$ vs time-matched STZ + Veh. B) Both MNCV and SNCV were decreased after 16 weeks of diabetes (0 weeks KU-32) and drug therapy improved these deficits. *, $p < 0.05$ vs Veh + Veh; ^, $p < 0.05$ vs STZ + Veh; #, $p < 0.05$ vs STZ + 1 week KU-32. (C) Correlation between recovery of SRC and improvement in SNCV.

Table 2.3-2: Weight, FBG, and HbA1c of Swiss Webster mice.

Week	Treatment	Weight g	FBG mg/dl	HbA1c %(mmol/mol)[a]	*n*
10	Veh + Veh	34.1 ± 2.5	127 ± 12	—	4
	STZ + Veh	27.3 ± 1.1*	540 ± 96*	—	4
12	Veh + Veh	34.0 ± 1.7	122 ± 10	5.0 ± 0.4 (31 ± 4.4)	6
	STZ+ Veh	30.3 ± 3.9*	600*	12.9 ± 0.2* (117 ± 2.2)	7
16	Veh + Veh	43.0 ± 3.1	117 ± 6	5.4 ± 0.7 (36 ± 7.7)	4
	STZ + Veh	28.6 ± 4.1*	573 ± 54*	11.7 ± 0.9* (104 ± 9.8)	4
18	Veh + Veh	43.8 ± 3.1	114 ± 15	4.7 ± 0.2 (28 ± 2.2)	4
	STZ + Veh	29.3 ± 4.2*	564 ± 35*	9.9 ± 1.8* (85 ± 19.7)	4
	Veh + KU-32	39.2 ± 2.2	138 ± 18	4.6 ± 0.3 (27 ± 3.3)	4
	STZ + KU-32	30.8 ± 1.7*	589 ± 21*	10.7 ± 0.8 * (93 ± 8.7)	4
20	Veh + Veh	40.2 ± 3.9	125 ± 9	4.9 ± 0.2 (30 ± 2.2)	4
	STZ + Veh	32.7 ± 2.8*	600*	12.1 ± 0.6* (109 ± 6.6)	4
	Veh + KU-32	41.4 ± 2.6	120 ± 1	5.2 ± 0.6 (33 ± 6.6)	4
	STZ + KU-32	33.0 ± 6.0*	600*	12.1 ± 0.9* (109 ± 9.8)	3
22	Veh + Veh	44.0 ± 0.6	123 ± 10	5.1 ± 0.1 (32 ± 1.1)	4
	STZ + Veh	30.3 ± 2.6*	600*	10.2 ± 1.7 * (88 ± 18.6)	3
	Veh + KU-32	43.0 ± 2.6	120 ± 1	4.8 ± 0.3 (29 ± 3.3)	4
	STZ + KU-32	35.9 ± 0.9*	600*	10.7 ± 1.6 * (93 ± 17.5)	3

Veh, vehicle.

[a] mmol of HbA1c/mol of hemoglobin.

* $p < 0.05$ versus Veh + Veh.

2.3.5. Hsp70 Is Necessary to Improve Mitochondrial Bioenergetics following KU-32 Therapy

We have shown previously that Hsp70 was necessary for the beneficial effect of KU-32 on improving insensate DPN (Urban et al., 2010). To examine whether the improvement in mtBE also required Hsp70, we compared the effect of KU-32 therapy on WT and Hsp70 KO mice rendered diabetic with STZ (Table 2.3-3). Diabetic WT and Hsp70 KO mice developed a mechanical hypoalgesia (Figure 2.3-6, A and B) and MNCV deficits (Figure 2.3-6, C and D). Thermal sensitivity and SNCV responded similarly (Figure 2.3-7, A–D). After 12 weeks of diabetes, the sensory deficits were well established, and although initiating weekly KU-32 therapy improved all the sensory endpoints in the WT mice, this response was totally absent in the drug-treated, diabetic, Hsp70 KO mice.

After 15 or 18 weeks of diabetes, MRC (Figure 2.3-8, A and B) and SRC (Figure 2.3-8, C and D) showed a similar decline in WT and Hsp70 KO mice. Thus, Hsp70 does not contribute to the diabetes-induced decline in mtBE. On the other hand, 3–6 weeks of KU-32 therapy improved MRC and SRC in diabetic WT mice but neither respiratory parameter was altered by the drug in diabetic Hsp70 KO mice. Importantly, the lack of efficacy of KU-32 in the Hsp70 KO mice is unlikely to result from differences in drug uptake or metabolism, since similar levels of KU-32 were present in DRG, sciatic nerve, and foot pads of WT and Hsp70 KO mice (data not shown). These data support the conclusion that Hsp70 is required to improve mtBE and sensory function following KU-32 therapy.

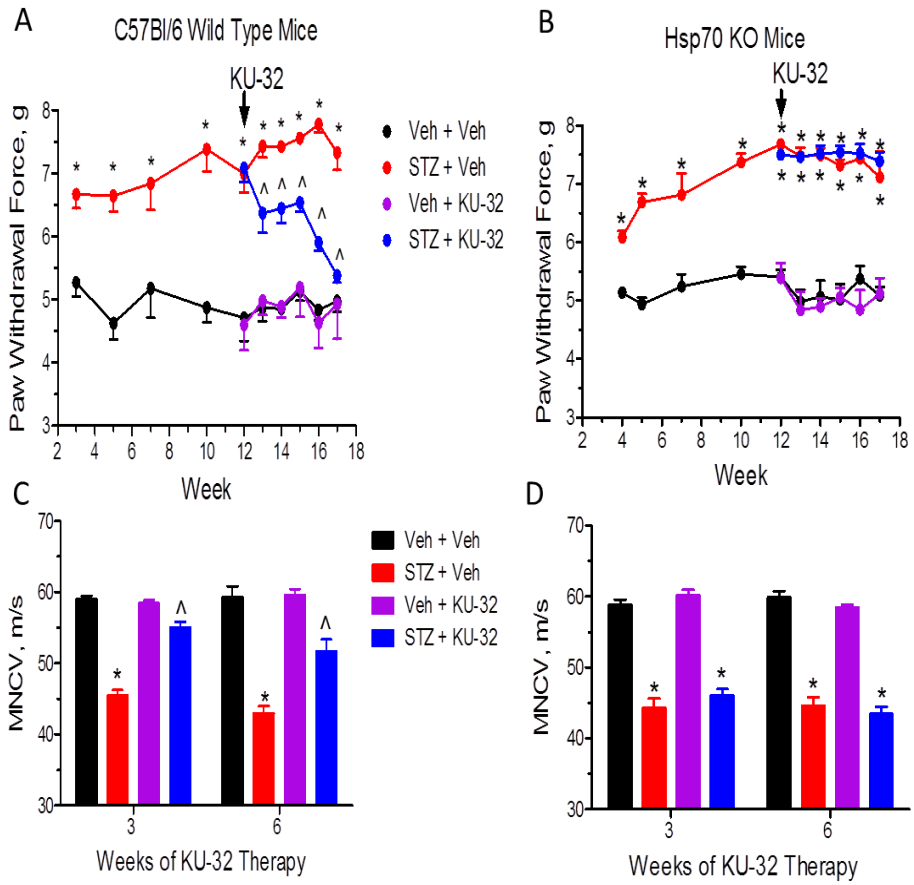

Figure 2.3-6: Hsp70 is necessary for KU-32 to reverse mechanical deficits of DPN.

C57Bl/6 wild type (A and C) and Hsp70 KO (B and D) mice were rendered diabetic with STZ and after 12 weeks of diabetes, KU-32 was given weekly for 6 weeks. Mechanical sensitivity (A and B) was assessed at the indicated weeks and MNCV (C and D) was assessed after 18 weeks of diabetes. In all panels, *, $p < 0.05$ versus time matched vehicle (Veh) + Veh; ^, $p < 0.05$ versus time-matched STZ + Veh.

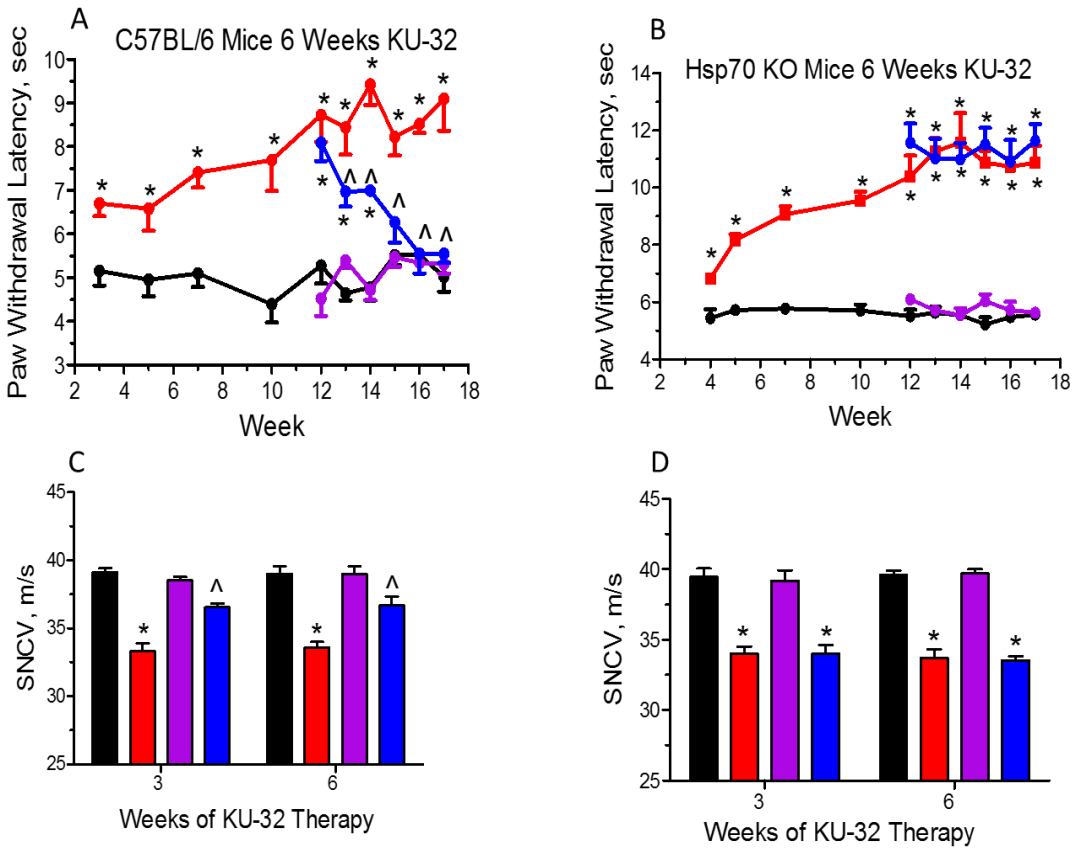

Figure 2.3-7: Hsp70 is necessary for KU-32 to reverse thermal deficits DPN.

C57Bl/6 (A, C) and Hsp70 KO (B, D) mice were rendered diabetic with STZ and at 12 weeks of diabetes, KU-32 was given weekly for 6 weeks. Thermal sensitivity (A, B) was assessed at the indicated weeks and SNCV (C, D) was assessed after 15 (3 weeks KU-32) and 18 weeks (6 weeks KU-32) of diabetes. *, $p < 0.05$ vs Veh + Veh; ^, $p < 0.05$ vs STZ + Veh. Symbol and bar colors in legend are shared between (A and B) and (C and D), respectively.

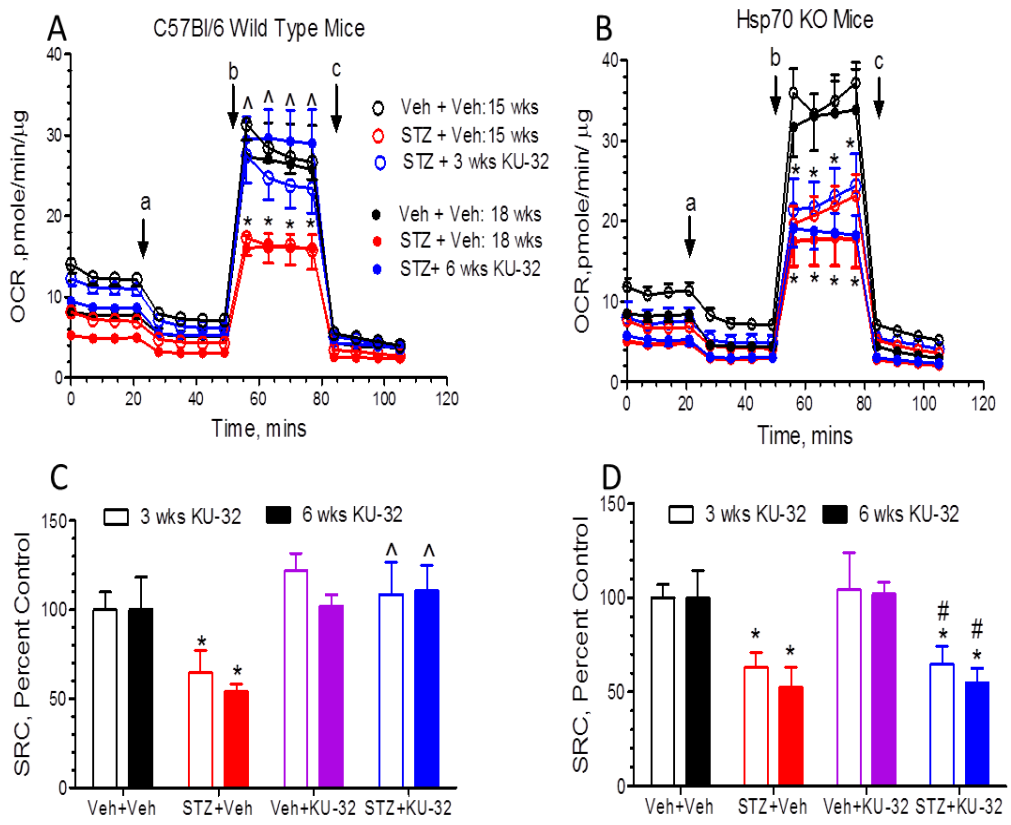

Figure 2.3-8: Hsp70 is necessary for KU-32 to improve mitochondrial bioenergetics.

C57Bl/6 wild-type (A and C) and Hsp70 KO (B and D) mice were rendered diabetic with STZ and after 12 weeks of diabetes, KU-32 was given weekly for 6 weeks. Sensory neurons were isolated 3 and 6 weeks after drug administration to assess mtBE. Diabetes decreased MRC (A and B) and SRC (C and D) in both C57Bl/6 and Hsp70 KO, but KU-32 therapy only improved these deficits in the diabetic C57Bl/6 mice. Oligomycin, FCCP, and rotenone/antimycin were injected at the times indicated by a, b, and c, respectively. *, $p < 0.05$ versus vehicle (Veh) + Veh; ^, $p < 0.05$ versus STZ + Veh; #, $p < 0.05$ versus C57Bl/6 STZ + KU-32.

Table 2.3-3: Weight, FBG, and HbA1c of C57Bl/6 and Hsp70 KO mice.

Weeks	Treatment	C57Bl/6				Hsp70 KO			
		Weight g	FBG mg/dl	HbA1c %(mmol/mol)[a]	*n*	Weight g	FBG Mg/dl	HbA1c %(mmol/mol)[a]	*n*
15	Veh + Veh	28.6 ± 3.4	149 ± 38	4.7 ± 0.2 (28 ± 2.2)	12	25.9 ± 3.1	137 ± 38	4.6 ± 0.2 (27 ± 2.2)	7
	STZ + Veh	20.7 ± 3.8	546 ± 75*	9.9 ± 1.58 (85 ± 17)	9	22.9 ± 3.4	431 ± 114*	8.7 ± 1.8* (72 ± 19.7)	6
	Veh + KU-32	24.4 ± 2.8	163 ± 47	4.5 ± 0.2 (26 ± 2.2)	12	24.2 ± 2.9	133 ± 18	4.6 ± 0.3 (27 ± 3.3)	8
	STZ + KU-32	21.6 ± 2.9	506 ± 98*	8.0 ± 1.5* (64 ± 17)	8	23.6 ± 3.9	478 ± 68*	8.4 ± 1.2* (68 ± 13.1)	5
18	Veh + Veh	25.5 ± 1.5	163 ± 45	4.7 ± 0.1 (28 ± 1.1)	4	23.7 ± 3.1	127 ± 15	5.0 ± 0.1 (31 ± 1.1)	8
	STZ + Veh	25.0 ± 2.7	419 ± 104*	8.2 ± 0.7* (66 ± 7.7)	3	25.4 ± 2.7	457 ± 66*	9.9 ± 0.9* (85 ± 9.8)	5
	Veh + KU-32	27.0 ± 0.6	151 ± 18	4.8 ± 0.2 (29 ± 2.2)	4	25.3 ± 2.3	141 ± 20	4.8 ± 0.3 (29 ± 3.3)	7
	STZ + KU-32	24.0 ± 2.2	415 ± 161*	8.5 ± 1.9* (69 ± 21)	3	22.9 ± 2.9	413 ± 57*	9.9 ± 1.8* (85 ± 19.7)	6

Veh, vehicle.
[a] mmol of HbA1c/mol of hemoglobin.
* $p < 0.05$ versus Veh + Veh.

2.4. Discussion

Mitochondrial Dysfunction and the Onset of DPN in Type 2 Diabetes

Similar to previous results in models of type 1 diabetes (Chowdhury et al., 2012; Urban et al., 2012b), we observed deficits in multiple bioenergetic parameters in sensory neurons obtained from $Lepr^{db/db}$ animals, a genetic model of type 2 diabetes. Although prior results have clearly implicated mitochondrial dysfunction in the development of insensate DPN in type 1 diabetes (Chowdhury et al., 2013; Fernyhough et al., 2010), our results are the first to temporally link the kinetics of onset of the bioenergetic deficits with the developing hypoalgesia in a model of type 2 diabetes.

The $Lepr^{db/db}$ mice showed significant deficits in MRC and SRC 4–6 weeks after the onset of hyperglycemia, which correlated with the rapidly developing sensory hypoalgesia. MRC measures the rate of maximal electron transport activity and substrate

oxidation that the sensory neurons can achieve in the absence of limitations imposed by the proton gradient across the inner mitochondrial membrane. The decrease in MRC suggests that electron transport in the diabetic mitochondria was impaired or that availability of substrates such as glucose and pyruvate was limiting. Although substrate availability might be affected by decreased activity of glycolysis and the tricarboxylic acid cycle as observed in 24-week-old $Lepr^{db/db}$ mice (Hinder et al., 2013b), the rate of extracellular acidification, a measure of glycolytic activity, was relatively similar between the $Lepr^{db/db}$ and $Lepr^{db/+}$ mice (data not shown). The similar levels of extracellular acidification suggest that the deficit in ATP production is either not sufficient to stimulate glycolysis or the diabetic neurons do not effectively revert to glycolysis to help produce ATP. Indeed, as observed by others (Chowdhury et al., 2012), the percent of the basal OCR that was attributable to ATP-linked respiration increased in the 10–18-week-old $Lepr^{db/db}$ compared with the $Lepr^{db/+}$ mice. Presumably, since the maximal rate of electron transport and substrate oxidation is compromised in the diabetic neurons, a greater portion of total respiration is commitment toward ATP-production to meet cellular demands.

SRC provides an indication of how close a cell is functioning to its bioenergetic limit (Sansbury et al., 2011). The progressive decline in SRC suggests that the diabetic neurons have a diminished energetic reserve to respond to the continued metabolic challenges associated with the chronic hyperglycemia and dyslipidemia in the $Lepr^{db/db}$ mice. Because KU-32 significantly improved SRC and NCV even after 4 weeks of drug withdrawal, moderate improvements in respiratory function via modulating chaperones may have long-term benefits for nerve electrophysiology. For example, decreased Na^+/K^+

ATPase activity is associated with slowing of MNCV in DPN (Coppey et al., 2001), and improved mitochondrial function may contribute to ameliorating this deficit.

Lastly, an unexpected outcome of our study was the significant improvement in SRC in the nondiabetic $Lepr^{db/+}$ mice treated with KU-32 for 8 weeks. The underlying reason for this improvement is unclear but may be related to the decreased mitochondrial respiratory capacity that was observed in the vehicle-treated 18-week-old $Lepr^{db/+}$ mice (compare black squares in Fig. 4, A and C). The decreased respiratory capacity between untreated 14- and 18-week-old $Lepr^{db/+}$ mice was observed in the testing of two separate groups of animals from different litters and suggests that the Lepr mutation may have an age-related effect on mitochondrial function.

Mitochondrial Dysfunction and the Onset of DPN in Type 1 Diabetes

In the type 1 model, diabetic mice developed a mechanical and thermal hypoalgesia between 6–12 weeks in the absence of significant decreases in SRC. However, mitochondrial respiration was significantly reduced after 16 weeks of diabetes. These data suggest that a fundamental difference may exist in the temporal role of altered mtBE in contributing to the early onset of hypoalgesia in type 1 versus type 2 diabetes. Because both models showed relatively similar levels of hyperglycemia, differences in the kinetics of onset of the bioenergetic decline may be influenced by insulin resistance, which is coincident with mitochondrial dysfunction in tissues such as oxidative skeletal muscle and liver of the $Lepr^{db/db}$ mice (Holmstrom et al., 2012). Alternatively, dyslipidemia is often associated with type 2 diabetes and has been suggested to contribute to DPN (Vincent et al., 2009). However, genetic deletion of apolipoprotein E to increase dyslipidemia in $Lepr^{db/db}$ mice did not exacerbate DPN assessed at 6 months of age

(Hinder et al., 2013a), suggesting that dyslipidemia may not significantly worsen sensory neuron mitochondrial dysfunction in type 2 diabetes.

Modulating Hsp70 Improves mtBE and DPN

Although the onset of a thermal and mechanical hypoalgesia does not require a significant change in mtBE in the type 1 model, the improvement in the psychosensory and electrophysiologic measures of nerve function in both diabetic animal models tightly correlated with an increase in mtBE following KU-32 therapy. The absence of this correlation in the diabetic Hsp70 KO mice provides the first evidence that modulating Hsp70 is a necessary effector for KU-32 to improve the bioenergetic profile of the sensory neurons and nerve function. This benefit was unrelated to any effect of KU-32 or Hsp70 on improving glucose disposal or any of the metabolic parameters in either model. However, a clear limitation of this work is that although a tight, Hsp70-dependent correlation exists between improved mtBE and the various measures of nerve function, a causal relationship between them is not established. Thus, we cannot rule out that Hsp70 may have independent and parallel effects on mtBE and other targets that contribute to improving psychosensory and electrophysiologic function following KU-32 therapy.

Although the etiology of DPN is not attributed to the accumulation of a specific misfolded or aggregated protein, the efficacy of Hsp70 in improving mtBE suggests that diabetic mitochondria are undergoing some level of proteotoxic stress. Because KU-32 can decrease oxidative stress and increase mitochondrial and cytosolic chaperones in hyperglycemically stressed primary sensory neurons, these factors may directly contribute to improving mtBE and SRC in diabetic mice (Zhang et al., 2012). In this regard, hyperglycemia can increase oxidative stress and the oxidative modification of

amino acids (Akude et al., 2010) that may impair protein folding within mitochondria (Muchowski and Wacker, 2005), decrease mitochondrial protein import (Baseler et al., 2011), and promote mitochondrial dysfunction (Tomlinson and Gardiner, 2008). In the mitochondrial proteome, ~99% of the mitochondrial proteins are encoded by nuclear genes and imported into the organelle from cytosol and Hsp70 serves as a chaperone for hydrophobic precursors of inner mitochondrial membrane proteins (Schmidt et al., 2010). Because Hsp70 is not a resident mitochondrial chaperone, determining whether it might mitigate diabetes-induced dysfunction in mtBE by facilitating the import, removal, and/or replacement of damaged mitochondrial proteins is an important biologic question with clear therapeutic relevance to treating DPN.

The reliance on Hsp70 for the tight correlation between improved mtBE and the physiologic measures of DPN adds to the evidence that modulating molecular chaperones may benefit various neurodegenerative diseases where mitochondrial respiratory function is compromised (Ouyang et al., 2006; Xu et al., 2010). However, it may be critical to limit the extent of Hsp70 induction since overexpression of Hsp70 in HeLa cells inhibited oxidative phosphorylation and augmented anaerobic glycolysis (Wang et al., 2012). As certain malignant phenotypes are characterized by Hsp70 overexpression and increased glycolytic rates, the efficacy of modulating Hsp70 to enhance neuronal mtBE might rely on pharmacologic agents that are weak or cell-selective inducers of Hsp70. Although glycolytic activity decreases in diabetic nerve (Hinder et al., 2013b), additional work will be needed to determine if long-term modulation of Hsp70 might negatively affect neuronal oxidative phosphorylation and be a liability in treating DPN.

In summary, numerous approaches toward treating insensate DPN have centered on inhibiting specific pathogenic pathways linked to glucotoxicity, with limited translational success (Calcutt et al., 2009). The pharmacologic management of insensate DPN is difficult since no single etiologic event has been unequivocally identified to contribute to disease development in a temporally and/or biochemically uniform fashion over the long natural history of the disease. Since pharmacologic modulation of endogenous neuroprotective chaperones does not rely on targeting a specific pathogenic enzyme (*i.e.*, aldose reductase) or pathway (*i.e.*, oxidative stress) that contributes to DPN, it provides a venue to complement etiocentric therapies. Coupled with close attention toward obtaining glycemic goals, modulating molecular chaperones may aid the medical management of DPN in patients with type 1 and type 2 diabetes.

Chapter 3: Novologue Therapy Improves Mitochondrial Bioenergetics and Modulates Transcriptome Changes Involved in Inflammatory Pathways and Production of Reactive Oxygen Species in Diabetic Sensory Neurons

Abstract

We have previously demonstrated that modulating heat shock protein 90 (Hsp90) and Hsp70 with the small molecule drug, KU-32, ameliorates physiologic and bioenergetic deficits of DPN in animal models of both type 1 and type 2 diabetes. In the current study, we sought to determine whether KU-596, an analogue of KU-32, offers similar therapeutic potential for treating DPN. Similar to KU-32, KU-596 improved psychosensory and bioenergetic deficits of DPN in a dose-dependent manner. However, the drug could not improve DPN in Hsp70 KO mice. Transcriptomic analysis using RNA sequencing (RNA-Seq) of DRG from diabetic wild type (WT) and Hsp70 KO mice revealed that KU-596 modulated transcription of genes involved in inflammatory pathways independently of Hsp70. In contrast, the effects of KU-596 on genes involved in the production of reactive oxygen species (ROS) are Hsp70-dependent. Our data indicate that modulation of molecular chaperones offers an effective approach towards correcting nerve dysfunction, and that normalization of inflammatory pathways alone by novologue therapy seems to be insufficient to reverse the deficits associated with insensate DPN in our model of type 1 diabetes.

3.1. Introduction

Diabetes has emerged as a major public health care concern worldwide, with the number of diabetic patients estimated to exceed 500 million by 2030 (Whiting et al., 2011). Diabetic peripheral neuropathy (DPN), as one of the most common diabetic

complications, affects patients with both type 1 and type 2 diabetes and greatly reduces quality of life. Thus, great efforts have been put into identifying mechanisms of disease pathogenesis in order to develop therapeutic approaches for its effective control and treatment. However, despite our increased understanding of the etiology of DPN, little progress has been made in treating the disease. To date, none of the agents targeting the pathogenic pathways have shown effectiveness in reversing, preventing, or even slowing disease progression. Currently, the only effective control of DPN remains to be tight glycemic control and lifestyle interventions, and this is only more effective in type 1 versus type 2 diabetics. Therefore, we have sought to target the disease from a different angle, through reinforcing innate cytoprotective mechanisms. Our results indicated that pharmacological manipulation of molecular chaperones might offer the therapeutic potential for reversing sensory deficits associated with DPN (Urban et al., 2010).

Hsp90 and Hsp70 function as molecular chaperones that are essential for the folding of nascent polypeptides and refolding of denatured proteins. Pharmacological inhibition of Hsp90 with KU-32, a first-generation novobiocin-based, C-terminal Hsp90 inhibitor, decreased glucose-induced death of primary sensory neurons and improved psychosensory, electrophysiologic, morphologic and bioenergetic deficits of DPN in an Hsp70-dependent manner (Li et al., 2012; Ma et al., 2014; Urban et al., 2012a; Urban et al., 2010; Zhang et al., 2012). Though KU-32 was found to be quite efficacious in treating DPN, it is cumbersome to make synthetically and efforts had been made to determine if diversification of its coumarin ring scaffold could identify structure-activity relationships (SAR) that might enhance the neuroprotective properties of the analogs, while also simplifying the synthetic scheme.

Based on molecular modeling of KU-32 docked to the Hsp90 C-terminal binding pocket, it was observed that the coumarin lactone of KU-32 appeared too distant from Lys539 to provide complementary interactions with this residue. Additionally, the 3-amido side chain of KU-32 projected into a large hydrophobic pocket that could accommodate more flexible linkers. Consequently, novologues (novobiocin analogues) were designed to contain a biphenyl scaffold that replaced the coumarin lactone of KU-32 (Figure 3.1-1A). It was hypothesized that the B-ring of the biphenyl would project into the Hsp90 C-terminal binding pocket and serve as a lead compound for further diversification. Subsequent modifications identified that electronegative atoms placed at the meta-position of the benzene ring exhibited improved cytoprotective activity, which is believed to result from favorable interactions with Lys539 in the Hsp90 C-terminal binding pocket (Kusuma et al., 2012). Consistent with these results, KU-596 (Figure 3.1-1B) was identified as a meta-3-fluorophenyl substituted novologue that exhibited a 14-fold lower ED_{50} for protecting primary sensory neurons against glucotoxicity compared with KU-32. In addition, treating 50B11 cells (an immortalized sensory neuron cell line) with KU-596 led to increased Hsp70 expression in the absence of client protein degradation (Kusuma et al., 2012). Thus, in the current study, we sought to determine if the novologue KU-596 displays similar cytoprotective effects in animal models of DPN in an Hsp70-dependent manner.

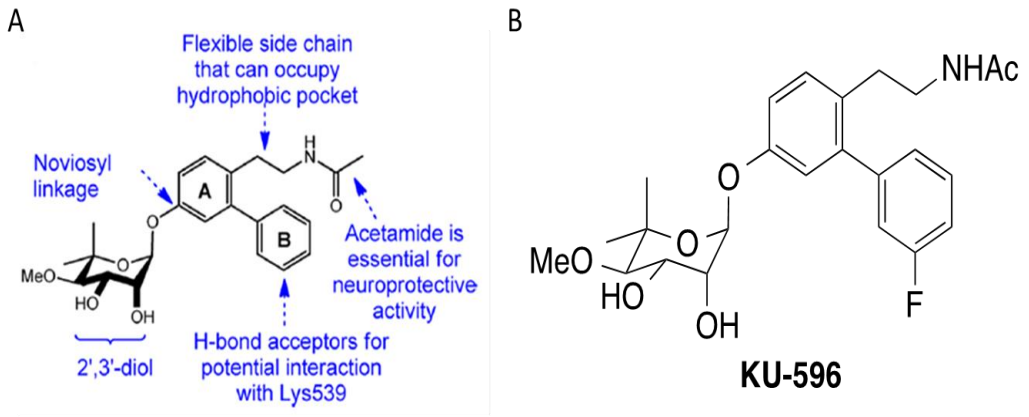

Figure 3.1-1: Structure-activity relationships of KU-32 analogues.
(A) Structure of novologue and its attributes. (B) Structure of KU-596.

Our previous studies have shown that manipulating molecular chaperones through improved multiple clinical indices of DPN, and that these neuroprotective effects were dependent on the stress-inducible form of Hsp70. Mechanistic studies have revealed that KU-32 restored mitochondrial respiratory capacity and reduced oxidative stress in the sensory neurons, which likely contributes to its protective efficacy (Zhang et al., 2012). However, since Hsp70 may contribute to improving insensate DPN by affecting diabetes-induced changes in protein folding, stability and clearance (Evans et al., 2010), we hypothesized that multiple genes/gene networks within sensory neurons may contribute to the reversal of insensate DPN in an Hsp70-dependent manner.

The application of system biology approaches has yielded novel insight into gene networks that contribute to the development of DPN in animal models of type 2 diabetes (Hinder et al., 2013b; Pande et al., 2011) and which distinguish humans with progressive versus non-progressive DPN, *i.e.*, induction of the c-jun network (Hur et al., 2011). Though the use of microarrays has successfully defined diabetes-induced changes in the peripheral nerve transcriptome, DNA microarrays have a small dynamic range (100-300

fold) and lack sensitivity for quantifying genes expressed either at low or very high levels due to background array signals or signal saturation (Wang et al., 2009). In contrast, high throughput transcript sequencing **(RNA-Seq)** has a dynamic range spanning five orders of magnitude and permits detecting abundant and even very rare transcripts, with sufficient sequencing depth (Mortazavi et al., 2008). RNA-Seq allows identifying and quantifying splice variants and provides a digital readout of gene expression since it is based on counting reads (# of sequence events), a direct measure of transcript abundance. Since RNA-Seq is emerging as a more versatile approach for quantitative transcriptomics, we examined transcriptomic changes within sensory neurons that contribute to the reversal of insensate DPN using RNA-Seq.

The RNA-Seq approach utilizes deep-sequencing technologies and is gaining prominence as a means of accurate transcriptome profiling (Wang et al., 2009). This method provides millions of sequences from expressed RNA molecules, and has been shown to provide highly accurate and reproducible results for quantitative characterization of the expressed complement of a genome with the requirement of less RNA sample (t Hoen et al., 2008). In general, a population of RNA (total or fractionated, for example poly(A)+ selected) is fragmented and converted to a library of cDNA fragments with adapters attached to one or both ends. The cDNA library is then sequenced in a high-throughput manner to obtain short sequences from one end (single-end sequencing) or both ends (paired-end sequencing). The reads are typically 30-400 base pairs (bp), depending on the DNA sequencing technology used. Following sequencing, the resulting reads are either aligned to a reference genome, or assembled *de novo* if no genomic sequence can be referred to. Qualitative and/or quantitative results

can be obtained through bioinformatics analysis of the sequencing data (Wang et al., 2009). Recent studies have shown that the RNA-Seq approach is more sensitive at detecting low expression transcripts compared to microarray technology. Direct determination of the cDNA sequences also circumvents background noise associated with fluorescence quantification in traditional microarrays (Fang et al., 2012). In addition, the entire transcriptome can be surveyed without the requirement of *a priori* knowledge of transcribed regions, which enables the discovery of novel transcripts. Furthermore, since RNA-Seq allows genome-wide analysis of transcription at single nucleotide resolution, transcript structures including alternatively spliced transcript isoforms and post-translational RNA editing events can also be identified (Wilhelm and Landry, 2009).

In this study, we define changes in the transcriptome of sensory neurons from C57Bl/6 and Hsp70 KO mice to determine the transcriptome targets of KU-596 and the Hsp70 dependency of these changes. Our results indicate that KU-596 improved sensory function and bioenergetic profile of sensory neurons. However, the effects of KU-596 on mitochondrial bioenergetics (mtBE) was likely exerted through post-translational modulation of mitochondrial proteins rather than through transcriptional modification of mitochondrial genes. In contrast, KU-596 reversed diabetes-associated transcriptome changes involved in inflammatory pathways and the production of ROS. Despite the lack of efficacy in reversing sensory deficits of DPN, the effects of KU-596 on inflammatory genes persisted in the absence of Hsp70. This finding suggests that normalization of inflammatory pathways alone might not be enough to reverse sensory deficits associated with insensate DPN. These data provide novel insight into the role of mitochondrial dysfunction, oxidative stress and inflammation in the onset of insensate DPN and further

consolidate the therapeutic potential of modulating molecular chaperones as a treatment for DPN.

3.2. Materials and Methods

Streptozotocin (STZ), carbonylcyanide-4-(trifluoromethoxy)-phenylhydrazone (FCCP), oligomycin, rotenone, antimycin A, Percoll, and poly(DL)ornithine were obtained from Sigma-Aldrich (St. Louis, MO). KU-596, N-(2-(5-(((3R,4S,5R)-3,4-Dihydroxy-5-methoxy-6,6-dimethyltetrahydro-2H-pyran-2-yl)oxy)-3'-fluoro-[1,1'-biphenyl]-2-yl)ethyl)-acetamide, was synthesized and structural purity (>95%) verified as described previously (Kusuma et al., 2012).

Animals

Male Swiss Webster Mice were purchased from Harlan Laboratories (Indianapolis, IN). Male and female wild-type (WT) C57Bl/6 and Hsp70.1/70.3 double knockout (KO) mice on a C57Bl/6 background (Hsp70 KO) were obtained from in-house breeding colonies (Urban et al., 2010). Diabetes was rendered in 8-week-old male and female mice with an intraperitoneal injection of 100 mg/kg STZ given on two consecutive day after 6-hour of fasting. Mice were fasted 6 hours for fasting blood glucose (FBG) measurement one week after the second injection, and mice with FBG $\geq$ 290 mg/dl (16 mM) were deemed diabetic. KU-596 was introduced to Swiss Webster mice after 8 weeks of diabetes through intraperitoneal injections with a dose of 2 mg/kg, 10 mg/kg, or 20 mg/kg in 0.1 M Captisol (β-cyclodextrin sulfobutylethers; CyDex Pharmaceuticals, Lenexa, KS). In C57Bl/6 and Hsp70 KO mice, a dose of 20 mg/kg KU-596 in 0.1 M Captisol was given through oral gavage after 12 weeks of diabetes. Weekly administration of KU-596 was continued in Swiss Webster mice for 6 weeks, and in C57Bl/6 and Hsp70 KO mice

for 4 weeks. Each group contained at least 8 mice and were randomly assigned to each of the 6 treatment groups using a random number generator.

All animals were maintained on a 12-hour light/dark cycle with ad libitum access to water and 7022 NIH-07 rodent chow (5.2% fat). All animal procedures were performed in accordance with protocols approved by the Institutional Animal Care and Use Committee and in compliance with standards and regulations for the care and use of laboratory rodents set by the National Institutes of Health.

Psychosensory and Electrophysiologic Analyses

Mechanical sensitivity was assessed using a Dynamic Plantar Aesthesiometer (Stoelting Inc.) fitted with a stiff monofilament that was applied to the plantar surface at an upward force of 10g for Swiss Webster mice or 8g for C57Bl/6 and Hsp70 KO mice. Thermal sensitivity was assessed by paw withdrawal latency to a ramping, focal heat using a Hargreaves Analgesiometer (Stoelting Inc.) (Urban et al., 2010). Responses from each animal were measured four times on alternate feet and averaged. At the end point of a study, animals were anesthetized prior to measuring motor and sensory nerve conduction velocities (MNCV and SNCV) as previously described (McGuire et al., 2009). Animals were then euthanized prior to tissue collection.

Mitochondrial Bioenergetics Assessment

Oxygen consumption rate (OCR) was assessed in intact lumbar DRG sensory neurons using the XF96 Extracellular Flux Analyzer (Seahorse Biosciences, North Billerica, MA). Lumbar sensory neurons were isolated as previously described (Ma et al., 2014), and maintained overnight in Ham's F10 medium (6.1 mM glucose) containing 50 ng/ml nerve growth factor and 1 ng/ml neurotrophin 3 and N2 supplement without insulin

(Invitrogen, Carlsbad, CA). The following day, the cells were placed in assay medium (unbuffered Dulbecco's modified Eagle's medium supplemented with 1 mM sodium pyruvate and 5.5 mM D-glucose) at 37℃ for one hour before being introduced to the XF96 analyzer. The initial readings provide a measure of the basal OCR before the addition of respiratory chain poisons (Brand and Nicholls, 2011). The addition of oligomycin (1 μg/ml), the ATP synthase inhibitor, leads to a decrease in OCR which represents the portion of basal OCR that is coupled to ATP synthesis. The residual OCR that persists after addition of oligomycin is from uncoupled respiration (proton leak). Next, maximal respiratory capacity (MRC) was assessed following addition of the protonophore FCCP (1 μM) which dissipates the proton gradient across the inner mitochondrial membrane. Non-mitochondrial respiration was then assessed by coinjection of 1 μM rotenone + 1 μM antimycin A. After the respiratory measures, the cells were harvested and OCR values were normalized to the total protein content of each well. Maximal respiratory capacity (MRC) and spare respiratory capacity (SRC) were determined and quantified as described previously (Brand and Nicholls, 2011; Chowdhury et al., 2012).

Isolation of RNA

L_4-L_6 lumbar DRG from two animals were pooled together for the isolation of one total RNA sample. Each treatment group consists of 3-4 biological replicates. Tissues were harvested and rapidly frozen in liquid nitrogen for storage, and subsequently ground in liquid nitrogen. After the homogenization, 900 ml of Trizol was added to each sample and RNA was isolated following the standard protocol of the Qiagen RNeasy Plus Universal Mini Kit (Qiagen, Venlo, Limburg). RNA quality and concentration was

checked with the Agilent 2200 TapeStation (Agilent Technologies, Santa Clara, CA) and Qubit Fluorometric Quantitation (Life Technologies, Carlsbad, CA), respectively. RNA with an integrity number (RIN) ≥ 7 was used for RNA-Seq analysis or qRT-PCR analysis (Figure 3.2-1).

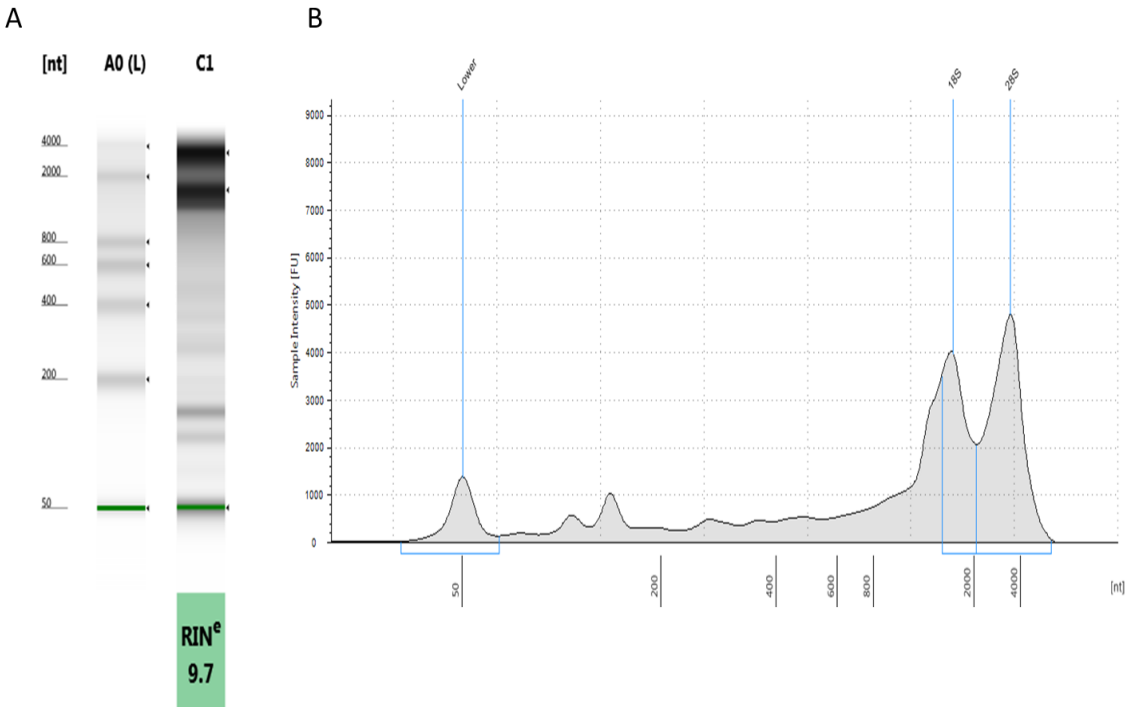

Figure 3.2-1: An example of RNA integrity analysis using the 2200 TapeStation instrument.

Tiny amounts of RNA samples (1-2 µl) were separated in the channels of the microfabricated chips according to their molecular weights and subsequently detected via laser-induced fluorescence detection. (A) Electrophoresis micro-gel image of the ladder (left lane) and the RNA sample (right lane). The two high intensity bands at the upper part of the gel indicated by arrow heads comprise the 28S and 18S ribosomal RNA (rRNA) species and other bands represent the migration of smaller RNA species. Increased intensity of lower molecular weight bands indicates RNA degradation. (B) Electropherogram of the RNA sample. The amplitude of each slope corresponds to the band intensity on the gel. A shift towards shorter fragment sizes reflects degradation of the RNA sample. (Schroeder et al., 2006)

Illumina RNA-Seq

For RNA-seq analysis, 100 ng of total RNA was used to prepare cDNA libraries with the TruSeq Stranded Total RNA Library Prep Kit (Illumina Inc., San Diego, CA). The procedures of library preparation is shown in Figure 3.2-2 (Corney, 2013). In general, poly(A)+ containing mRNA molecules were purified with oligo-dT attached magnetic beads. Purified mRNA was then fragmented and primed with random hexamers, which were subsequently reverse transcribed into first strand cDNA using reverse transcriptase. The RNA templates were then removed from the single-strand cDNA, and a replacement strand was synthesized to generate double-strand cDNA. The double-strand cDNA was end-repaired and adenylated at the 3' ends. For each sample, Illumina-specific adaptors that contain a unique 6 bp index sequence that specifically identifies each sample were ligated to the 3' adenine-tail of the fragments to permit the single read, multiplex sequencing of transcripts within each lane of the flow cell. cDNA products (~260 bp) were amplified and submitted to quality control with the Agilent 2200 TapeStation (Agilent Technologies, Santa Clara, CA). cDNA libraries prepared from 3-4 biological replicates from each treatment group were then randomly assigned to two lanes of the flow cell for subsequent single-end sequencing with a read length of 100 bases using the Illumina HiSeq 2500 System (Illumina Inc., San Diego, CA).

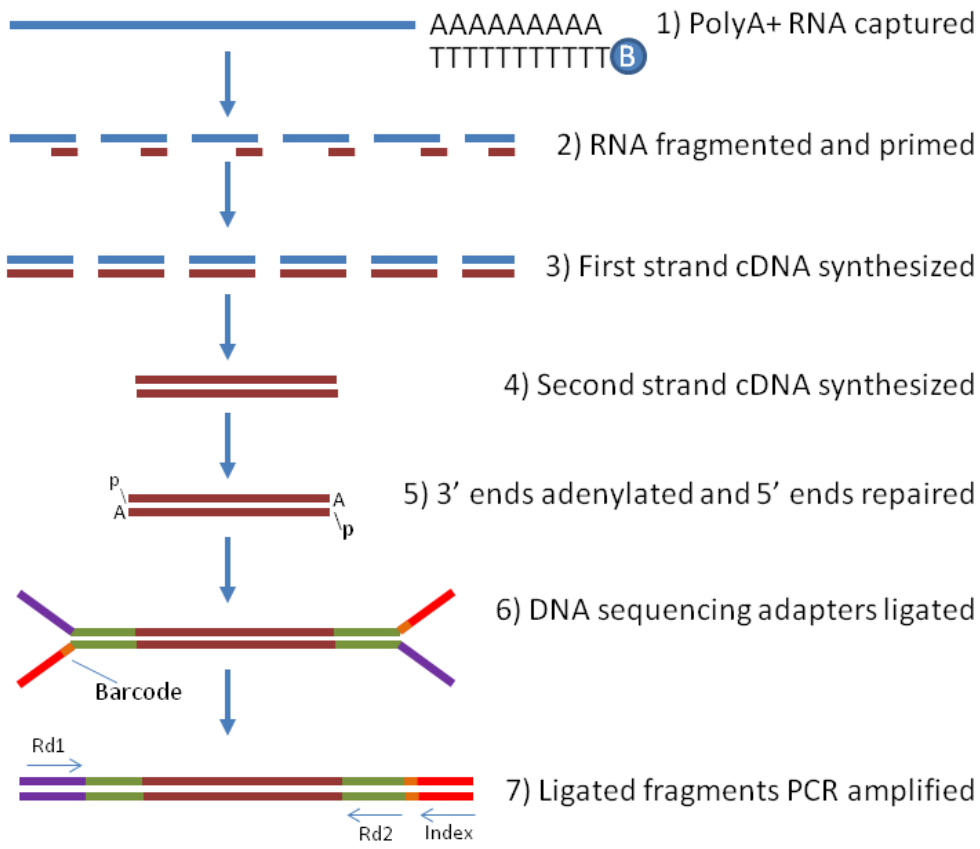

Figure 3.2-2: Process of library preparation.

Poly(A)+ RNA is enriched using oligo(dT) beads followed by fragmentation and reverse transcription. The 5' and 3' ends of cDNA fragments are next prepared to allow efficient ligation of "Y" adapters containing a unique barcode and primer binding sites. Finally, ligated cDNAs are PCR-amplified and ready for cluster generation and sequencing. (Corney, 2013)

Bioinformatics Analysis of RNA-Seq Data

After the initial processing and de-multiplexing steps, the resulting FASTQ files were analyzed via the Galaxy Project web-based interface (http://usegalaxy.org/) linked to the freely available Tuxedo Suite (Figure 3.2-3) (Trapnell et al., 2012). FASTQ files were quality checked, groomed if necessary, and then submitted to the Tophat module to align the short read sequences to the mouse genome (mm9). The Cufflinks package was then used for transcript assembly, and annotation of each sample. The resulting files were merged using CuffMerge. The CuffMerge output and Tophat files were loaded into the CuffDiff module to quantify significant changes in transcript expression between groups (Goecks et al., 2010; Trapnell et al., 2013). Gene level expression data were normalized to obtain fragments per kb per millions of aligned reads (FPKM), and the log 2 fold changes between groups were calculated based on the FPKM data. A t-test was used to calculate the p-value for differential gene expression in the Cuffdiff module, the resulting p values were adjusted by the Benjamini-Hochberg method to compute false discovery rate (FDR, *i.e.* q-value) (Rapaport et al., 2013). Those with q-value < 0.05 were deemed significant. CummeRbund was used for data visualization, and Ingenuity Pathway Analysis (http://www.ingenuity.com/products/ipa) was employed to identify and model gene networks.

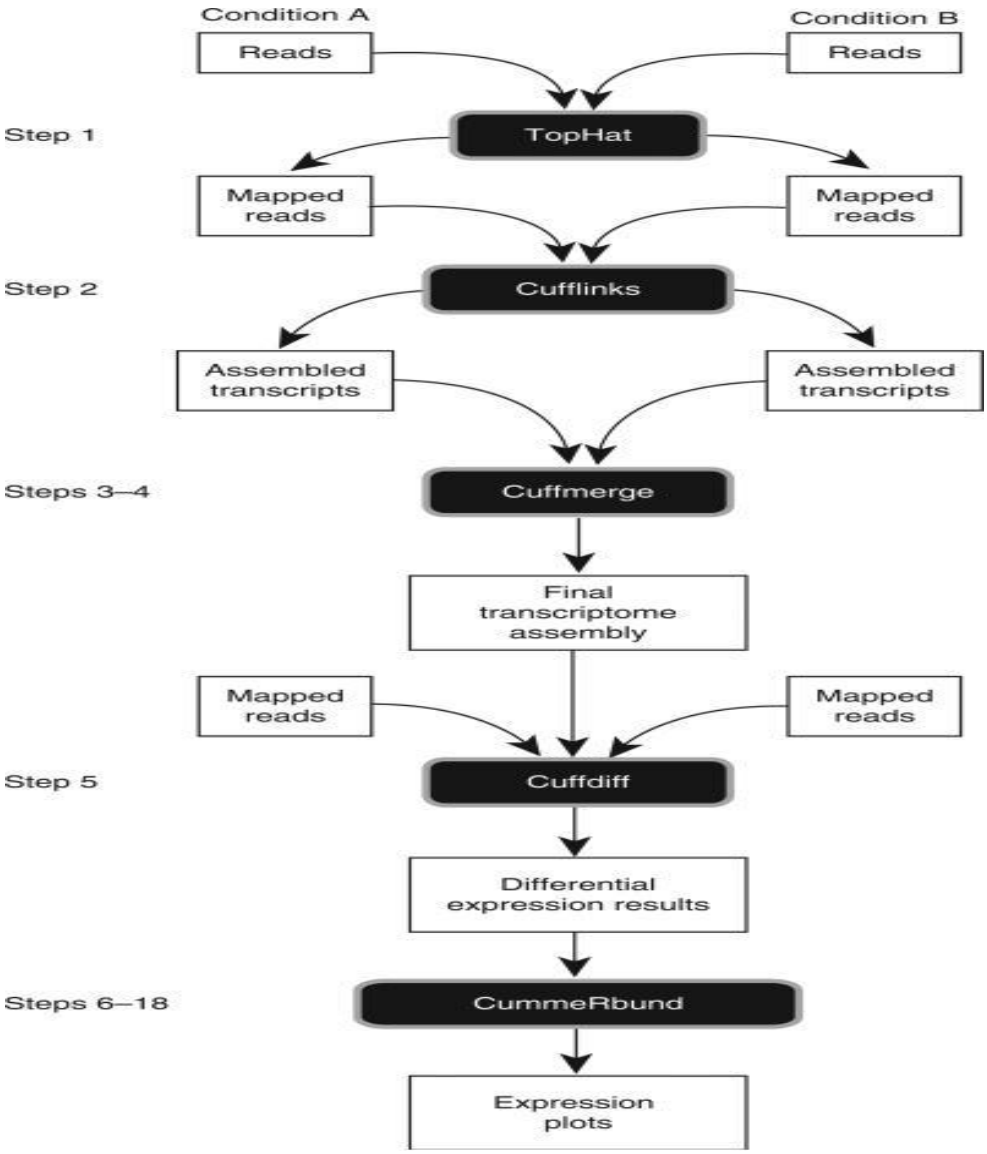

Figure 3.2-3: An overview of the Tuxedo protocol.

In an experiment involving various conditions, reads (FASTQ files) are first mapped to the genome with TopHat. The reads for each biological replicate are mapped independently. These mapped reads are provided as input to Cufflinks, which produces one file of assembled transcripts for each replicate. The assembly files are merged with the reference transcriptome annotation into a unified annotation for further analysis. This merged annotation is quantified in each condition by Cuffdiff, which produces expression data in a set of tabular files. These files are indexed and visualized with CummeRbund to facilitate exploration of genes identified by Cuffdiff as differentially expressed genes. (Trapnell et al., 2012)

Real-time PCR

Quantitative Real-time PCR (qRT-PCR) was performed using the Step One Plus Real-Time PCR System (Life Techonologies, Carlsbad, CA). Total RNA (150 ng) was reverse transcribed with oligo$(dT)_{20}$ primers and superscript III reverse transcriptase (Life Techonologies, Carlsbad, CA). 1 µl of the cDNA was used as template in subsequent qRT-PCR reactions. The qRT-PCR reaction was performed with the Power SYBR Green Master Mix (Life Techonologies, Carlsbad, CA) and custom primers (Appendix 1). The integrity of the PCR reaction was verified by melt curve analysis.

Statistical Analysis

Student's t tests, one-way analysis of variance (AVONA), and repeated measures one-way ANOVA were used for between-group comparisons. Post hoc analysis were conducted using Tukey's test. All data are presented as mean ± S.E.M.

3.3. Results

3.3.1. KU-596 Improves Sensory Functions and Mitochondrial Bioenergetics in Diabetic Swiss Webster Mice in a Dose-dependent Manner

Because it is unclear whether KU-596 exhibited similar *in vivo* effects on improving sensory and bioenergetic deficits of DPN, this was examined using Swiss Webster mice rendered diabetic with STZ. By 8 weeks of diabetes, the mice developed significant mechanical and thermal hypoalgesia (Figure 3.3-1, B and C). Once a week dosing of 2 mg/kg, 10 mg/kg, or 20 mg/kg KU-596 was initiated at week 9, and the treatment was continued for 6 weeks before termination of the study. After 14 weeks of diabetes, STZ-rendered diabetic mice displayed significantly elevated FBG and HbA1c levels, and KU-596 did not affect these metabolic parameters in the mice (Table 3.3-1). In contrast, 6-

week of KU-596 treatment resulted in significantly improved mechanical, thermal sensitivity. KU-596 also dose-dependently improved motor and sensory NCV (Figure 3.3-1, B-D). Both the 10 and 20 mg/kg doses showed similar efficacy in improving the sensory and NCV deficits suggesting that 10 mg/kg is likely a saturating dose. As the drug is dosed once per week, this translates to 1.42 mg/kg/day. Based on allometric scaling, the corresponding dose in a 70 kg human would be 0.73 mg/kg/day.

Table 3.3-1: Weight, FBG, and HbA1c of Swiss Webster mice.

Treatment	**Weight g**	**FBG mg/dl**	**HbA1c %(mmol/mol)[a]**	***n***
Veh + Veh	35.6 ±2.4	153 ±42	5.2 ±0.1 (33.3 ±1.1)	6
STZ + Veh	27.9 ±2.2*	596 ±7*	13.0 ±0.0* (118.6 ±0.0)	5
STZ + 2mg/kg KU-596	30.4 ±2.5*	554 ±113*	12.6 ±0.6* (114.2 ±6.6)	6
STZ + 10mg/kg KU-596	30.6 ±2.1*	525 ±128*	11.9 ±1.3* (106.6 ±14.3)	7
STZ + 20mg/kg KU-596	29.0 ±2.0*	600*	12.9 ±0.1* (117.5 ±1.1)	7
Veh + 20mg/kg KU-596	34.1 ±1.4	128 ±10	5.1 ±0.2 (32.2 ±0.2)	7

Veh, vehicle.
[a] mmol of HbA1c/mol of hemoglobin.
*$p < 0.05$ versus Veh + Veh.

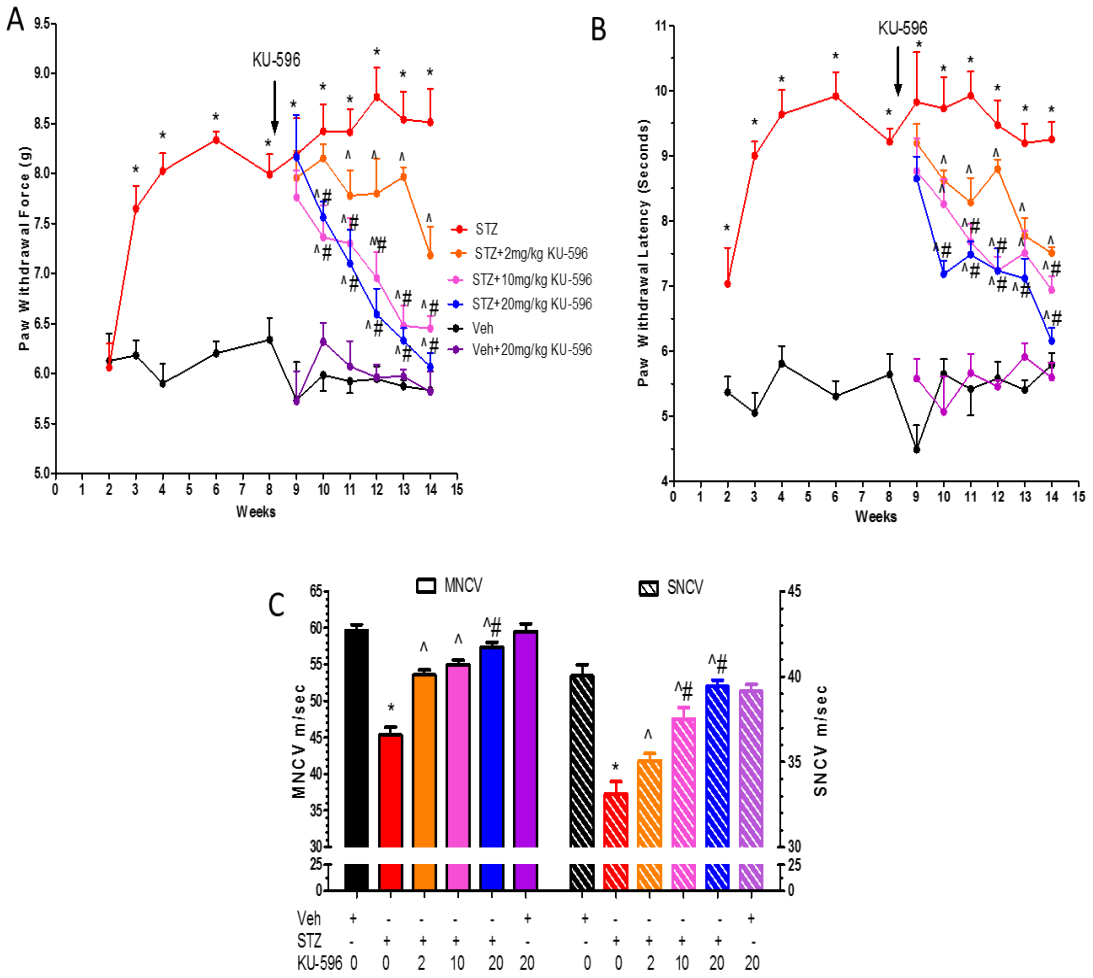

Figure 3.3-1: Dose response of KU-596 in reversing mechanical, thermal hypoalgesia and NCV deficits in diabetic Swiss Webster mice.

(A) Mechanical and (B) Thermal hypoalgesia in Swiss Webster mice at the indicated week of diabetes and weekly KU-596 therapy initiated after being diabetic for 8 weeks. (C) Effects of 6 weeks of KU-596 treatment on MNCV and SNCV. *, $p < 0.05$ vs. Veh+Veh; ^, $p < 0.05$ vs. STZ+Veh; #, $p < 0.05$ versus time-matched STZ + 2 mg/kg KU-596.

To determine whether the changes in psychosensory function and NCV were accompanied by improvements in mtBE, sensory neurons were isolated from the L_4-L_6 lumbar ganglia at the end point of the study for bioenergetics measurement. After 14 weeks of diabetes, the diabetic sensory neurons showed a significant decline in maximal respiratory capacity (MRC) and spare respiratory capacity (SRC) (Figure 3.3-2). Consistent with improvements in the sensory parameters of DPN, 6-week of KU-596 treatment significantly improved mtBE of diabetic sensory neurons in a dose-dependent manner, with the 20mg/kg dose being the most effective. Thus, all subsequent studies were performed using a once per week 20 mg/kg dosing of KU-596.

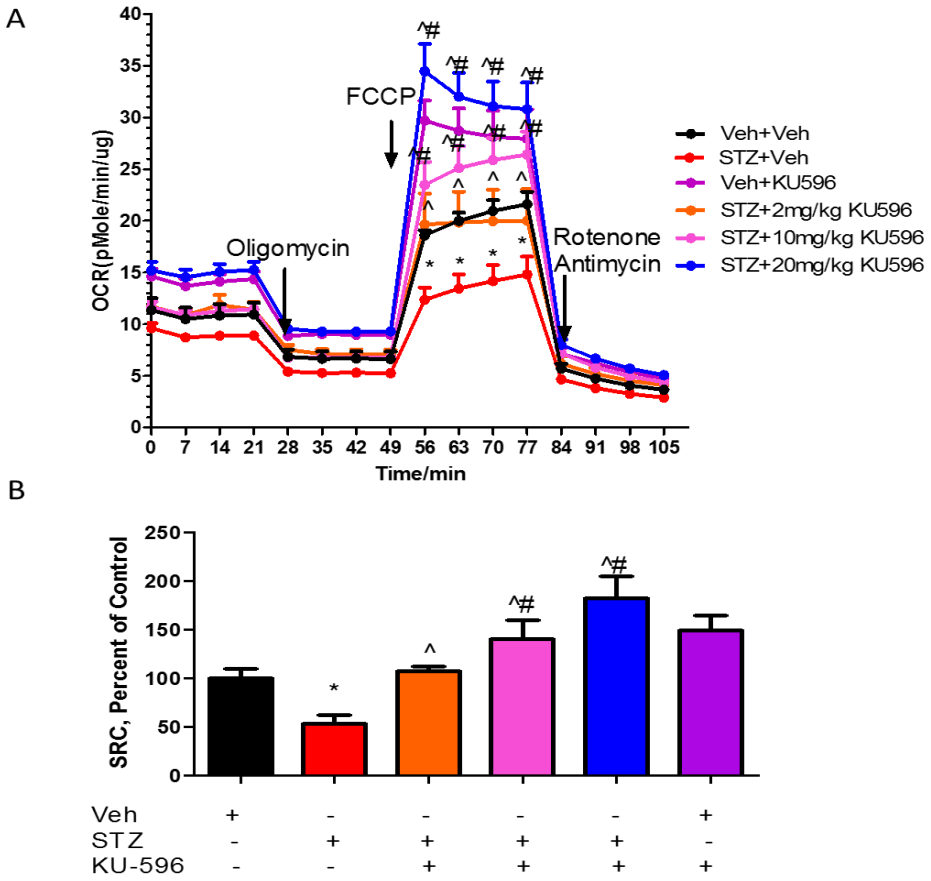

Figure 3.3-2: KU-596 improves mitochondrial bioenergetics in Swiss Webster mice.

(A) KU-596 improves mitochondrial bioenergetics in the sensory neurons of diabetic Swiss Webster mice in a dose-dependent manner. B) Spare respiratory capacity (SRC) was quantified and expressed as percent of the control group (Veh +Veh). Weekly injection of KU-596 increased SRC in a dose-dependent manner. *, $p < 0.05$ vs. Veh+Veh; ^, $p < 0.05$ vs. STZ+Veh; #, $p < 0.05$ versus time-matched STZ + 2 mg/kg KU-596.

3.3.2. KU-596 Improves Sensory Parameters in an Hsp70-dependent Manner

In our previous studies, the neuroprotective efficacy of KU-32 in reversing the psychosensory, electrophysiologic and bioenergetic deficits required the presence of Hsp70 as neuropathic Hsp70 KO mice were insensitive to drug treatment (Ma et al., 2014; Urban et al., 2010). In the current study, we determined whether the efficacy of KU-596 also requires stress-inducible Hsp70. In this regard, C57Bl/6 and Hsp70 KO mice were rendered diabetic with STZ. After 12 weeks of diabetes, the mice were administered 20 mg/kg KU-596 via oral gavage weekly for 4 weeks. By 12 weeks of diabetes, WT and Hsp70 KO diabetic mice showed significant decreases in their response to mechanical or thermal stimuli (Figure 3.3-3). In contrast, whereas 4-week of KU-596 treatment significantly reversed sensory hypoalgesia in the WT mice (Figure 3.3-3, A and C), drug treatment did not alter any of the sensory parameters in Hsp70 KO mice (Figure 3.3-3, B and D). Similar to our previous results with KU-32, both genotypes developed extensive diabetes and neither FBG, a measure of immediate blood glucose levels, nor HbA1c, a long-term measure of blood glucose control, were affected by novologue therapy (Table 3.3.2). Thus, the above results suggest that the novologue KU-596 also reverses sensory deficits of DPN in an Hsp70-dependent manner.

Of note, since RNA-Seq analysis of the DRG was to be performed, we did not assess NCV in these animals to avoid any potential changes in transcript expression due to insertion of the electrophysiolgic probes. Similarly, mtBE were not assessed as the DRG were used to isolate RNA.

Table 3.3-2: Weight and FBG of C57Bl/6 and Hsp70 KO Mice.

	C57Bl/6				Hsp70 KO			
Treatment	**Weight g**	**FBG mg/dl**	**HbA1c %(mmol/mol)[a]**	**n**	**Weight g**	**FBG mg/dl**	**HbA1c %(mmol/mol)[a]**	**n**
Veh + Veh	34.6 ± 6.7	145 ±12	4.6 ±0.2 (26.8 ±2.2)	7	28.1 ± 5.5	177 ±20	5.0 ±0.3 (31.1 ±3.3)	9
STZ + Veh	22.6 ± 2.0*	540 ±48*	9.1 ±1.3* (76.0 ±14.3)	6	23.2 ± 3.0*	524 ±80*	11.1 ±3.3* (97.8 ±36.3)	10
Veh + KU-596	33.9 ± 4.5	157 ±20	4.4 ±0.2 (24.6 ±2.2)	7	27.0 ± 5.1	168 ±19	5.2 ±0.2 (33.3 ±2.2)	8
STZ + KU-596	25.1 ± 3.2*	499 ±82*	9.3 ±2.7* (78.1 ±29.7)	7	22.0 ± 2.8*	573 ±32*	10.3 ±2.4* (89.1 ±26.4)	9

Veh, vehicle.

[a] mmol of HbA1c/mol of hemoglobin.

*$p < 0.05$ versus Veh + Veh.

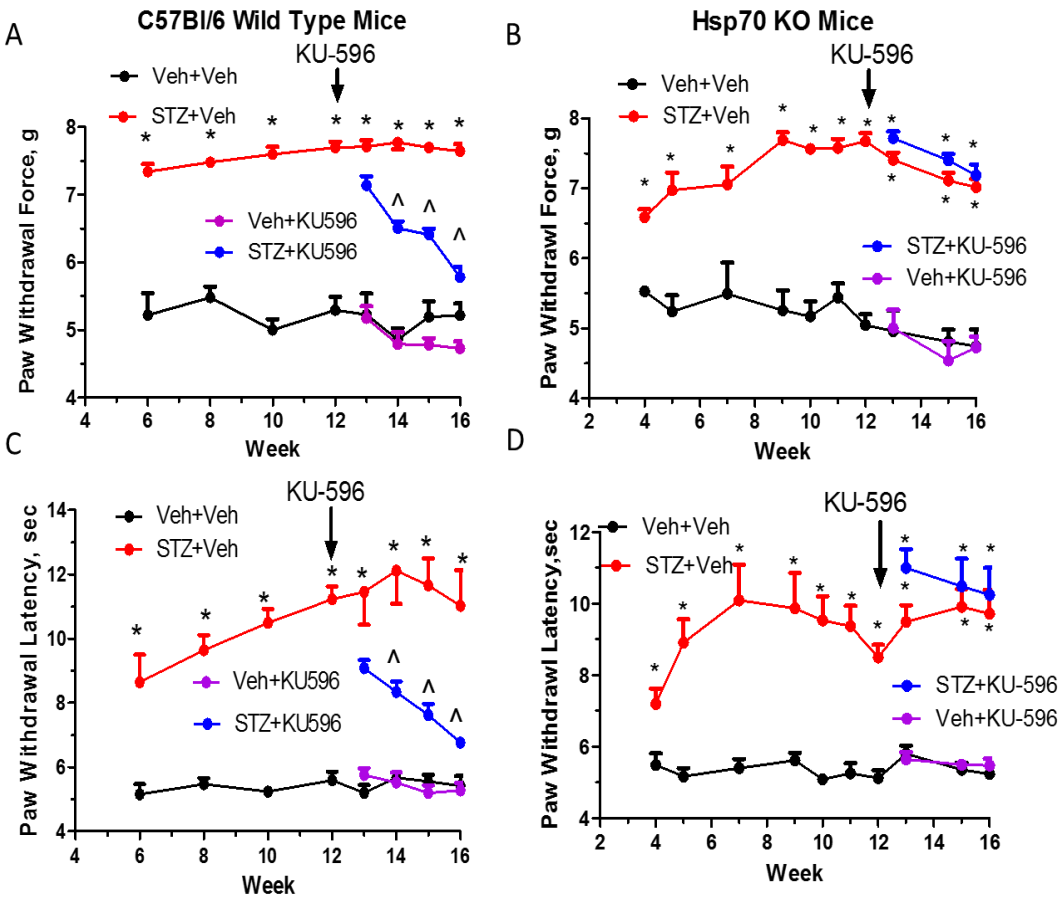

Figure 3.3-3: KU-596 Reverses Sensory Deficits in Diabetic Mice in an Hsp70-dependent manner.

STZ-rendered diabetic mice developed significant sensory hypoalgesia regardless of genotype by 12-week of diabetes, at which time point KU-596 treatment was initiated. Mechanical (A) and thermal (C) hypoalgesia was partially reversed by 4 weeks of KU-596 treatment in C57Bl/6 mice. In contrast, 4-week of drug treatment did not have any effect in reversing mechanical (B) or thermal (D) deficits in the Hsp70 KO mice. *, $p < 0.05$ vs. Veh+Veh; ^, $p < 0.05$ vs. STZ+Veh.

3.3.3. RNA-Seq Analysis of Sensory Neurons in C57Bl/6 Mice

To determine the transcriptome changes within sensory neurons that contribute to the reversal of insensate DPN, we performed a RNA-Seq analysis using RNA isolated from L_4-L_6 lumbar DRG. In diabetic sensory neurons from WT mice, of the 23,112 genes detected by RNA-Seq, 39.6% were expressed too low or went undetected for statistical analysis yielding 13,959 genes that were statistically analyzed. Of these genes, 343 were significantly modified in diabetic WT compared to control neurons (Figure 3.3-4A). KU-596 treatment induced significant alterations in 174 genes in diabetic sensory neurons (Figure 3.3-4B) and 42 genes in control sensory neurons. Among the subset of transcripts that were significantly altered by diabetes in the absence or presence of KU-596, 67/70 were increased in expression in the diabetic neurons. Impressively, KU-596 treatment reversed this trend and consistently decreased transcript expression in an almost quantitatively opposite direction (Table 3.3-3).

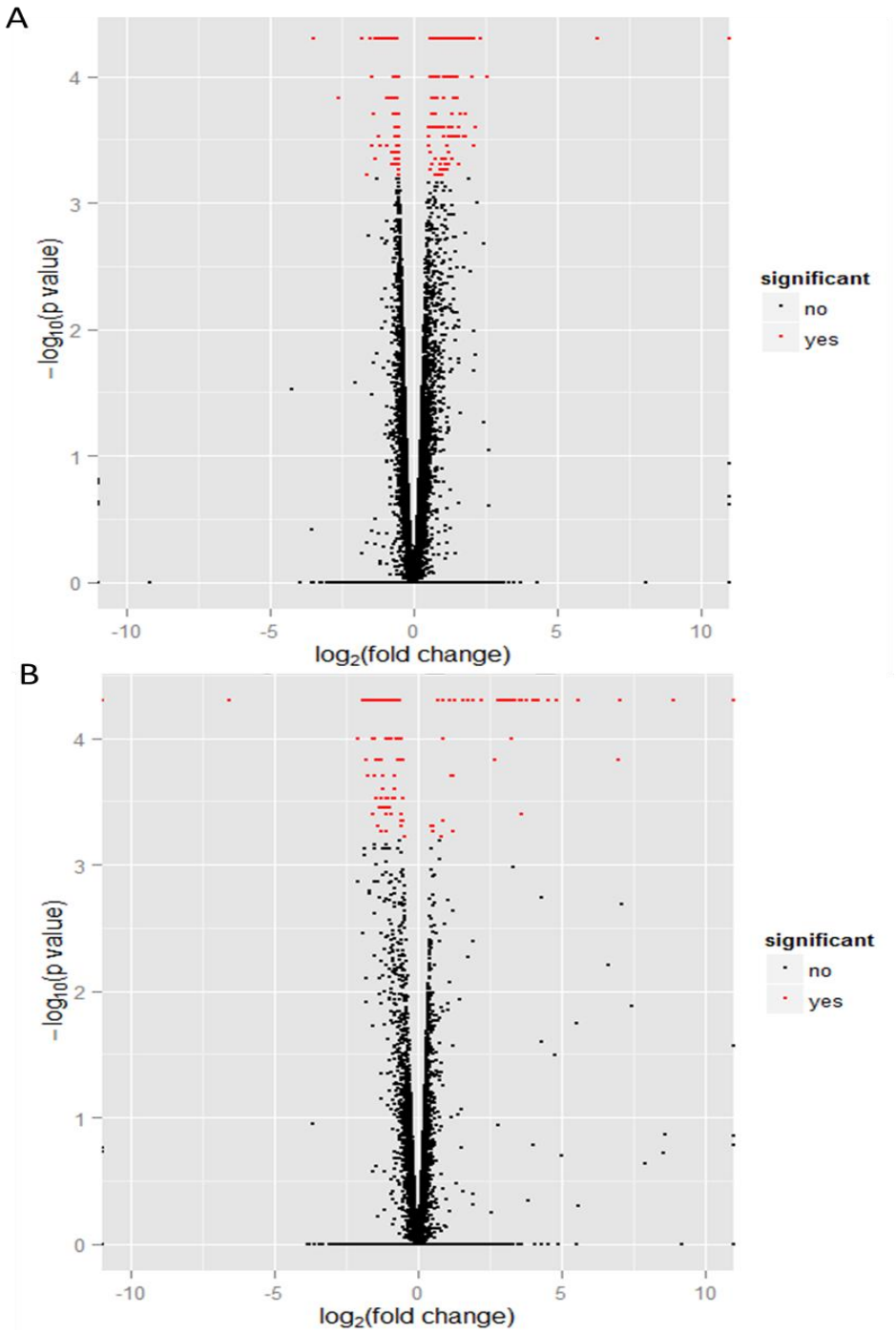

Figure 3.3-4: Volcano plots for differential gene expression in C57Bl/6 mice.

Volcano plots comparing the normalized expression of genes in the sensory neurons of STZ+Veh versus Veh+Veh group (A), and STZ+KU-596 versus STZ+Veh group (B). Y-axis, negative log of p value; x-axis, log_2-transformed fold change; red dots, significantly altered genes; black dots, non-significant genes.

Table 3.3-3: List of significantly altered transcripts common to diabetic sensory neurons from vehicle and KU-596 treated mice.

	Veh+Veh vs STZ+Veh	STZ+Veh vs STZ+KU-596		Veh+Veh vs STZ+Veh	STZ+Veh vs STZ+KU-596
Gene	Log_2(fold change)	Log_2(fold change)	Gene	Log_2(fold change)	Log_2(fold change)
Acer2	0.90	-0.94	Lrg1	1.17	-1.15
Agxt2l1	1.47	-0.83	Ltf	0.98	-1.43
Alas2	1.66	-1.25	Ly6c2	1.38	-1.53
Anxa1	0.91	-1.03	Lyz2	1.29	-0.98
Arhgdib	1.15	-0.99	Mki67	0.63	-1.02
Beta-s	2.01	-1.40	Mmp8	1.45	-1.68
C1qa	1.17	-0.84	Mmp9	1.10	-1.52
C1qb	1.06	-0.61	Mpeg1	0.75	-0.71
C1qc	1.30	-0.68	Mpo	1.26	-1.66
C3	0.70	-0.92	Ms4a6b	1.34	-1.10
Camp	1.36	-1.20	Mt2	1.53	-0.87
Ccl6	1.51	-1.24	Ncf1	1.15	-1.01
Cd163	1.59	-1.09	Nckap1l	0.84	-0.74
Cd177	1.52	-1.83	Net1	0.89	-0.53
Cd53	1.16	-0.98	Ngp	1.25	-1.43
Chi3l3	1.89	-1.82	Npy1r	0.77	-0.51
Ctgf	1.38	-0.91	Plbd1	1.00	-0.93
Ctss	0.91	-0.66	Pld4	1.10	-0.79
Cybb	0.97	-0.99	Prg2	1.53	-1.58
F13a1	1.05	-0.84	Prtn3	1.45	-1.34
F3	0.81	-0.60	Rac2	1.08	-0.91
Fabp4	1.62	-1.69	Retnlg	1.51	-1.69
Fam107a	1.18	-0.71	S100a8	1.26	-1.57
Fcgr3	1.04	-0.85	S100a9	1.30	-1.54
Fkbp5	0.54	-0.56	Slc4a1	1.31	-1.60
Fmo2	0.73	-0.54	Slfn2	1.43	-1.10
Galntl2	1.04	-0.85	Sult1a1	1.00	-0.56
Gypa	1.25	-1.33	Txnip	1.12	-0.46
Hbb-b1/2	2.08	-1.44	Tyrobp	1.17	-1.12
Hcls1	1.02	-0.94	Zbtb16	1.00	-1.09
Hp	1.52	-1.68	4632428N05Rik	0.87	-0.96
Ifitm6	1.55	-1.56			
Igj	1.66	-1.57	Hal	-1.17	0.82
Itgam	0.87	-1.12	Hivep3	-0.73	0.55
Itgb2	1.00	-1.12	Zfhx2	-0.76	0.52
Lcn2	1.52	-1.65			

Ingenuity Pathway Analysis of differentially expressed transcripts revealed that inflammatory pathways were among the top canonical pathways enriched in STZ+Veh as well as STZ+KU-596 genes (Figure 3.3-5). Other top enriched canonical pathways mainly involved chemotaxis of immune cells, which are also indicative of altered inflammatory responses. The majority of inflammatory genes altered in STZ+Veh group were upregulated (Figure 3.3-6A), which further support the involvement of inflammation in the pathogenesis of DPN (Navarro and Mora, 2005). KU-596 significantly reversed diabetes-induced changes in a number of inflammatory genes in the sensory neurons (Figure 3.3-6B), suggesting that modulation of inflammatory pathways might contribute to the neuroprotective effects of KU-596. Unexpectedly, differential expression of the mitochondrial transcriptome was not overrepresented in either STZ+Veh or STZ+KU-596 group. This observation suggests that the alterations in mtBE observed in our study were not due to transcriptome changes in genes involved in mitochondrial function, although we have previously reported that diabetes decreases the expression of numerous mitochondrial proteins (Akude et al., 2011). Thus, diabetes and KU-596 likely exert effects on mtBE at the protein level. In contrast, a number of genes encoding proteins involved in the production of ROS were increased in the STZ+Veh group (Figure 3.3-7A) and decreased in the STZ+KU-596 group (Figure 3.3-7B). These data are consistent with the ability of KU-32 to decrease glucose-induced superoxide production in hyperglycemically stressed embryonic sensory neurons (Zhang et al., 2012).

A

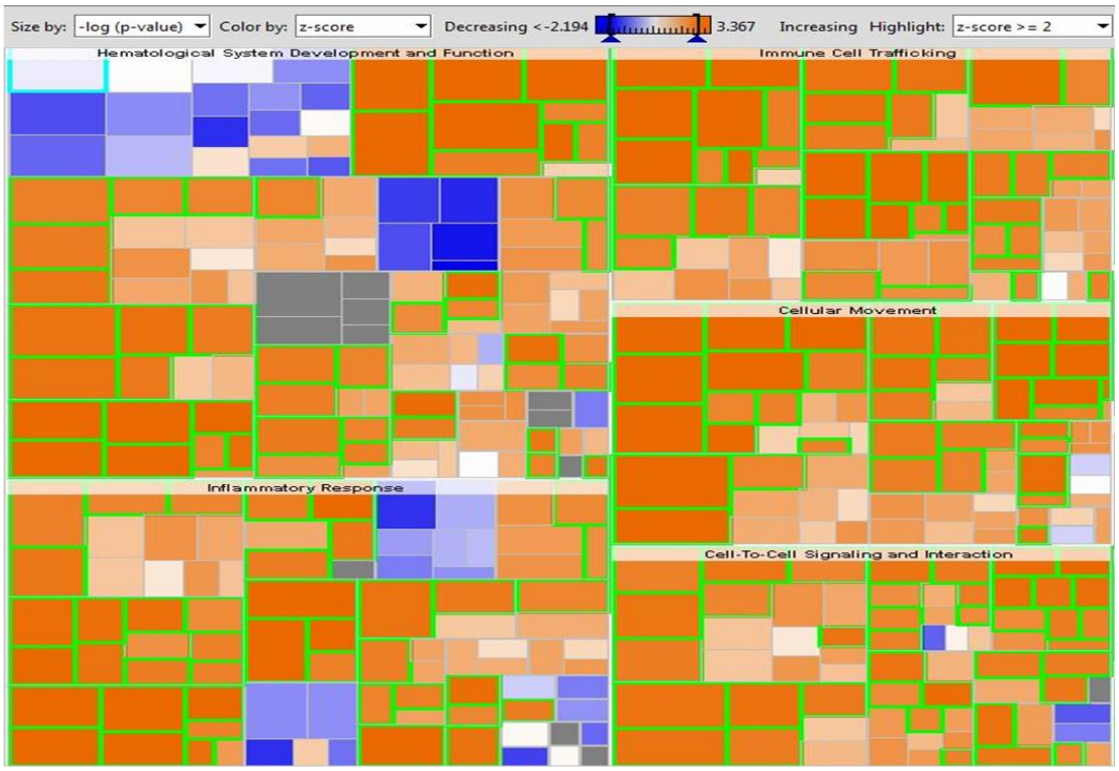
Size by: -log (p-value)
Color by: z-score
Decreasing <-2.194
3.367
Increasing
Highlight: z-score >= 2
Hematological System Development and Function
Immune Cell Trafficking
Cellular Movement
Inflammatory Response
Cell-To-Cell Signaling and Interaction

B

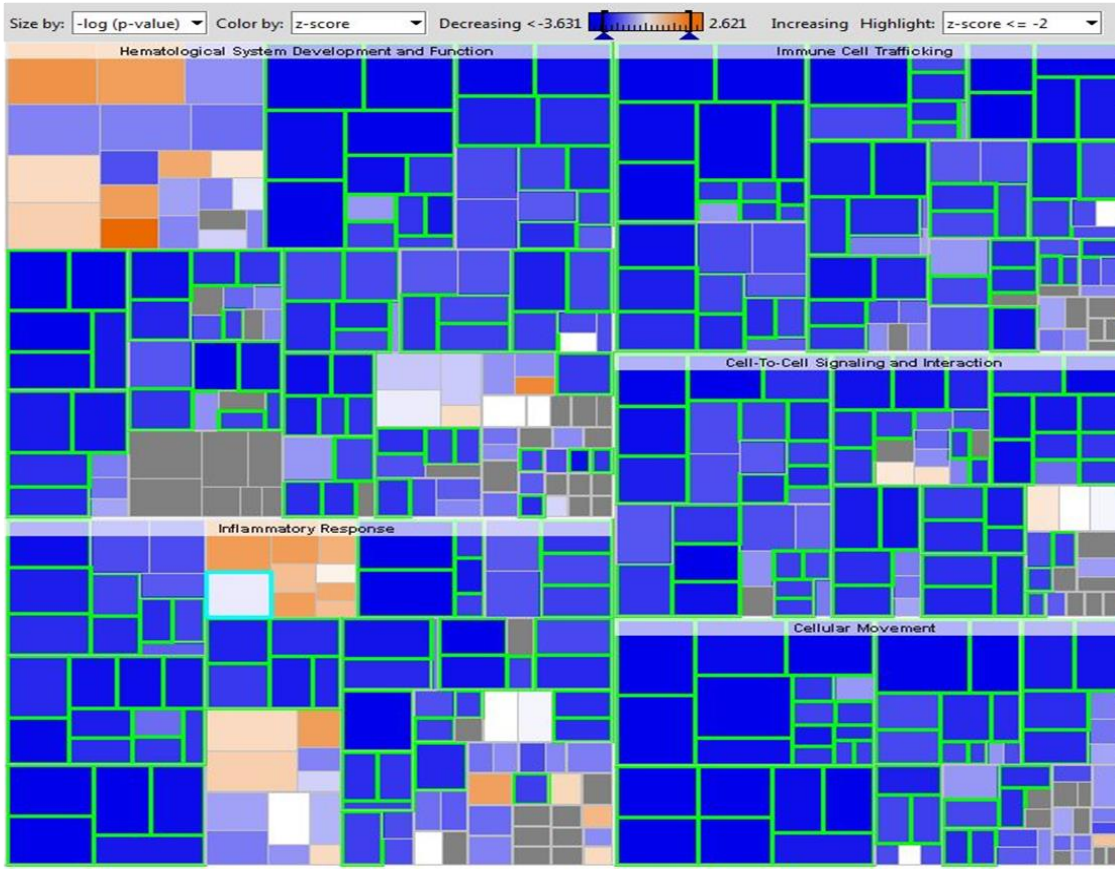
Size by: -log (p-value)
Color by: z-score
Decreasing <-3.631
2.621
Increasing
Highlight: z-score <= -2
Hematological System Development and Function
Immune Cell Trafficking
Cell-To-Cell Signaling and Interaction
Inflammatory Response
Cellular Movement

Figure 3.3-5: Heatmap representation of significantly altered gene categories in C57Bl/6 mice.

Significantly altered gene categories in STZ+Veh versus Veh+Veh group (A), and STZ+KU-596 versus STZ+Veh group (B). The squares represent significantly altered genes under each category; the size of the square was determined by the negative log of the p-value of the gene it represents; the color of the square was determined by the activation z-score, with orange representing increasing and blue representing decreasing. Genes with a z-score ≥ 2 in (A) or ≤ 2 in (B) were highlighted in green lines.

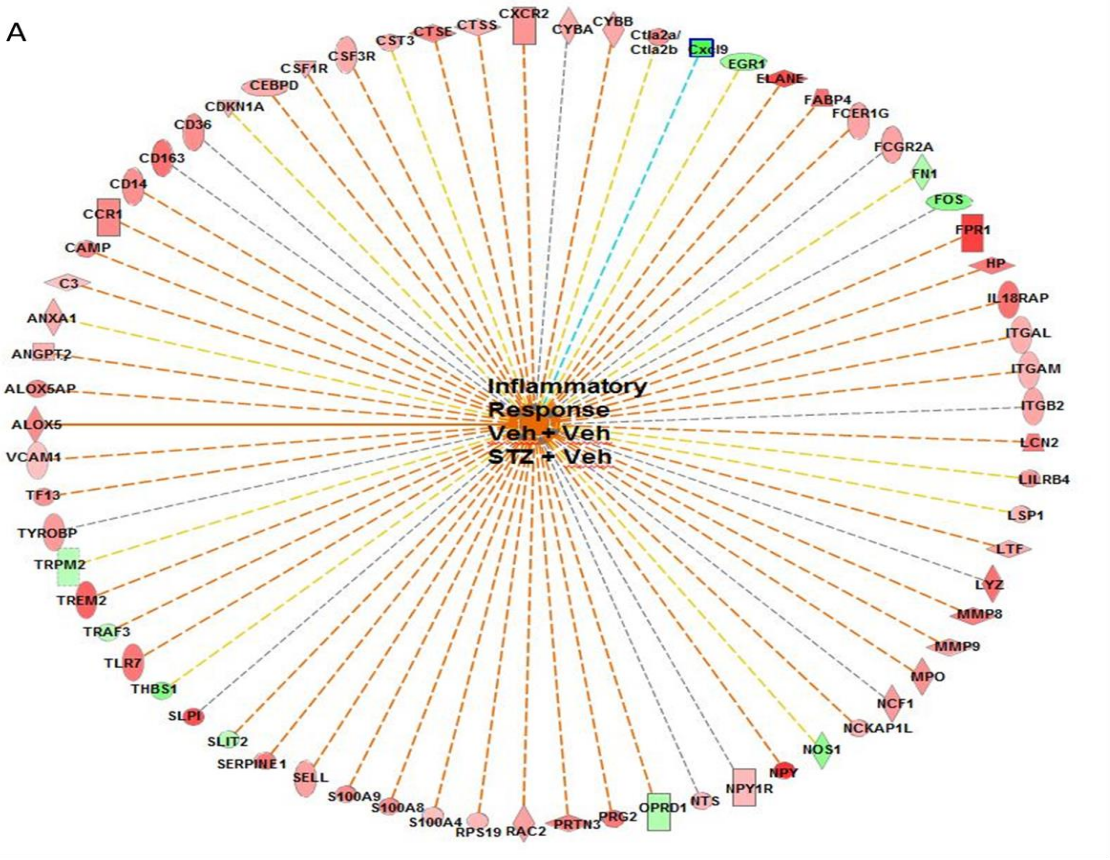
A
Inflammatory Response Veh + Veh STZ + Veh
CXCR2
CYBA
CYBB
Ctla2a/ Ctla2b
Cxcl9
EGR1
ELANE
FABP4
FCER1G
FCGR2A
FN1
FOS
FPR1
HP
IL18RAP
ITGAL
ITGAM
ITGB2
LCN2
LILRB4
LSP1
LTF
LYZ
MMP8
MMP9
MPO
NCF1
NCKAP1L
NOS1
NPY
NPY1R
NTS
OPRD1
PRG2
PRTN3
RAC2
RPS19
S100A4
S100A8
S100A9
SELL
SERPINE1
SLIT2
SLPI
THBS1
TLR7
TRAF3
TREM2
TRPM2
TYROBP
TF13
VCAM1
ALOX5
ALOX5AP
ANGPT2
ANXA1
C3
CAMP
CCR1
CD14
CD163
CD36
CDKN1A
CEBPD
CSF1R
CSF3R
CST3
CTSE
CTSS

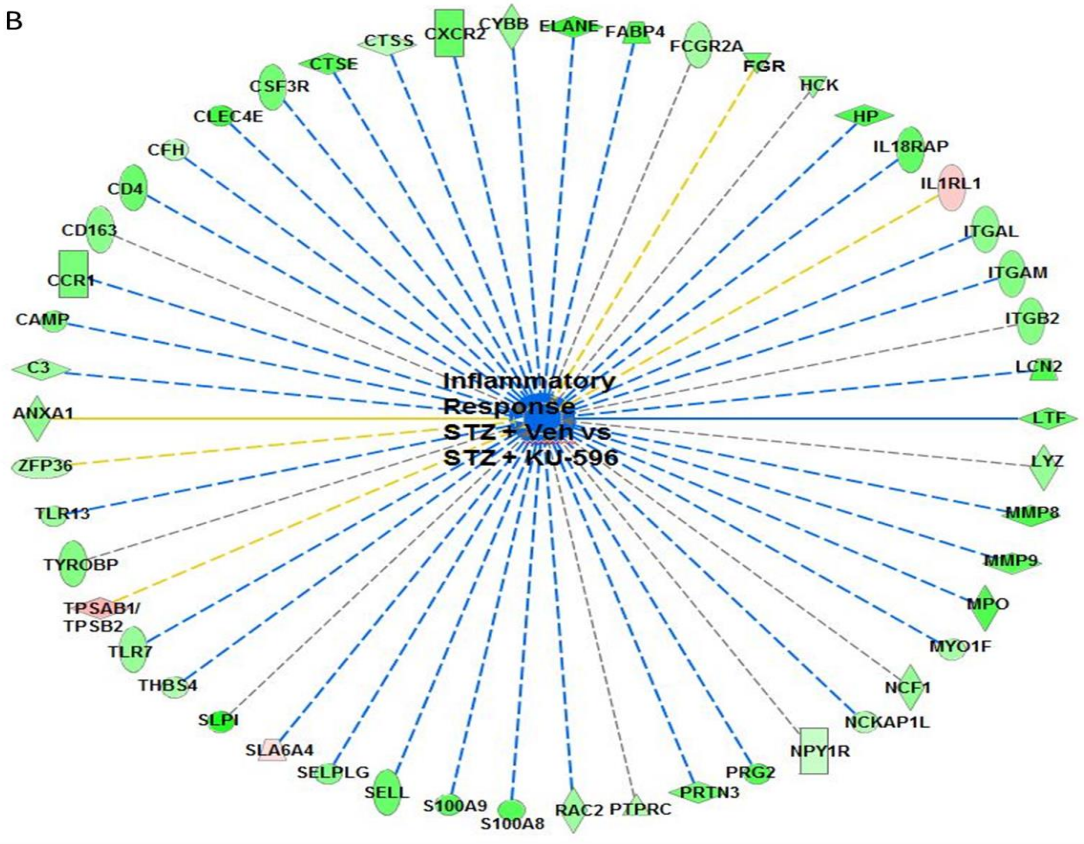
B
Inflammatory Response STZ + Veh vs STZ + KU-596
CXCR2
CYBB
ELANE
FABP4
FCGR2A
FGR
HCK
HP
IL18RAP
IL1RL1
ITGAL
ITGAM
ITGB2
LCN2
LTF
LYZ
MMP8
MMP9
MPO
MYO1F
NCF1
NCKAP1L
NPY1R
PRG2
PRTN3
PTPRC
RAC2
S100A8
S100A9
SELL
SELPLG
SLA6A4
SLPI
THBS4
TLR7
TPSAB1/ TPSB2
TYROBP
TLR13
ZFP36
ANXA1
C3
CAMP
CCR1
CD163
CD4
CFH
CLEC4E
CSF3R
CTSE
CTSS

Figure 3.3-6: Significantly altered genes involved in inflammatory response in C57Bl/6 mice.

Significantly altered genes involved in inflammatory response between Veh+Veh and STZ+Veh conditions (A), and between STZ+Veh and STZ+KU-596 conditions (B). Red indicates upregulation of the genes, and green indicates downregulation of the genes. The degree of change is indicated by the color intensity, a higher color intensity indicating a more extreme change. Different colors of the connecting lines represent predicted effects of the change of a molecule to the inflammatory response: orange line leads to activation, blue line leads to inhibition, yellow line indicates a finding inconsistent with the activation state of the downstream molecule, and gray line indicates an effect is not predicted.

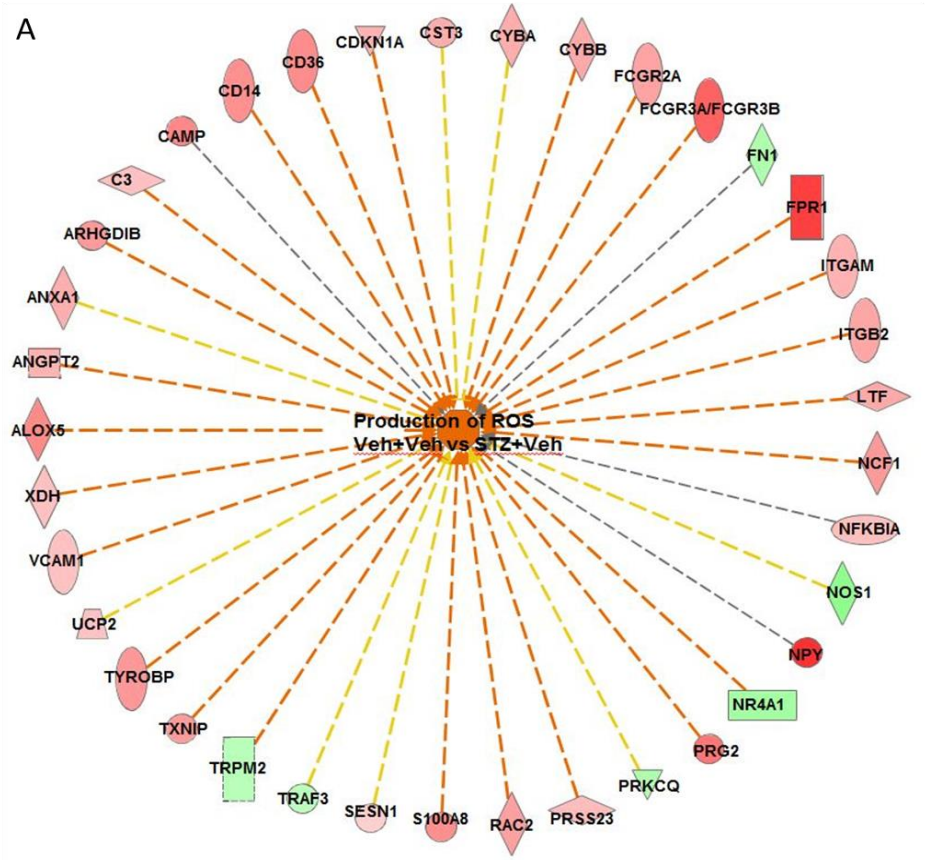
A
CDKN1A
CST3
CYBA
CYBB
CD36
CD14
FCGR2A
FCGR3A/FCGR3B
CAMP
FN1
C3
FPR1
ARHGDIB
ITGAM
ANXA1
ITGB2
ANGPT2
LTF
Production of ROS
Veh+Veh vs STZ+Veh
ALOX5
NCF1
XDH
NFKBIA
VCAM1
NOS1
UCP2
NPY
TYROBP
NR4A1
TXNIP
PRG2
TRPM2
PRKCQ
TRAF3
SESN1
S100A8
RAC2
PRSS23

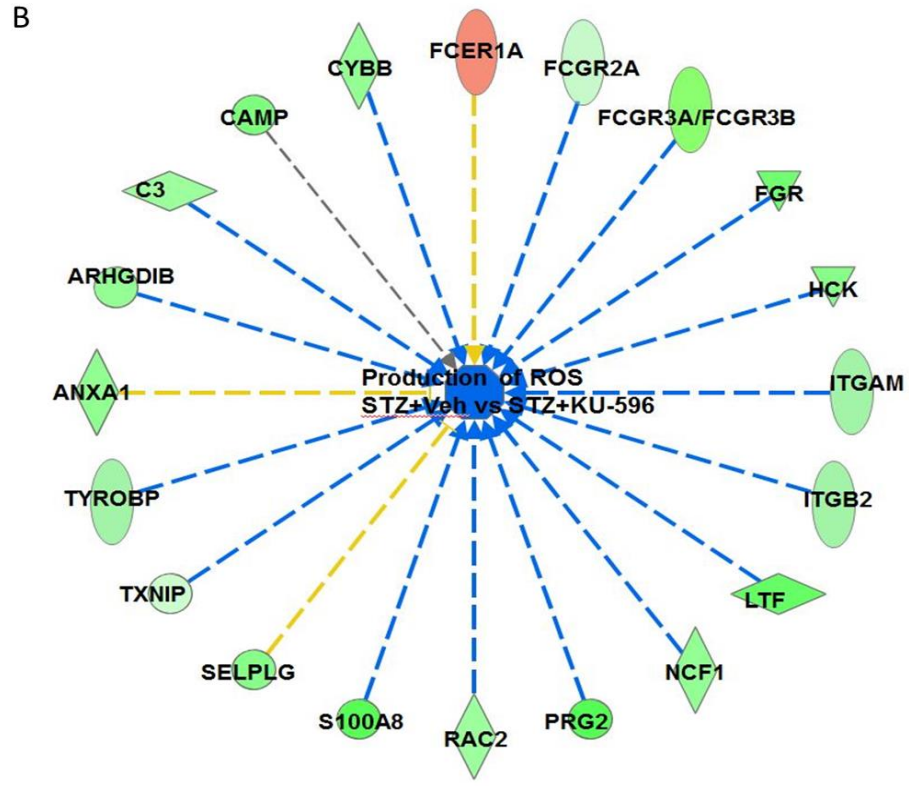
B
CYBB
FCER1A
FCGR2A
CAMP
FCGR3A/FCGR3B
C3
FGR
ARHGDIB
HCK
ANXA1
Production of ROS
STZ+Veh vs STZ+KU-596
ITGAM
TYROBP
ITGB2
TXNIP
LTF
SELPLG
NCF1
S100A8
RAC2
PRG2

Figure 3.3-7: Significantly altered genes involved in the production of ROS in C57Bl/6 mice.

Significantly altered genes involved in ROS production between Veh+Veh and STZ+Veh conditions (A), and between STZ+Veh and STZ+KU-596 conditions (B). Red indicates upregulation of the genes, and green indicates downregulation of the genes. The degree of change is indicated by the color intensity, the higher the color intensity indicates a more extreme change. Different colors of the connecting lines represent the predicted effects of the change of a molecule to the production of ROS: orange line leads to activation, blue line leads to inhibition, yellow line indicates a finding inconsistent with the activation state of the downstream molecule, and a gray line indicates an effect is not predicted.

To validate the RNA-seq analysis, several genes that were altered in both STZ+Veh and STZ+KU-596 group were chosen for qRT-PCR analysis in independent samples. Due to limits in the amounts of RNA we obtained from each DRG sample, we selected 8 genes with FPKM $\geq$ 5 for qRT-PCR analysis (TXNIP, S100A8, LTF, FKBP5, ARHGDIB, FABP4, LCN2, CCL6). Although due to small sample sizes (n=3 in each group), only TXNIP and FKBP5 showed statistical significance, the other selected genes also followed similar trends in the qRT-PCR analysis (Figure 3.3-7A) as compared to the RNA-Seq data (Figure 3.3-7B). Collectively, these data suggest that KU-596 can reverse transcriptome alternations in the sensory neurons of STZ-rendered type 1 diabetic mice.

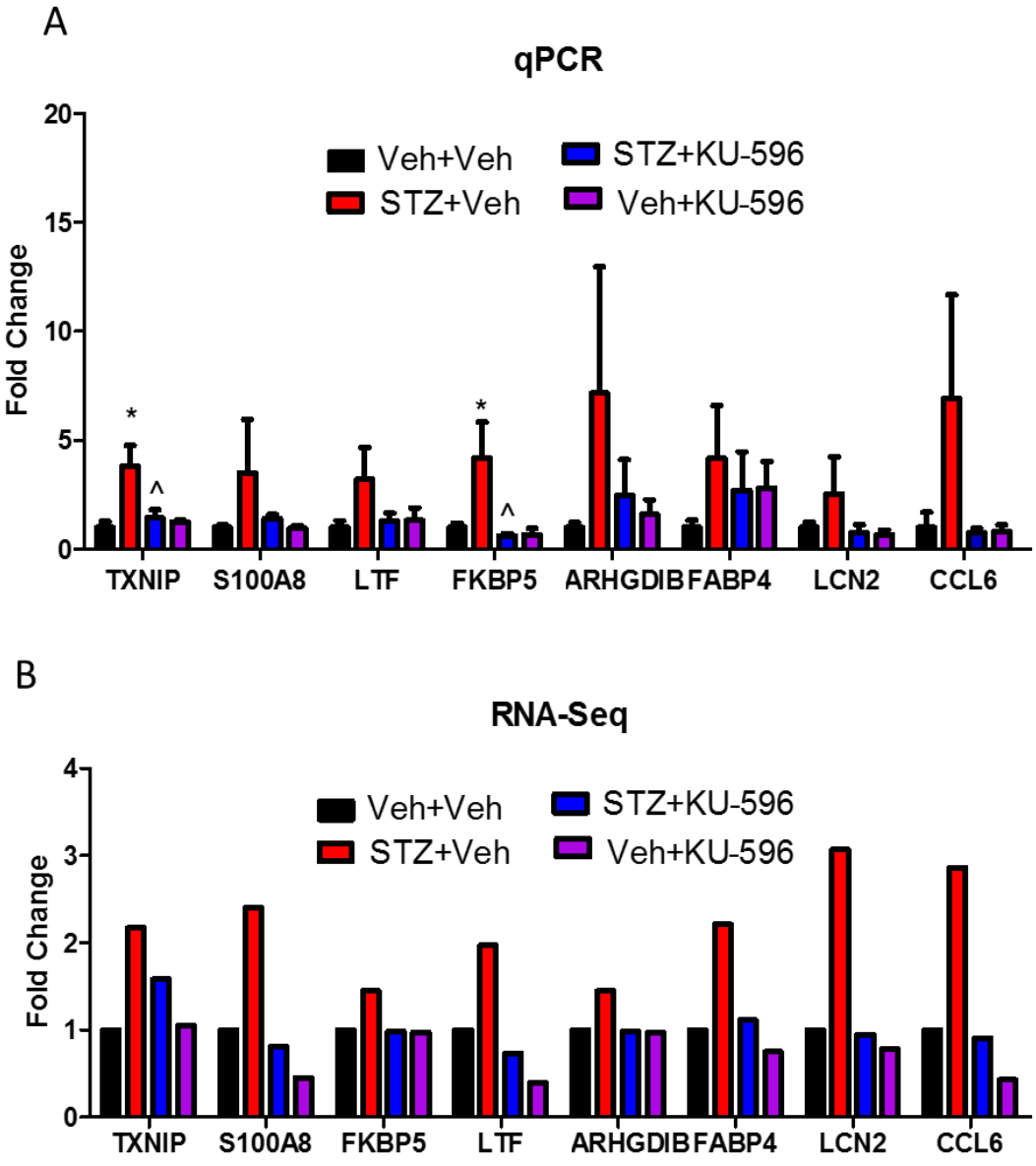

Figure 3.3-8: qRT-PCR validation of RNA-Seq data in C57Bl/6 mice.

(A) Total RNA was prepared for mRNA quantification by standard qRT-PCR. Tubulin was used as the internal control. Each group consisted of three samples. The data were expressed as fold change versus Veh+Veh for each gene. *, $p < 0.05$ vs. Veh+Veh; ^, $p < 0.05$ vs. STZ+Veh; n=3. (B) Fold change versus Veh+Veh using the FPKM normalized reads obtained from RNA-Seq.

3.3.4. RNA-Seq Analysis of Sensory Neurons from Hsp70 KO Mice

To determine transcriptome changes induced by KU-596 that were Hsp70-dependent, RNA was isolated from the Hsp70 KO mice and used for RNA-seq analysis. The genomic structures of Hsp70 in WT versus the Hsp70 KO mice were displayed in the Appendix 2. Unexpectedly, of the 23,112 genes detected by RNA-seq, only 101 were significantly modified in diabetic sensory neurons (Figure 3.3-9A). On the other hand, KU-596 treatment significantly altered 242 genes in the diabetic sensory neurons (Figure 3.3-9B) and 37 genes in control sensory neurons. Among the significantly altered transcripts, 31 were increased in diabetic neurons and decreased by KU-596 treatment (Table 3.3-4). Comparison between genes significantly altered in WT and Hsp70 KO mice revealed little overlap: of the genes affected by KU-596 in diabetic sensory neurons, there were 8 genes altered in both genotypes and 8 genes altered only in C57Bl/6 but not Hsp70 KO mice.

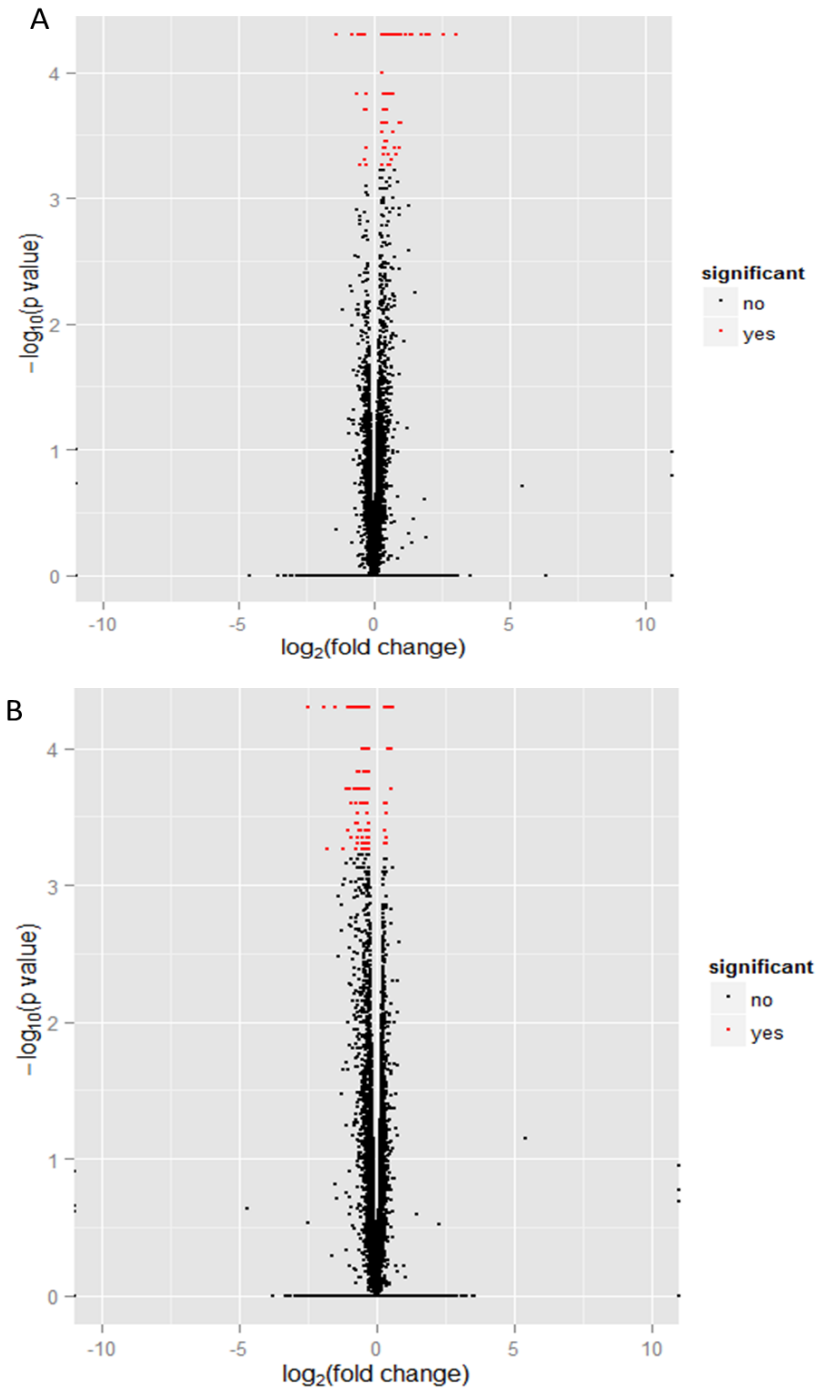

Figure 3.3-9: Volcano plots for differential gene expression in Hsp70 KO mice.

Volcano plots comparing the normalized expression of genes in the sensory neurons of STZ+Veh versus Veh+Veh group (A), and STZ+KU-596 versus STZ+Veh group (B). Y-axis, negative log of p value; x-axis, log_2-transformed fold change; red dots, significantly altered genes; black dots, non-significant genes.

Table 3.3-4：List of genes upregulated in diabetic sensory neurons and downregulated by KU-596 treatment in Hsp70 KO mice.

	Veh+Veh vs STZ+Veh	STZ+Veh vs STZ+KU-596		Veh+Veh vs STZ+Veh	STZ+Veh vs STZ+KU-596
Gene	**Log_2(fold change)**	**Log_2(fold change)**	**Gene**	**Log_2(fold change)**	**Log_2(fold change)**
1500015A07Rik	2.0436	-0.62406	**H2-Ab1**	0.317947	-0.65519
Acp5	1.31424	-1.5356	**Ifi27l2a**	0.881136	-1.05258
Apod	0.344651	-0.64443	**Ifit1**	0.396187	-0.40826
C1qa	0.57526	-0.76349	**Ifitm3**	0.408975	-0.34488
C1qb	0.39586	-0.76585	**Iigp1**	0.973369	-0.53836
C1qc	0.390653	-0.56792	**Lyz2**	0.525966	-0.55338
Ccl8	1.7593	-1.11681	**Mmp9**	0.530685	-0.63794
Cd74,Mir5107	0.331849	-0.60352	**Mpo**	0.655659	-1.06418
Col1a1	0.588773	-0.94085	**Ms4a7**	0.921042	-0.94733
Col1a2	0.393786	-0.5556	**Nckap1l**	0.594368	-0.6136
Cst3	0.294541	-0.27093	**Ndufb2**	0.351165	-0.51403
Ctss	0.56015	-0.71955	**Rpl39**	0.477781	-0.55082
Cxcl16	0.564734	-0.81446	**S100a1**	0.379494	-0.52036
Fam65a,Mir1966	2.557	-2.48583	**S100a4**	0.456091	-0.55616
Gfap	1.18752	-0.97605	**Trf**	0.374662	-0.48973
H2-Aa	0.406471	-0.70817			

Despite the stark difference between the gene sets affected in the Hsp70 KO and WT mice, Ingenuity Pathway Analysis revealed that inflammation was still among the top canonical pathways significantly enriched in the STZ+Veh and STZ+KU-596 groups (Figure 3.3-10 and Figure 3.3-11). This observation suggests that KU-596 likely decreased the inflammatory response in diabetic sensory neurons through an Hsp70-independent pathway. In contrast to inflammatory pathways, the effects of KU-596 on the production of ROS was blunted (Figure 3.3-12), suggesting that KU-596 may reduce oxidative stress in diabetic sensory neurons in an Hsp70-dependent manner. Unexpectedly, KU-596 slightly decreased the transcription of several mitochondrial genes in diabetic sensory neurons (Table 3.3-5). This effect was not observed in either Hsp70 KO control mice or WT mice treated with KU-596. Though mtBE was not measured in KU-596-treated Hsp70 KO mice, the decrease in mRNA levels of these mitochondrial proteins was unlikely to result in changes in mitochondrial respiration since KU-32 did not decrease mtBE in sensory neurons isolated from diabetic Hsp70 KO mice in our previous study (Ma et al., 2014). In addition to affecting mitochondrial transcripts, KU-596 also decreased a subset of 25 genes involved in the eIF2 pathway in diabetic sensory neurons, all of which encoded ribosomal proteins. Considering the role of eIF2 pathway in protein synthesis and translation, the decrease in genes involved in this pathway would suggest an overall decrease in protein synthesis. Regardless of the consequence of these changes, they are not associated with changes in sensory pathophysiology since KU-596-treated Hsp70 KO diabetic mice behaved similar to vehicle-treated mice (Figure 3.3-3).

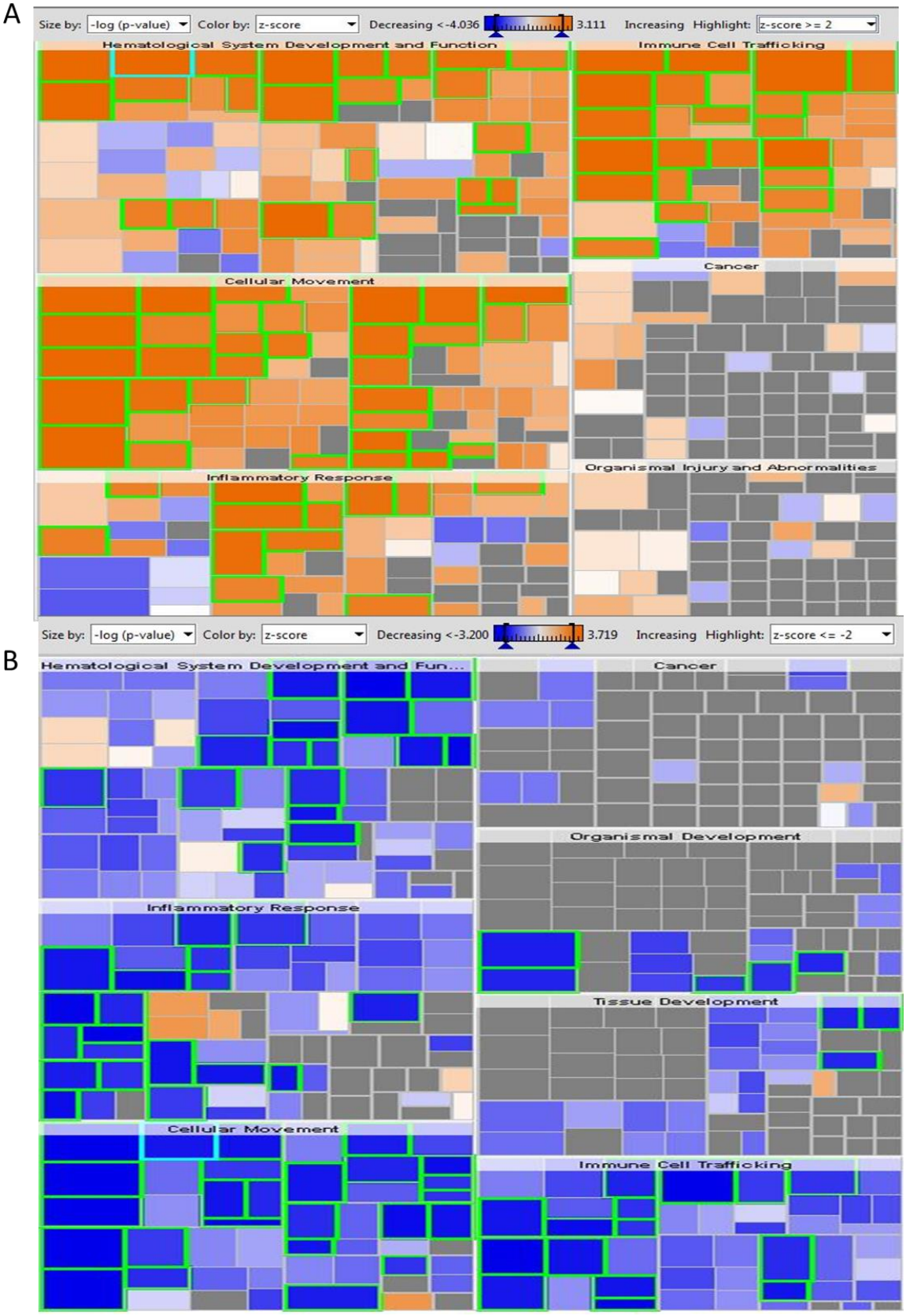
A
Size by: -log (p-value)
Color by: z-score
Decreasing <-4.036
3.111
Increasing
Highlight: z-score >= 2
Hematological System Development and Function
Immune Cell Trafficking
Cellular Movement
Cancer
Inflammatory Response
Organismal Injury and Abnormalities
Size by: -log (p-value)
Color by: z-score
Decreasing <-3.200
3.719
Increasing
Highlight: z-score <= -2
B
Hematological System Development and Fun...
Cancer
Organismal Development
Inflammatory Response
Tissue Development
Cellular Movement
Immune Cell Trafficking

Figure 3.3-10: Heat map representation of significantly altered gene categories in Hsp70 KO mice.

Significantly altered gene categories in STZ+Veh versus Veh+Veh group (A), and STZ+KU-596 versus STZ+Veh group (B). The squares represent significantly altered genes under each category; the size of the square was determined by the negative log of the p-value of the gene it represents; the color of the square was determined by the activation z-score, with orange representing increasing and blue representing decreasing. Genes with a z-score ≥ 2 in (A) or ≤ 2 in (B) were highlighted in green lines.

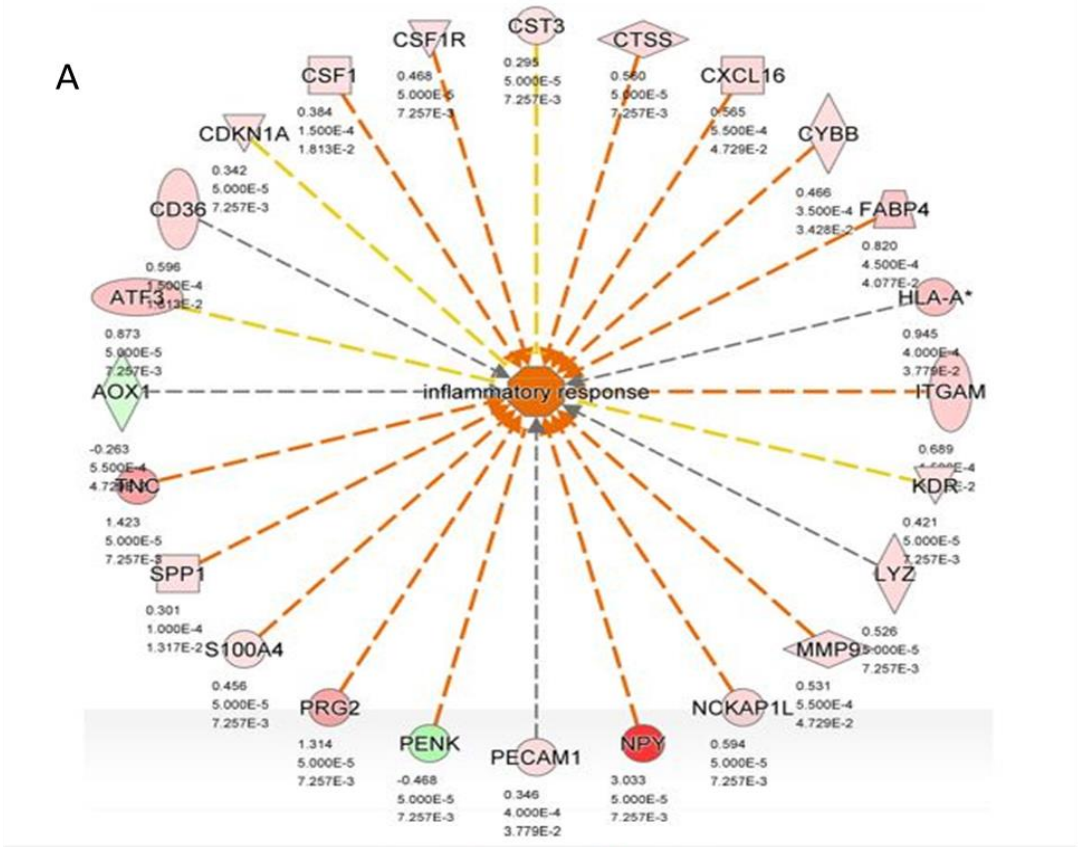
A
CSF1R
CST3
CTSS
CSF1
CXCL16
CDKN1A
CYBB
CD36
FABP4
ATF3
HLA-A*
AOX1
inflammatory response
ITGAM
TNC
KDR
SPP1
LYZ
S100A4
MMP9
PRG2
NCKAP1L
PENK
PECAM1
NPY

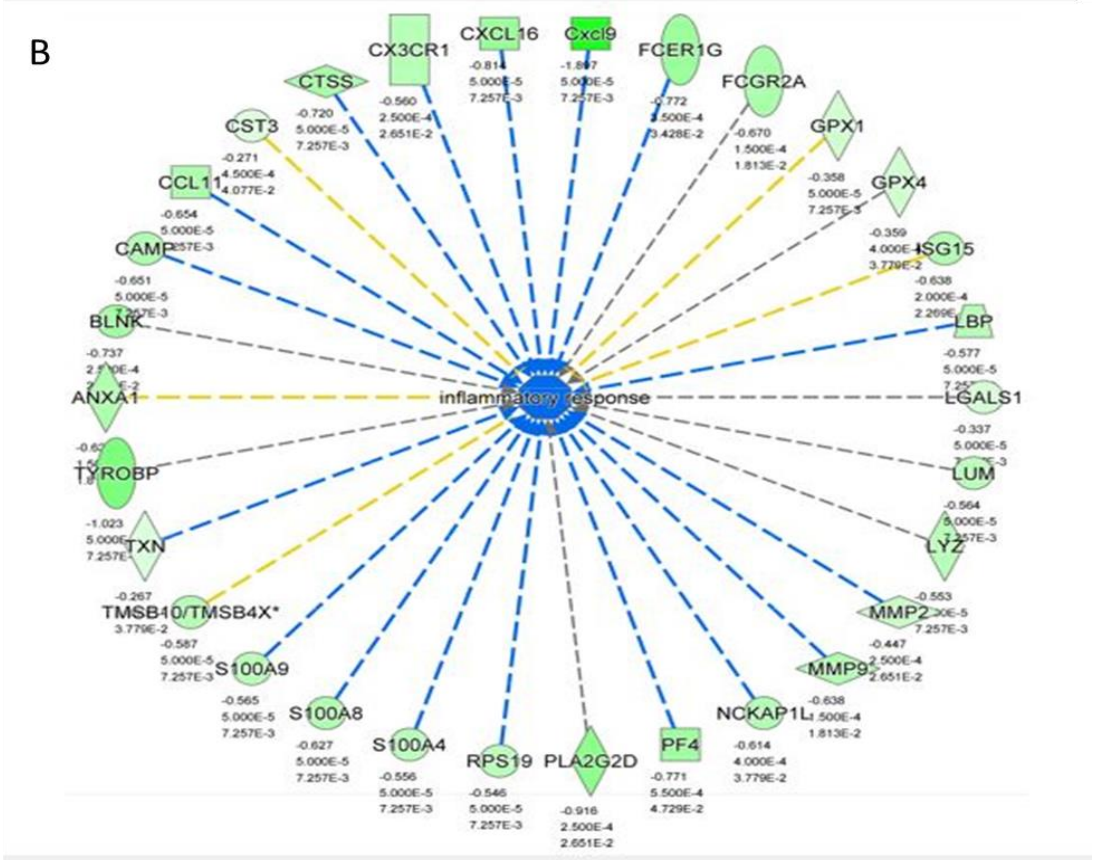
B
CX3CR1
CXCL16
Cxcl9
FCER1G
CTSS
FCGR2A
CST3
GPX1
CCL11
GPX4
CAMP
ISG15
BLNK
LBP
ANXA1
inflammatory response
LGALS1
TYROBP
LUM
TXN
LYZ
TMSB10/TMSB4X*
MMP2
S100A9
MMP9
S100A8
NCKAP1L
S100A4
RPS19
PLA2G2D
PF4

Figure 3.3-11: Significantly altered genes involved in inflammatory response in Hsp70 KO mice.

Significantly altered genes involved in inflammatory response between Veh+Veh and STZ+Veh conditions (A), and between STZ+Veh and STZ+KU-596 conditions (B). Red indicates upregulation of the genes, and green indicates downregulation of the genes. The degree of change is indicated by the color intensity, a higher color intensity indicating a more extreme change. Different colors of the connecting lines represent predicted effects of the change of a molecule to the inflammatory response: orange line leads to activation, blue line leads to inhibition, yellow line indicates a finding inconsistent with the activation state of the downstream molecule, and gray line indicates an effect is not predicted.

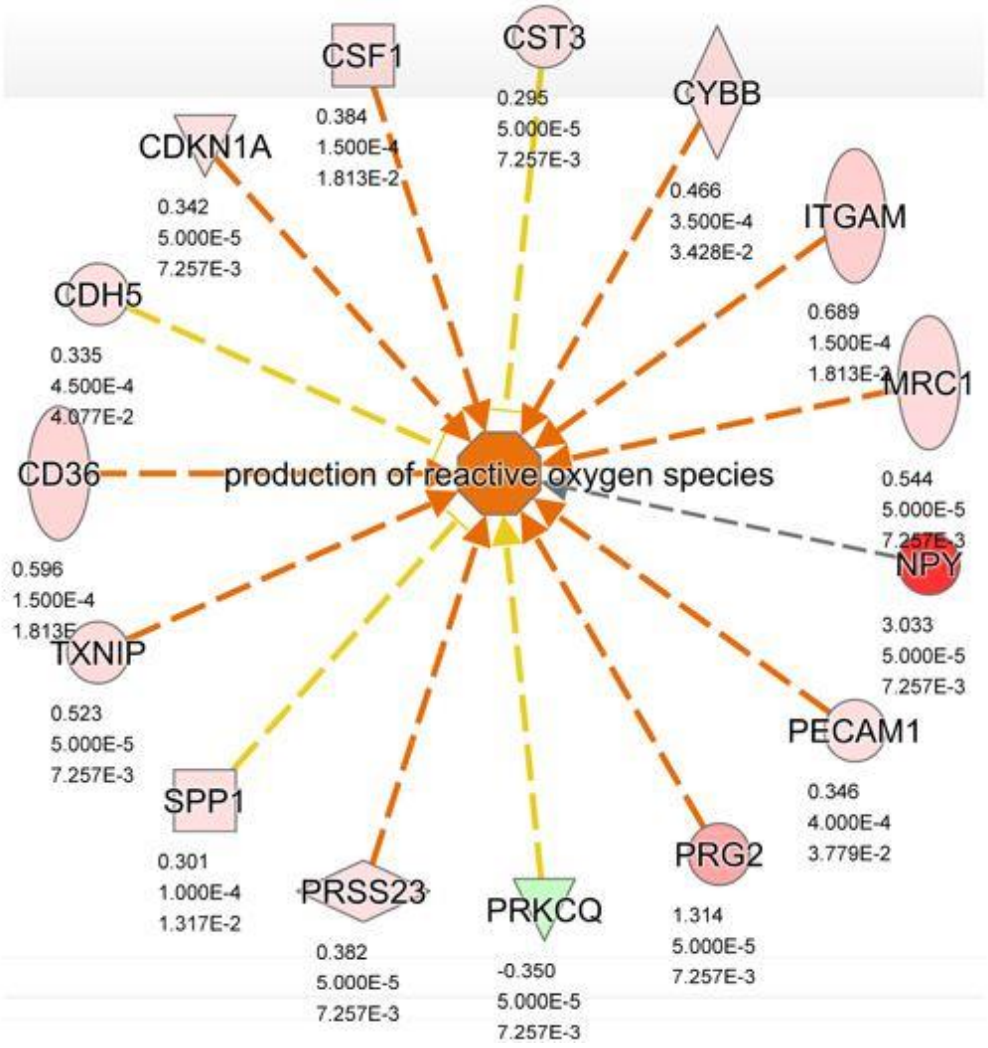

Figure 3.3-12: Significantly altered genes involved in the production of ROS in Hsp70 KO mice.

Significantly altered genes involved in ROS production between Veh+Veh and STZ+Veh conditions. Red indicates upregulation of the genes, and green indicates downregulation of the genes. The degree of change is indicated by the color intensity, the higher the color intensity indicates a more extreme change. Different colors of the connecting lines represent the predicted effects of the change of a molecule to the production of ROS: orange line leads to activation, blue line leads to inhibition, yellow line indicates a finding inconsistent with the activation state of the downstream molecule, and a gray line indicates an effect is not predicted.

Table 3.3-5: List of mitochondrial genes downregulated by KU-596 treatment in diabetic sensory neurons in Hsp70 KO mice.

Gene	Entrez Gene Name	Log_2(fold change)
Atp5e	ATP synthase, H+ transporting, mitochondrial F1 complex, epsilon subunit	-0.757
ATP5J2	ATP synthase, H+ transporting, mitochondrial Fo complex, subunit F2	-0.363
COX17	COX17 cytochrome c oxidase copper chaperone	-0.340
COX6B1	cytochrome c oxidase subunit VIb polypeptide 1 (ubiquitous)	-0.274
Cox6c	cytochrome c oxidase subunit VIc	-0.358
Cox7a2/Cox7a2l2	cytochrome c oxidase subunit VIIa polypeptide 2-like 2	-0.363
COX7B	cytochrome c oxidase subunit VIIb	-0.438
FIS1	fission 1 (mitochondrial outer membrane) homolog (S. cerevisiae)	-0.286
GPX4	glutathione peroxidase 4	-0.359
NDUFA4	NDUFA4, mitochondrial complex associated	-0.448
NDUFA7	NADH dehydrogenase (ubiquinone) 1 alpha subcomplex, 7, 14.5kDa	-0.325
NDUFB2	NADH dehydrogenase (ubiquinone) 1 beta subcomplex, 2, 8kDa	-0.514
NDUFB9	NADH dehydrogenase (ubiquinone) 1 beta subcomplex, 9, 22kDa	-0.284
NDUFB11	NADH dehydrogenase (ubiquinone) 1 beta subcomplex, 11, 17.3kDa	-0.321
UQCR10	ubiquinol-cytochrome c reductase, complex III subunit X	-0.370
UQCR11	ubiquinol-cytochrome c reductase, complex III subunit XI	-0.396
UQCRQ	ubiquinol-cytochrome c reductase, complex III subunit VII, 9.5kDa	-0.341

3.4. Summary and Discussion

KU-596 Reverses Physiologic and Bioenergetic Deficits of DPN

In the current study, the next-generation novologue KU-596 reversed psychosensory, electrophysiologic and bioenergetic deficits of DPN in animal models of type 1 diabetes. KU-596 was identified through SAR analysis of KU-32 derivatives. Mechanistically, substitution of the coumarin lactone of KU-32 with a 3'-fluoro-benzene ring in KU-596 may enhance the molecule's interaction with Lys539 in the Hsp90 C-terminal binding pocket. In addition, the flexible ethyl amide projecting from KU-596 accommodates a number of orientations that could better occupy the large hydrophobic pocket of Hsp90 that remains vacant in the presence of KU-32. Previous studies have shown that KU-596 induced Hsp70 expression and exhibited enhanced neuroprotective properties in *in vitro* models of glucotoxicity (Kusuma et al., 2012). In the current study, we provided further evidence that KU-596 is orally bioavailable, and is effective at reversing multiple clinical indices of DPN in *in vivo* models of type 1 diabetes in an Hsp70-dependent manner.

KU-596 Reverses Transcriptome Changes involved in Inflammatory Pathways and Production of ROS

Transcriptome analysis of sensory neurons using the RNA-Seq approach revealed that KU-596 primarily modulated genes involved in inflammatory responses (Figure 3.3-5). Inflammation has been proposed as a key mechanism underlying the pathogenesis as well as progression of DPN (Zhou and Zhou, 2014). Patients with diabetic neuropathy exhibit features of low-grade subclinical inflammation (Herder et al., 2009). Increased levels of pro-inflammatory cytokines, especially interleukin (IL)-6 and C-reactive peptides (CRP), have been found to correlate closely with the incidence of DPN (Herder

et al., 2009; Shelbaya et al., 2012). These pro-inflammatory cytokines produced locally by resident and infiltrating immune cells exhibit neuropoietic effects on glial and neuronal cells, further disturbing cellular homeostasis in diabetic tissues (Skundric and Lisak, 2003).

In the current study, diabetic sensory neurons exhibited enhanced markers of inflammation and immune cell infiltration, which were partially abolished by 4 weeks of KU-596 treatment. Among these inflammation genes, one of interest is CD163. CD163 is an endocytic haptoglobin–hemoglobin receptor expressed on macrophages and monocytes and serves as a macrophage-derived low-grade inflammation marker reflecting macrophage activation (Kristiansen et al., 2001). It was increased ~3-fold in diabetic sensory neurons and decreased ~2-fold by KU-596 treatment. A case-control study involving a small number of type 2 diabetic patients indicated that an increase in soluble CD163 levels in cerebrospinal fluid and serum was associated with impaired peripheral nerve function and incidence of DPN (Kallestrup et al., 2015). Thus, the upregulation of cytokines, chemokines and genes such as CD163 in diabetic sensory neurons suggests that recruitment of activated macrophages and activation of inflammatory pathways are likely involved in the pathogenesis of DPN. KU-596 reduced inflammatory markers in the sensory neurons, suggesting that modulation of molecular chaperones alters inflammatory responses in the sensory neurons, which might contribute to reversing the sensory deficits. CD163 was also upregulated 1.4 fold in diabetic Hsp70 KO neurons, but this did not quite reach statistical significance ($q < 0.06$). However, CD163 was significantly increased when comparing non-diabetic animals to diabetic mice treated with KU-596 (1.65 fold, $q < 0.007$). Thus, this inflammatory marker was not

as strongly increased between the diabetic WT and Hsp70 KO mice and its expression was not decreased by novologue treatment of the diabetic Hsp70 KO mice. Therefore, Hsp70 may have a role in altering the expression of CD163. Given the putative link that diabetic patients with neuropathy show a greater increase in serum CD163 levels than diabetic patients without neuropathy (Kallestrup et al., 2015), the ability of KU-596 therapy to decrease its expression may provide a biomarker for drug efficacy.

Another overrepresented biologic process in diabetic sensory neurons comprised genes involved in the production of ROS (Figure 3.3-6A). Oxidative stress has been considered as an essential pathogenic mechanism for DPN (Figueroa-Romero et al., 2008; Kasznicki et al., 2012; Vincent et al., 2004b). Hyperglycemia changes multiple biochemical and metabolic pathways, including the polyol pathway, activation of PKC isoforms and the AGE/RAGE pathway. In addition to causing damage to the peripheral nerves themselves, these pathophysiological changes intersect at the level of ROS production to further contribute to the development and progression of DPN (Edwards et al., 2008). Our previous study indicated that KU-32 increased the translation of MnSOD and decreased oxidative stress in hyperglycemically stressed rat embryonic sensory neurons (Zhang et al., 2012). In the current study, transcriptome analysis of sensory neurons revealed that KU-596 also affected gene networks involved in the production of ROS (Figure 3.3-6B). For example, Cybb (also known as cytochrome b(558) subunit beta or NADPH oxidase 2/Nox2), a superoxide generating enzyme that forms ROS (Tammariello et al., 2000), increased ~2-fold in diabetic sensory neurons and was reduced ~2-fold by KU-596 treatment. Thioredoxin interacting/inhibiting protein (Txnip) is an early response gene induced by diabetes and hyperglycemia (Devi et al., 2012). It

promotes oxidative stress through interacting with thioredoxin (Trx) and blocking its ROS scavenging activity (Schulze et al., 2004). In the current study, Txnip was also upregulated ~2-fold in diabetic neurons and downregulated about 1.4-fold by KU-596. Similarly, diabetes significantly increased the expression of Txnip in the Hsp70 KO DRG but this was unaffected by KU-596 treatment. Therefore, limiting ROS production and reducing oxidative stress in the sensory neurons might represent an important Hsp70-dependent pathway through which KU-596 exhibits efficacy on reversing sensory deficits of DPN.

KU-596 (Figure 3.1-1B) and KU-32 (Ma et al., 2014) have been shown to reverse mtBE deficits in diabetic sensory neurons. Thus, we were expecting that transcriptome analysis would reveal gene clusters connecting to aspects of mitochondrial function. However, none of the genes involved in cellular bioenergetic activities were significantly altered in WT mice of the STZ+Veh or STZ+KU-596 groups. These results suggest that modulation of molecular chaperones likely exerts effects on mitochondrial function post-translationally, for example, through refolding of damaged proteins, directing protein import into mitochondria, or as mentioned above by decreasing oxidative stress. In addition, it has been suggested that inflammatory signaling leads to changes in the phosphorylation state of mitochondrial proteins, which results in an inhibition of respiratory chain activity, a reduction of the mitochondrial membrane potential, and consequently a lack of energy production (Lee and Huttemann, 2014). Thus, modulation of mtBE could also be achieved indirectly through mediating inflammatory responses. In this regard, the effect of KU-596 to improve mitochondrial bioenergetics might be

partially attributed to its effects in ameliorating inflammatory signaling in the sensory neurons.

Hsp70 KO Mice Display Different Gene Sets altered by STZ and KU-596

Comparison between genes significantly altered in WT and Hsp70 KO mice revealed little overlap in either STZ+Veh or STZ+KU596 group (Figure 3.4-1). Compared to 343 genes in WT mice, only 101 genes were significantly altered in diabetic sensory neurons of Hsp70 KO mice. Further analysis of the genes revealed decreases in the number of genes involved in inflammatory pathways, immune cell recruitment and ROS production. Though unexpected, this change might be related to a role of Hsp70 in the stimulation of pro-inflammatory cytokine production and recruitment of macrophages/monocytes (Huang et al., 2013; Senf et al., 2013). A recent study revealed that Hsp70.1-deficent mice were more resistant to developing autoimmune encephalomyelitis, suggesting the involvement of Hsp70.1 in promoting an effective myelin oligodendrocyte glycoprotein T cell response (Mansilla et al., 2014). It has been reported that under stress conditions, Hsp70 is actively released into the extracellular milieu to promote innate and adaptive immune responses (Hunter-Lavin et al., 2004). Recent studies indicate that the physiological function of Hsp70 largely depends on the location of the protein (Krause et al., 2015). For example, increased extracellular Hsp70 is associated with inflammatory and oxidative stress conditions (Whitham and Fortes, 2008), whereas increased intracellular Hsp70 confers cellular protection through anti-inflammatory effects (Jones et al., 2011). In this regard, increased concentrations of extracellular Hsp70 and decreased concentrations of intracellular Hsp70 have been reported in type 2 diabetic patients (Rodrigues-Krause et al., 2012). In the current study, extracellular Hsp70 likely

mediated the activation of inflammatory pathways in WT diabetic sensory neurons, which may contribute to the partial blockage of transcriptome changes involved in these pathways in the Hsp70 KO mice.

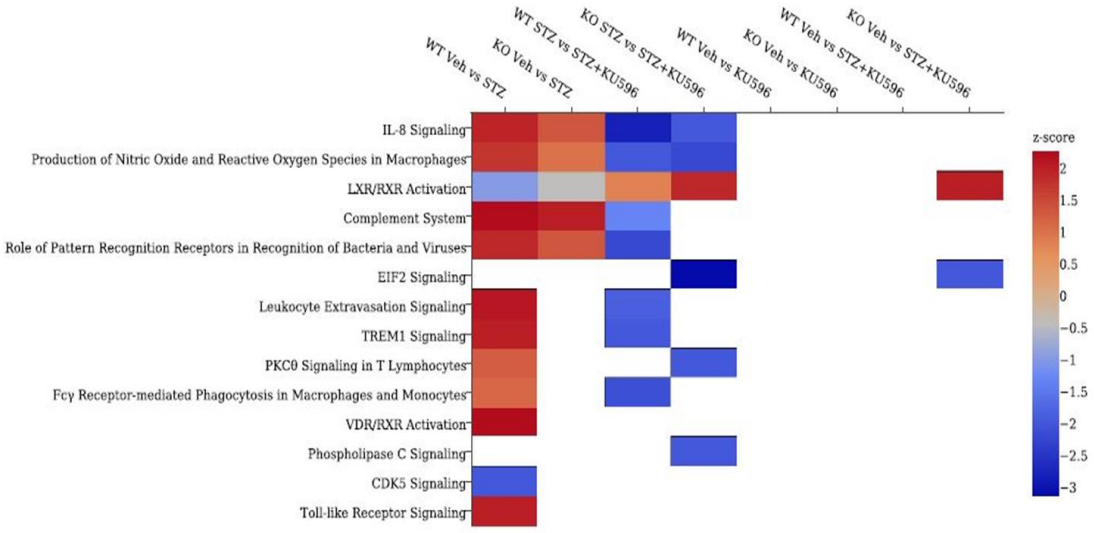

Figure 3.4-1: Heatmap representation of top canonical pathways enriched in WT and Hsp70 KO mice.

Top canonical pathways revealed by comparison analysis of transcriptomic changes in WT versus Hsp70 KO mice. The squares were colored by the activation z-score: red indicates increasing, blue indicates decreasing, intensity of the color is indicative of the degree of change.

In contrast to decreased number of affected genes in STZ+Veh group, KU-596 induced changes in 242 genes in diabetic sensory neurons in Hsp70 KO mice (compared to 174 in C57Bl/6 mice). Among these altered genes, 220 out of 242 were decreased, including 17 genes involved in mitochondrial function and oxidative phosphorylation. Although the exact underlying reason is unknown, this effect of KU-596 on mitochondrial transcripts might be associated with a role of Hsp90 in mitochondrial protein turnover. In the absence of Hsp70, the effects of KU-596 on transcriptome changes may be exerted through inhibiting Hsp90 activity. A previous *in vitro* study

showed that Hsp90 inhibition led to post-translational accumulation of several mitochondrial oxidative phosphorylation complex subunits without corresponding changes in mRNA abundance (Margineantu et al., 2007). Thus, the decrease in transcription observed in our study might be an innate response mechanism to the accumulation of these mitochondrial proteins due to inhibition of Hsp90 over the 4 weeks of drug treatment. As an essential molecular chaperone that assures the correct folding and maturation of a number of cellular proteins, Hsp90 inhibition leads to a global repression of protein synthesis and an increase in the degradation of its client proteins (Fierro-Monti et al., 2013). A recent proteomics study using human T cells revealed that Hsp90 inhibition resulted in the depletion of proteins involved in transcription and DNA damage response as well as a mild but general decrease of ribosomal proteins and other components of the protein synthesis machinery (Quadroni et al., 2015). This finding is consistent with our observation that KU-596 led to a decrease in the eIF2 signaling pathway and an overall decrease in transcription. In this regard, the differences in the gene sets affected by KU-596 in WT versus Hsp70 KO mice might be explained by the different downstream pathways induced by drug treatment in the different genotypes: whereas KU-596 exerts cytoprotective effects through induction of Hsp70 in WT cells, the effects of KU-596 are largely exerted through inhibiting the activity of Hsp90 in Hsp70 KO cells.

KU-596 Exerts Alterations in Transcriptome through both Hsp70-dependent and Hsp70-independent mechanisms

An anti-inflammatory role of Hsp70 has been implicated by various studies. It is reported that Hsp70 inhibited lipopolysaccharide (LPS)-induced activation of NF-κB and

production of pro-inflammatory cytokines (Dokladny et al., 2010; Shi et al., 2006). Mechanistic studies suggest that the modulatory effect of Hsp70 on the inflammatory response is likely through directing the degradation of the p65 subunit of NF-κB (Tanaka et al., 2014). However, in the current study, KU-596-induced alterations in inflammatory pathways were not solely dependent on Hsp70 (Figure 3.3-9). Mechanistically, different Hsp90 inhibitors may attenuate inflammation through disparate pathways. For example, the N-terminal Hsp90 inhibitor 17-AAG suppressed glial inflammatory responses in experimental autoimmune encephalomyelitis through transcriptional activation of HSF-1 and induction of a HSR (Dello Russo et al., 2006). In contrast, novobiocin inhibited pro-inflammatory cytokine production through disruption of Hsp90 chaperone function and decreasing the level of IKK-α. The decease of IKK-α in novobiocin-treated cells subsequently led a reduction in the nuclear translocation of the NF-κB p65 subunit and inhibition of inflammatory pathway (Collins et al., 2014). As a structural analogue of novobiocin, KU-596 may mediate inflammatory responses through degradation of IKK-α but not induction of Hsp70, which might explain its Hsp70-independent anti-inflammatory effects in diabetic sensory neurons. However, the preserved anti-inflammatory effects of KU-596 in Hsp70 KO mice was not associated with improvements in psychosensory functions of diabetic mice. This suggests that inhibition of inflammatory responses alone was not sufficient to reverse sensory deficits of insensate DPN in our model of type 1 diabetes.

In contrast to the Hsp70-independent anti-inflammatory effects, KU-596 exerted its effects on the production of ROS in an Hsp70-dependent manner (Figure 3.3-10). The alterations induced by KU-596 in several genes involved in ROS production, including

Cybb and Txnip, were blunted in Hsp70 KO mice. Though the exact mechanism through which Hsp70 modulates ROS production remains undetermined, overexpression of Hsp70 has been associated with protection against age-related oxidative stress (Broome et al., 2006). In our previous study, we identified that modulation of molecular chaperones reversed deficits in sensory functions and mitochondrial bioenergetics in an Hsp70-dependent manner (Ma et al., 2014). The reliance on Hsp70 for a tight correlation between reduced gene networks involved in ROS production and improved mtBE suggests that the effects of KU-596 to improve mitochondrial respiration might be partly attributed to reduced oxidative stress in the sensory neurons.

Chapter 4: Outlooks

Progress in developing effective therapies for DPN has largely been disappointing despite increased understanding of its pathophysiological mechanisms. The multifaceted biochemical abnormalities associated with DPN occur in an individual-based, non-uniform fashion, hindering disease treatment with simple monotherapeutic strategies that directly target a specific pathogenic factor. In this regard, modulating molecular chaperones offers promising therapeutic alternatives and may provide a powerful tool for ameliorating deficits of DPN through reinforcing innate protective mechanisms. In other words, modulating molecular chaperones may help neurons and glia to more effectively tolerate ongoing diabetic stress.

Mitochondrial dysfunction, oxidative stress and activation of the inflammatory pathways have been implicated as important pathogenic factors for DPN (Callaghan et al., 2012a). We have shown that novologues improved mitochondrial bioenergetics and reversed transcriptomic changes associated with the production of ROS in an Hsp70-dependent manner, which correlated with the Hsp70-dependent improvements in sensory performances. However, the exact mechanism through which modulation of Hsp70 mediates mitochondrial bioenergetics remains to be elucidated. As revealed by the RNA-Seq analysis of sensory neurons, the effects of KU-596 on mitochondrial function were not exerted through transcriptional modulation of genes encoding proteins involved in cellular bioenergetic activities. Therefore, KU-596 likely modulates mitochondrial bioenergetics post-translationally, for example, through facilitating the import, removal, and/or replacement of damaged mitochondrial proteins. Despite the presence of mtDNA, 99% of mitochondrial proteins are encoded by the nucleus and require import into the

organelle. In this regard, Hsp70 serves as a chaperone for importing hydrophobic precursors of inner mitochondrial membrane proteins (Schmidt et al., 2010). Our previous proteomic study using hyperglycemically-stressed rat embryonic sensory neurons indicated that KU-32 increased the level of MnSOD, which correlated with decreased mitochondrial superoxide production and enhanced bioenergetic profile (Zhang et al., 2010a). MnSOD is synthesized in the cytosol and imported into the mitochondrial matrix, and it has been reported that the import of MnSOD is dependent on its interaction with the inducible HSP70 (Afolayan et al., 2014). Therefore, it seems reasonable to hypothesize that modulation of Hsp70 might improve mitochondrial bioenergetics through enhancing the mitochondrial protein import machinery.

Txnip was identified in the RNA-Seq study as a KU-596 target gene which displayed Hsp70 dependency. It acts as a physiological inhibitor of thioredoxin (Trx) and promotes oxidative stress through blocking the ROS scavenging activity of Trx (Schulze et al., 2004). It was later found that Txnip shuttles between various intracellular locations, and its actions largely depend on its intracellular distribution. Whereas under basal conditions, Txnip is located entirely in the nucleus where it binds to a number of intranuclear proteins such as PARP-1, it translocates to mitochondria or cell surface under certain stress conditions (Spindel et al., 2012). For example, in response to oxidative stress, Txnip translocated to mitochondria where it bound thioredoxin-2 (Trx-2), the mitochondrial isoform of Trx, and led to mitochondrial dysfunction and activation of apoptosis (Saxena et al., 2010). Furthermore, binding of Txnip to Trx-2 is critical to the development of intra-mitochondrial redox stress and activation of inflammatory pathways (Lane et al., 2013). Therefore, Txnip acts as an important link for oxidative stress,

mitochondrial dysfunction and inflammatory responses in diabetic sensory neurons, and might represent a critical target for Hsp70 modulation in the treatment of DPN.

The RNA-Seq analysis revealed that KU-596 reversed transcriptomic changes associated with the inflammatory pathways in an Hsp70-independent manner, and that reversing the inflammatory responses alone was not enough to reverse sensory deficits of insensate DPN in our type 1 diabetes model. However, the efficacy of KU-596 to reverse activation of the inflammatory pathways might enable the expansion of its application to other sensory neuropathies that exhibit more profound features of inflammation, for example, painful diabetic peripheral neuropathy (PDPN). The symptoms of PDPN range from uncomfortable tingling, pain with a variety of different characteristics (burning, lancinating, shooting, electric-shock-like, aching and crawling pain) to evoked pain such as allodynia or hyperaesthesia (Gandhi and Selvarajah, 2015). PDPN is associated with an increased pro-inflammatory cytokine profile (Doupis et al., 2009), implicating the role of cytokine-mediated neuroimmune interactions in the development and maintenance of pain. Therefore, as a modulator of inflammatory responses, KU-596 might be effective in ameliorating neuropathic pain associated with PDPN. Management of the chemotherapy-induced peripheral neuropathy (CIPN) represents another possible application for KU-596. CIPN is a common dose-limiting complication of cancer chemotherapy and exhibits bilaterally symmetrical sensory symptoms (numbness, tingling, and pain) appearing in the extremities after cumulative dosing (Argyriou et al., 2012; Paice, 2011). Recent studies indicated that chemotherapeutics, such as paclitaxel and oxaliplatin, produced a long-lasting dysfunction in mitochondria in primary afferent sensory neurons (Xiao and Bennett, 2012). In addition, it was reported that intravenous paclitaxel infusion induced

peripheral neuropathy was characterized by macrophage infiltration in both the DRG and peripheral nerve, and microglial activation within the spinal cord (Peters et al., 2007). Therefore, considering its role in improving mitochondrial bioenergetics and reducing the inflammatory responses, KU-596 might provide a novel therapy against CIPN and aid in the treatment of cancer. However, caution must be taken in the application of KU-596 as an adjuvant therapy to treat CIPN. As certain cancers are characterized by Hsp70 overexpression (Ricaniadis et al., 2001; Yoshida et al., 2009), modulation of Hsp70 in cancer subjects might lead to deterioration of the malignant phenotypes. Though KU-32 and KU-596 were shown to be weak inducers of Hsp70 and demonstrated safety in animal models of DPN, their actions in malignant phenotypes are hard to predict without careful experimental examinations.

In summary, this dissertation provides further evidence that pharmacologic modulation of endogenous neuroprotective chaperones offers a novel therapeutic opportunity for the management of DPN. Though future studies are needed to further elucidate the protective mechanism of novologue therapy, we have identified mtBE and oxidative stress as key targets for Hsp70 modulation which correlated closely with improved sensory parameters in animal models of DPN. Coupled with close attention towards good glycemic control, modulating molecular chaperones shows great promise in the therapeutic management of DPN in patients with type 1 and type 2 diabetes.

Appendix 1

Table 5-1: List of primer sequences.

TUBA1A	Forward	5'-TCTTGTCACTTGGCATCTGG-3'
	Reverse	5'-CGCGAAGCAGCAACCAT-3'
TXNIP	Forward	5'-TCTTTTGAGGTGGTCTTCAACG-3'
	Reverse	5'-GCTTTGACTCGGGTAACTTCACA-3'
S100A8	Forward	5'-AAATCACCATGCCCTCTACAAG-3'
	Reverse	5'-CCCACTTTTATCACCATCGCAA-3'
LTF	Forward	5'-TGAGGCCCTTGGACTCTGT-3'
	Reverse	5'-ACCCACTTTTCTCATCTCGTTC-3'
FKBP5	Forward	5'-TGAGGGCACCAGTAACAATGG-3'
	Reverse	5'-CAACATCCCTTTGTAGTGGACAT-3'
ARHGDIB	Forward	5'-ATGACGGAGAAGGATGCACAG-3'
	Reverse	5'-CTCCCAGCAGTGTTTTCTTGTA-3'
FABP4	Forward	5'-AAGGTGAAGAGCATCATAACCCT-3'
	Reverse	5'-TCACGCCTTTCATAACACATTCC-3'
LCN2	Forward	5'-ATGTATGGCCGGTACACTCAG-3'
	Reverse	5'-AACAAATGCGACATCTGGCAC-3'
CCL6	Forward	5'-GCTGGCCTCATACAAGAAATGG-3'
	Reverse	5'-GCTTAGGCACCTCTGAACTCTC-3'

Appendix 2

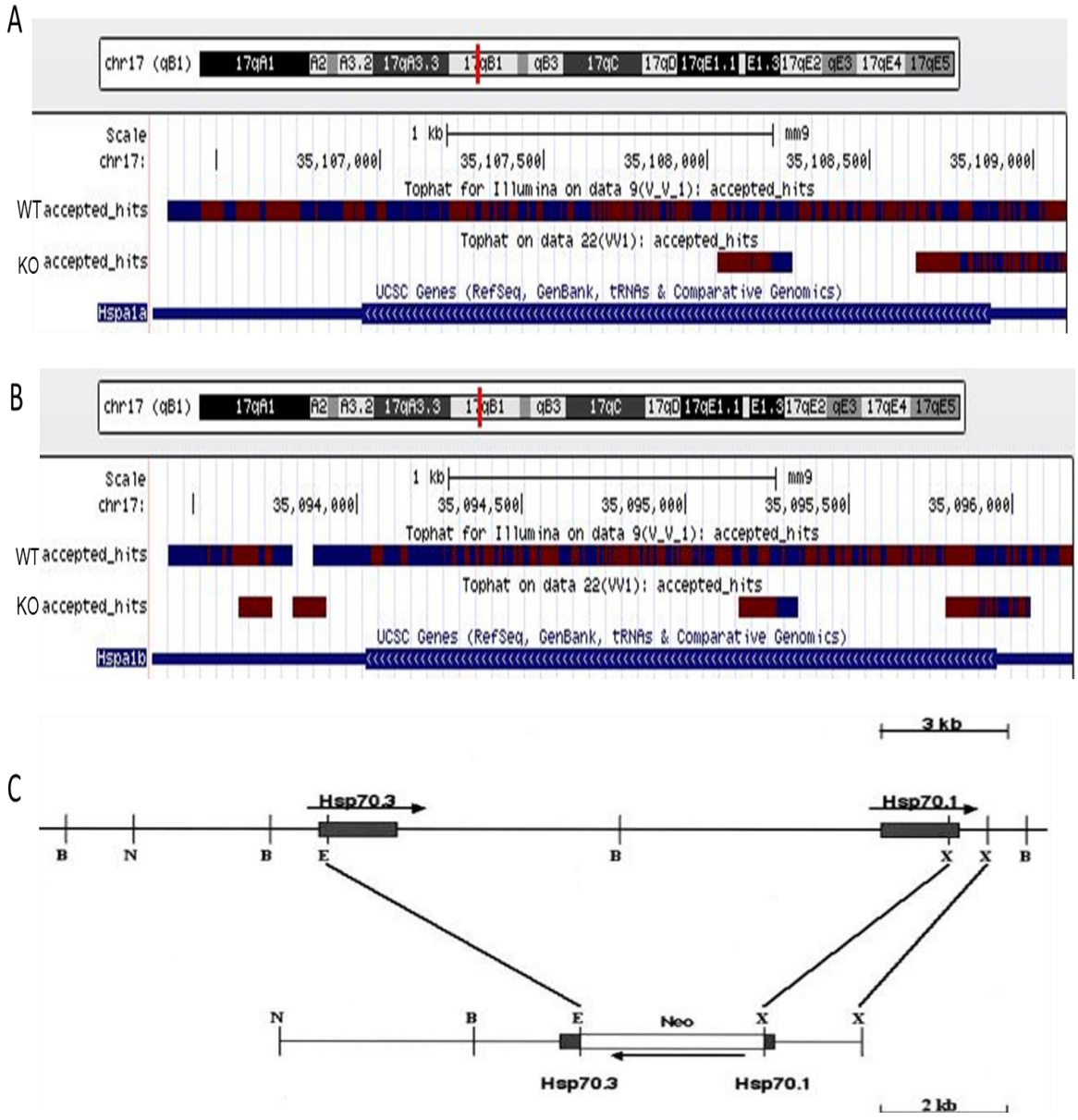

Figure 5-1: RNA-seq confirmation of the Hsp70 KO phenotype.

The phenotype of the Hsp70.1/70.3 double KO mice used in our study was confirmed by RNA-seq. (A) Accepted hits of Hspa1a (Hsp70.3) in WT (upper band) versus Hsp70 KO mice (lower band). (B) Accepted hits of Hspa1b (Hsp70.1) in WT (upper band) versus Hsp70 KO mice (lower band). (C) Genomic structure of Hsp70.1/3 and design of targeting construct. The Hsp70 gene deletion vector was constructed by replacement of approximately 11 kb of genomic DNA separating the 5' end of the Hsp70.3 gene and the 3' end of the Hsp70.1 gene with a 3.1 kb neo gene, thereby simultaneously inactivating both genes (Hunt et al., 2004).

References

1993a. The effect of intensive treatment of diabetes on the development and progression of long-term complications in insulin-dependent diabetes mellitus. The Diabetes Control and Complications Trial Research Group. *N Engl J Med*. 329:977-986.

1993b. UK Prospective Diabetes Study (UKPDS). X. Urinary albumin excretion over 3 years in diet-treated type 2, (non-insulin-dependent) diabetic patients, and association with hypertension, hyperglycaemia and hypertriglyceridaemia. *Diabetologia*. 36:1021-1029.

1997. Report of the Expert Committee on the Diagnosis and Classification of Diabetes Mellitus. *Diab Care*. 20:1183-1197.

1998a. Tight blood pressure control and risk of macrovascular and microvascular complications in type 2 diabetes: UKPDS 38. UK Prospective Diabetes Study Group. *BMJ*. 317:703-713.

1998b. United Kingdom Prospective Diabetes Study 24: a 6-year, randomized, controlled trial comparing sulfonylurea, insulin, and metformin therapy in patients with newly diagnosed type 2 diabetes that could not be controlled with diet therapy. United Kingdom Prospective Diabetes Study Group. *Ann Intern Med*. 128:165-175.

2003. Report of the expert committee on the diagnosis and classification of diabetes mellitus. *Diab Care*. 26 Suppl 1:S5-20.

Afolayan, A.J., R.J. Teng, A. Eis, U. Rana, K.A. Broniowska, J.A. Corbett, K. Pritchard, and G.G. Konduri. 2014. Inducible HSP70 regulates superoxide dismutase-2 and mitochondrial oxidative stress in the endothelial cells from developing lungs. *Am J Physiol Lung Cell Mol Physiol*. 306:L351-360.

Agrawal, Y., J.P. Carey, C.C. Della Santina, M.C. Schubert, and L.B. Minor. 2010. Diabetes, vestibular dysfunction, and falls: analyses from the National Health and Nutrition Examination Survey. *Otol Neurotol*. 31:1445-1450.

Aguirre, V., E.D. Werner, J. Giraud, Y.H. Lee, S.E. Shoelson, and M.F. White. 2002. Phosphorylation of Ser307 in insulin receptor substrate-1 blocks interactions with the insulin receptor and inhibits insulin action. *J Biol Chem*. 277:1531-1537.

Ahmed, N. 2005. Advanced glycation endproducts--role in pathology of diabetic complications. *Diabetes Res Clin Pract*. 67:3-21.

Akerfelt, M., R.I. Morimoto, and L. Sistonen. 2010. Heat shock factors: integrators of cell stress, development and lifespan. *Nat Rev Mol Cell Biol*. 11:545-555.

Akude, E., E. Zherebitskaya, S.K. Chowdhury, D.R. Smith, R.T. Dobrowsky, and P. Fernyhough. 2011. Diminished superoxide generation is associated with respiratory chain dysfunction

and changes in the mitochondrial proteome of sensory neurons from diabetic rats. *Diabetes*. 60:288-297.

Akude, E., E. Zherebitskaya, S.K. Roy Chowdhury, K. Girling, and P. Fernyhough. 2010. 4-Hydroxy-2-nonenal induces mitochondrial dysfunction and aberrant axonal outgrowth in adult sensory neurons that mimics features of diabetic neuropathy. *Neurotox Res*. 17:28-38.

Albers, J.W., W.H. Herman, R. Pop-Busui, E.L. Feldman, C.L. Martin, P.A. Cleary, B.H. Waberski, J.M. Lachin, C. Diabetes, I. Complications Trial /Epidemiology of Diabetes, and G. Complications Research. 2010. Effect of prior intensive insulin treatment during the Diabetes Control and Complications Trial (DCCT) on peripheral neuropathy in type 1 diabetes during the Epidemiology of Diabetes Interventions and Complications (EDIC) Study. *Diab Care*. 33:1090-1096.

American Diabetes, A. 2007. Standards of medical care in diabetes--2007. *Diab Care*. 30 Suppl 1:S4-S41.

American Diabetes, A. 2013. Diagnosis and classification of diabetes mellitus. *Diab Care*. 36 Suppl 1:S67-74.

American Diabetes, A. 2014. The Cost of Diabetes. *http://www.diabetes.org/advocacy/news-events/cost-of-diabetes.html*.

Amin, V., D.V. Cumming, R.S. Coffin, and D.S. Latchman. 1995. The degree of protection provided to neuronal cells by a pre-conditioning stress correlates with the amount of heat shock protein 70 it induces and not with the similarity of the subsequent stress. *Neurosci Lett*. 200:85-88.

Anckar, J., and L. Sistonen. 2007. Heat shock factor 1 as a coordinator of stress and developmental pathways. *Adv Exp Med Biol*. 594:78-88.

Andre, I., A. Gonzalez, B. Wang, J. Katz, C. Benoist, and D. Mathis. 1996. Checkpoints in the progression of autoimmune disease: lessons from diabetes models. *Proc Natl Acad Sci U S A*. 93:2260-2263.

Ansar, S., J.A. Burlison, M.K. Hadden, X.M. Yu, K.E. Desino, J. Bean, L. Neckers, K.L. Audus, M.L. Michaelis, and B.S. Blagg. 2007. A non-toxic Hsp90 inhibitor protects neurons from Abeta-induced toxicity. *Bioorg Med Chem Lett*. 17:1984-1990.

Apfel, S.C. 1999. Neurotrophic factors in peripheral neuropathies: therapeutic implications. *Brain Pathol*. 9:393-413.

Apfel, S.C., J.A. Kessler, B.T. Adornato, W.J. Litchy, C. Sanders, and C.A. Rask. 1998. Recombinant human nerve growth factor in the treatment of diabetic polyneuropathy. NGF Study Group. *Neurology*. 51:695-702.

Argyriou, A.A., J. Bruna, P. Marmiroli, and G. Cavaletti. 2012. Chemotherapy-induced peripheral neurotoxicity (CIPN): an update. *Crit Rev Oncol Hematol*. 82:51-77.

Arnoult, D., N. Rismanchi, A. Grodet, R.G. Roberts, D.P. Seeburg, J. Estaquier, M. Sheng, and C. Blackstone. 2005. Bax/Bak-dependent release of DDP/TIMM8a promotes Drp1-mediated mitochondrial fission and mitoptosis during programmed cell death. *Curr Biol*. 15:2112-2118.

Azad, N., N.V. Emanuele, C. Abraira, W.G. Henderson, J. Colwell, S.R. Levin, F.Q. Nuttall, J.P. Comstock, C.T. Sawin, C. Silbert, and F.A. Rubino. 1999. The effects of intensive glycemic control on neuropathy in the VA cooperative study on type II diabetes mellitus (VA CSDM). *J Diabetes Complicat*. 13:307-313.

Bach, D., D. Naon, S. Pich, F.X. Soriano, N. Vega, J. Rieusset, M. Laville, C. Guillet, Y. Boirie, H. Wallberg-Henriksson, M. Manco, M. Calvani, M. Castagneto, M. Palacin, G. Mingrone, J.R. Zierath, H. Vidal, and A. Zorzano. 2005. Expression of Mfn2, the Charcot-Marie-Tooth neuropathy type 2A gene, in human skeletal muscle: effects of type 2 diabetes, obesity, weight loss, and the regulatory role of tumor necrosis factor alpha and interleukin-6. *Diabetes*. 54:2685-2693.

Bach, D., S. Pich, F.X. Soriano, N. Vega, B. Baumgartner, J. Oriola, J.R. Daugaard, J. Lloberas, M. Camps, J.R. Zierath, R. Rabasa-Lhoret, H. Wallberg-Henriksson, M. Laville, M. Palacin, H. Vidal, F. Rivera, M. Brand, and A. Zorzano. 2003. Mitofusin-2 determines mitochondrial network architecture and mitochondrial metabolism. A novel regulatory mechanism altered in obesity. *J Biol Chem*. 278:17190-17197.

Bailey, C.J., and R.C. Turner. 1996. Metformin. *N Engl J Med*. 334:574-579.

Barile, G.R., S.I. Pachydaki, S.R. Tari, S.E. Lee, C.M. Donmoyer, W. Ma, L.L. Rong, L.G. Buciarelli, T. Wendt, H. Horig, B.I. Hudson, W. Qu, A.D. Weinberg, S.F. Yan, and A.M. Schmidt. 2005. The RAGE axis in early diabetic retinopathy. *Invest Ophthalmol Vis Sci*. 46:2916-2924.

Baseler, W.A., E.R. Dabkowski, C.L. Williamson, T.L. Croston, D. Thapa, M.J. Powell, T.T. Razunguzwa, and J.M. Hollander. 2011. Proteomic alterations of distinct mitochondrial subpopulations in the type 1 diabetic heart: contribution of protein import dysfunction. *Am J Physiol Regul Integr Comp Physiol*. 300:R186-200.

Batuman, V. 2014. Diabetic Nephropathy, eMedicine from WebMD.

Baumann, C.A., V. Ribon, M. Kanzaki, D.C. Thurmond, S. Mora, S. Shigematsu, P.E. Bickel, J.E. Pessin, and A.R. Saltiel. 2000. CAP defines a second signalling pathway required for insulin-stimulated glucose transport. *Nature*. 407:202-207.

Berlett, B.S., and E.R. Stadtman. 1997. Protein oxidation in aging, disease, and oxidative stress. *J Biol Chem*. 272:20313-20316.

Bhavsar, A. 2014. Diabetic Retinopathy, eMedicine from WebMD.

Bierhaus, A., K.M. Haslbeck, P.M. Humpert, B. Liliensiek, T. Dehmer, M. Morcos, A.A. Sayed, M. Andrassy, S. Schiekofer, J.G. Schneider, J.B. Schulz, D. Heuss, B. Neundorfer, S. Dierl, J. Huber, H. Tritschler, A.M. Schmidt, M. Schwaninger, H.U. Haering, E. Schleicher, M. Kasper, D.M. Stern, B. Arnold, and P.P. Nawroth. 2004a. Loss of pain perception in diabetes is dependent on a receptor of the immunoglobulin superfamily. *J Clin Invest*. 114:1741-1751.

Bierhaus, A., K.M. Haslbeck, P.M. Humpert, B. Liliensiek, T. Dehmer, M. Morcos, A.A. Sayed, M. Andrassy, S. Schiekofer, J.G. Schneider, J.B. Schulz, D. Heuss, B. Neundorfer, S. Dierl, J. Huber, H. Tritschler, A.M. Schmidt, M. Schwaninger, H.U. Haering, E. Schleicher, M. Kasper, D.M. Stern, B. Arnold, and P.P. Nawroth. 2004b. Loss of pain perception in diabetes is dependent on a receptor of the immunoglobulin superfamily. *J Clin Invest*. 114:1741-1751.

Biessels, G.J., V. Bril, N.A. Calcutt, N.E. Cameron, M.A. Cotter, R. Dobrowsky, E.L. Feldman, P. Fernyhough, J. Jakobsen, R.A. Malik, A.P. Mizisin, P.J. Oates, I.G. Obrosova, R. Pop-Busui, J.W. Russell, A.A. Sima, M.J. Stevens, R.E. Schmidt, S. Tesfaye, A. Veves, A.I. Vinik, D.E. Wright, S. Yagihashi, M.A. Yorek, D. Ziegler, and D.W. Zochodne. 2014. Phenotyping animal models of diabetic neuropathy: a consensus statement of the diabetic neuropathy study group of the EASD (Neurodiab). *J Peripher Nerv Syst*. 19:77-87.

Boden, G., and G.I. Shulman. 2002. Free fatty acids in obesity and type 2 diabetes: defining their role in the development of insulin resistance and beta-cell dysfunction. *Eur J Clin Invest*. 32 Suppl 3:14-23.

Bonifacio, E., and A.G. Ziegler. 2010. Advances in the prediction and natural history of type 1 diabetes. *Endocrinol Metab Clin North Am*. 39:513-525.

Boulton, A.J., A.I. Vinik, J.C. Arezzo, V. Bril, E.L. Feldman, R. Freeman, R.A. Malik, R.E. Maser, J.M. Sosenko, D. Ziegler, and A. American Diabetes. 2005. Diabetic neuropathies: a statement by the American Diabetes Association. *Diab Care*. 28:956-962.

Boulton, T.G., S.H. Nye, D.J. Robbins, N.Y. Ip, E. Radziejewska, S.D. Morgenbesser, R.A. DePinho, N. Panayotatos, M.H. Cobb, and G.D. Yancopoulos. 1991. ERKs: a family of

protein-serine/threonine kinases that are activated and tyrosine phosphorylated in response to insulin and NGF. *Cell*. 65:663-675.

Brady, M.J., A.C. Nairn, and A.R. Saltiel. 1997. The regulation of glycogen synthase by protein phosphatase 1 in 3T3-L1 adipocytes. Evidence for a potential role for DARPP-32 in insulin action. *J Biol Chem*. 272:29698-29703.

Brand, M.D., and D.G. Nicholls. 2011. Assessing mitochondrial dysfunction in cells. *Biochem J*. 435:297-312.

Brandenburg, D. 2008. History and diagnostic significance of C-peptide. *Exp Diabetes Res*. 2008:576862.

Broome, C.S., A.C. Kayani, J. Palomero, W.H. Dillmann, R. Mestril, M.J. Jackson, and A. McArdle. 2006. Effect of lifelong overexpression of HSP70 in skeletal muscle on age-related oxidative stress and adaptation after nondamaging contractile activity. *FASEB J*. 20:1549-1551.

Brown, G.C. 1999. Nitric oxide and mitochondrial respiration. *Biochim Biophys Acta*. 1411:351-369.

Brownlee, M. 2005. The pathobiology of diabetic complications: a unifying mechanism. *Diabetes*. 54:1615-1625.

Bruce, C.R., A.L. Carey, J.A. Hawley, and M.A. Febbraio. 2003. Intramuscular heat shock protein 72 and heme oxygenase-1 mRNA are reduced in patients with type 2 diabetes: evidence that insulin resistance is associated with a disturbed antioxidant defense mechanism. *Diabetes*. 52:2338-2345.

Brussee, V., F.A. Cunningham, and D.W. Zochodne. 2004. Direct insulin signaling of neurons reverses diabetic neuropathy. *Diabetes*. 53:1824-1830.

Calcutt, N.A., M.E. Cooper, T.S. Kern, and A.M. Schmidt. 2009. Therapies for hyperglycaemia-induced diabetic complications: from animal models to clinical trials. *Nat Rev Drug Discov*. 8:417-429.

Calcutt, N.A., D.R. Tomlinson, G.B. Willars, and P. Keen. 1990. Axonal transport of substance P-like immunoreactivity in ganglioside-treated diabetic rats. *J Neurol Sci*. 96:283-291.

Callaghan, B.C., H.T. Cheng, C.L. Stables, A.L. Smith, and E.L. Feldman. 2012a. Diabetic neuropathy: clinical manifestations and current treatments. *Lancet Neurol*. 11:521-534.

Callaghan, B.C., J. Hur, and E.L. Feldman. 2012b. Diabetic neuropathy: one disease or two? *Curr Opin Neurol*. 25:536-541.

Cameron, N.E., and M.A. Cotter. 1996. Effects of a nonpeptide endothelin-1 ETA antagonist on neurovascular function in diabetic rats: interaction with the renin-angiotensin system. *J Pharmacol Exp Ther*. 278:1262-1268.

Cameron, N.E., and M.A. Cotter. 2008. Pro-inflammatory mechanisms in diabetic neuropathy: focus on the nuclear factor kappa B pathway. *Curr Drug Targets*. 9:60-67.

Cameron, N.E., M.A. Cotter, A.M. Jack, M.D. Basso, and T.C. Hohman. 1999. Protein kinase C effects on nerve function, perfusion, Na(+), K(+)-ATPase activity and glutathione content in diabetic rats. *Diabetologia*. 42:1120-1130.

Carls, G.S., T.B. Gibson, V.R. Driver, J.S. Wrobel, M.G. Garoufalis, R.R. Defrancis, S. Wang, J.E. Bagalman, and J.R. Christina. 2011. The economic value of specialized lower-extremity medical care by podiatric physicians in the treatment of diabetic foot ulcers. *J Am Podiatr Med Assoc*. 101:93-115.

Carlson, C.J., M.F. White, and C.M. Rondinone. 2004. Mammalian target of rapamycin regulates IRS-1 serine 307 phosphorylation. *Biochem Biophys Res Commun*. 316:533-539.

CDC. 2014. National Diabetes Statistics Report.

Chang, L., S.H. Chiang, and A.R. Saltiel. 2004. Insulin signaling and the regulation of glucose transport. *Mol Med*. 10:65-71.

Chen, S., and D.F. Smith. 1998. Hop as an adaptor in the heat shock protein 70 (Hsp70) and hsp90 chaperone machinery. *J Biol Chem*. 273:35194-35200.

Cheng, C., and D.W. Zochodne. 2003. Sensory neurons with activated caspase-3 survive long-term experimental diabetes. *Diabetes*. 52:2363-2371.

Chiang, J.L., Kirkman, M.S., Laffel, L.M.B., and Peters, A.L., on behalf of the Type 1 Diabetes Sourcebook Authors. 2014. Type 1 Diabetes Through the Life Span: A Position Statement of the American Diabetes Association. *Diab Care*. 37:2034-2054.

Chiang, S.H., C.A. Baumann, M. Kanzaki, D.C. Thurmond, R.T. Watson, C.L. Neudauer, I.G. Macara, J.E. Pessin, and A.R. Saltiel. 2001. Insulin-stimulated GLUT4 translocation requires the CAP-dependent activation of TC10. *Nature*. 410:944-948.

Chiosis, G., B. Lucas, H. Huezo, D. Solit, A. Basso, and N. Rosen. 2003. Development of purine-scaffold small molecule inhibitors of Hsp90. *Curr Cancer Drug Targets*. 3:371-376.

Chowdhury, S.K., R.T. Dobrowsky, and P. Fernyhough. 2011. Nutrient excess and altered mitochondrial proteome and function contribute to neurodegeneration in diabetes. *Mitochondrion*. 11:845-854.

Chowdhury, S.K., D.R. Smith, and P. Fernyhough. 2013. The role of aberrant mitochondrial bioenergetics in diabetic neuropathy. *Neurobiol Dis*. 51:56-65.

Chowdhury, S.K., D.R. Smith, A. Saleh, J. Schapansky, A. Marquez, S. Gomes, E. Akude, D. Morrow, N.A. Calcutt, and P. Fernyhough. 2012. Impaired adenosine monophosphate-activated protein kinase signalling in dorsal root ganglia neurons is linked to mitochondrial dysfunction and peripheral neuropathy in diabetes. *Brain*. 135:1751-1766.

Chowdhury, S.K., E. Zherebitskaya, D.R. Smith, E. Akude, S. Chattopadhyay, C.G. Jolivalt, N.A. Calcutt, and P. Fernyhough. 2010. Mitochondrial respiratory chain dysfunction in dorsal root ganglia of streptozotocin-induced diabetic rats and its correction by insulin treatment. *Diabetes*. 59:1082-1091.

Clements, R.S., Jr. 1986. The polyol pathway. A historical review. *Drugs*. 32 Suppl 2:3-5.

Cocozza, S., A. Porcellini, G. Riccardi, A. Monticelli, G. Condorelli, A. Ferrara, L. Pianese, C. Miele, B. Capaldo, F. Beguinot, and et al. 1992. NIDDM associated with mutation in tyrosine kinase domain of insulin receptor gene. *Diabetes*. 41:521-526.

Collins, C.B., D. Strassheim, C.M. Aherne, A.R. Yeckes, P. Jedlicka, and E.F. de Zoeten. 2014. Targeted inhibition of heat shock protein 90 suppresses tumor necrosis factor-alpha and ameliorates murine intestinal inflammation. *Inflamm Bowel Dis*. 20:685-694.

Connell, P., C.A. Ballinger, J. Jiang, Y. Wu, L.J. Thompson, J. Hohfeld, and C. Patterson. 2001. The co-chaperone CHIP regulates protein triage decisions mediated by heat-shock proteins. *Nat Cell Biol*. 3:93-96.

Conti, G., E. Scarpini, P. Baron, S. Livraghi, M. Tiriticco, R. Bianchi, C. Vedeler, and G. Scarlato. 2002. Macrophage infiltration and death in the nerve during the early phases of experimental diabetic neuropathy: a process concomitant with endoneurial induction of IL-1beta and p75NTR. *J Neurol Sci*. 195:35-40.

Coppey, L.J., E.P. Davidson, T.W. Rinehart, J.S. Gellett, C.L. Oltman, D.D. Lund, and M.A. Yorek. 2006. ACE inhibitor or angiotensin II receptor antagonist attenuates diabetic neuropathy in streptozotocin-induced diabetic rats. *Diabetes*. 55:341-348.

Coppey, L.J., J.S. Gellett, E.P. Davidson, J.A. Dunlap, D.D. Lund, and M.A. Yorek. 2001. Effect of antioxidant treatment of streptozotocin-induced diabetic rats on endoneurial blood flow, motor nerve conduction velocity, and vascular reactivity of epineurial arterioles of the sciatic nerve. *Diabetes*. 50:1927-1937.

Corney, D.C. 2013. RNA-seq Using Next Generation Sequencing., http://www.labome.com/method/RNA-seq-Using-Next-Generation-Sequencing.html.

Corvera, S., and M.P. Czech. 1998. Direct targets of phosphoinositide 3-kinase products in membrane traffic and signal transduction. *Trends Cell Biol*. 8:442-446.

Craparo, A., R. Freund, and T.A. Gustafson. 1997. 14-3-3 (epsilon) interacts with the insulin-like growth factor I receptor and insulin receptor substrate I in a phosphoserine-dependent manner. *J Biol Chem*. 272:11663-11669.

Crawford, T.N., D.V. Alfaro, 3rd, J.B. Kerrison, and E.P. Jablon. 2009. Diabetic retinopathy and angiogenesis. *Curr Diabetes Rev*. 5:8-13.

Cross, D.A., D.R. Alessi, P. Cohen, M. Andjelkovich, and B.A. Hemmings. 1995. Inhibition of glycogen synthase kinase-3 by insulin mediated by protein kinase B. *Nature*. 378:785-789.

Cullum, N.A., J. Mahon, K. Stringer, and W.G. McLean. 1991. Glycation of rat sciatic nerve tubulin in experimental diabetes mellitus. *Diabetologia*. 34:387-389.

Cusi, K., A. Consoli, and R.A. DeFronzo. 1996. Metabolic effects of metformin on glucose and lactate metabolism in noninsulin-dependent diabetes mellitus. *J Clin Endocrinol Metab*. 81:4059-4067.

Dale, A.C., L.J. Vatten, T.I. Nilsen, K. Midthjell, and R. Wiseth. 2008. Secular decline in mortality from coronary heart disease in adults with diabetes mellitus: cohort study. *BMJ*. 337:a236.

Das Evcimen, N., and G.L. King. 2007. The role of protein kinase C activation and the vascular complications of diabetes. *Pharmacol Res*. 55:498-510.

Daugaard, M., M. Rohde, and M. Jaattela. 2007. The heat shock protein 70 family: Highly homologous proteins with overlapping and distinct functions. *FEBS Lett*. 581:3702-3710.

DeFronzo, R.A. 2004. Pathogenesis of type 2 diabetes mellitus. *Med Clin North Am*. 88:787-835, ix.

DeFronzo, R.A., R.C. Bonadonna, and E. Ferrannini. 1992. Pathogenesis of NIDDM. A balanced overview. *Diab Care*. 15:318-368.

Dello Russo, C., P.E. Polak, P.R. Mercado, A. Spagnolo, A. Sharp, P. Murphy, A. Kamal, F.J. Burrows, L.C. Fritz, and D.L. Feinstein. 2006. The heat-shock protein 90 inhibitor 17-allylamino-17-demethoxygeldanamycin suppresses glial inflammatory responses and ameliorates experimental autoimmune encephalomyelitis. *J Neurochem*. 99:1351-1362.

Delree, P., P. Leprince, J. Schoenen, and G. Moonen. 1989. Purification and culture of adult rat dorsal root ganglia neurons. *J Neurosci Res*. 23:198-206.

Devi, T.S., I. Lee, M. Huttemann, A. Kumar, K.D. Nantwi, and L.P. Singh. 2012. TXNIP links innate host defense mechanisms to oxidative stress and inflammation in retinal Muller glia under chronic hyperglycemia: implications for diabetic retinopathy. *Exp Diabetes Res*. 2012:438238.

Dickey, C.A., A. Kamal, K. Lundgren, N. Klosak, R.M. Bailey, J. Dunmore, P. Ash, S. Shoraka, J. Zlatkovic, C.B. Eckman, C. Patterson, D.W. Dickson, N.S. Nahman, Jr., M. Hutton, F. Burrows, and L. Petrucelli. 2007. The high-affinity HSP90-CHIP complex recognizes and selectively degrades phosphorylated tau client proteins. *J Clin Invest*. 117:648-658.

Diemel, L.T., W.J. Brewster, P. Fernyhough, and D.R. Tomlinson. 1994. Expression of neuropeptides in experimental diabetes; effects of treatment with nerve growth factor or brain-derived neurotrophic factor. *Brain Res Mol Brain Res*. 21:171-175.

Dix, D.J., J.W. Allen, B.W. Collins, C. Mori, N. Nakamura, P. Poorman-Allen, E.H. Goulding, and E.M. Eddy. 1996. Targeted gene disruption of Hsp70-2 results in failed meiosis, germ cell apoptosis, and male infertility. *Proc Natl Acad Sci U S A*. 93:3264-3268.

Dodson, G., and D. Steiner. 1998. The role of assembly in insulin's biosynthesis. *Curr Opin Struct Biol*. 8:189-194.

Dokladny, K., R. Lobb, W. Wharton, T.Y. Ma, and P.L. Moseley. 2010. LPS-induced cytokine levels are repressed by elevated expression of HSP70 in rats: possible role of NF-kappaB. *Cell Stress Chaperon*. 15:153-163.

Dorrell, M., H. Uusitalo-Jarvinen, E. Aguilar, and M. Friedlander. 2007. Ocular neovascularization: basic mechanisms and therapeutic advances. *Surv Ophthalmol*. 52 Suppl 1:S3-19.

Dotta, F., S. Censini, A.G. van Halteren, L. Marselli, M. Masini, S. Dionisi, F. Mosca, U. Boggi, A.O. Muda, S. Del Prato, J.F. Elliott, A. Covacci, R. Rappuoli, B.O. Roep, and P. Marchetti. 2007. Coxsackie B4 virus infection of beta cells and natural killer cell insulitis in recent-onset type 1 diabetic patients. *Proc Natl Acad Sci U S A*. 104:5115-5120.

Doupis, J., T.E. Lyons, S. Wu, C. Gnardellis, T. Dinh, and A. Veves. 2009. Microvascular reactivity and inflammatory cytokines in painful and painless peripheral diabetic neuropathy. *J Clin Endocrinol Metab*. 94:2157-2163.

Drake, P.G., and B.I. Posner. 1998. Insulin receptor-associated protein tyrosine phosphatase(s): role in insulin action. *Mol Cell Biochem*. 182:79-89.

Drel, V.R., P. Pacher, I. Vareniuk, I.A. Pavlov, O. Ilnytska, V.V. Lyzogubov, S.R. Bell, J.T. Groves, and I.G. Obrosova. 2007. Evaluation of the peroxynitrite decomposition catalyst Fe(III) tetra-mesitylporphyrin octasulfonate on peripheral neuropathy in a mouse model of type 1 diabetes. *Int J Mol Med*. 20:783-792.

Dyck, P.J. 1988. Detection, characterization, and staging of polyneuropathy: assessed in diabetics. *Muscle Nerve*. 11:21-32.

Edwards, J.L., A.M. Vincent, H.T. Cheng, and E.L. Feldman. 2008. Diabetic neuropathy: mechanisms to management. *Pharmacol Ther*. 120:1-34.

Ekberg, K., T. Brismar, B.L. Johansson, B. Jonsson, P. Lindstrom, and J. Wahren. 2003. Amelioration of sensory nerve dysfunction by C-Peptide in patients with type 1 diabetes. *Diabetes*. 52:536-541.

Ekberg, K., T. Brismar, B.L. Johansson, P. Lindstrom, L. Juntti-Berggren, A. Norrby, C. Berne, H.J. Arnqvist, J. Bolinder, and J. Wahren. 2007. C-Peptide replacement therapy and sensory nerve function in type 1 diabetic neuropathy. *Diab Care*. 30:71-76.

Elchebly, M., P. Payette, E. Michaliszyn, W. Cromlish, S. Collins, A.L. Loy, D. Normandin, A. Cheng, J. Himms-Hagen, C.C. Chan, C. Ramachandran, M.J. Gresser, M.L. Tremblay, and B.P. Kennedy. 1999. Increased insulin sensitivity and obesity resistance in mice lacking the protein tyrosine phosphatase-1B gene. *Science*. 283:1544-1548.

Engelgau, M.M., L.S. Geiss, J.B. Saaddine, J.P. Boyle, S.M. Benjamin, E.W. Gregg, E.F. Tierney, N. Rios-Burrows, A.H. Mokdad, E.S. Ford, G. Imperatore, and K.M. Narayan. 2004. The evolving diabetes burden in the United States. *Ann Intern Med*. 140:945-950.

Engerman, R.L., and T.S. Kern. 1987. Progression of incipient diabetic retinopathy during good glycemic control. *Diabetes*. 36:808-812.

Evans, C.G., L. Chang, and J.E. Gestwicki. 2010. Heat shock protein 70 (hsp70) as an emerging drug target. *J Med Chem*. 53:4585-4602.

Fang, Z., J. Martin, and Z. Wang. 2012. Statistical methods for identifying differentially expressed genes in RNA-Seq experiments. *Cell Biosci*. 2:26.

Farmer, K., S.J. Williams, L. Novikova, K. Ramachandran, S. Rawal, B.S. Blagg, R. Dobrowsky, and L. Stehno-Bittel. 2012a. KU-32, a novel drug for diabetic neuropathy, is safe for human islets and improves in vitro insulin secretion and viability. *Exp Diabetes Res*. 2012:671673.

Farmer, K.L., C. Li, and R.T. Dobrowsky. 2012b. Diabetic peripheral neuropathy: should a chaperone accompany our therapeutic approach? *Pharmacol Rev*. 64:880-900.

Feder, M.E., and G.E. Hofmann. 1999. Heat-shock proteins, molecular chaperones, and the stress response: evolutionary and ecological physiology. *Annu Rev Physiol*. 61:243-282.

Fernyhough, P., A. Gallagher, S.A. Averill, J.V. Priestley, L. Hounsom, J. Patel, and D.R. Tomlinson. 1999. Aberrant neurofilament phosphorylation in sensory neurons of rats with diabetic neuropathy. *Diabetes*. 48:881-889.

Fernyhough, P., S.K. Roy Chowdhury, and R.E. Schmidt. 2010. Mitochondrial stress and the pathogenesis of diabetic neuropathy. *Expert Rev Endocrinol Metab*. 5:39-49.

Fierro-Monti, I., J. Racle, C. Hernandez, P. Waridel, V. Hatzimanikatis, and M. Quadroni. 2013. A novel pulse-chase SILAC strategy measures changes in protein decay and synthesis rates induced by perturbation of proteostasis with an Hsp90 inhibitor. *PLoS One*. 8:e80423.

Figueroa-Romero, C., M. Sadidi, and E.L. Feldman. 2008. Mechanisms of disease: the oxidative stress theory of diabetic neuropathy. *Rev Endocr Metab Disord*. 9:301-314.

Fioretto, P., M.W. Steffes, D.E. Sutherland, F.C. Goetz, and M. Mauer. 1998. Reversal of lesions of diabetic nephropathy after pancreas transplantation. *N Engl J Med*. 339:69-75.

Florin, L., K.A. Becker, C. Sapp, C. Lambert, H. Sirma, M. Muller, R.E. Streeck, and M. Sapp. 2004. Nuclear translocation of papillomavirus minor capsid protein L2 requires Hsc70. *J Virol*. 78:5546-5553.

Foulis, A.K., M.A. Farquharson, and A. Meager. 1987. Immunoreactive alpha-interferon in insulin-secreting beta cells in type 1 diabetes mellitus. *Lancet*. 2:1423-1427.

Frank, R.N. 2004. Diabetic retinopathy. *N Engl J Med*. 350:48-58.

Gandhi, R.A., and D. Selvarajah. 2015. Understanding and treating painful diabetic neuropathy: time for a paradigm shift. *Diabet Med*.

Ganesh Yerra, V., G. Negi, S.S. Sharma, and A. Kumar. 2013. Potential therapeutic effects of the simultaneous targeting of the Nrf2 and NF-kappaB pathways in diabetic neuropathy. *Redox Biol*. 1:394-397.

Gao, Z., D. Hwang, F. Bataille, M. Lefevre, D. York, M.J. Quon, and J. Ye. 2002. Serine phosphorylation of insulin receptor substrate 1 by inhibitor kappa B kinase complex. *J Biol Chem*. 277:48115-48121.

Gao, Z., X. Zhang, A. Zuberi, D. Hwang, M.J. Quon, M. Lefevre, and J. Ye. 2004. Inhibition of insulin sensitivity by free fatty acids requires activation of multiple serine kinases in 3T3-L1 adipocytes. *Mol Endocrinol*. 18:2024-2034.

Gibbons, C.H., and R. Freeman. 2010. Treatment-induced diabetic neuropathy: a reversible painful autonomic neuropathy. *Ann Neurol*. 67:534-541.

Gilbertson, D.T., J. Liu, J.L. Xue, T.A. Louis, C.A. Solid, J.P. Ebben, and A.J. Collins. 2005. Projecting the number of patients with end-stage renal disease in the United States to the year 2015. *J Am Soc Nephrol*. 16:3736-3741.

Glass, D.J., and G.D. Yancopoulos. 1993. The neurotrophins and their receptors. *Trends Cell Biol*. 3:262-268.

Goecks, J., A. Nekrutenko, J. Taylor, and G. Team. 2010. Galaxy: a comprehensive approach for supporting accessible, reproducible, and transparent computational research in the life sciences. *Genome Biol*. 11.

Gonzalez-Clemente, J.M., D. Mauricio, C. Richart, M. Broch, A. Caixas, A. Megia, O. Gimenez-Palop, I. Simon, A. Martinez-Riquelme, G. Gimenez-Perez, and J. Vendrell. 2005. Diabetic neuropathy is associated with activation of the TNF-alpha system in subjects with type 1 diabetes mellitus. *Clin Endocrinol (Oxf)*. 63:525-529.

Gordois, A., P. Scuffham, A. Shearer, A. Oglesby, and J.A. Tobian. 2003. The health care costs of diabetic peripheral neuropathy in the US. *Diab Care*. 26:1790-1795.

Griffin, M.E., M.J. Marcucci, G.W. Cline, K. Bell, N. Barucci, D. Lee, L.J. Goodyear, E.W. Kraegen, M.F. White, and G.I. Shulman. 1999. Free fatty acid-induced insulin resistance is associated with activation of protein kinase C theta and alterations in the insulin signaling cascade. *Diabetes*. 48:1270-1274.

Gruessner, A.C. 2011. 2011 update on pancreas transplantation: comprehensive trend analysis of 25,000 cases followed up over the course of twenty-four years at the International Pancreas Transplant Registry (IPTR). *Rev Diabet Stud*. 8:6-16.

Gual, P., Y. Le Marchand-Brustel, and J.F. Tanti. 2005. Positive and negative regulation of insulin signaling through IRS-1 phosphorylation. *Biochimie*. 87:99-109.

Guariguata, L. 2012. By the numbers: new estimates from the IDF Diabetes Atlas Update for 2012. *Diabetes Res Clin Pract*. 98:524-525.

Guariguata, L. 2013. Contribute data to the 6th edition of the IDF Diabetes Atlas. *Diabetes Res Clin Pract*. 100:280-281.

Guettouche, T., F. Boellmann, W.S. Lane, and R. Voellmy. 2005. Analysis of phosphorylation of human heat shock factor 1 in cells experiencing a stress. *BMC Biochem*. 6:4.

Guilford, B.L., J.M. Ryals, and D.E. Wright. 2011. Phenotypic changes in diabetic neuropathy induced by a high-fat diet in diabetic C57BL/6 mice. *Exp Diabetes Res*. 2011:848307.

Ha, H.C., L.D. Hester, and S.H. Snyder. 2002. Poly(ADP-ribose) polymerase-1 dependence of stress-induced transcription factors and associated gene expression in glia. *Proc Natl Acad Sci U S A*. 99:3270-3275.

Hamilton, R.T., A. Bhattacharya, M.E. Walsh, Y. Shi, R. Wei, Y. Zhang, K.A. Rodriguez, R. Buffenstein, A.R. Chaudhuri, and H. Van Remmen. 2013. Elevated protein carbonylation, and misfolding in sciatic nerve from db/db and Sod1(-/-) mice: plausible link between oxidative stress and demyelination. *PLoS One*. 8:e65725.

Harrison, J.F., S.B. Hollensworth, D.R. Spitz, W.C. Copeland, G.L. Wilson, and S.P. LeDoux. 2005. Oxidative stress-induced apoptosis in neurons correlates with mitochondrial DNA base excision repair pathway imbalance. *Nucleic Acids Res*. 33:4660-4671.

Haslbeck, K.M., B. Neundorfer, U. Schlotzer-Schrehardtt, A. Bierhaus, E. Schleicher, E. Pauli, M. Haslbeck, M. Hecht, P. Nawroth, and D. Heuss. 2007. Activation of the RAGE pathway: a general mechanism in the pathogenesis of polyneuropathies? *Neurol Res*. 29:103-110.

Haslbeck, K.M., E. Schleicher, A. Bierhaus, P. Nawroth, M. Haslbeck, B. Neundorfer, and D. Heuss. 2005. The AGE/RAGE/NF-(kappa)B pathway may contribute to the pathogenesis of polyneuropathy in impaired glucose tolerance (IGT). *Exp Clin Endocrinol Diabetes*. 113:288-291.

Hellweg, R., G. Raivich, H.D. Hartung, C. Hock, and G.W. Kreutzberg. 1994. Axonal transport of endogenous nerve growth factor (NGF) and NGF receptor in experimental diabetic neuropathy. *Exp Neurol*. 130:24-30.

Hellweg, R., M. Wohrle, H.D. Hartung, H. Stracke, C. Hock, and K. Federlin. 1991. Diabetes mellitus-associated decrease in nerve growth factor levels is reversed by allogeneic pancreatic islet transplantation. *Neurosci Lett*. 125:1-4.

Herder, C., M. Lankisch, D. Ziegler, W. Rathmann, W. Koenig, T. Illig, A. Doring, B. Thorand, R. Holle, G. Giani, S. Martin, and C. Meisinger. 2009. Subclinical inflammation and diabetic polyneuropathy: MONICA/KORA Survey F3 (Augsburg, Germany). *Diab Care*. 32:680-682.

Hevener, A.L., D. Reichart, A. Janez, and J. Olefsky. 2001. Thiazolidinedione treatment prevents free fatty acid-induced insulin resistance in male wistar rats. *Diabetes*. 50:2316-2322.

Hietakangas, V., J.K. Ahlskog, A.M. Jakobsson, M. Hellesuo, N.M. Sahlberg, C.I. Holmberg, A. Mikhailov, J.J. Palvimo, L. Pirkkala, and L. Sistonen. 2003. Phosphorylation of serine 303 is a prerequisite for the stress-inducible SUMO modification of heat shock factor 1. *Mol Cell Biol*. 23:2953-2968.

Hietakangas, V., J. Anckar, H.A. Blomster, M. Fujimoto, J.J. Palvimo, A. Nakai, and L. Sistonen. 2006. PDSM, a motif for phosphorylation-dependent SUMO modification. *Proc Natl Acad Sci U S A*. 103:45-50.

Hinder, L.M., A.M. Vincent, J.M. Hayes, L.L. McLean, and E.L. Feldman. 2013a. Apolipoprotein E knockout as the basis for mouse models of dyslipidemia-induced neuropathy. *Exp Neurol*. 239:102-110.

Hinder, L.M., A. Vivekanandan-Giri, L.L. McLean, S. Pennathur, and E.L. Feldman. 2013b. Decreased glycolytic and tricarboxylic acid cycle intermediates coincide with peripheral

nervous system oxidative stress in a murine model of type 2 diabetes. *J Endocrinol*. 216:1-11.

Ho, E.C., K.S. Lam, Y.S. Chen, J.C. Yip, M. Arvindakshan, S. Yamagishi, S. Yagihashi, P.J. Oates, C.A. Ellery, S.S. Chung, and S.K. Chung. 2006. Aldose reductase-deficient mice are protected from delayed motor nerve conduction velocity, increased c-Jun NH2-terminal kinase activation, depletion of reduced glutathione, increased superoxide accumulation, and DNA damage. *Diabetes*. 55:1946-1953.

Holman, R.R., S.K. Paul, M.A. Bethel, D.R. Matthews, and H.A. Neil. 2008. 10-year follow-up of intensive glucose control in type 2 diabetes. *N Engl J Med*. 359:1577-1589.

Holmberg, C.I., V. Hietakangas, A. Mikhailov, J.O. Rantanen, M. Kallio, A. Meinander, J. Hellman, N. Morrice, C. MacKintosh, R.I. Morimoto, J.E. Eriksson, and L. Sistonen. 2001. Phosphorylation of serine 230 promotes inducible transcriptional activity of heat shock factor 1. *EMBO J*. 20:3800-3810.

Holmstrom, M.H., E. Iglesias-Gutierrez, J.R. Zierath, and P.M. Garcia-Roves. 2012. Tissue-specific control of mitochondrial respiration in obesity-related insulin resistance and diabetes. *Am J Physiol Endocrinol Metab*. 302:E731-739.

Hotamisligil, G.S. 2000. Molecular mechanisms of insulin resistance and the role of the adipocyte. *Int J Obes Relat Metab Disord*. 24 Suppl 4:S23-27.

Hotamisligil, G.S., P. Peraldi, A. Budavari, R. Ellis, M.F. White, and B.M. Spiegelman. 1996. IRS-1-mediated inhibition of insulin receptor tyrosine kinase activity in TNF-alpha- and obesity-induced insulin resistance. *Science*. 271:665-668.

Hu, J., J. Liu, R. Ghirlando, A.R. Saltiel, and S.R. Hubbard. 2003. Structural basis for recruitment of the adaptor protein APS to the activated insulin receptor. *Mol Cell*. 12:1379-1389.

Huang, C., J. Wang, Z. Chen, Y. Wang, and W. Zhang. 2013. 2-phenylethynesulfonamide Prevents Induction of Pro-inflammatory Factors and Attenuates LPS-induced Liver Injury by Targeting NHE1-Hsp70 Complex in Mice. *PLoS One*. 8:e67582.

Huang, T.J., S.A. Price, L. Chilton, N.A. Calcutt, D.R. Tomlinson, A. Verkhratsky, and P. Fernyhough. 2003. Insulin prevents depolarization of the mitochondrial inner membrane in sensory neurons of type 1 diabetic rats in the presence of sustained hyperglycemia. *Diabetes*. 52:2129-2136.

Huang, T.J., N.M. Sayers, A. Verkhratsky, and P. Fernyhough. 2005. Neurotrophin-3 prevents mitochondrial dysfunction in sensory neurons of streptozotocin-diabetic rats. *Exp Neurol*. 194:279-283.

Huang, Y.T., and B.S. Blagg. 2007. A library of noviosylated coumarin analogues. *J Org Chem*. 72:3609-3613.

Hunt, C.R., D.J. Dix, G.G. Sharma, R.K. Pandita, A. Gupta, M. Funk, and T.K. Pandita. 2004. Genomic instability and enhanced radiosensitivity in Hsp70.1- and Hsp70.3-deficient mice. *Mol Cell Biol*. 24:899-911.

Hunter-Lavin, C., E.L. Davies, M.M. Bacelar, M.J. Marshall, S.M. Andrew, and J.H. Williams. 2004. Hsp70 release from peripheral blood mononuclear cells. *Biochem Biophys Res Commun*. 324:511-517.

Hur, J., K.A. Sullivan, M. Pande, Y. Hong, A.A.F. Sima, H.V. Jagadish, M. Kretzler, and E.L. Feldman. 2011. The identification of gene expression profiles associated with progression of human diabetic neuropathy. *Brain*. 134:3222-3235.

Huttunen, H.J., J. Kuja-Panula, G. Sorci, A.L. Agneletti, R. Donato, and H. Rauvala. 2000. Coregulation of neurite outgrowth and cell survival by amphoterin and S100 proteins through receptor for advanced glycation end products (RAGE) activation. *J Biol Chem*. 275:40096-40105.

Ido, Y., J. McHowat, K.C. Chang, E. Arrigoni-Martelli, Z. Orfalian, C. Kilo, P.B. Corr, and J.R. Williamson. 1994. Neural dysfunction and metabolic imbalances in diabetic rats. Prevention by acetyl-L-carnitine. *Diabetes*. 43:1469-1477.

Idris, I., S. Gray, and R. Donnelly. 2001. Protein kinase C activation: isozyme-specific effects on metabolism and cardiovascular complications in diabetes. *Diabetologia*. 44:659-673.

Imam, K. 2012. Clinical features, diagnostic criteria and pathogenesis of diabetes mellitus. *Adv Exp Med Biol*. 771:340-355.

Institute, N.E. 2014. Facts About Diabetic Retinopathy, http://www.nei.nih.gov/health/diabetic/retinopathy.asp.

Isakoff, S.J., C. Taha, E. Rose, J. Marcusohn, A. Klip, and E.Y. Skolnik. 1995. The inability of phosphatidylinositol 3-kinase activation to stimulate GLUT4 translocation indicates additional signaling pathways are required for insulin-stimulated glucose uptake. *Proc Natl Acad Sci U S A*. 92:10247-10251.

Ismail-Beigi, F., T. Craven, M.A. Banerji, J. Basile, J. Calles, R.M. Cohen, R. Cuddihy, W.C. Cushman, S. Genuth, R.H. Grimm, Jr., B.P. Hamilton, B. Hoogwerf, D. Karl, L. Katz, A. Krikorian, P. O'Connor, R. Pop-Busui, U. Schubart, D. Simmons, H. Taylor, A. Thomas, D. Weiss, I. Hramiak, and A.t. group. 2010. Effect of intensive treatment of hyperglycaemia on microvascular outcomes in type 2 diabetes: an analysis of the ACCORD randomised trial. *Lancet*. 376:419-430.

Itani, S.I., N.B. Ruderman, F. Schmieder, and G. Boden. 2002. Lipid-induced insulin resistance in human muscle is associated with changes in diacylglycerol, protein kinase C, and IkappaB-alpha. *Diabetes*. 51:2005-2011.

Jack, M.M., J.M. Ryals, and D.E. Wright. 2011. Characterisation of glyoxalase I in a streptozocin-induced mouse model of diabetes with painful and insensate neuropathy. *Diabetologia*. 54:2174-2182.

Jagtap, P., and C. Szabo. 2005. Poly(ADP-ribose) polymerase and the therapeutic effects of its inhibitors. *Nat Rev Drug Discov*. 4:421-440.

Jayakumar, J., K. Suzuki, I.A. Sammut, R.T. Smolenski, M. Khan, N. Latif, H. Abunasra, B. Murtuza, M. Amrani, and M.H. Yacoub. 2001. Heat shock protein 70 gene transfection protects mitochondrial and ventricular function against ischemia-reperfusion injury. *Circulation*. 104:I303-307.

JDRF, P.G.f. Type 1 Diabetes, 2010.

Jiang, J., E.G. Maes, A.B. Taylor, L. Wang, A.P. Hinck, E.M. Lafer, and R. Sousa. 2007. Structural basis of J cochaperone binding and regulation of Hsp70. *Mol Cell*. 28:422-433.

Jones, Q., T.S. Voegeli, G. Li, Y. Chen, and R.W. Currie. 2011. Heat shock proteins protect against ischemia and inflammation through multiple mechanisms. *Inflamm Allergy Drug Targets*. 10:247-259.

Joy, S.V., A.C. Scates, S. Bearelly, M. Dar, C.A. Taulien, J.A. Goebel, and M.J. Cooney. 2005. Ruboxistaurin, a protein kinase C beta inhibitor, as an emerging treatment for diabetes microvascular complications. *Ann Pharmacother*. 39:1693-1699.

Kallestrup, M., H.J. Moller, H. Tankisi, and H. Andersen. 2015. Soluble CD163 levels are elevated in cerebrospinal fluid and serum in people with Type 2 diabetes mellitus and are associated with impaired peripheral nerve function. *Diabet Med*. 32:54-61.

Kamiya, H., J. Nakamura, Y. Hamada, E. Nakashima, K. Naruse, K. Kato, Y. Yasuda, and N. Hotta. 2003. Polyol pathway and protein kinase C activity of rat Schwannoma cells. *Diabetes Metab Res Rev*. 19:131-139.

Kamiya, H., W. Zhang, and A.A. Sima. 2006. Degeneration of the Golgi and neuronal loss in dorsal root ganglia in diabetic BioBreeding/Worcester rats. *Diabetologia*. 49:2763-2774.

Kamiya, H., W. Zhangm, and A.A. Sima. 2005. Apoptotic stress is counterbalanced by survival elements preventing programmed cell death of dorsal root ganglions in subacute type 1 diabetic BB/Wor rats. *Diabetes*. 54:3288-3295.

Karachalias, N., R. Babaei-Jadidi, N. Ahmed, and P.J. Thornalley. 2003. Accumulation of fructosyl-lysine and advanced glycation end products in the kidney, retina and peripheral nerve of streptozotocin-induced diabetic rats. *Biochem Soc Trans*. 31:1423-1425.

Kass, D.A., E.P. Shapiro, M. Kawaguchi, A.R. Capriotti, A. Scuteri, R.C. deGroof, and E.G. Lakatta. 2001. Improved arterial compliance by a novel advanced glycation end-product crosslink breaker. *Circulation*. 104:1464-1470.

Kasznicki, J., M. Kosmalski, A. Sliwinska, M. Mrowicka, M. Stanczyk, I. Majsterek, and J. Drzewoski. 2012. Evaluation of oxidative stress markers in pathogenesis of diabetic neuropathy. *Mol Biol Rep*. 39:8669-8678.

Kellogg, A.P., T.D. Wiggin, D.D. Larkin, J.M. Hayes, M.J. Stevens, and R. Pop-Busui. 2007. Protective effects of cyclooxygenase-2 gene inactivation against peripheral nerve dysfunction and intraepidermal nerve fiber loss in experimental diabetes. *Diabetes*. 56:2997-3005.

Kempen, J.H., B.J. O'Colmain, M.C. Leske, S.M. Haffner, R. Klein, S.E. Moss, H.R. Taylor, and R.F. Hamman. 2004. The prevalence of diabetic retinopathy among adults in the United States. *Arch Ophthalmol*. 122:552-563.

Kern, T.S. 2007. Contributions of inflammatory processes to the development of the early stages of diabetic retinopathy. *Exp Diabetes Res*. 2007:95103.

Kim, J., E.H. Rushovich, T.P. Thomas, T. Ueda, B.W. Agranoff, and D.A. Greene. 1991. Diminished specific activity of cytosolic protein kinase C in sciatic nerve of streptozocin-induced diabetic rats and its correction by dietary myo-inositol. *Diabetes*. 40:1545-1554.

Kimura, A., C.A. Baumann, S.H. Chiang, and A.R. Saltiel. 2001. The sorbin homology domain: a motif for the targeting of proteins to lipid rafts. *Proc Natl Acad Sci U S A*. 98:9098-9103.

Kishi, Y., J.D. Schmelzer, J.K. Yao, P.J. Zollman, K.K. Nickander, H.J. Tritschler, and P.A. Low. 1999. Alpha-lipoic acid: effect on glucose uptake, sorbitol pathway, and energy metabolism in experimental diabetic neuropathy. *Diabetes*. 48:2045-2051.

Kluding, P.M., M. Pasnoor, R. Singh, S. Jernigan, K. Farmer, J. Rucker, N.K. Sharma, and D.E. Wright. 2012. The effect of exercise on neuropathic symptoms, nerve function, and cutaneous innervation in people with diabetic peripheral neuropathy. *J Diabetes Complicat*. 26:424-429.

Knudsen, B.S., S.M. Feller, and H. Hanafusa. 1994. Four proline-rich sequences of the guanine-nucleotide exchange factor C3G bind with unique specificity to the first Src homology 3 domain of Crk. *J Biol Chem*. 269:32781-32787.

Knudsen, L.B. 2004. Glucagon-like peptide-1: the basis of a new class of treatment for type 2 diabetes. *J Med Chem*. 47:4128-4134.

Kohn, A.D., A. Barthel, K.S. Kovacina, A. Boge, B. Wallach, S.A. Summers, M.J. Birnbaum, P.H. Scott, J.C. Lawrence, Jr., and R.A. Roth. 1998. Construction and characterization of a conditionally active version of the serine/threonine kinase Akt. *J Biol Chem*. 273:11937-11943.

Kohn, A.D., S.A. Summers, M.J. Birnbaum, and R.A. Roth. 1996. Expression of a constitutively active Akt Ser/Thr kinase in 3T3-L1 adipocytes stimulates glucose uptake and glucose transporter 4 translocation. *J Biol Chem*. 271:31372-31378.

Kondo, T., S. Koga, R. Matsuyama, K. Miyagawa, R. Goto, H. Kai, and E. Araki. 2011. Heat shock response regulates insulin sensitivity and glucose homeostasis: pathophysiological impact and therapeutic potential. *Curr Diabetes Rev*. 7:264-269.

Koster, J.C., B.A. Marshall, N. Ensor, J.A. Corbett, and C.G. Nichols. 2000. Targeted overactivity of beta cell K(ATP) channels induces profound neonatal diabetes. *Cell*. 100:645-654.

Krause, M., T.G. Heck, A. Bittencourt, S.P. Scomazzon, P. Newsholme, R. Curi, and P.I. Homem de Bittencourt, Jr. 2015. The Chaperone Balance Hypothesis: The Importance of the Extracellular to Intracellular HSP70 Ratio to Inflammation-Driven Type 2 Diabetes, the Effect of Exercise, and the Implications for Clinical Management. *Mediators Inflamm*. 2015:249205.

Kregel, K.C. 2002. Heat shock proteins: modifying factors in physiological stress responses and acquired thermotolerance. *J Appl Physiol (1985)*. 92:2177-2186.

Kristiansen, M., J.H. Graversen, C. Jacobsen, O. Sonne, H.J. Hoffman, S.K. Law, and S.K. Moestrup. 2001. Identification of the haemoglobin scavenger receptor. *Nature*. 409:198-201.

Kusari, J., U.S. Verma, J.B. Buse, R.R. Henry, and J.M. Olefsky. 1991. Analysis of the gene sequences of the insulin receptor and the insulin-sensitive glucose transporter (GLUT-4) in patients with common-type non-insulin-dependent diabetes mellitus. *J Clin Invest*. 88:1323-1330.

Kusuma, B.R., L. Zhang, T. Sundstrom, L.B. Peterson, R.T. Dobrowsky, and B.S. Blagg. 2012. Synthesis and evaluation of novologues as C-terminal Hsp90 inhibitors with cytoprotective activity against sensory neuron glucotoxicity. *J Med Chem*. 55:5797-5812.

Lane, T., B. Flam, R. Lockey, and N. Kolliputi. 2013. TXNIP shuttling: missing link between oxidative stress and inflammasome activation. *Front Physiol*. 4:50.

Lebovitz, H.E., and M.A. Banerji. 2001. Insulin resistance and its treatment by thiazolidinediones. *Recent Prog Horm Res*. 56:265-294.

Lee, I., and M. Huttemann. 2014. Energy crisis: the role of oxidative phosphorylation in acute inflammation and sepsis. *Biochim Biophys Acta*. 1842:1579-1586.

Lee, J.S., K. Kawakubo, S. Inoue, and A. Akabayashi. 2006. Effect of beta(3)-adrenergic receptor gene polymorphism on body weight change in middle-aged, overweight women. *Environ Health Prev Med*. 11:69-74.

Leinninger, G.M., C. Backus, A.M. Sastry, Y.B. Yi, C.W. Wang, and E.L. Feldman. 2006a. Mitochondria in DRG neurons undergo hyperglycemic mediated injury through Bim, Bax and the fission protein Drp1. *Neurobiol Dis*. 23:11-22.

Leinninger, G.M., J.L. Edwards, M.J. Lipshaw, and E.L. Feldman. 2006b. Mechanisms of disease: mitochondria as new therapeutic targets in diabetic neuropathy. *Nat Clin Pract Neurol*. 2:620-628.

Li, C., J. Ma, H. Zhao, B.S. Blagg, and R.T. Dobrowsky. 2012. Induction of heat shock protein 70 (Hsp70) prevents neuregulin-induced demyelination by enhancing the proteasomal clearance of c-Jun. *ASN Neuro*. 4:e00102.

Li, F., C. Szabo, P. Pacher, G.J. Southan, O.I. Abatan, T. Charniauskaya, M.J. Stevens, and I.G. Obrosova. 2004. Evaluation of orally active poly(ADP-ribose) polymerase inhibitor in streptozotocin-diabetic rat model of early peripheral neuropathy. *Diabetologia*. 47:710-717.

Lietzke, S.E., S. Bose, T. Cronin, J. Klarlund, A. Chawla, M.P. Czech, and D.G. Lambright. 2000. Structural basis of 3-phosphoinositide recognition by pleckstrin homology domains. *Mol Cell*. 6:385-394.

Lindquist, S., and E.A. Craig. 1988. The heat-shock proteins. *Annu Rev Genet*. 22:631-677.

Linnenkamp, U., L. Guariguata, J. Beagley, D.R. Whiting, and N.H. Cho. 2014. The IDF Diabetes Atlas methodology for estimating global prevalence of hyperglycaemia in pregnancy. *Diabetes Res Clin Pract*. 103:186-196.

Liu, J., A. Kimura, C.A. Baumann, and A.R. Saltiel. 2002. APS facilitates c-Cbl tyrosine phosphorylation and GLUT4 translocation in response to insulin in 3T3-L1 adipocytes. *Mol Cell Biol*. 22:3599-3609.

Lohmueller, K.E., C.L. Pearce, M. Pike, E.S. Lander, and J.N. Hirschhorn. 2003. Meta-analysis of genetic association studies supports a contribution of common variants to susceptibility to common disease. *Nat Genet*. 33:177-182.

Ludwig, S., and G.X. Shen. 2006. Statins for diabetic cardiovascular complications. *Curr Vasc Pharmacol*. 4:245-251.

Lund, A., F.K. Knop, and T. Vilsboll. 2014. Glucagon-like peptide-1 receptor agonists for the treatment of type 2 diabetes: differences and similarities. *Eur J Intern Med*. 25:407-414.

Luo, W., A. Rodina, and G. Chiosis. 2008. Heat shock protein 90: translation from cancer to Alzheimer's disease treatment? *BMC Neurosci*. 9 Suppl 2:S7.

Luo, Z.J., R.H. King, J. Lewin, and P.K. Thomas. 2002. Effects of nonenzymatic glycosylation of extracellular matrix components on cell survival and sensory neurite extension in cell culture. *J Neurol*. 249:424-431.

Ma, J., K.L. Farmer, P. Pan, M.J. Urban, H. Zhao, B.S. Blagg, and R.T. Dobrowsky. 2014. Heat shock protein 70 is necessary to improve mitochondrial bioenergetics and reverse diabetic sensory neuropathy following KU-32 therapy. *J Pharmacol Exp Ther*. 348:281-292.

Maehama, T., and J.E. Dixon. 1999. PTEN: a tumour suppressor that functions as a phospholipid phosphatase. *Trends Cell Biol*. 9:125-128.

Mamputu, J.C., N.F. Wiernsperger, and G. Renier. 2003. Antiatherogenic properties of metformin: the experimental evidence. *Diabetes Metab*. 29:6S71-76.

Mansilla, M.J., C. Costa, H. Eixarch, V. Tepavcevic, M. Castillo, R. Martin, C. Lubetzki, M.S. Aigrot, X. Montalban, and C. Espejo. 2014. Hsp70 regulates immune response in experimental autoimmune encephalomyelitis. *PLoS One*. 9:e105737.

Marcu, M.G., T.W. Schulte, and L. Neckers. 2000. Novobiocin and related coumarins and depletion of heat shock protein 90-dependent signaling proteins. *J Natl Cancer Inst*. 92:242-248.

Margineantu, D.H., C.B. Emerson, D. Diaz, and D.M. Hockenbery. 2007. Hsp90 inhibition decreases mitochondrial protein turnover. *PLoS One*. 2:e1066.

Martin, S.S., T. Haruta, A.J. Morris, A. Klippel, L.T. Williams, and J.M. Olefsky. 1996. Activated phosphatidylinositol 3-kinase is sufficient to mediate actin rearrangement and GLUT4 translocation in 3T3-L1 adipocytes. *J Biol Chem*. 271:17605-17608.

Matschinsky, F., Y. Liang, P. Kesavan, L. Wang, P. Froguel, G. Velho, D. Cohen, M.A. Permutt, Y. Tanizawa, T.L. Jetton, and et al. 1993. Glucokinase as pancreatic beta cell glucose sensor and diabetes gene. *J Clin Invest*. 92:2092-2098.

Mattila, T.K., and A. de Boer. 2010. Influence of intensive versus conventional glucose control on microvascular and macrovascular complications in type 1 and 2 diabetes mellitus. *Drugs*. 70:2229-2245.

Matts, R.L., G.E. Brandt, Y. Lu, A. Dixit, M. Mollapour, S. Wang, A.C. Donnelly, L. Neckers, G. Verkhivker, and B.S. Blagg. 2011. A systematic protocol for the characterization of Hsp90 modulators. *Bioorg Med Chem*. 19:684-692.

McGarry, J.D., and R.L. Dobbins. 1999. Fatty acids, lipotoxicity and insulin secretion. *Diabetologia*. 42:128-138.

McGuire, J.F., S. Rouen, E. Siegfreid, D.E. Wright, and R.T. Dobrowsky. 2009. Caveolin-1 and altered neuregulin signaling contribute to the pathophysiological progression of diabetic peripheral neuropathy. *Diabetes*. 58:2677-2686.

Migdalis, I.N., K. Kalogeropoulou, L. Kalantzis, C. Nounopoulos, A. Bouloukos, and M. Samartzis. 1995. Insulin-like growth factor-I and IGF-I receptors in diabetic patients with neuropathy. *Diabet Med*. 12:823-827.

Mizukami, H., S. Ogasawara, S. Yamagishi, K. Takahashi, and S. Yagihashi. 2011. Methylcobalamin effects on diabetic neuropathy and nerve protein kinase C in rats. *Eur J Clin Invest*. 41:442-450.

Mogensen, C.E., C.K. Christensen, and E. Vittinghus. 1983. The stages in diabetic renal disease. With emphasis on the stage of incipient diabetic nephropathy. *Diabetes*. 32 Suppl 2:64-78.

Molitch, M.E., R.A. DeFronzo, M.J. Franz, W.F. Keane, C.E. Mogensen, H.H. Parving, M.W. Steffes, and A. American Diabetes. 2004. Nephropathy in diabetes. *Diab Care*. 27 Suppl 1:S79-83.

Mootha, V.K., C.M. Lindgren, K.F. Eriksson, A. Subramanian, S. Sihag, J. Lehar, P. Puigserver, E. Carlsson, M. Ridderstrale, E. Laurila, N. Houstis, M.J. Daly, N. Patterson, J.P. Mesirov, T.R. Golub, P. Tamayo, B. Spiegelman, E.S. Lander, J.N. Hirschhorn, D. Altshuler, and L.C. Groop. 2003. PGC-1alpha-responsive genes involved in oxidative phosphorylation are coordinately downregulated in human diabetes. *Nat Genet*. 34:267-273.

Mora, A., D. Komander, D.M. van Aalten, and D.R. Alessi. 2004. PDK1, the master regulator of AGC kinase signal transduction. *Semin Cell Dev Biol*. 15:161-170.

Morimoto, R.I. 2011. The heat shock response: systems biology of proteotoxic stress in aging and disease. *Cold Spring Harb Symp Quant Biol*. 76:91-99.

Morino, K., K.F. Petersen, and G.I. Shulman. 2006. Molecular mechanisms of insulin resistance in humans and their potential links with mitochondrial dysfunction. *Diabetes*. 55 Suppl 2:S9-S15.

Mortazavi, A., B.A. Williams, K. McCue, L. Schaeffer, and B. Wold. 2008. Mapping and quantifying mammalian transcriptomes by RNA-Seq. *Nat Meth*. 5:621-628.

Muchowski, P.J., and J.L. Wacker. 2005. Modulation of neurodegeneration by molecular chaperones. *Nat Rev Neurosci*. 6:11-22.

Mylonas, C., and D. Kouretas. 1999. Lipid peroxidation and tissue damage. *In Vivo*. 13:295-309.

Nakamura, J., K. Kato, Y. Hamada, M. Nakayama, S. Chaya, E. Nakashima, K. Naruse, Y. Kasuya, R. Mizubayashi, K. Miwa, Y. Yasuda, H. Kamiya, K. Ienaga, F. Sakakibara, N. Koh, and N. Hotta. 1999. A protein kinase C-beta-selective inhibitor ameliorates neural dysfunction in streptozotocin-induced diabetic rats. *Diabetes*. 48:2090-2095.

Nakhooda, A.F., C.N. Wei, A.A. Like, and E.B. Marliss. 1978. The spontaneously diabetic Wistar rat (the "BB" rat): the significance of transient glycosuria. *Diabete Metab*. 4:255-259.

Nathan, D.F., M.H. Vos, and S. Lindquist. 1997. In vivo functions of the Saccharomyces cerevisiae Hsp90 chaperone. *Proc Natl Acad Sci U S A*. 94:12949-12956.

Nathan, D.M., P.A. Cleary, J.Y. Backlund, S.M. Genuth, J.M. Lachin, T.J. Orchard, P. Raskin, B. Zinman, C. Diabetes, I. Complications Trial/Epidemiology of Diabetes, and G. Complications Study Research. 2005. Intensive diabetes treatment and cardiovascular disease in patients with type 1 diabetes. *N Engl J Med*. 353:2643-2653.

Navarro, J.F., and C. Mora. 2005. Role of inflammation in diabetic complications. *Nephrol Dial Transplant*. 20:2601-2604.

Newton, A.C. 2003. Regulation of the ABC kinases by phosphorylation: protein kinase C as a paradigm. *Biochem J*. 370:361-371.

NIDDK. 2011. Diagnosis of Diabetes and Prediabetes, http://diabetes.niddk.nih.gov/dm/pubs/diagnosis/.

Nishikawa, T., D. Edelstein, and M. Brownlee. 2000a. The missing link: a single unifying mechanism for diabetic complications. *Kidney Int Suppl*. 77:S26-30.

Nishikawa, T., D. Edelstein, X.L. Du, S. Yamagishi, T. Matsumura, Y. Kaneda, M.A. Yorek, D. Beebe, P.J. Oates, H.P. Hammes, I. Giardino, and M. Brownlee. 2000b. Normalizing mitochondrial superoxide production blocks three pathways of hyperglycaemic damage. *Nature*. 404:787-790.

O'Rahilly, S., W.H. Choi, P. Patel, R.C. Turner, J.S. Flier, and D.E. Moller. 1991. Detection of mutations in insulin-receptor gene in NIDDM patients by analysis of single-stranded conformation polymorphisms. *Diabetes*. 40:777-782.

Oates, P.J. 2002. Polyol pathway and diabetic peripheral neuropathy. *Int Rev Neurobiol*. 50:325-392.

Oates, P.J. 2008. Aldose reductase, still a compelling target for diabetic neuropathy. *Curr Drug Targets*. 9:14-36.

Obrosova, I.G. 2005. Increased sorbitol pathway activity generates oxidative stress in tissue sites for diabetic complications. *Antioxid Redox Signal*. 7:1543-1552.

Obrosova, I.G. 2009. Diabetes and the peripheral nerve. *Biochim Biophys Acta*. 1792:931-940.

Obrosova, I.G., V.R. Drel, C.L. Oltman, N. Mashtalir, J. Tibrewala, J.T. Groves, and M.A. Yorek. 2007a. Role of nitrosative stress in early neuropathy and vascular dysfunction in streptozotocin-diabetic rats. *Am J Physiol Endocrinol Metab*. 293:E1645-1655.

Obrosova, I.G., V.R. Drel, P. Pacher, O. Ilnytska, Z.Q. Wang, M.J. Stevens, and M.A. Yorek. 2005a. Oxidative-Nitrosative Stress and Poly(ADP-Ribose) Polymerase (PARP) Activation in Experimental Diabetic Neuropathy: The Relation Is Revisited. *Diabetes*. 54:3435-3441.

Obrosova, I.G., L. Fathallah, and M.J. Stevens. 2001. Taurine counteracts oxidative stress and nerve growth factor deficit in early experimental diabetic neuropathy. *Exp Neurol*. 172:211-219.

Obrosova, I.G., O. Ilnytska, V.V. Lyzogubov, I.A. Pavlov, N. Mashtalir, J.L. Nadler, and V.R. Drel. 2007b. High-fat diet induced neuropathy of pre-diabetes and obesity: effects of "healthy" diet and aldose reductase inhibition. *Diabetes*. 56:2598-2608.

Obrosova, I.G., F. Li, O.I. Abatan, M.A. Forsell, K. Komjati, P. Pacher, C. Szabo, and M.J. Stevens. 2004. Role of poly(ADP-ribose) polymerase activation in diabetic neuropathy. *Diabetes*. 53:711-720.

Obrosova, I.G., J.G. Mabley, Z. Zsengeller, T. Charniauskaya, O.I. Abatan, J.T. Groves, and C. Szabo. 2005b. Role for nitrosative stress in diabetic neuropathy: evidence from studies with a peroxynitrite decomposition catalyst. *FASEB J*. 19:401-403.

Ohkubo, Y., H. Kishikawa, E. Araki, T. Miyata, S. Isami, S. Motoyoshi, Y. Kojima, N. Furuyoshi, and M. Shichiri. 1995. Intensive insulin therapy prevents the progression of diabetic microvascular complications in Japanese patients with non-insulin-dependent diabetes mellitus: a randomized prospective 6-year study. *Diabetes Res Clin Pract*. 28:103-117.

Okada, T., Y. Kawano, T. Sakakibara, O. Hazeki, and M. Ui. 1994. Essential role of phosphatidylinositol 3-kinase in insulin-induced glucose transport and antilipolysis in rat adipocytes. Studies with a selective inhibitor wortmannin. *J Biol Chem*. 269:3568-3573.

Oltman, C.L., E.P. Davidson, L.J. Coppey, T.L. Kleinschmidt, D.D. Lund, E.T. Adebara, and M.A. Yorek. 2008. Vascular and neural dysfunction in Zucker diabetic fatty rats: a difficult condition to reverse. *Diabetes Obes Metab*. 10:64-74.

Ouyang, Y.B., L.J. Xu, Y.J. Sun, and R.G. Giffard. 2006. Overexpression of inducible heat shock protein 70 and its mutants in astrocytes is associated with maintenance of mitochondrial physiology during glucose deprivation stress. *Cell Stress Chaperon*. 11:180-186.

Ozes, O.N., H. Akca, L.D. Mayo, J.A. Gustin, T. Maehama, J.E. Dixon, and D.B. Donner. 2001. A phosphatidylinositol 3-kinase/Akt/mTOR pathway mediates and PTEN antagonizes tumor necrosis factor inhibition of insulin signaling through insulin receptor substrate-1. *Proc Natl Acad Sci U S A*. 98:4640-4645.

Ozturk, G., M.R. Sekeroglu, E. Erdogan, and M. Ozturk. 2006. The effect of non-enzymatic glycation of extracellular matrix proteins on axonal regeneration in vitro. *Acta Neuropathol*. 112:627-632.

Paice, J.A. 2011. Chronic treatment-related pain in cancer survivors. *Pain*. 152:S84-89.

Pande, M., J. Hur, Y. Hong, C. Backus, J.M. Hayes, S.S. Oh, M. Kretzler, and E.L. Feldman. 2011. Transcriptional profiling of diabetic neuropathy in the BKS db/db mouse: a model of type 2 diabetes. *Diabetes*. 60:1981-1989.

Panunti, B., and V. Fonseca. 2006. Effects of PPAR gamma agonists on cardiovascular function in obese, non-diabetic patients. *Vascul Pharmacol*. 45:29-35.

Patti, M.E., A.J. Butte, S. Crunkhorn, K. Cusi, R. Berria, S. Kashyap, Y. Miyazaki, I. Kohane, M. Costello, R. Saccone, E.J. Landaker, A.B. Goldfine, E. Mun, R. DeFronzo, J. Finlayson, C.R. Kahn, and L.J. Mandarino. 2003. Coordinated reduction of genes of oxidative metabolism in humans with insulin resistance and diabetes: Potential role of PGC1 and NRF1. *Proc Natl Acad Sci U S A*. 100:8466-8471.

Patti, M.E., and C.R. Kahn. 1998. The insulin receptor--a critical link in glucose homeostasis and insulin action. *J Basic Clin Physiol Pharmacol*. 9:89-109.

Pekiner, C., N.A. Cullum, J.N. Hughes, A.J. Hargreaves, J. Mahon, I.F. Casson, and W.G. McLean. 1993. Glycation of brain actin in experimental diabetes. *J Neurochem*. 61:436-442.

Pessin, J.E., and A.R. Saltiel. 2000. Signaling pathways in insulin action: molecular targets of insulin resistance. *J Clin Invest*. 106:165-169.

Peters AL, L.L.E. 2013. American Diabetes Association/JDRF Type 1 Diabetes Sourcebook. A.D. Association, editor.

Peters, C.M., J.M. Jimenez-Andrade, B.M. Jonas, M.A. Sevcik, N.J. Koewler, J.R. Ghilardi, G.Y. Wong, and P.W. Mantyh. 2007. Intravenous paclitaxel administration in the rat induces a peripheral sensory neuropathy characterized by macrophage infiltration and injury to sensory neurons and their supporting cells. *Exp Neurol*. 203:42-54.

Peterson, L.B., and B.S. Blagg. 2009. To fold or not to fold: modulation and consequences of Hsp90 inhibition. *Future Med Chem*. 1:267-283.

Pierce, M., H. Keen, and C. Bradley. 1995. Risk of diabetes in offspring of parents with non-insulin-dependent diabetes. *Diabet Med*. 12:6-13.

Pilkis, S.J., and D.K. Granner. 1992. Molecular physiology of the regulation of hepatic gluconeogenesis and glycolysis. *Annu Rev Physiol*. 54:885-909.

Pirkkala, L., P. Nykanen, and L. Sistonen. 2001. Roles of the heat shock transcription factors in regulation of the heat shock response and beyond. *FASEB J*. 15:1118-1131.

Pittenger, G., and A. Vinik. 2003. Nerve growth factor and diabetic neuropathy. *Exp Diabesity Res*. 4:271-285.

Polier, S., Z. Dragovic, F.U. Hartl, and A. Bracher. 2008. Structural basis for the cooperation of Hsp70 and Hsp110 chaperones in protein folding. *Cell*. 133:1068-1079.

Polonsky, K.S. 2012. The past 200 years in diabetes. *N Engl J Med*. 367:1332-1340.

Pop-Busui, R., J. Lu, M.M. Brooks, S. Albert, A.D. Althouse, J. Escobedo, J. Green, P. Palumbo, B.A. Perkins, F. Whitehouse, T.L. Jones, and B.D.S. Group. 2013. Impact of glycemic control strategies on the progression of diabetic peripheral neuropathy in the Bypass Angioplasty Revascularization Investigation 2 Diabetes (BARI 2D) Cohort. *Diab Care*. 36:3208-3215.

Pop-Busui, R., V. Marinescu, C. Van Huysen, F. Li, K. Sullivan, D.A. Greene, D. Larkin, and M.J. Stevens. 2002. Dissection of metabolic, vascular, and nerve conduction interrelationships in experimental diabetic neuropathy by cyclooxygenase inhibition and acetyl-L-carnitine administration. *Diabetes*. 51:2619-2628.

Price, S.A., S. Agthong, A.B. Middlemas, and D.R. Tomlinson. 2004. Mitogen-activated protein kinase p38 mediates reduced nerve conduction velocity in experimental diabetic neuropathy: interactions with aldose reductase. *Diabetes*. 53:1851-1856.

Proud, C.G. 2006. Regulation of protein synthesis by insulin. *Biochem Soc Trans*. 34:213-216.

Pugliese, A. 2013. The multiple origins of Type 1 diabetes. *Diabet Med*. 30:135-146.

Purves, T., A. Middlemas, S. Agthong, E.B. Jude, A.J. Boulton, P. Fernyhough, and D.R. Tomlinson. 2001. A role for mitogen-activated protein kinases in the etiology of diabetic neuropathy. *FASEB J*. 15:2508-2514.

Quadroni, M., A. Potts, and P. Waridel. 2015. Hsp90 inhibition induces both protein-specific and global changes in the ubiquitinome. *J Proteomics*.

Ramasamy, R., S.J. Vannucci, S.S. Yan, K. Herold, S.F. Yan, and A.M. Schmidt. 2005. Advanced glycation end products and RAGE: a common thread in aging, diabetes, neurodegeneration, and inflammation. *Glycobiology*. 15:16R-28R.

Ramasamy, R., S.F. Yan, and A.M. Schmidt. 2007. Arguing for the motion: yes, RAGE is a receptor for advanced glycation endproducts. *Mol Nutr Food Res*. 51:1111-1115.

Rapaport, F., R. Khanin, Y. Liang, M. Pirun, A. Krek, P. Zumbo, C.E. Mason, N.D. Socci, and D. Betel. 2013. Comprehensive evaluation of differential gene expression analysis methods for RNA-seq data. *Genome Biol*. 14:R95.

Ribon, V., R. Herrera, B.K. Kay, and A.R. Saltiel. 1998. A role for CAP, a novel, multifunctional Src homology 3 domain-containing protein in formation of actin stress fibers and focal adhesions. *J Biol Chem*. 273:4073-4080.

Ribon, V., S. Hubbell, R. Herrera, and A.R. Saltiel. 1996. The product of the cbl oncogene forms stable complexes in vivo with endogenous Crk in a tyrosine phosphorylation-dependent manner. *Mol Cell Biol*. 16:45-52.

Ribon, V., and A.R. Saltiel. 1997. Insulin stimulates tyrosine phosphorylation of the proto-oncogene product of c-Cbl in 3T3-L1 adipocytes. *Biochem J*. 324 (Pt 3):839-845.

Ricaniadis, N., A. Kataki, N. Agnantis, G. Androulakis, and C.P. Karakousis. 2001. Long-term prognostic significance of HSP-70, c-myc and HLA-DR expression in patients with malignant melanoma. *Eur J Surg Oncol*. 27:88-93.

Rich, K.M., J.R. Luszczynski, P.A. Osborne, and E.M. Johnson, Jr. 1987. Nerve growth factor protects adult sensory neurons from cell death and atrophy caused by nerve injury. *J Neurocytol*. 16:261-268.

Robertson, R.P., J. Harmon, P.O. Tran, Y. Tanaka, and H. Takahashi. 2003. Glucose toxicity in beta-cells: type 2 diabetes, good radicals gone bad, and the glutathione connection. *Diabetes*. 52:581-587.

Rodbard, H.W., S. Gough, W. Lane, L. Korsholm, D.M. Bretler, and Y. Handelsman. 2014. Reduced risk of hypoglycemia with insulin degludec versus insulin glargine in patients with type 2 diabetes requiring high doses of Basal insulin: a meta-analysis of 5 randomized begin trials. *Endocr Pract*. 20:285-292.

Rodrigues-Krause, J., M. Krause, C. O'Hagan, G. De Vito, C. Boreham, C. Murphy, P. Newsholme, and G. Colleran. 2012. Divergence of intracellular and extracellular HSP72 in type 2 diabetes: does fat matter? *Cell Stress Chaperon*. 17:293-302.

Roe, S.M., C. Prodromou, R. O'Brien, J.E. Ladbury, P.W. Piper, and L.H. Pearl. 1999. Structural basis for inhibition of the Hsp90 molecular chaperone by the antitumor antibiotics radicicol and geldanamycin. *J Med Chem*. 42:260-266.

Roy, M.S., R. Klein, B.J. O'Colmain, B.E. Klein, S.E. Moss, and J.H. Kempen. 2004. The prevalence of diabetic retinopathy among adult type 1 diabetic persons in the United States. *Arch Ophthalmol*. 122:546-551.

Rubio-Cabezas, O., and J. Argente. 2008. Current insights into the genetic basis of diabetes mellitus in children and adolescents. *J Pediatr Endocrinol Metab*. 21:917-940.

Russell, J.W., D. Golovoy, A.M. Vincent, P. Mahendru, J.A. Olzmann, A. Mentzer, and E.L. Feldman. 2002. High glucose-induced oxidative stress and mitochondrial dysfunction in neurons. *FASEB J*. 16:1738-1748.

Ryle, C., C.K. Leow, and M. Donaghy. 1997. Nonenzymatic glycation of peripheral and central nervous system proteins in experimental diabetes mellitus. *Muscle Nerve*. 20:577-584.

Ryu, H., J. Lee, S. Impey, R.R. Ratan, and R.J. Ferrante. 2005. Antioxidants modulate mitochondrial PKA and increase CREB binding to D-loop DNA of the mitochondrial genome in neurons. *Proc Natl Acad Sci U S A*. 102:13915-13920.

Saibil, H. 2013. Chaperone machines for protein folding, unfolding and disaggregation. *Nat Rev Mol Cell Biol*. 14:630-642.

Saltiel, A.R., and C.R. Kahn. 2001. Insulin signalling and the regulation of glucose and lipid metabolism. *Nature*. 414:799-806.

Sansbury, B.E., S.P. Jones, D.W. Riggs, V.M. Darley-Usmar, and B.G. Hill. 2011. Bioenergetic function in cardiovascular cells: the importance of the reserve capacity and its biological regulation. *Chem Biol Interact*. 191:288-295.

Santos, J.M., S. Tewari, A.F. Goldberg, and R.A. Kowluru. 2011. Mitochondrial biogenesis and the development of diabetic retinopathy. *Free Radic Biol Med*. 51:1849-1860.

Sasaoka, T., and M. Kobayashi. 2000. The functional significance of Shc in insulin signaling as a substrate of the insulin receptor. *Endocr J*. 47:373-381.

Sasase, T., H. Yamada, K. Sakoda, N. Imagawa, T. Abe, M. Ito, S. Sagawa, M. Tanaka, and M. Matsushita. 2005. Novel protein kinase C-beta isoform selective inhibitor JTT-010 ameliorates both hyper- and hypoalgesia in streptozotocin- induced diabetic rats. *Diabetes Obes Metab*. 7:586-594.

Saxena, G., J. Chen, and A. Shalev. 2010. Intracellular shuttling and mitochondrial function of thioredoxin-interacting protein. *J Biol Chem*. 285:3997-4005.

Schmidt, O., N. Pfanner, and C. Meisinger. 2010. Mitochondrial protein import: from proteomics to functional mechanisms. *Nat Rev Mol Cell Biol*. 11:655-667.

Schmidt, R.E., D.A. Dorsey, K.A. Roth, C.A. Parvin, L. Hounsom, and D.R. Tomlinson. 2000. Effect of streptozotocin-induced diabetes on NGF, P75(NTR) and TrkA content of prevertebral and paravertebral rat sympathetic ganglia. *Brain Res*. 867:149-156.

Schroeder, A., O. Mueller, S. Stocker, R. Salowsky, M. Leiber, M. Gassmann, S. Lightfoot, W. Menzel, M. Granzow, and T. Ragg. 2006. The RIN: an RNA integrity number for assigning integrity values to RNA measurements. *BMC Mol Biol*. 7:3.

Schulze, P.C., J. Yoshioka, T. Takahashi, Z. He, G.L. King, and R.T. Lee. 2004. Hyperglycemia promotes oxidative stress through inhibition of thioredoxin function by thioredoxin-interacting protein. *J Biol Chem*. 279:30369-30374.

Senf, S.M., T.M. Howard, B. Ahn, L.F. Ferreira, and A.R. Judge. 2013. Loss of the inducible Hsp70 delays the inflammatory response to skeletal muscle injury and severely impairs muscle regeneration. *PLoS One*. 8:e62687.

Sharma, P.M., K. Egawa, Y. Huang, J.L. Martin, I. Huvar, G.R. Boss, and J.M. Olefsky. 1998. Inhibition of phosphatidylinositol 3-kinase activity by adenovirus-mediated gene transfer and its effect on insulin action. *J Biol Chem*. 273:18528-18537.

Shelbaya, S., H. Amer, S. Seddik, A.A. Allah, I.M. Sabry, T. Mohamed, and M. El Mosely. 2012. Study of the role of interleukin-6 and highly sensitive C-reactive protein in diabetic nephropathy in type 1 diabetic patients. *Eur Rev Med Pharmacol Sci*. 16:176-182.

Shepherd, P.R., B.T. Nave, and K. Siddle. 1995. Insulin stimulation of glycogen synthesis and glycogen synthase activity is blocked by wortmannin and rapamycin in 3T3-L1 adipocytes: evidence for the involvement of phosphoinositide 3-kinase and p70 ribosomal protein-S6 kinase. *Biochem J*. 305 (Pt 1):25-28.

Shi, Y., D.D. Mosser, and R.I. Morimoto. 1998. Molecular chaperones as HSF1-specific transcriptional repressors. *Genes Dev*. 12:654-666.

Shi, Y., Z. Tu, D. Tang, H. Zhang, M. Liu, K. Wang, S.K. Calderwood, and X. Xiao. 2006. The inhibition of LPS-induced production of inflammatory cytokines by HSP70 involves inactivation of the NF-kappaB pathway but not the MAPK pathways. *Shock*. 26:277-284.

Shimomura, I., Y. Bashmakov, S. Ikemoto, J.D. Horton, M.S. Brown, and J.L. Goldstein. 1999. Insulin selectively increases SREBP-1c mRNA in the livers of rats with streptozotocin-induced diabetes. *Proc Natl Acad Sci U S A*. 96:13656-13661.

Singleton, J.R., A.G. Smith, J.W. Russell, and E.L. Feldman. 2003. Microvascular complications of impaired glucose tolerance. *Diabetes*. 52:2867-2873.

Singleton, K.D., and P.E. Wischmeyer. 2006. Effects of HSP70.1/3 gene knockout on acute respiratory distress syndrome and the inflammatory response following sepsis. *Am J Physiol Lung Cell Mol Physiol*. 290:L956-961.

Sivitz, W.I., and M.A. Yorek. 2010. Mitochondrial dysfunction in diabetes: from molecular mechanisms to functional significance and therapeutic opportunities. *Antioxid Redox Signal*. 12:537-577.

Skundric, D.S., and R.P. Lisak. 2003. Role of neuropoietic cytokines in development and progression of diabetic polyneuropathy: from glucose metabolism to neurodegeneration. *Exp Diabesity Res*. 4:303-312.

Sladek, R., G. Rocheleau, J. Rung, C. Dina, L. Shen, D. Serre, P. Boutin, D. Vincent, A. Belisle, S. Hadjadj, B. Balkau, B. Heude, G. Charpentier, T.J. Hudson, A. Montpetit, A.V. Pshezhetsky, M. Prentki, B.I. Posner, D.J. Balding, D. Meyre, C. Polychronakos, and P. Froguel. 2007. A genome-wide association study identifies novel risk loci for type 2 diabetes. *Nature*. 445:881-885.

Smith, A.G., J. Russell, E.L. Feldman, J. Goldstein, A. Peltier, S. Smith, J. Hamwi, D. Pollari, B. Bixby, J. Howard, and J.R. Singleton. 2006. Lifestyle intervention for pre-diabetic neuropathy. *Diab Care*. 29:1294-1299.

Soedamah-Muthu, S.S., N. Chaturvedi, D.R. Witte, L.K. Stevens, M. Porta, J.H. Fuller, and E.P.C.S. Group. 2008. Relationship between risk factors and mortality in type 1 diabetic patients in Europe: the EURODIAB Prospective Complications Study (PCS). *Diab Care*. 31:1360-1366.

Sorger, P.K. 1991. Heat shock factor and the heat shock response. *Cell*. 65:363-366.

Soti, C., A. Vermes, T.A. Haystead, and P. Csermely. 2003. Comparative analysis of the ATP-binding sites of Hsp90 by nucleotide affinity cleavage: a distinct nucleotide specificity of the C-terminal ATP-binding site. *Eur J Biochem*. 270:2421-2428.

Spindel, O.N., C. Yan, and B.C. Berk. 2012. Thioredoxin-interacting protein mediates nuclear-to-plasma membrane communication: role in vascular endothelial growth factor 2 signaling. *Arterioscler Thromb Vasc Biol*. 32:1264-1270.

Srinivasan, S., M. Stevens, and J.W. Wiley. 2000. Diabetic peripheral neuropathy: evidence for apoptosis and associated mitochondrial dysfunction. *Diabetes*. 49:1932-1938.

Steiner, D.F., J.L. Clark, C. Nolan, A.H. Rubenstein, E. Margoliash, B. Aten, and P.E. Oyer. 1969. Proinsulin and the biosynthesis of insulin. *Recent Prog Horm Res*. 25:207-282.

Steiner, D.F., S.Y. Park, J. Stoy, L.H. Philipson, and G.I. Bell. 2009. A brief perspective on insulin production. *Diabetes Obes Metab*. 11 Suppl 4:189-196.

Stern, D.M., S.D. Yan, S.F. Yan, and A.M. Schmidt. 2002. Receptor for advanced glycation endproducts (RAGE) and the complications of diabetes. *Ageing Res Rev*. 1:1-15.

Stevens, M.J., I. Obrosova, X. Cao, C. Van Huysen, and D.A. Greene. 2000. Effects of DL-alpha-lipoic acid on peripheral nerve conduction, blood flow, energy metabolism, and oxidative stress in experimental diabetic neuropathy. *Diabetes*. 49:1006-1015.

Stirban, A., M. Negrean, B. Stratmann, T. Gawlowski, T. Horstmann, C. Gotting, K. Kleesiek, M. Mueller-Roesel, T. Koschinsky, J. Uribarri, H. Vlassara, and D. Tschoepe. 2006. Benfotiamine prevents macro- and microvascular endothelial dysfunction and oxidative stress following a meal rich in advanced glycation end products in individuals with type 2 diabetes. *Diab Care*. 29:2064-2071.

Strokov, I.A., E.B. Manukhina, L.Y. Bakhtina, I.Y. Malyshev, G.K. Zoloev, S.I. Kazikhanova, and A.S. Ametov. 2000. The function of endogenous protective systems in patients with insulin-dependent diabetes mellitus and polyneuropathy: effect of antioxidant therapy. *Bull Exp Biol Med*. 130:986-990.

Stuart, R.A., D.M. Cyr, and W. Neupert. 1994. Hsp70 in mitochondrial biogenesis: from chaperoning nascent polypeptide chains to facilitation of protein degradation. *Experientia*. 50:1002-1011.

Stumvoll, M., B.J. Goldstein, and T.W. van Haeften. 2005. Type 2 diabetes: principles of pathogenesis and therapy. *Lancet*. 365:1333-1346.

Sugimoto, K., M. Yasujima, and S. Yagihashi. 2008. Role of advanced glycation end products in diabetic neuropathy. *Curr Pharm Des*. 14:953-961.

Suzen, S., and E. Buyukbingol. 2003. Recent studies of aldose reductase enzyme inhibition for diabetic complications. *Curr Med Chem*. 10:1329-1352.

Szwergold, B.S., F. Kappler, and T.R. Brown. 1990. Identification of fructose 3-phosphate in the lens of diabetic rats. *Science*. 247:451-454.

t Hoen, P.A., Y. Ariyurek, H.H. Thygesen, E. Vreugdenhil, R.H. Vossen, R.X. de Menezes, J.M. Boer, G.J. van Ommen, and J.T. den Dunnen. 2008. Deep sequencing-based expression analysis shows major advances in robustness, resolution and inter-lab portability over five microarray platforms. *Nucleic Acids Res*. 36:e141.

Tammariello, S.P., M.T. Quinn, and S. Estus. 2000. NADPH oxidase contributes directly to oxidative stress and apoptosis in nerve growth factor-deprived sympathetic neurons. *J Neurosci*. 20:RC53.

Tanaka, T., A. Shibazaki, R. Ono, and T. Kaisho. 2014. HSP70 mediates degradation of the p65 subunit of nuclear factor kappaB to inhibit inflammatory signaling. *Sci Signal*. 7:ra119.

Tavaria, M., T. Gabriele, I. Kola, and R.L. Anderson. 1996. A hitchhiker's guide to the human Hsp70 family. *Cell Stress Chaperon*. 1:23-28.

Tesfaye, S., A.J. Boulton, P.J. Dyck, R. Freeman, M. Horowitz, P. Kempler, G. Lauria, R.A. Malik, V. Spallone, A. Vinik, L. Bernardi, P. Valensi, and G. Toronto Diabetic Neuropathy Expert. 2010. Diabetic neuropathies: update on definitions, diagnostic criteria, estimation of severity, and treatments. *Diab Care*. 33:2285-2293.

Thomas, P.J., B.H. Qu, and P.L. Pedersen. 1995. Defective protein folding as a basis of human disease. *Trends Biochem Sci*. 20:456-459.

Thomas, T.P., F. Porcellati, K. Kato, M.J. Stevens, W.R. Sherman, and D.A. Greene. 1994. Effects of glucose on sorbitol pathway activation, cellular redox, and metabolism of myo-inositol, phosphoinositide, and diacylglycerol in cultured human retinal pigment epithelial cells. *J Clin Invest*. 93:2718-2724.

Tomlinson, D.R., and N.J. Gardiner. 2008. Glucose neurotoxicity. *Nat Rev Neurosci*. 9:36-45.

Torres, M., and H.J. Forman. 2003. Redox signaling and the MAP kinase pathways. *Biofactors*. 17:287-296.

Toth, C., L.L. Rong, C. Yang, J. Martinez, F. Song, N. Ramji, V. Brussee, W. Liu, J. Durand, M.D. Nguyen, A.M. Schmidt, and D.W. Zochodne. 2008. Receptor for advanced glycation end products (RAGEs) and experimental diabetic neuropathy. *Diabetes*. 57:1002-1017.

Trapnell, C., D.G. Hendrickson, M. Sauvageau, L. Goff, J.L. Rinn, and L. Pachter. 2013. Differential analysis of gene regulation at transcript resolution with RNA-seq. *Nat Biotechnol*. 31:46-+.

Trapnell, C., A. Roberts, L. Goff, G. Pertea, D. Kim, D.R. Kelley, H. Pimentel, S.L. Salzberg, J.L. Rinn, and L. Pachter. 2012. Differential gene and transcript expression analysis of RNA-seq experiments with TopHat and Cufflinks. *Nat Protoc*. 7:562-578.

Unger, R.H. 1995. Lipotoxicity in the pathogenesis of obesity-dependent NIDDM. Genetic and clinical implications. *Diabetes*. 44:863-870.

Unger, R.H., and Y.T. Zhou. 2001. Lipotoxicity of beta-cells in obesity and in other causes of fatty acid spillover. *Diabetes*. 50 Suppl 1:S118-121.

Unwin, N., D. Gan, and D. Whiting. 2010. The IDF Diabetes Atlas: providing evidence, raising awareness and promoting action. *Diabetes Res Clin Pract*. 87:2-3.

Urban, M.J., R.T. Dobrowsky, and B.S. Blagg. 2012a. Heat shock response and insulin-associated neurodegeneration. *Trends Pharmacol Sci*. 33:129-137.

Urban, M.J., C. Li, C. Yu, Y. Lu, J.M. Krise, M.P. McIntosh, R.A. Rajewski, B.S. Blagg, and R.T. Dobrowsky. 2010. Inhibiting heat-shock protein 90 reverses sensory hypoalgesia in diabetic mice. *ASN Neuro*. 2:e00040.

Urban, M.J., P. Pan, K.L. Farmer, H. Zhao, B.S. Blagg, and R.T. Dobrowsky. 2012b. Modulating molecular chaperones improves sensory fiber recovery and mitochondrial function in diabetic peripheral neuropathy. *Exp Neurol*. 235:388-396.

van Haeften, T.W., W. Pimenta, A. Mitrakou, M. Korytkowski, T. Jenssen, H. Yki-Jarvinen, and J.E. Gerich. 2002. Disturbances in beta-cell function in impaired fasting glycemia. *Diabetes*. 51 Suppl 1:S265-270.

Vareniuk, I., I.A. Pavlov, V.R. Drel, V.V. Lyzogubov, O. Ilnytska, S.R. Bell, J. Tibrewala, J.T. Groves, and I.G. Obrosova. 2007. Nitrosative stress and peripheral diabetic neuropathy in leptin-deficient (ob/ob) mice. *Exp Neurol*. 205:425-436.

Vehik, K., C.A. Beam, J.L. Mahon, D.A. Schatz, M.J. Haller, J.M. Sosenko, J.S. Skyler, J.P. Krischer, and G. TrialNet Natural History Study. 2011. Development of autoantibodies in the TrialNet Natural History Study. *Diab Care*. 34:1897-1901.

Veves, A., M. Backonja, and R.A. Malik. 2008. Painful diabetic neuropathy: epidemiology, natural history, early diagnosis, and treatment options. *Pain Med*. 9:660-674.

Vincent, A.M., J.M. Hayes, L.L. McLean, A. Vivekanandan-Giri, S. Pennathur, and E.L. Feldman. 2009. Dyslipidemia-induced neuropathy in mice: the role of oxLDL/LOX-1. *Diabetes*. 58:2376-2385.

Vincent, A.M., L.L. McLean, C. Backus, and E.L. Feldman. 2005. Short-term hyperglycemia produces oxidative damage and apoptosis in neurons. *FASEB J*. 19:638-640.

Vincent, A.M., J.A. Olzmann, M. Brownlee, W.I. Sivitz, and J.W. Russell. 2004a. Uncoupling proteins prevent glucose-induced neuronal oxidative stress and programmed cell death. *Diabetes*. 53:726-734.

Vincent, A.M., L. Perrone, K.A. Sullivan, C. Backus, A.M. Sastry, C. Lastoskie, and E.L. Feldman. 2007. Receptor for advanced glycation end products activation injures primary sensory neurons via oxidative stress. *Endocrinology*. 148:548-558.

Vincent, A.M., J.W. Russell, P. Low, and E.L. Feldman. 2004b. Oxidative stress in the pathogenesis of diabetic neuropathy. *Endocr Rev*. 25:612-628.

Vlassara, H., M. Brownlee, and A. Cerami. 1983. Excessive nonenzymatic glycosylation of peripheral and central nervous system myelin components in diabetic rats. *Diabetes*. 32:670-674.

Vlassara, H., M. Brownlee, and A. Cerami. 1985. Recognition and uptake of human diabetic peripheral nerve myelin by macrophages. *Diabetes*. 34:553-557.

Voellmy, R., and F. Boellmann. 2007. Chaperone regulation of the heat shock protein response. *Adv Exp Med Biol*. 594:89-99.

Vollenweider, P., M. Clodi, S.S. Martin, T. Imamura, W.M. Kavanaugh, and J.M. Olefsky. 1999. An SH2 domain-containing 5' inositolphosphatase inhibits insulin-induced GLUT4 translocation and growth factor-induced actin filament rearrangement. *Mol Cell Biol*. 19:1081-1091.

Wang, L., U. Schumann, Y. Liu, O. Prokopchuk, and J.M. Steinacker. 2012. Heat shock protein 70 (Hsp70) inhibits oxidative phosphorylation and compensates ATP balance through enhanced glycolytic activity. *J Appl Physiol (1985)*. 113:1669-1676.

Wang, Y., A.M. Schmeichel, H. Iida, J.D. Schmelzer, and P.A. Low. 2006. Enhanced inflammatory response via activation of NF-kappaB in acute experimental diabetic neuropathy subjected to ischemia-reperfusion injury. *J Neurol Sci*. 247:47-52.

Wang, Z., M. Gerstein, and M. Snyder. 2009. RNA-Seq: a revolutionary tool for transcriptomics. *Nat Rev Genet*. 10:57-63.

Ways, D.K., and M.J. Sheetz. 2000. The role of protein kinase C in the development of the complications of diabetes. *Vitam Horm*. 60:149-193.

Waza, M., H. Adachi, M. Katsuno, M. Minamiyama, C. Sang, F. Tanaka, A. Inukai, M. Doyu, and G. Sobue. 2005. 17-AAG, an Hsp90 inhibitor, ameliorates polyglutamine-mediated motor neuron degeneration. *Nat Med*. 11:1088-1095.

Wendt, T., N. Tanji, J. Guo, B.I. Hudson, A. Bierhaus, R. Ramasamy, B. Arnold, P.P. Nawroth, S.F. Yan, V. D'Agati, and A.M. Schmidt. 2003. Glucose, glycation, and RAGE: implications for amplification of cellular dysfunction in diabetic nephropathy. *J Am Soc Nephrol*. 14:1383-1395.

Westerheide, S.D., J. Anckar, S.M. Stevens, Jr., L. Sistonen, and R.I. Morimoto. 2009. Stress-inducible regulation of heat shock factor 1 by the deacetylase SIRT1. *Science*. 323:1063-1066.

White, M.F. 1998. The IRS-signalling system: a network of docking proteins that mediate insulin action. *Mol Cell Biochem*. 182:3-11.

White, M.F. 2002. IRS proteins and the common path to diabetes. *Am J Physiol Endocrinol Metab*. 283:E413-422.

Whitham, M., and M.B. Fortes. 2008. Heat shock protein 72: release and biological significance during exercise. *Front Biosci*. 13:1328-1339.

Whiting, D.R., L. Guariguata, C. Weil, and J. Shaw. 2011. IDF diabetes atlas: global estimates of the prevalence of diabetes for 2011 and 2030. *Diabetes Res Clin Pract*. 94:311-321.

WHO. 2006. Definition and diagnosis of diabetes mellitus.

WHO. 2013a. Diabetes, http://www.who.int/mediacentre/factsheets/fs312/en/.

WHO. 2013b. Diabetes Fact sheet N ̊312.

Wiese, R.J., C.C. Mastick, D.F. Lazar, and A.R. Saltiel. 1995. Activation of mitogen-activated protein kinase and phosphatidylinositol 3'-kinase is not sufficient for the hormonal stimulation of glucose uptake, lipogenesis, or glycogen synthesis in 3T3-L1 adipocytes. *J Biol Chem*. 270:3442-3446.

Wilhelm, B.T., and J.R. Landry. 2009. RNA-Seq-quantitative measurement of expression through massively parallel RNA-sequencing. *Methods*. 48:249-257.

Williams, M.D., and J.L. Nadler. 2007. Inflammatory mechanisms of diabetic complications. *Curr Diab Rep*. 7:242-248.

Williams, S.K., N.L. Howarth, J.J. Devenny, and M.W. Bitensky. 1982. Structural and functional consequences of increased tubulin glycosylation in diabetes mellitus. *Proc Natl Acad Sci U S A*. 79:6546-6550.

Wolffenbuttel, B.H. 1993. The DCCT: "metabolic control matters". Diabetes Control and Complications Trial. *Neth J Med*. 43:241-245.

Wright, D.E., M.S. Johnson, M.G. Arnett, S.E. Smittkamp, and J.M. Ryals. 2007. Selective changes in nocifensive behavior despite normal cutaneous axon innervation in leptin receptor-null mutant (db/db) mice. *J Peripher Nerv Syst*. 12:250-261.

Wright, G., K. Terada, M. Yano, I. Sergeev, and M. Mori. 2001. Oxidative stress inhibits the mitochondrial import of preproteins and leads to their degradation. *Experimental cell research*. 263:107-117.

Wuarin, L., D.M. Guertin, and D.N. Ishii. 1994. Early reduction in insulin-like growth factor gene expression in diabetic nerve. *Exp Neurol*. 130:106-114.

Xia, P., T. Inoguchi, T.S. Kern, R.L. Engerman, P.J. Oates, and G.L. King. 1994. Characterization of the mechanism for the chronic activation of diacylglycerol-protein kinase C pathway in diabetes and hypergalactosemia. *Diabetes*. 43:1122-1129.

Xiao, W.H., and G.J. Bennett. 2012. Effects of mitochondrial poisons on the neuropathic pain produced by the chemotherapeutic agents, paclitaxel and oxaliplatin. *Pain*. 153:704-709.

Xu, L., J.F. Emery, Y.B. Ouyang, L.A. Voloboueva, and R.G. Giffard. 2010. Astrocyte targeted overexpression of Hsp72 or SOD2 reduces neuronal vulnerability to forebrain ischemia. *Glia*. 58:1042-1049.

Xu, L., D. Tang, M. Guan, C. Xie, and Y. Xue. 2014. Effect of high-fat diet on peripheral neuropathy in C57BL/6 mice. *Int J Endocrinol*. 2014:305205.

Xu, Y., and S. Lindquist. 1993. Heat-shock protein hsp90 governs the activity of pp60v-src kinase. *Proc Natl Acad Sci U S A*. 90:7074-7078.

Yagihashi, S., S.I. Yamagishi, R. Wada Ri, M. Baba, T.C. Hohman, C. Yabe-Nishimura, and Y. Kokai. 2001. Neuropathy in diabetic mice overexpressing human aldose reductase and effects of aldose reductase inhibitor. *Brain*. 124:2448-2458.

Yamagishi, S., S. Ogasawara, H. Mizukami, N. Yajima, R. Wada, A. Sugawara, and S. Yagihashi. 2008. Correction of protein kinase C activity and macrophage migration in peripheral nerve by pioglitazone, peroxisome proliferator activated-gamma-ligand, in insulin-deficient diabetic rats. *J Neurochem*. 104:491-499.

Yki-Jarvinen, H. 1992. Glucose toxicity. *Endocr Rev*. 13:415-431.

Yki-Jarvinen, H. 2004. Thiazolidinediones. *N Engl J Med*. 351:1106-1118.

Yoshida, S., S. Hazama, K. Tokuno, K. Sakamoto, M. Takashima, T. Tamesa, T. Torigoe, N. Sato, and M. Oka. 2009. Concomitant overexpression of heat-shock protein 70 and HLA class-I in hepatitis C virus-related hepatocellular carcinoma. *Anticancer Res*. 29:539-544.

Young, J.C., N.J. Hoogenraad, and F.U. Hartl. 2003. Molecular chaperones Hsp90 and Hsp70 deliver preproteins to the mitochondrial import receptor Tom70. *Cell*. 112:41-50.

Young, J.C., I. Moarefi, and F.U. Hartl. 2001. Hsp90: a specialized but essential protein-folding tool. *J Cell Biol*. 154:267-273.

Zhang, L., C. Yu, F.E. Vasquez, N. Galeva, I. Onyango, R.H. Swerdlow, and R.T. Dobrowsky. 2010a. Hyperglycemia alters the schwann cell mitochondrial proteome and decreases coupled respiration in the absence of superoxide production. *J Proteome Res*. 9:458-471.

Zhang, L., H. Zhao, B.S. Blagg, and R.T. Dobrowsky. 2012. C-terminal heat shock protein 90 inhibitor decreases hyperglycemia-induced oxidative stress and improves mitochondrial bioenergetics in sensory neurons. *J Proteome Res*. 11:2581-2593.

Zhang, X., J.B. Saaddine, C.F. Chou, M.F. Cotch, Y.J. Cheng, L.S. Geiss, E.W. Gregg, A.L. Albright, B.E. Klein, and R. Klein. 2010b. Prevalence of diabetic retinopathy in the United States, 2005-2008. *JAMA*. 304:649-656.

Zhao, H., M.L. Michaelis, and B.S. Blagg. 2012. Hsp90 modulation for the treatment of Alzheimer's disease. *Adv Pharmacol*. 64:1-25.

Zhou, J., and S. Zhou. 2014. Inflammation: therapeutic targets for diabetic neuropathy. *Mol Neurobiol*. 49:536-546.

Ziegler, A.G., M. Rewers, O. Simell, T. Simell, J. Lempainen, A. Steck, C. Winkler, J. Ilonen, R. Veijola, M. Knip, E. Bonifacio, and G.S. Eisenbarth. 2013. Seroconversion to multiple islet autoantibodies and risk of progression to diabetes in children. *JAMA*. 309:2473-2479.

Ziegler, D., A. Ametov, A. Barinov, P.J. Dyck, I. Gurieva, P.A. Low, U. Munzel, N. Yakhno, I. Raz, M. Novosadova, J. Maus, and R. Samigullin. 2006. Oral treatment with alpha-lipoic acid improves symptomatic diabetic polyneuropathy: the SYDNEY 2 trial. *Diab Care*. 29:2365-2370.

Ziegler, D., L. Movsesyan, B. Mankovsky, I. Gurieva, Z. Abylaiuly, and I. Strokov. 2009. Treatment of symptomatic polyneuropathy with actovegin in type 2 diabetic patients. *Diab Care*. 32:1479-1484.

Ziegler, D., H. Nowak, P. Kempler, P. Vargha, and P.A. Low. 2004. Treatment of symptomatic diabetic polyneuropathy with the antioxidant alpha-lipoic acid: a meta-analysis. *Diabet Med*. 21:114-121.

Zou, J., Y. Guo, T. Guettouche, D.F. Smith, and R. Voellmy. 1998. Repression of heat shock transcription factor HSF1 activation by HSP90 (HSP90 complex) that forms a stress-sensitive complex with HSF1. *Cell*. 94:471-480.